



Baba, Yahaya Danjuma

**Experimental Investigation of High Viscous Multiphase  
Flow in Horizontal Pipelines**

Oil & Gas Engineering Centre,  
School of Energy, Environment and Agrifood,  
**CRANFIELD UNIVERSITY**

PhD Thesis  
Academic Year: 2016

Supervisor: Prof. Hoi Yeung



CRANFIELD UNIVERSITY

Oil & Gas Engineering Centre,  
School of Energy, Environment and Agrifood,

PhD Thesis

Academic Year 2012 -2015

Baba, Yahaya Danjuma

**Experimental Investigation of High Viscous Multiphase  
Flows in Horizontal Pipelines**

Supervisor: Prof. Hoi Yeung

This thesis is submitted in partial fulfilment of the requirements for  
the degree of PhD

© Cranfield University 2016. All rights reserved. No part of this  
publication may be reproduced without the written permission of the  
copyright owner.



## **ABSTRACT**

Diminishing reserves of “conventional” light crude oil, increased production costs amidst increased world energy demand over the last decade has spurred industrial interest in the production of the significantly and more abundant “unconventional” heavy crude oil.

Recent findings have shown that unconventional oil being a veritable energy source accounts for over two-thirds of the world total oil reserve. The exploration of this vast resource for easy production and transportation requires a good understanding of multiphase system for which the knowledge of the effect of fluid viscosity is of great importance.

Heavy oils are known for their high liquid viscosities which make them even more difficult and expensive to produce and transport in pipelines at ambient temperatures. In the light of this, it has become imperative to investigate the rheology of high viscosity oils and ways of enhancing its production and transportation since a critical understanding of multiphase flow characteristics are vital to aid engineering design.

It is clear from experimental investigation reported so far in literatures and in Cranfield University that the behaviour of high viscosity oil-gas flows differs significantly from that of low viscosity oils. This means that most of the existing prediction models in the literature which were developed from observations of low viscosity liquid-gas flow will not perform accurately when compared to oil-gas flow data for high viscosity oil. Therefore, this research work seek to extend databank and provide a clearer understanding of the physics of high viscous multiphase flows.

Experimental investigation have been conducted using 3-inch and 1-inch ID horizontal test facilities for oil-gas and oil-water respectively using different oil viscosities. The effects of liquid viscosities on oil-gas two phase flow parameters (i.e. pressure gradient, mean liquid holdup, slug frequency, slug translational velocity and slug body length) have been discussed. Assessment of existing

prediction models and correlations in the literature are also carried out and their performance highlighted.

New/improved prediction correlations for high viscosity oil-gas flow slug frequency, slug translational velocity and slug body have been proposed with their performance evaluated against the results obtained for this study and in literature. As for high viscosity oil-water flows, a new flow pattern maps have been established for high viscous oil-water two-phase flow in horizontal pipe with ID = 0.0254 m for which four flow patterns were observed namely; rivulet, core annular, plug and dispersed flows were observed. Generally, it was observed that increase in oil viscosity favoured the Core Annular Flow pattern, similar behaviour was also observed for increased oil holdup. Comparatively analysis of results obtained here with low viscous kerosene and water flow study obtained under similar flow geometry and conditions shows significant difference in flow patterns under similar flow conditions.

**Keywords:**

Pressure gradient, flow pattern, liquid holdup, high viscosity, gamma densitometer.

## **ACKNOWLEDGEMENTS**

This research work was funded by the Petroleum Technology Development Fund (PTDF), a parastatal under the Nigerian Ministry of Petroleum Resources charged with the mandate of building capacities and capabilities in Nigeria's Oil and Gas industry through the development of human capacities.

A special acknowledgement to my supervisor, Professor Hoi Yeung for his guidance, encouragement and constructive criticisms which were indispensable towards the successful completion of this study. I am very thankful of this and the support provided.

Dr. Archibong Archibong is immensely appreciated for his support throughout the period of this study. I benefitted greatly from his practical knowledge of multiphase flow which was a source of inspiration and encouragements. Many thanks for the brotherly counselling and support.

Special thanks goes to Stan Collins; the laboratory manager, Sheridan Cross, Dimitry Gazin of Neftemer for their technical assistance with respect to the experimental facility and instrumentation and for their quick solutions for many facility problems.

I will remain indebted to Aliyu Aliyu, Shi Jing, and Muhammad Ilham for been always there at odds hours to support my experiments despite their individual schedule. I appreciate your kind help and friendship.

My appreciation goes to Sam Skears and Sasha Quill for remarkably discharging their administrative responsibilities. You both are wonderful.

I wish to thank my friends; Muhammad Basheer of the University of Bradford and Kaigama Usman of Cardiff University for being supportive.

This acknowledgement will be incomplete without the mentioning the patience from my beloved wife Jamila Muhammad and daughter A'matullah. The unalloyed support and prayers from my parents and siblings is greatly acknowledged.

# TABLE OF CONTENTS

ABSTRACT .....	i
ACKNOWLEDGEMENTS.....	iii
LIST OF FIGURES.....	vii
LIST OF TABLES .....	xii
NOMENCLATURE .....	xiii
LIST OF ABBREVIATIONS .....	xv
1 INTRODUCTION.....	1
1.1 Background.....	1
1.2 Overview of Heavy Oil .....	1
1.3 Motivation .....	3
1.4 Research Aim and Objectives.....	4
1.5 Thesis Outline .....	5
2 LITERATURE REVIEW .....	6
2.1 Multiphase Flow .....	6
2.2 Basic Definition .....	6
2.2.1 Superficial phase velocity.....	6
2.2.2 Slip: .....	7
2.2.3 Slip velocity .....	7
2.2.4 Slip ratio .....	7
2.2.5 Water Cut (WC).....	7
2.2.6 Mixture Density .....	7
2.2.7 Viscosity Mixture .....	8
2.2.8 Volume Fraction .....	8
2.2.9 Void Fraction and Liquid Hold up .....	8
2.3 Gas-Liquid Two Phase Flow .....	8
2.3.1 Gas-Liquid Flow patterns .....	9
2.3.2 Flow Pattern Maps .....	10
2.3.3 Effects of Viscosity on Flow Patterns .....	12
2.3.4 Oil-Gas Two-Phase Flow Modelling Studies .....	15
2.3.5 Closure Relationships .....	22
2.3.6 Summary of Gas-Liquid Two-Phase Flow .....	34
2.4 Liquid-Liquid Two-Phase Flow .....	38
2.4.1 Flow Patterns in Liquid-Liquid Flow.....	38
2.4.2 Two Phase Liquid-Liquid Flow Modelling Studies.....	43
2.4.3 Summary of Liquid-Liquid Flow .....	48
3 EXPERIMENTAL SETUP .....	51
3.1 Description of One-Inch Test Facility.....	51
3.1.1 Fluid Handling Section .....	51
3.1.2 Unit Operation Equipment Section .....	52
3.1.3 Instrumentation and Data Acquisition Section .....	57



3.2	Description of Three-Inch Test Facility .....	59
3.2.1	Test Fluid Handling Section .....	60
3.2.2	Unit Operation Equipment Section .....	61
3.2.3	Instrumentation and Data Acquisition Section .....	63
3.3	Gamma Densitometer .....	68
3.3.1	Basic Concept Gamma Rays .....	68
3.4	Quick Closing Valves .....	72
3.5	Test Materials and Matrix .....	74
3.5.1	Test Fluids .....	74
3.6	Experimental Procedure .....	75
3.7	Data Processing .....	76
3.8	Cross-correlation Procedure .....	78
3.9	Uncertainty Measurements .....	79
4	LOW VISCOUS GAS LIQUID FLOW IN HORIZONTAL PIPE .....	80
4.1	Single Phase Water Test .....	80
4.1.1	Comparison of measurements with Friction Factor Correlations .....	80
4.2	Two Phase Air-Water Test .....	82
4.3	Flow Pattern Characterization .....	82
4.4	Flow Pattern Visualization with Gamma Densitometer .....	86
4.5	Pressure Gradient .....	88
4.6	Comparison of Measured Pressure Gradient with Predictions Models ...	89
4.7	Liquid Holdup .....	90
4.8	Slug Translational Velocity .....	92
4.8.1	Evaluation of Slug Translational Velocity Prediction Models .....	92
4.9	Slug Body length .....	94
4.9.1	Comparison with Prediction Models .....	96
4.10	Chapter Summary .....	96
5	HIGH VISCOUS OIL-GAS FLOW IN HORIZONTAL PIPELINE .....	98
5.1	Flow pattern Characterization .....	98
5.2	Flow Regime Map .....	104
5.3	Liquid Holdup .....	107
5.3.1	Viscosity Effects on Mean Liquid Holdup .....	109
5.3.2	Comparisons Against Liquid Holdup Prediction Models .....	110
5.4	Pressure Gradient .....	112
5.4.1	Viscosity Effects on Pressure Gradient .....	115
5.4.2	Comparisons with previous pressure gradient data .....	115
5.4.3	Comparisons with prediction methods .....	117
5.5	Slug Body Holdup .....	120
5.5.1	Slug Liquid Holdup Prediction Models Evaluation .....	124
5.6	Slug Frequency .....	125
5.6.1	Comparison of slug frequency against prediction models .....	129
5.7	Slug Translational Velocity .....	131

5.7.1 Comparison with Prediction Models .....	133
5.8 Slug Body Length.....	134
5.9 Chapter Summary.....	137
6 HIGH VISCOSITY LIQUID-GAS SLUG FLOW MODELLING STUDY.....	139
6.1 Slug Frequency.....	140
6.1.1 Evaluation and comparison of Proposed Slug Frequency Prediction Model .....	141
6.2 Slug Body length.....	146
6.2.1 Validation of Proposed Correlation.....	147
6.3 Slug Translational Velocity .....	150
6.3.1 Calculation Method.....	154
6.3.2 Model validation and comparison.....	154
6.4 Evaluation of Proposed Correlation .....	158
6.5 Chapter Summary.....	162
7 OIL–WATER TWO–PHASE FLOW .....	164
7.1 Flow Pattern Visualization.....	164
7.1.1 Flow Pattern Map .....	165
7.1.2 Comparison of Flow Patterns in this Study with Flow Patterns observed for Low Viscous Liquid –Liquid Flow.....	167
7.2 Oil Holdup .....	168
7.3 Water Holdup .....	170
7.3.1 Comparison of Predictive Models with Experimental Results.....	171
7.3.2 Water Holdup and Water Cut .....	172
7.4 Pressure Drop.....	172
7.5 Conclusion .....	174
8 CONCLUSIONS AND RECOMMENDATION .....	176
8.1 Conclusions .....	176
8.1.1 Air-Water Two Phase Flow .....	176
8.1.2 High Viscous Oil-Gas Flow.....	177
8.1.3 High Viscous Oil-Water Flow.....	178
8.2 Recommendations for Further Work.....	178
REFERENCES.....	180
APPENDICES .....	191
A Estimating Uncertainties .....	191
B Error Analysis .....	196
C List of Models/Correlations Used For Comparison.....	198

## LIST OF FIGURES

Figure 1-1: Heavy oil vs. conventional oil reserve (Falcone et al., 2009). .....	2
Figure 1-2: An illustration of knowledge gap existing in the literature and the present study focus. ....	4
Figure 2-1: Flow patterns of gas-liquid flow in horizontal pipes (Taitel and Dukler, 1976). ....	9
Figure 2-2: Beggs and Brill (1973) flow pattern map for horizontal pipeline .....	12
Figure 2-3: Marquez & Trujillo (2010) gas-liquid flow pattern maps in horizontal pipe. ....	14
Figure 2-4: Oil-water flow patterns (Trallero 1995) .....	38
Figure 2-5: Flow Patterns Observed in Vuong et al. (2009) study .....	40
Figure 2-6: Flow Patterns Observed in Bannwart et al., (2004).....	41
Figure 2-7: Viscous oil-water flow patterns schematics by (Al-Awadi, 2012)....	42
Figure 3-1: The schematic of one-inch test facility .....	53
Figure 3-2: Pictorial view of one-inch test facility .....	54
Figure 3-3: Temperature Regulator for 1-Inch Rig .....	57
Figure 3-4: (a) & (b) GE Druck Static and Differential Pressure Transducers (c) Thermocouple .....	58
Figure 3-5: Sony camcorders .....	58
Figure 3-6: Pictorial view of the installed Ball Valves for water holdup measurement .....	59
Figure 3-7: Mineral oil (CYL 680) used for the study .....	61
Figure 3-8: The 3-inch test facility chiller unit .....	62
Figure 3-9: 3-Inch test facility separator with its viewing window.....	62
Figure 3-10: 3-inch multiphase flow facility schematics.....	64
Figure 3-11: Injection and test sections in 3-inch facility (Zhao, 2014) .....	66
Figure 3-12: Brookfield DV-I™ prime viscometer .....	67
Figure 3-13: Viscosity versus temperature measurement .....	68
Figure 3-14: A gamma densitometer clamped onto the 3-inch multiphase flow test facility .....	69
Figure 3-15: Actual liquid holdup versus gamma estimated holdup.....	71

Figure 3-16: Gamma photon count rate for single phase oil and air bench test	71
Figure 3-17: Quick closing valve section for water holdup measurement.....	73
Figure 3-18: (I) calibration samples collected for the fluid sampling section volume. (a) $V_{sw}= 0.6$ m/s; (b) $V_{sw}= 0.8$ m/s; (c) $V_{sw}= 1.0$ m/s. (II) Collected samples of two-phase flow for different flow conditions.....	74
Figure 3-19: Raw signal output from gamma photon counts .....	77
Figure 3-20: Sample of a filtered signal output.....	77
Figure 3-21: Cross-Correlation results between Gamma Densitometer 1 and Gamma Densitometer 2 .....	78
Figure 4-1: Frictional pressure gradient as a function of water velocity. ....	81
Figure 4-2: Frictional pressure gradient Vs single phase prediction models ....	81
Figure 4-3 Comparison of air-water test and Beggs & Brill (1973) flow pattern map .....	85
Figure 4-4: Comparison of air-water test and Mandhane (1974) flow pattern map .....	86
Figure 4-5: Pressure gradient as a function of gas superficial velocities for different superficial water velocities.....	88
Figure 4-6: Pressure Gradient Prediction as a Function Experimental Measurement .....	89
Figure 4-7: Measured Liquid Holdup versus Superficial Gas Velocity .....	90
Figure 4-8 Comparison of measured liquid holdup and prediction models.....	91
Figure 4-9: Slug translational velocity plotted as a function of mixture velocity	93
Figure 4-10: Comparison between measured data and prediction models .....	93
Figure 4-11: Slug length as a function of mixture velocity.....	95
Figure 4-12: Slug length distribution and log-normal fits for flow conditions investigated ( $V_{sg}=0.3-7$ m/s and $V_{sw}=0.2-0.4$ m/s).....	95
Figure 5-1 Gamma Densitometer Liquid Holdup Time series .....	101
Figure 5-2 Probability Mass Function (PMF) of Gamma Densitometer Liquid Holdup Time Series.....	103
Figure 5-3: Flow Pattern Map for Gas-Liquid Two phase Flow.....	106
Figure 5-4 Comparison of Flow Pattern Map with Taitel and Dukler (1976)....	107
Figure 5-5: A typical time varying instantaneous liquid holdup time trace derived from the gamma densitometer. ....	108

Figure 5-6: Measured mean liquid holdup as function of liquid superficial velocity for different liquid superficial velocities.....	109
Figure 5-7: Measured mean liquid holdup as function of liquid superficial velocity for different liquid viscosities. ....	110
Figure 5-8 Comparison of experimental measured liquid holdup versus predicted mean liquid holdup .....	111
Figure 5-9: Pressure gradient versus gas superficial velocity for viscosity range (1.2-1.5 Pa.s) .....	113
Figure 5-10: Pressure gradient versus gas superficial velocity for viscosity range (a) 2.2-2.9 Pa.s, (b) 3.4-3.9 Pa.s.....	114
Figure 5-11: Pressure gradient versus gas superficial velocity for viscosity range (4.2-5.0 Pa.s) .....	114
Figure 5-12: Pressure gradient as a function of gas superficial velocity for different viscosities.....	115
Figure 5-13: Comparison of the present data with Gokcal (2008) data. ....	116
Figure 5-14: Comparison of the present data with Gokcal (2008) data. ....	117
Figure 5-15: Comparison of measured pressure gradient with model predictions. ....	118
Figure 5-16: Comparison of measured pressure gradient with model predictions .....	119
Figure 5-17: Measured pressure gradient versus model predictions.....	119
Figure 5-18: A typical gamma densitometer time series liquid holdup plot. ....	121
Figure 5-19: Measured slug body holdup as a function of superficial gas velocities for different viscosities.....	122
Figure 5-20: Measured slug body holdup as a function of superficial gas velocities for different superficial liquid velocity.....	123
Figure 5-21: Liquid viscosity effects on slug body holdup.....	123
Figure 5-22: Liquid viscosity effects on slug body holdup for different viscosities .....	124
Figure 5-23: Prediction of slug holdup as function of measured slug holdup .	125
Figure 5-24: Slug frequency vs. gas superficial velocity.....	127
Figure 5-25: Slug frequency vs. gas superficial velocity.....	127
Figure 5-26: Slug frequency vs. gas superficial velocity.....	128
Figure 5-27: Slug frequency vs. gas superficial velocity for diff. viscosities....	128

Figure 5-28a and b: Measured slug frequency versus prediction models .....	130
Figure 5-29: Liquid holdup time trace for the two Gamma densitometer used. .....	132
Figure 5-30: Measured translational velocity as a function mixture velocity ...	133
Figure 5-31: Comparison between measured and predicted translational velocity .....	134
Figure 5-32: Measured slug length versus superficial gas velocity for different superficial liquid velocity $V_{sl}=0.06-0.3\text{m/s}$ .....	135
Figure 5-33 Mean Slug Length as a Function of Mixture Velocity.....	136
Figure 5-34: Comparison of experimental result for slug length and Log-Normal distribution.....	137
Figure 6-1 Slug Flow Unit Cell.....	140
Figure 6-2 Cross-plot of measured slug frequency against predicted for present data set. ....	143
Figure 6-3 Cross-plot of measured slug frequency versus predicted (Gokcal, 2008 dataset) .....	144
Figure 6-4 Cross-plot of predictive model predictions against experimental measurement. ....	148
Figure 6-5 Cross-plot of predictive model predictions against experimental measurement. ....	149
Figure 6-6 a, b: Partial correlation of the dimensionless groupings of equation. .....	153
Figure 6-7 Cross-plot of model prediction vs. measurement from experiment from (Gokcal, 2008).....	156
Figure 6-8 Plot of comparison between model predictions and proposed models for present study .....	157
Figure 6-10: Performance of Xiao <i>et al</i> (1990) model using present data. ....	159
Figure 6-11: Cross-plot of present data against (Modified Xiao, 1990) Prop Corr. .....	160
Figure 6-13: Cross-plot of present data against (Choi, 2012) prediction model .....	160
Figure 6-14: Cross-plot of present data against (Bestion, 1990) prediction model .....	161
Figure 6-15: Cross-plot of present data against (Zuber and Findlay, 1965) prediction model.....	161

Figure 6-16: Cross-plot of present data against (Beggs & Brill, 1973) model.	162
Figure 7-1: Oil-Water Two-Phase Flow (Oil Viscosity = 3.3 Pa.s).....	166
Figure 7-2: Oil-Water Two-Phase Flow (Oil Viscosity = 5.0 Pa.s).....	166
Figure 7-3: Effect of increasing oil viscosity in Oil-Water Two-Phase Flow.....	166
Figure 7-4 Comparison of Flow Pattern obtained in this study with the Flow Pattern Map of Sugimoto and Mazza (2015).....	168
Figure 7-5: Oil Holdup as a function of Water Superficial Velocity, $\mu_o = 3.3 \text{ Pa.s}$ .....	169
Figure 7-6: Oil Holdup as a function of Water Superficial Velocity, $\mu_o = 5.0 \text{ Pa.s}$ .....	170
Figure 7-7: Oil Holdup as a function of Water Superficial Velocity.....	170
Figure 7-8: Water Holdup as a function of Water Superficial Velocity.....	171
Figure 7-9: Comparison of measured water holdup with predictive models ...	171
Figure 7-10: Water Holdup as a Function of Water Cut.....	172
Figure 7-11: Pressure Drop versus Water Superficial Velocity $\mu_o = 3.3 \text{ Pa.s}$	173
Figure 7-12: Pressure Drop versus Water Superficial Velocity $\mu_o = 5.0 \text{ Pa.s}$	174
Figure 7-13: Pressure Drop versus Water Superficial Velocity $\mu_o = 5.0 \text{ Pa.s}$	174

## LIST OF TABLES

Table 1-1: Oil classification based on API gravity, viscosity and mobility .....	3
Table 2-1: Beggs and Brill (1973) flow pattern transition .....	11
Table 3-1 specification for 1-inch facility .....	55
Table 3-2: The specification for 3-inch facility .....	65
Table 3-3: Summary of test fluid properties .....	75
Table 3-4 Uncertainty of measurement.....	79
Table 4-1: Air-Water Test Matrix.....	82
Table 4-2: Pictorial representation of observed flow patterns .....	84
Table 4-3: PMF plots of Air-Water experiment .....	87
Table 4-4 Evaluation of Liquid Holdup correlations using Statistics.....	92
Table 4-5: Performance evaluation of prediction models for present data.....	94
Table 4-6: Evaluation of slug length prediction against present data.....	96
Table 5-1 Representative video images and flow condition.....	99
Table 5-2: Statistical evaluation of prediction models with respect to experimental liquid holdup values.....	111
Table 6-1 Performance evaluation of proposed model against existing prediction models (Present data).....	145
Table 6-2 Performance evaluation of proposed model against existing prediction models (Gokcal, '08 data) .....	145
Table 6-3 Statistical evaluation of slug length predictive models.....	150
Table 6-4 Proposed and existing correlation comparison .....	155
Table 6-5: Statistical performance evaluation of proposed correlation in comparison to models in the literature .....	162
Table 7-1: Flow Patterns in High Viscosity Oil-Water Two-Phase Flow .....	164



## NOMENCLATURE

<b>Symbols</b>	<b>Denotes</b>	<b>Units</b>
$A$	Area	$m^2$
$C$	Constants	
$C_w$	Water cut	
$D$	Pipe diameter	$m$
$E$	Volume fraction	
$E_o$	EÖtvös number	
$FE$	liquid entrainment fraction	
$Fr$	Froude number	
$f_s$	Frequency	$s^{-1}$
$g$	Acceleration due to gravity	$m \cdot s^{-2}$
$G$	Mass flow rate	$kg/s$
$G_k$	Turbulence kinetic energy	$J/kg$
$h$	Liquid height	$m$
$I$	Turbulent intensity	
$k$	Wave numbers or curvature	$m^{-1}$ or $m$
$L$	length	$m$
$M$	Momentum exchanges	$Kg \ m/s$
$N_{lu}$	Liquid velocity number	
$N_{\square}$	Viscous number	
$P$	Pressure	$kPa$
$Re$	Reynolds number	
$R_H$	Slip ratio	
$R_P$	Pressure drop reduction factor	
$S$	Perimeter or slip ratio	$m$
$s$	sheltering coefficient	
$U$	Velocity	$m/s$
$X$	Lockhart Martinelli parameter	
$Y$	Lockhart Martinelli parameter	
$y$	Length for first cell close to the wall	$m$
$z$	Axial direction	

**Greek letter**

$\mu$	Viscosity	<i>cP</i>
$\rho$	Density	<i>kg/m<sup>3</sup></i>
$\tau$	Shear stress	<i>Pa</i>
$\gamma$	Shear rate	<i>s<sup>-1</sup></i>
$\Gamma$	Effective diffusivity	<i>m<sup>2</sup>/s</i>
$\alpha$	Input liquid volume fraction	
$\delta$	Film thickness	<i>m</i>
$\varepsilon$	Relative error	
$\lambda$	Liquid content	
$\theta$	Pipe inclination angle	<i>°</i>
$\sigma$	Surface tension	<i>N/m</i>
$\nu$	Kinetic viscosity	<i>Pa s</i>
$\omega$	Turbulence dissipation rate	<i>J/(kg·s)</i>

**Subscripts**

<i>c</i>	Gas core
<i>f</i>	Film zone
<i>g</i>	Gas phase
<i>i</i>	interface
<i>l</i>	Liquid phase
<i>m</i>	Mixture phase
<i>ns</i>	No slip
<i>o</i>	Oil phase
<i>s</i>	Superficial or slug body
<i>t</i>	Translational
<i>tp</i>	Two phase
<i>u</i>	Slug unit
<i>wg</i>	Wall and gas
<i>wl</i>	Wall and liquid

## LIST OF ABBREVIATIONS

<i>BP</i>	British Petroleum
<i>PSE</i>	Process Systems Engineering
<i>SG</i>	Specific gravity
<i>PMF</i>	Probability Mass Function
<i>K-H</i>	Kelvin-Helmholtz
<i>API</i>	American Petroleum Institute gravity
<i>PCP</i>	Progressive Cavity Pump
<i>VOF</i>	Volume of Fraction
<i>WAF</i>	Water Assisted Flow
<i>CAF</i>	Core-Annular Flow
<i>GVF</i>	Gas Volume Fraction



# 1 INTRODUCTION

## 1.1 Background

As a result of the increasing world oil demand in the face of limited supplies, the exploration of non-conventional oil sources (i.e. heavy oil) is increasingly gaining attention so as to relieve the pressure exerted on conventional stocks. Latest findings from the “*British Petroleum (BP) Statistical Review of World Energy 2015*” reports shows that global primary energy consumption increased by 0.9% with oil been the world leading fuel accounting for 32.6% of global energy consumption. The aforementioned trend among other factors have resulted to exhaustion of conventional oil reserves to assuage demand.

However, the high viscosity and density of heavy oils poses challenge during extraction, processing and transportation. Several technologies are already at work with differing levels of success, recovery ranging from as low as 5% to more than 70% (Shah et al., 2010).

The existing technologies for the extraction, processing and transportation adopted for heavy oil is costly due to their natural composition (i.e. viscosity) thereby making their production expensive, difficult to transport and refine. This whole process is quite expensive when compared to conventional crude oil. However, with improvement in technology, this once costly energy source is quickly becoming a more viable alternative. Hence, there is the need to carry out further investigation so as to enhance its further production at reduced cost.

To date, not only has there been limitation in the existing empirical correlations and mechanistic models of low viscosity oil to precisely predict characteristics of flow such as flow regime, pressure gradient and liquid hold up for heavy oils transport in pipelines but also limited experimental data for very high viscous oil hence the need for further investigation is imperative.

## 1.2 Overview of Heavy Oil

Heavy oils are commonly referred to as unconventional oil due to their nature and composition (i.e. high viscosity and asphaltic content) with high density and a low

API gravity. There are basically three forms of unconventional oil, namely heavy oil, extra heavy oil and bitumen accounting for about 2/3 of the world's total oil reserve of 9-15 trillion barrels (Zhang et al., 2012) as indicated in Figure 1-1. Geologically, unconventional oil are thought to be expelled from source rocks as light or medium oil and later converted to heavier components by bacterial degradation in subsurface reservoirs (Zhang et al., 2012).

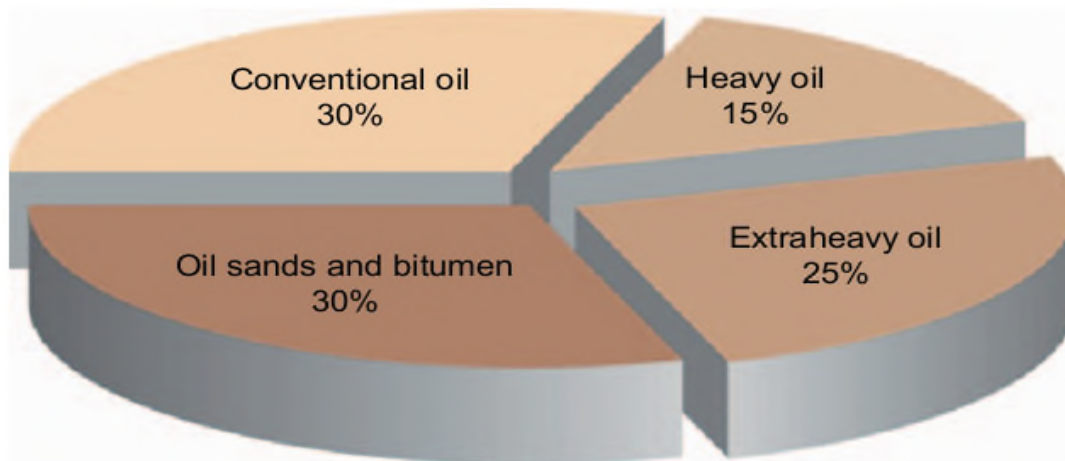


Figure 1-1: Heavy oil vs. conventional oil reserve (Falcone et al., 2009).

Heavy oil are characterised by their high viscosity ( $>0.1$  Pa.s) and low API gravity ( $<22^\circ$  API), consisting of asphaltenes (which contains large molecular compounds with 90% sulphur & metal constituents) with the presence of impure substances such as waxes and carbon residue (Richard and Emil, 2003).

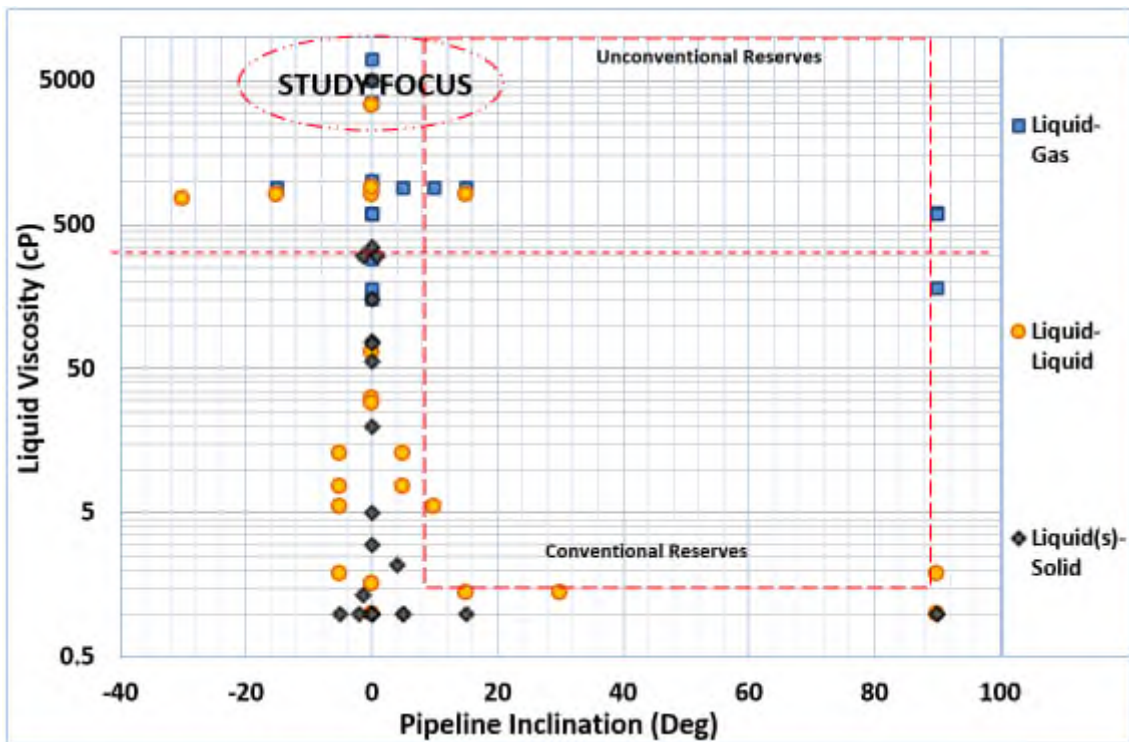
Heavy oil and tar sands occur in many countries representing at least more than half of the recoverable oil resources of the world. Recent studies estimate that unconventional oil reserves, including heavy oils, extra-heavy oils and bitumen exceed 6 trillion barrels. This amount is equivalent to about 70% of all energy resources derived from fossil fuels in the world (Oilfield Review Summer, 2006). Table 1.1 describes oil classification based on API gravity, viscosity and mobility.

Table 1-1: Oil classification based on API gravity, viscosity and mobility

<b>Oil type</b>	<b>API° Gravity</b>	<b>Viscosity (cP)</b>	<b>Mobility</b>
Light oil	>22.7	1-100	Mobile
Heavy oil	15-22.7	100-1000	Mobile
Extra heavy oil	10-15	1000-10000	Slightly mobile
Tar sand/Bitumen	7-12	>10000	Immobile

### **1.3 Motivation**

Investigation has shown that most published works reported in the literature for multiphase flow in pipelines were carried out based on observations from low viscous liquids with viscosities of less than 1.0 Pa.s. Very few of these studies focus on high viscosity liquids as illustrated in Figure 1-2. The figure clearly reflects the knowledge gap that needs to be filled vis-à-vis heavy oil multiphase flow, thus emphasizing the need to improve understanding of the flow dynamics. This is more so since heavy oils have been identified as a veritable energy source to augment the fast depleting reserves of conventional oil. Furthermore, since heavy oils are more difficult and expensive to produce and transport in pipelines at ambient operating conditions, a critical understanding of their flow characteristics is vital for engineering design. It has therefore become imperative to investigate high viscous oils and find out ways of enhancing its production and transportation. For example, widely used mechanistic models developed by investigators such as Beggs and Brill, (1973); Taitel and Dukler, (1976); Xiao et al. (1990); Zhang et al. (2003a, 2003b) still rely on closure relationships developed using data obtained from low viscous liquids such as water and light oils. The current investigation therefore aims to develop a new empirical correlations for slug flow characteristics for multiphase flow with viscosities >1.0 Pa.s. Not only will the current data bank on high viscous oil-gas two-phase flow be extended, the developed correlation will provides improved the estimation of fundamental slug flow characteristics. This will in turn provide better predictions of pressure gradient useful for the design and operation of pipeline systems in the oil and gas industry.



**Figure 1-2: An illustration of knowledge gap existing in the literature and the present study focus.**

#### 1.4 Research Aim and Objectives

This research work is aimed at improving the understanding of the hydrodynamics and the effects of high viscosity liquids on flow characteristics of multiphase flows in horizontal pipelines.

The following objectives were required(?) towards achieving this aim.

1. To carryout experimental investigation on high viscous oil-gas and viscous oil-water flows in horizontal pipelines.
2. To study the effects of liquid viscosity on two phase flow characteristics i.e. pressure gradient, liquid holdup.
3. Performance evaluation of the existing gas-liquid prediction models and correlations against experimental data.



4. Modification of existing prediction models to account for the effects of viscosity on gas-liquid two phase flow based on the new data and others from the literature.

## **1.5 Thesis Outline**

This thesis report is divided into chapters with each highlighting the contents as presented below

Chapter 2 presents the fundamentals of multiphase flow, review of previous work on gas-liquid flow systems on low and high viscous multiphase flow in pipelines and the measurement techniques.

A detailed description of the test facility used for this experimental study is presented in chapter 3 with notes on instrumentation calibration, physical properties of test fluids, test matrix and methodology adopted for this study.

Experimental results for air-water two phase flow characteristics; flow patterns, pressure gradient, liquid holdup, slug frequency, slug translational velocity and slug body length are reported in chapter 4. Results of the comparison between experimental results and predictive model are also presented.

Chapter 5 focuses on high viscosity oil-gas flows. Results on pressure gradient, flow pattern, liquid holdup, slug frequency, slug translational velocity and body length are reported. comparison between experimental results and prediction models

Chapter 6 reports the modification and development of new prediction correlations for high viscosity two phase flow. It also reports performance of the new correlation against those found in the literature for high viscosity oil data.

Experimental results in viscous oil-water two-phase flow are reported in chapter 7. Results include flow pattern visualization, water cut, oil holdup and pressure gradient measurements. Discussions of these results are also presented.

While chapter 8 summarises the findings of this study with recommendation notes for future study.



## 2 LITERATURE REVIEW

In this chapter, the fundamentals of multiphase flows in addition to existing literature on two phase oil-air, oil-water flows is reviewed in the context of the present study. This is to carry out an in-depth literature survey of the previous studies on multiphase flow and subsequently establish the need for further studies by showing the existing gap. Strong emphasis has been laid on models/correlations as their predictive performance has been evaluated using present experimental dataset.

### 2.1 Multiphase Flow

Multiphase flow may be defined as a concurrent flow of materials in the same phase for instance liquid-liquid or different phases; gas-liquid-solid with different chemical properties. It may also be in the same phase but immiscible (i.e. liquid-liquid). Fluidised beds, slug catchers, risers, slurry pipelines, nuclear reactors and bubble columns reactors are some of the industrial application of multiphase flow which makes it important. Also the transportation of reservoir fluids which may consist of crude oil, water, sand and gas through well tubing to the risers and pre-production and production facilities are typical examples of multiphase flow in the petroleum industry.

### 2.2 Basic Definition

The most relevant terminologies associated with multiphase flows are presented in the flowing subsections in order to facilitate a good understanding of this write-up.

#### 2.2.1 Superficial phase velocity

This is described as the velocity of one phase of a multiphase flow assuming that it is the only phase occupying the whole pipeline itself. It can also be defined as the ratio of phase volume flow rate to pipe cross-sectional area. Mathematically it can be defined for each phase as follow

$$V_{SL} = \frac{Q_L}{A} \quad (2-1)$$

$$V_{SG} = \frac{Q_G}{A} \quad (2-2)$$

Where  $A$  is the total cross-sectional area of the pipe while  $V_{SL}$  and  $V_{SG}$  are the gas and liquid superficial velocity term. The mixture velocity  $V_M$  is given by

$$V_m = V_{SL} + V_{SG} \quad (2-3)$$

### 2.2.2 Slip:

Slip is a term which describes the condition of flow that exists when the phases in the cross-section of a pipe have different velocities. Or simply put as the phase velocity difference between phases in a cross section.

### 2.2.3 Slip velocity

This is the instantaneous difference in the superficial velocities between two or more different fluids flowing together in a pipe. It is given by the relationship:

$$V_{slip} = V_{SG} - V_{SL} \quad (2-4)$$

### 2.2.4 Slip ratio

Slip ratio which is also referred to as velocity ratio is defined as the ratio of the gas phase velocity relative to the liquid phase velocity. It is assumed to be unity (i.e. no slip) for homogeneous two-phase flow.

$$S = \frac{V_G}{V_L} \quad (2-5)$$

Where  $V_G$  and  $V_L$  are the respective phase superficial velocities.

### 2.2.5 Water Cut (WC)

This is the volume flow rate of water, relative to the total volume flow rate of liquid (oil and water) and normally expressed as a percentage.

$$W_c = \frac{Q_w}{Q_w + Q_o} \quad (2-6)$$

### 2.2.6 Mixture Density

The mixture density of homogeneous flows can be expressed as

$$\rho_m = \rho_L H_L + \rho_G (1 - H_L) \quad (2-7)$$

Where  $\rho_L$  and  $\rho_G$  are the liquid and gas densities respectively.

### 2.2.7 Viscosity Mixture

For homogeneous gas-liquid mixture, the viscosity mixture  $\mu_m$  is given by:

$$\mu_m = \mu_L H_L + \mu_G (1 - H_L) \quad (2-8)$$

Where  $\mu_G$  and  $\mu_L$  are the liquid and gas viscosity respectively.

### 2.2.8 Volume Fraction

Volume fraction can either be gas volume fraction or liquid volume fraction which is the ratio of a particular phase volumetric flow rate to the total volumetric flow rate.

### 2.2.9 Void Fraction and Liquid Hold up

Void fraction and liquid holdup are parameters of utmost significance in the characterization of two-phase flows and key factors critical for the determination of numerous other important parameters (Thome, 2004). Void fraction ( $\alpha_G$ ) is defined as the gas phase volume occupying a given two phase flow in a pipe relative to that of the total two-phase mixture. The void fraction is given by;

$$\alpha_G = \frac{A_G}{A_G + A_L} \quad (2-9)$$

Liquid hold up ( $H_L$ ) been the complement of void fraction is the cross sectional area of a pipe is defined as the instantaneous fraction of an element of pipe which is occupied by liquid given by

$$H_L = 1 - \alpha_G = \frac{A_L}{A_G + A_L} \quad (2-10)$$

## 2.3 Gas-Liquid Two Phase Flow

One of the most common multiphase flows encountered in the industry is the gas-liquid two phase flow. Therefore, understanding its flow characteristics is important in many industrial processes such as separators, risers, slug catchers, nuclear reactors,

oil-gas pipelines etc. Detail literature review of the experimental and modelling studies is presented below.

### 2.3.1 Gas-Liquid Flow patterns

Flow Patterns are the description of geometric distribution of the relative positions, shape and size of different phases in multiphase flow. In oil and gas flows, the interfacial deformation and the compressibility of the gas phase leads to the complex nature of of gas-liquid flows relative to other possible two-phase combinations such as oil-water (Hewitt, 1982) . The key influencers of flow patterns are the superficial velocities of the phases, pipeline geometry/orientation and physical properties of the phases. Differing terminologies in the definition of flow patterns is due to its subjectivity, nevertheless, gas-liquid flow in horizontal and slightly inclined pipelines are classified mainly into four types namely; annular (A), stratified (S), dispersed bubble (D) and intermittent (I) flows. The flow patterns with corresponding subsets are illustrated in Figure 2-1 below.

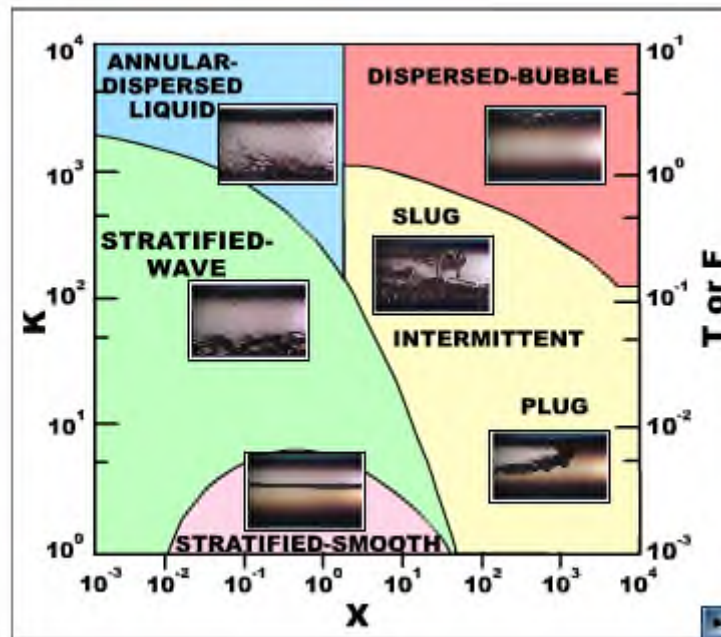


Figure 2-1: Flow patterns of gas-liquid flow in horizontal pipes (Taitel and Dukler, 1976).

- **Stratified Flow:** This flow pattern involves the movement of phases along the pipeline in completely separated sections mainly due to density differences and gravity, it is also called segregated flow. In stratified flow in gas-liquid systems, the less dense gas phase traditionally flows on top of the liquid which flows

along the bottom of the pipeline. Stratified wavy, smooth and rolling wave flows are the classification of stratified flow which differ in their function of the interfacial hydrodynamics of the oil-gas interface.

- **Intermittent Flow:** This flow pattern consists of two characteristic units; the elongated liquid body and the film region. This flow pattern is characterised by the film region similar to the stratified flow separated intermittently by elongated liquid body flowing through the pipe. Slug, Elongated Bubble (Plug) and Froth flows are the sub-divisions of intermittent flow. The entrained gas bubbles in the elongated liquid body is visible for the slug flow pattern while plug flow is the limiting case of slug flow with the entrained gas bubbles not visible. Froth flow occurs when the elongated liquid body becomes fragments in the film region at very high gas flowrates.
- **Bubble Flow:** This is characterised by the distribution of gas phase in the liquid phase as spherical or near-spherical bubbles dispersed within the liquid phase both of which have very similar velocities. The spherical bubbles are driven towards the top section of the pipe by buoyancy forces. Bubble flow occurs at very high gas and liquid flowrates.
- **Annular Flow:** Annular flow pattern occurs when the gas that flows at the core of the pipe is enveloped by an annulus around the periphery of the pipe in the liquid phase flow. It is possible to observe some entrainments of gas in the liquid annulus and vice versa

### 2.3.2 Flow Pattern Maps

. Flow pattern maps are maps that shows the different patterns at a certain flow conditions in multiphase flow. They can be plotted in a variety of ways, mostly with superficial gas and liquid velocities plotted on 2-dimensional Cartesian plane. Others are plotted using Froude number as a function of liquid content. Several researchers have carried out works in the area of gas-liquid flow in pipelines resulting to the development of a number flow regime maps. some of these works are presented below..

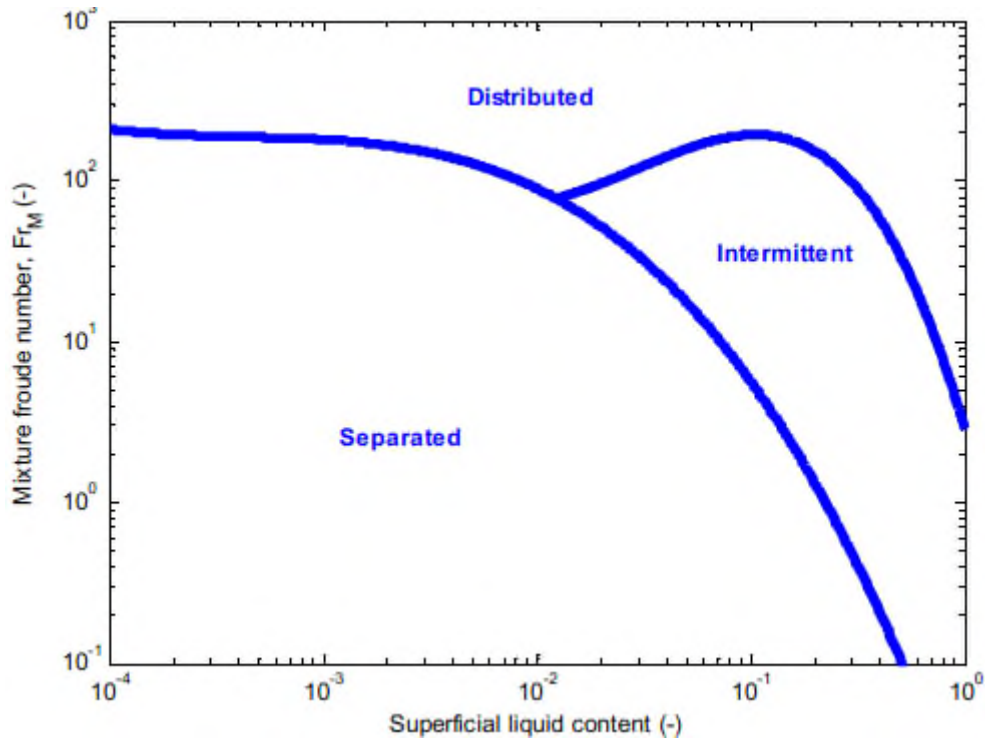
Beggs & Brill,(1973) grouped flow pattern based on three main types, namely; separated, intermittent and distributed. While stratified, stratified wavy and annular flow as separated flow; plug, slug and bubbly flows are classified as intermittent flow



and distributed flow respectively. The Froude number and the input liquid content respectively represent the abscissa and ordinate of their maps. Their flow pattern map was constructed based on experimental data obtained in a flow loop constructed with transparent acrylic pipe 90 ft long with gas flow rates ranging from 0 - 300 Mscf/D; liquid flow rates, 0 - 30 gal/min with average system pressure of 35 - 95 psia at different inclination angles from  $-90^{\circ}$  to  $+90^{\circ}$ . As can be seen on Table 2-1 below,  $L1, L2, L3$  and  $L4$  are the flow transition parameters while  $\varepsilon_L$  and  $\varepsilon_{L0}$  are the no slip liquid holdup. Also represented on table is the flow pattern prediction lines given as  $Fr_m, V_m, V_{SL}$  representing mixture Froude number, the mixture velocity and the liquid superficial velocity. Figure 2-2 below presents the flow pattern map constructed by (Pan, 2010) which is a typical of (Beggs and Brill, 1973).

**Table 2-1: Beggs and Brill (1973) flow pattern transition**

Flow Transition Criteria	Flow Pattern	Parameter Definition
$\varepsilon_L < 0.01 \ \& \ Fr_m < L1$ or $\varepsilon_L \geq 0.01 \ \& \ Fr_m < L2$	Separated	$Fr_m = \frac{V_m^2}{gD}$
$0.01 < \varepsilon_L < 0.4 \ \& \ L3 < Fr_m < L1$ or $\varepsilon_L \geq 0.4 \ \& \ L3 < Fr_m \leq L4$	Intermittent	$\varepsilon_L = \frac{V_{SL}}{V_m}$  $L1 = 316\varepsilon_L^{0.302}$
$\varepsilon_L < 0.4 \ \& \ Fr_m \geq L1$ or $\varepsilon_L \geq 0.4 \ \& \ Fr_m > L4$	Distributed	$L2 = 0.0009252\varepsilon_L^{-2.46}$
$\varepsilon_L \geq 0.01 \ \& \ L2 < Fr_m < L3$	Transition	$L3 = 0.1\varepsilon_L^{-1.4516}$  $L4 = 0.5\varepsilon_L^{-1.4516}$



**Figure 2-2: Beggs and Brill (1973) flow pattern map for horizontal pipeline**

Generally, the boundaries existing between the various flow patterns in a flow pattern map occur because of instability of the regime as the boundary is approached thereby resulting to transition to another flow pattern (Brennen, 2005). The slight difference in the developed flow pattern maps available in the literature is an indication of different experimental setups and the parameters used by different researchers in experiments.

### **2.3.3 Effects of Viscosity on Flow Patterns**

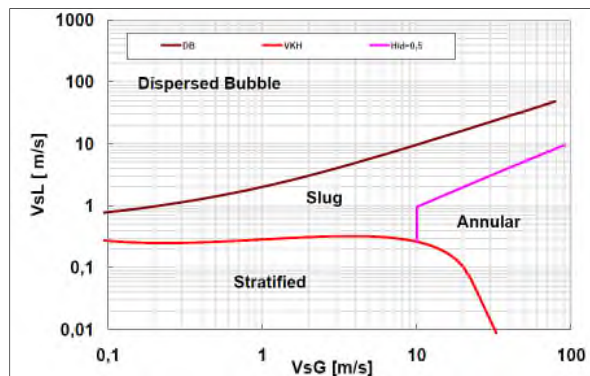
Viscosity is an important physical property that affects flow patterns; therefore it is crucial to study its effect on oil-gas two phase flow. Presented below are reviews of some studies on the effect of liquid viscosity on two phase flow.

Weisman et al (1979) conducted experiments in a 0.012, 0.025 and 0.051 m ID with pipe length of 6.1 m to study the effects of liquid viscosity on flow pattern transition boundaries. They used glycerol-water solutions and Air with viscosity of 0.15 and 0.075 Pa.s respectively as the test fluids. Surface active agent was used to decrease the surface tension from 0.068 to 0.038 N/m. They concluded that both surface tension and liquid viscosity had little effect on the flow pattern transition boundary within the range of experimental test condition. This is in contrast to the finding of this

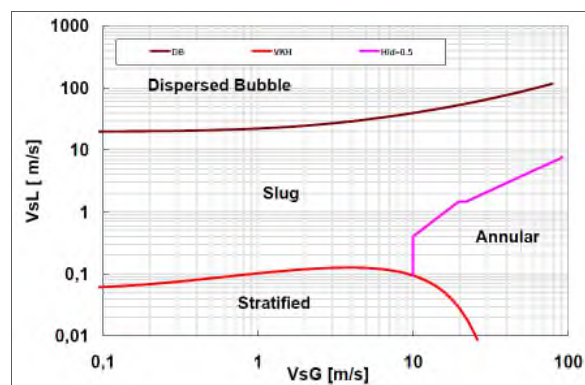
experimental investigation however their conclusion may be due to the fact that the viscosity difference was not large enough.

The effect of liquid viscosity was studied by (Gokcal et al., 2006) using a liquid viscosity ranging from 0.18 – 0.59 Pa.s with air as the gas phase. It was carried out on an 18.9 m long test section and 0.0508 m internal diameter pipe. In comparison with the results of (Zhang et al., 2003) and (Barnea, 1991) for low viscosity studies, their conclusion was that that the flow transition boundaries increasingly varied with the low viscosity transition boundaries as viscosity increased. They also noted that intermittent flow pattern was enhanced as liquid viscosity increases.

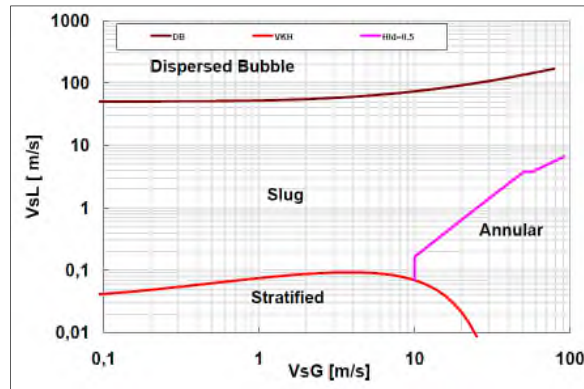
Márquez and Trujillo (2010) in their study considered three liquid viscosities; 0.181, 0.392 and 1.0 Pa.s to investigate the effect of liquid viscosity on flow pattern transition boundaries. They analysed the (Taitel and Dukler, 1976) flow pattern maps mathematically and concluded that increase in liquid viscosity led to increased slug flow pattern. The flow pattern maps obtained in the study is shown in Figure 2-3 below.



a.) Oil viscosity,  $\mu_o = 0.181$  Pa.s



b.) Oil viscosity,  $\mu_o = 0.392$  Pa.s



c.) Oil viscosity,  $\mu_o = 1.0 \text{ Pa}\cdot\text{s}$

**Figure 2-3: Marquez & Trujillo (2010) gas-liquid flow pattern maps in horizontal pipe.**

Foletti et al (2011) experimentally studied two-phase oil-gas flow in a horizontal pipeline of 0.022 m ID. A liquid phase of oil viscosity 0.896 Pa.s and surface tension 0.03 N/m was used while air as the gas phase. The observed flow patterns in their study were compared with the flow pattern maps of (Baker, 1954) and (Mandhane et al., 1974) resulting to large discrepancies. The dominant flow pattern for their investigation was the intermittent flow which they attributed to viscosity effect.

Zhao et al (2013) also investigated the effects of viscosity on flow patterns characteristics for high viscosity oil-gas two phase flow in an experiment conducted in a 0.0254 m Pipe ID facility of length of 5.5 m using oil with nominal viscosities ranging from 1.0 – 7.0 Pa.s. It was observed that intermittent flow pattern was under predicted when their flow patterns were compared with the (Beggs and Brill, 1973) flow pattern map. They also noted that the discrepancies increased as the viscosity of oil increases. The authors did not consider the effects of liquid viscosities on slug flow parameters like slug translational velocity and slug body length. The present study aims towards filling this research gap and hence contributing to knowledge.

Brito et al (2013) carried out an experimental study which focused on the effect of medium viscosity oil on two phase oil-gas flow behaviour in horizontal pipes. The study was conducted in 0.0508 m-ID horizontal test pipe for oil viscosities ranging 0.039-0.166 Pa.s. They noted that the stratified smooth region shrinks as oil viscosity increases. Also, larger bubble concentration were associated with dispersed bubble and are at the top of the pipe as compared with low viscosity case.

Khaledi et al (2014) used oil with viscosities of 0.032 and 0.1 Pa.s and sulphur hexafluoride gas (SF<sub>6</sub>) as test fluids in a 0.069 m pipe ID to investigate oil-gas flow characteristics in horizontal pipe. Their results were compared with a slug fraction calculation which was based on pre-defined sets of rules, they stated that the model gave a better prediction at lower viscosity but observed that discrepancies increased with increasing liquid viscosity.

In general, the studies of high viscosity oil-gas two phase flow are very few in the literature, most of the available studies have noted that the existing maps considerably differ from experimental observations involving high viscosity liquid -gas. This implied the need for further studies in order to arrive at possible improvements on the existing flow transition correlations and flow patterns prediction.

### **2.3.4 Oil-Gas Two-Phase Flow Modelling Studies**

Over the last half-century, several theoretical and experimental studies have been carried out on low viscous liquid-gas flows in pipelines. The predictive models from these studies seemed to be less reliable and inaccurate especially when evaluated against dataset that are significantly different from those from which they were developed from. The error margin in their prediction could be as a result of the complexities associated with single phase flow such as non-linearity, instabilities and transition from laminar to turbulence. Others are two-phase flow characteristics such as motion and interfacial deformation, non-equilibrium effects and interactions between phases. These models are generally developed using one of the following techniques; Theoretical, Empirical and Phenomenological which are mostly used for the prediction of important two-phase flow parameter.

#### **2.3.4.1 Empirical Correlations**

The relative simplicity and accuracy in prediction of empirical correlations made it the most common models for two phase flow models especially when used within the range of experimental flow conditions from which it was developed. Production operators in the oil and gas industry can easily use it owing to its simplicity and less computational time. The performance of this model tends to be poor when tested against dataset from experimental flow conditions outside its scope of development and this is often considered as the paradox for this class of models. Summarily, it can be said that its greatest advantage is also its disadvantage. Some examples of

empirical correlations are those proposed by Lockhart-Martinelli, (1949); Chisholm, (1967) and Zhang, (2010)

### 2.3.4.2 Phenomenological Models

The models derived from the physical phenomenon observed during experiments are known as phenomenological models. They consist of some prior knowledge which may be implicit in some cases. (Beggs and Brill, 1973) model is an example of the phenomenological model widely used in the petroleum industry.

#### 2.3.4.2.1 Beggs and Brill (1973)

A phenomenological model for the prediction of pressure gradient for three different flow patterns was developed by (Beggs & Brill, 1973) as stated earlier in sub-section 2.3.2 for low viscosity two-phase flow. An energy balance was considered for the two fluids from one point to the other, and for a steady-state mechanical energy balance; the total pressure gradient was considered to be the summation of the static, acceleration, and frictional pressure losses, the relationship is given by:

$$-\frac{dP}{dx} = \left(\frac{\partial P}{\partial x}\right)_{ACN} + \left(\frac{\partial P}{\partial x}\right)_{ST} + \left(\frac{\partial P}{\partial x}\right)_F \quad (2-11)$$

The static or elevation pressure gradient is given by:

$$\left(\frac{\partial P}{\partial x}\right)_{ST} = \frac{g}{g_c} [\rho_L H_L + \rho_G (1 - H_L)] \sin \theta \quad (2-12)$$

Where  $\rho_L, \rho_G, g, g_c, H_L$  and  $\theta$  are the liquid density, gas density, gravitational acceleration, gravitational constant, liquid holdup and the angle of inclination of the flowing conduit from the horizontal.

The pressure gradient due to acceleration is given by:

$$\left(\frac{\partial P}{\partial x}\right)_{ACN} = -\frac{\rho_{TP} V_M V_{SG}}{144 g_c D} \quad (2-13)$$

Where  $\rho_{TP} V_M V_{SG}$  and  $g_c$  are the two-phase density, the mixture velocity, gas superficial velocity and the gravitational constant.

And the frictional pressure gradient (psi) was further evaluated as:

$$\left(\frac{\partial P}{\partial x}\right)_F = \frac{2f_{TP}V_m^2\rho_{ns}}{2g_cD} \quad (2-14)$$

Where  $f_{TP}$ ,  $V_m$ ,  $g_c$  and  $\rho_{ns}$  are respectively the two phase friction factor, the mixture velocity, the gravitational constant and the no-slip density.

### 2.3.4.3 Theoretical Models

Theoretical models are relatively complex than the empirical models and are developed on the basis of the physics of the flow. An optimum solution of a theoretical model often requires series of iterative computations. It is worth noting that theoretical models also contain some form of phenomenological theories and their evaluation often require closure relationship. The models by Taitel and Dukler, (1976); Xiao et al (1990); Zhang et al (2003a, 2003b); Zhao, (2014) are some of the common theoretical models widely used. A detailed review of Xiao et al (1990) is presented below.

To solve the Taitel and Dukler (1976) model, iteration procedures are required, in addition; evaluation of the model against high viscosity database has not been conducted.

#### 2.3.4.3.1 Xiao et al. (1990)

A comprehensive mechanistic model for two-phase gas-liquid flow for the prediction of pressure gradient was developed by (Xiao et al., 1990) in the stratified, annular and intermittent flow patterns.

(Xiao et al., 1990) adopted the one-dimensional steady state two-fluid model technique for the stratified flow, while the changes in the liquid height was neglected; the momentum equation for the two fluids was stated thus:

$$-A_L \left(\frac{dP}{dx}\right) + \tau_i s_i - \tau_{wL} s_L - A_L \rho_L g \sin \alpha = 0 \quad (2-15)$$

$$-A_g \left(\frac{dP}{dx}\right) + \tau_i s_i - \tau_{wg} s_g - A_g \rho_g g \sin \alpha = 0 \quad (2-16)$$

Based on the assumptions that surface tension and hydrostatic pressure gradient are negligible, equal pressure gradient for both phases were considered. By combining equations (2-15) and (2-16), the combined momentum equation obtained is:

$$\tau_{wL} \frac{s_L}{A_L} - \tau_{wg} \left[ \left( \frac{s_g}{A_g} \right) + \frac{\tau_i}{\tau_{wg}} \left( \frac{s_i}{A_L} + \frac{s_g}{A_g} \right) \right] + (\rho_L - \rho_g)g \sin \alpha = 0 \quad (2-17)$$

By rearranging Equation (2-15), the following was obtained:

$$\tau_i = \frac{A_L}{s_i} \left( \frac{dP}{dx} \right) + \tau_{wL} \frac{s_L}{s_i} + \frac{A_L}{s_i} \rho_L g \sin \alpha \quad (2-18)$$

The pressure gradient can then be computed by Substituting Equation (2-18) in (2-16) thus;

$$-\left( \frac{dP}{dx} \right) = \frac{\tau_{wL}s_L - \tau_{wg}s_g}{A} + \left( \frac{A_L}{A} \rho_L + \frac{A_g}{A} \rho_g \right) g \sin \alpha \quad (2-19)$$

The interfacial, liquid wall and gas wall shear stress are given by:

$$\tau_{wL} = f_L \frac{\rho_L V_L^2}{2} \quad \tau_{wg} = f_G \frac{\rho_G V_G^2}{2} \quad \tau_i = f_i \frac{\rho_G V_G^2}{2} \quad (2-20)$$

Equation (2-20) is similar to **Error! Reference source not found.** with the exception being  $\tau_i$  dependence on  $V_G$  and not  $(V_G - V_i)$ .

$f_L$  and  $f_g$  are obtained as follows:

$$f = \begin{cases} \frac{16}{Re} & Re \leq 2000 \\ \left[ 3.48 - 4 \log \left( \frac{2\varepsilon}{D} + \frac{9.35}{Re\sqrt{f}} \right) \right]^{-2} & Re > 2000 \end{cases} \quad (2-21)$$

$\varepsilon$  is defined as the pipe wall roughness, while the gas and liquid Reynolds number are defined as;

$$Re_L = \frac{\rho_L V_L D_L}{\mu_L} ; \quad Re_G = \frac{\rho_g V_g D_G}{\mu_G} \quad (2-22)$$

$D_L$  and  $D_G$  are further defined as:

$$D_L = \frac{4A_L}{s_L} ; \quad D_G = \frac{4A_G}{s_G + s_i} \quad (2-23)$$

$s_L$ ,  $s_G$  and  $s_i$  are the wetted periphery of the liquid, gas and liquid-gas interface respectively. (Xiao et al., 1990) used interfacial friction factor  $f_i = 0.0142$ .



**Intermittent Flow:** Xiao et al (1990) considered the mechanism of flow essentially being a slow moving stratified liquid-layer in intermittent flow, flowing along the pipe's bottom with gas at the top and a fast moving liquid body overriding it. The liquid was considered to be aerated by gas bubbles at the slug front and the top of the pipe. The model was developed on a basis of a uniform liquid level stratified gas-liquid film region. Fluids in flow were considered the to be;

$$V_{SL}L_u = V_L E_S L_S + V_f E_f L_f \quad (2-24)$$

$E_S$  and  $E_f$  are the liquid body and stratified film region liquid holdup respectively. Applying a mass balance to the two cross-sections with respect to a coordinate system moving at the same velocity with the translational velocity, they proposed the following for the liquid phase:

$$(V_T - V_L)E_S = (V_T - V_f)E_f \quad (2-25)$$

In a slug unit, the sum of the volumetric flow rate is constant at a given cross sections, thus:

$$V_S = V_{SL} + V_{SG} = V_L E_S + V_b(1 - E_S) \quad (2-26)$$

$$V_S = V_f E_f + V_G(1 - E_f) \quad (2-27)$$

The average liquid holdup in the slug unit can thus be obtained by:

$$E_L = \frac{E_S L_S + E_f L_f}{L_u} = \frac{V_T E_S + V_b(1 - E_S) - V_{SG}}{V_T} \quad (2-28)$$

Recalling that a uniform liquid height in the film zone,  $E_f$  was assumed, an equation similar to that of the stratified flow is given as;

$$\tau_f \frac{S_f}{A_f} - \tau_g \left[ \left( \frac{S_g}{A_g} \right) + \frac{\tau_i}{\tau_g} \left( \frac{S_i}{A_f} + \frac{S_i}{A_g} \right) \right] + (\rho_L - \rho_g)g \sin \alpha = 0 \quad (2-29)$$

The average pressure gradient for intermittent flow computed based on the force balance over a slug unit is given by:

$$-\left( \frac{dP}{dx} \right) = \frac{1}{L_u} \left[ \left( \frac{\tau_s \pi D}{A} L_S \right) + \left( \frac{\tau_s S_f + \tau_g S_g}{A} L_f \right) \right] + \rho_u g \sin \alpha \quad (2-30)$$

Where  $\rho_u$  and  $L_u$  are the average fluid density of the slug unit and the slug unit length respectively. They are given as:

$$\rho_u = E_L \rho_L + (1 - E_L) \rho_g \quad (2-31)$$

$$L_u = L_S \frac{V_L E_S + V_f E_f}{V_{SL} - V_f E_f} \quad (2-32)$$

The shear stresses are given by:

$$\tau_f = f_f \frac{\rho_L |V_f| V_f}{2} \quad \tau_G = f_G \frac{\rho_G |V_G| V_G}{2} \quad \tau_i = f_i \frac{\rho_G |V_G - V_f| (V_G - V_f)}{2} \quad (2-33)$$

Equation (2-21) is used to evaluate gas,  $f_G$  and liquid,  $f_f$  interfacial friction factors using  $Re_f = \rho_L V_f D_L / \mu_L$  and  $Re_G = \rho_G V_G D_G / \mu_G$ .  $f_i = 0.0142$ .

Slug body shear stress is given as:

$$\tau_f = f_S \frac{\rho_S V_S^2}{2} \quad (2-34)$$

$f_S$  is obtained from Equation (2-21) with  $Re_S = \rho_S V_S D_S / \mu_S$ .  $\rho_S$  and  $\mu_S$  are the slug mixture density and viscosity. They are given by:

$$\rho_S = E_S \rho_L + (1 - E_S) \rho_g \quad (2-35)$$

$$\mu_S = E_S \mu_L + (1 - E_S) \mu_g \quad (2-36)$$

The relationships used to close out the model will be discussed subsequently in the later sections.

**Annular flow:** The two-fluid model approach was used by (Xiao et al., 1990) to model a fully developed steady state annular flow in pipelines. The following assumptions were made; an assumed film thickness value, the droplets and gas phase travel at the same velocity in the gas core therefore making it similar to homogenous flow. The difference in the analysis of the annular and stratified flow is in geometrical relationships of the flow, otherwise they are similar.

Momentum balance on both phases is given by:

$$-A_f \left( \frac{dP}{dx} \right) + \tau_i s_i - \tau_{wL} s_L - A_f \rho_L g \sin \alpha = 0 \quad (2-37)$$

$$-A_C \left( \frac{dP}{dx} \right) + \tau_i s_i - A_C \rho_C g \sin \alpha = 0 \quad (2-38)$$

$\rho_C$  Is the density of mixture in the gas core and is defined by:

$$\rho_C = E_C \rho_L + (1 - E_C) \rho_g \quad (2-39)$$

$E_C$  Is the liquid holdup in the gas core, it is related to liquid entrainment,  $FE$  thus:

$$E_C = \frac{V_{SL} FE}{V_{SG} + V_{SL} FE} \quad (2-40)$$

A combination of Equation (2-37) and (2-38) yields:

$$\tau_{wL} \frac{s_L}{A_F} - \tau_i s_i \left[ \left( \frac{s_g}{A_g} \right) + \frac{\tau_i}{\tau_{wg}} \left( \frac{1}{A_f} + \frac{1}{A_C} \right) \right] + (\rho_L - \rho_C) g \sin \alpha = 0 \quad (2-41)$$

The geometrical parameters are functions of the non-dimensional mean film thickness. Evaluation of the combined momentum equation allows for the computation of the liquid holdup which is defined as:

$$E_L = 1 - \left( 1 - 2 \frac{\delta}{D} \right)^2 \frac{V_{SG}}{V_{SG} + V_{SL} FE} \quad (2-42)$$

By evaluating (2-37) and (2-38), the pressure gradient is obtained by:

$$-\left( \frac{dP}{dx} \right) = \frac{\tau_{wL} s_L}{A} + \left( \frac{A_F}{A} \rho_L + \frac{A_C}{A} \rho_C \right) g \sin \alpha \quad (2-43)$$

Shear stresses are defined as:

$$\tau_{wL} = f_f \frac{\rho_L V_f^2}{2} \quad \tau_i = f_i \frac{\rho_C (V_C - V_f)^2}{2} \quad (2-44)$$

$f_f$  is evaluated from Equation (2-21) with  $Re_L = \rho_L V_f D_L / \mu_L$ . The hydraulic diameter,  $D_L = 4\delta(D - \delta)/D$

The liquid film velocity is given as:

$$V_f = \frac{V_{SL}(1 - FE)}{\left( 1 - 2 \frac{\delta}{D} \right)^2} \quad (2-45)$$

$FE$  and  $f_i$  are defined based on Oliemans *et al.* (1986) correlations given by:

$$\frac{FE}{1 - FE} = 10^{\beta_0} \rho_L^{\beta_1} \rho_G^{\beta_2} \mu_L^{\beta_3} \mu_G^{\beta_4} \sigma^{\beta_5} D^{\beta_6} V_{SL}^{\beta_7} V_{SG}^{\beta_8} g^{\beta_9} \quad (2-46)$$

$$f_i = f_c \left[ 1 + 2250 \frac{\frac{\delta}{D}}{\frac{\rho_c (V_c - V_f)^2 \delta}{\sigma}} \right] \quad (2-47)$$

$\beta$  Parameters are defined as the regression coefficients. Reynolds number in the gas core is defined as;

$$Re_c = \frac{\rho_c V_c D_c}{\mu_c} \quad (2-48)$$

Where:

$$\mu_c = E_c \mu_L + (1 - E_c) \mu_g \quad (2-49)$$

$$D_c = D - 2\delta \quad (2-50)$$

**Dispersed flow:** The least complex flow pattern to model is the dispersed flow pattern with an assumptions that the average properties obtained for a homogenous flow similar to single phase flow and no slippage between the gas and liquid phase. The no slip liquid holdup was obtained as;

$$E_L = \frac{V_{SL}}{V_M} \quad (2-51)$$

The pressure gradient is obtained from the Darcy-Weisbach equation by defining the average mixture density and velocity, thus:

$$-\left(\frac{dP}{dx}\right) = \frac{2f_M \rho_M V_M^2}{D} + \rho_M g \sin \alpha \quad (2-52)$$

The (Xiao et al., 1990) performed well when evaluated against a low viscosity dataset, however this model has not been used for high viscosity dataset.

### 2.3.5 Closure Relationships

Closure relationships are input parameters required by most of the phenomenological and analytical models in literatures for their estimation. An example of such models is the (Zhao, 2014) mechanistic model which requires the input of mean liquid holdup,

slug unit holdup, slug body length, slug body void fraction, film length, film height and interfacial friction as input parameters for its estimation. Some closure relationships which may be used subsequently in this work.

### 2.3.5.1 Slug Body Liquid Holdup

Experimental studies on liquid holdup in the slug body have been reported by many authors most of which focused on low viscosity oil-gas two-phase flow. The (Gregory et al., 1978) slug body liquid holdup prediction correlation is one of the earliest and widely used. This was obtained from experiments conducted in a gas-liquid two phase flow system. Air was used as the gas phase and light oil of viscosity 0.0067 Pa.s as the liquid phase. A test facility of pipes used for the study are of 0.0258 and 0.0512 m IDs. The correlation is given by:

$$H_s = \frac{1}{1 + \left(\frac{V_M}{8.66}\right)^{1.39}} \quad (2-53)$$

$V_M$  is defined as the mixture velocity ( $V_{SG} + V_{SL}$ ) in m/s. (Gregory et al., 1978) highlighted that the correlation was not reliable beyond 10 m/s mixture velocity. The fluid physical properties such as viscosity and surface tension were not accounted for, therefore it is dimensionally inconsistent. It was as well developed on the basis of low viscosity liquid-gas two-phase flow and was not validated against high viscosity data.

Malnes, (1983) included the fluid physical properties; surface tension and liquid density as an extension of the (Gregory et al., 1978) model, the predictive correlation is proposed as follows:

$$H_s = 1 - \frac{V_M}{\left[V_M + 83 \left(\frac{g\sigma_{GL}}{\rho_L}\right)^{1/4}\right]} \quad (2-54)$$

This model was also not validated against high viscosity data.

Gomez et al (2000) proposed the following correlation for liquid holdup in slug body by correlating numerous experimental data from a variety of pipe diameters and inclinations:

$$E_s = e^{-(0.45\theta + C Re)} \quad 0 < \theta \leq 90^\circ \quad (2-55)$$

Where  $\theta$  is the angle of inclination from the horizontal,  $C = 2.48 \times 10^{-6}$  and the Reynolds number,  $Re$  is defined as:  $Re = \frac{\rho_L V_M D}{\mu_L}$

Zhang et al (2003c) developed an analytical model for the prediction of slug body liquid holdup based on a balance between the turbulent kinetic energy of the liquid phase and the surface free energy of dispersed spherical gas bubbles, it is proposed thus:

$$E_s = \frac{1}{1 + \frac{T_{sm}}{3.16[(\rho_L - \rho_G)g\sigma_L]}} \quad (2-56)$$

Where

$$T_{sm} = \frac{1}{C_e} \left[ \frac{f_s}{2} \rho_s V_M^2 + \frac{D \rho_L E_f (V_T - V_f)(V_M - V_f)}{4 L_s} \right] \quad (2-57)$$

$$C_e = \frac{2.5 - |\sin \theta|}{2}$$

$T_{sm}$  is a function of the wall shear stress, slug length, translational velocity and is also affected by momentum exchange between liquid slug and liquid film in the slug unit. It is however a complex model with iterative solution.

A nonlinear regression model was developed by (Al-Safran, 2009a) using a database that is comprised of 410 experimental data for a wide range of fluid physical properties, geometrical and operational conditions. He implemented a mechanistic feature which was defined as the dimensionless momentum transfer rate between the slug body and liquid film was in the model. Below is the simplified form of the parameter:

$$\Theta = \frac{H_f (V_T - V_f)(V_M - V_f)}{V_M^2} \quad (2-58)$$

The final expression for the model is given as;

$$H_{LS} = 1.05 - \frac{0.0417}{\Theta - 0.123} \quad (2-59)$$

The model was validated against limited data for an air-oil two phase flow system and in addition, it required the computation of complex slug features and measurements.

The effect of high liquid viscosity on slug liquid holdup was investigated by (Kora et al., 2011) using a test facility of 0.0508 m pipe ID. They tested oil with 0.587, 0.378, 0.257 and 0.181 Pa.s viscosities and observed an insignificant effect of liquid viscosity on slug body within the matrix of the experimental test and fluid physical properties studied. The performance of the (Gregory et al., 1978), Zhang et al., 2003) and Al-Safran, 2009) correlations were evaluated. It was observed that when mixture velocity was less than 2.0 m/s, the proposed correlation gave good predictions relative to others while significant discrepancies in prediction were however observed at high mixture velocities. (Kora et al., 2011) then used non-dimensional groupings of (Wallis, 1969) to account for the influence of viscous forces and inertia forces. The dimensionless viscosity number,  $N_\mu$  accounts for viscosity and gravity while dimensionless Froude number,  $Fr$  accounts for inertia and gravity forces as defined by (Wallis, 1969):

$$N_\mu = \frac{V_m \mu_l}{g D^2 (\rho_l - \rho_g)} \quad (2-60)$$

$$Fr = \frac{V_m}{(gD)^{0.5}} \sqrt{\frac{\rho_l}{\rho_l - \rho_g}} \quad (2-61)$$

(Kora et al., 2011) proposed a new slug holdup based on experimental data, thus:

$$E_S = \begin{cases} 1.012 \exp(-0.085 Fr N_\mu^{0.2}) & 0.15 < Fr N_\mu^{0.2} < 1.5 \\ 0.9473 \exp(-0.041 Fr N_\mu^{0.2}) & Fr N_\mu^{0.2} \geq 1.5 \\ 1.0 & Fr N_\mu^{0.2} \leq 0.15 \end{cases} \quad (2-62)$$

Kora et al (2011) model gave a very good performance when tested against high viscosity data, however predicted poorly at certain flow conditions (producing values greater than unity).

Al-safran et al (2013) conducted experimentally investigation in horizontal pipes to study the effects of high viscosity liquid on slug liquid holdup. An empirical non-linear

regression model was developed as a function of two dimensionless numbers. The dimensionless numbers were defined by (Wallis, 1969) and used by (Kora et al., 2011). A liquid viscosity data ranging from of 0.180 – 0.587 Pa.s were utilized for the model development and the results obtained in the study were comparatively analysed with data obtained from (Gregory et al., 1978) and (Nadler and Mewes, 1995) which were for liquid viscosities of 0.001 and 0.007 Pa.s respectively. It was observed that a critical mixture velocity exist at which slug aeration process was initiated. Above the critical mixture velocity, it was also reported that high viscosity liquid had higher slug liquid holdup in comparison to low viscosity data. This was attributed to the thicker liquid film on the slug body and less turbulent energy in the slug mixing zone for high viscous liquid. The proposed model of (Al-safran et al., 2013) is expressed as:

$$E_S = 0.85 - 0.75\varphi + 0.057\sqrt{\varphi^2 + 2.27}; \quad \varphi = FrN_\mu^{0.2} - 0.89 \quad (2-63)$$

In general, this model gave good predictions at high slug holdup values (values above 0.93). The model however performed relatively poor below this value within the matrix of their experimental test.

Recently (Archibong, 2015) also developed a new general non-linear relationship for the slug holdup in high viscosity oil-gas based on experimental data from 0.026 m Pipe ID. He used groupings similar to those reported and utilized by (Kora et al., 2011) and (Al-safran et al., 2013). In both studies, the dimensionless numbers were defined based on (Wallis, 1969), this was necessary to ensure the influence of inertia and viscous force on liquid holdup is accounted for. The new correlation is given as;

$$H_{lS} = 1 - 0.03336 N_{Fr}N_\mu^{0.11} \quad (2-64)$$

### 2.3.5.2 Slug Frequency

The number of slugs observed by a fixed observer passing at a specific point along a pipeline over a certain period of time is referred to as slug frequency.

Gregory and Scott (1969) used a 0.019 m Pipe ID with CO<sub>2</sub> and water as the gas and liquid phase respectively to investigate slug frequency experimentally for which they came to a conclusion that slug frequency is a function of Froude number and pipe



diameter. This investigation saw them proposing a new correlation for slug frequency as follows:

$$f_s = 0.0226 \left( \frac{V_{SL}}{gD} \right)^{1.2} \cdot \left( \frac{19.75}{V_M} + V_M \right)^{1.2} \quad (2-65)$$

Gregory and Scot (1969) was later modified by (Greskovich and Shrier, 1972) to give;

$$f_s = 0.0226 \left( \frac{V_{SL}}{V_M} \right)^{1.2} \cdot \left( \frac{19.75}{D} + \frac{V_M^2}{gD} \right)^{1.2} \quad (2-66)$$

Heywood and Richardson (1979) proposed slight modifications to the (Gregory and Scott, 1969) correlation and came up with;

$$f_s = 0.0434 \left[ \left( \frac{V_{SL}}{gD} \right) \left( \frac{19.75}{V_M} + V_M \right) \right]^{1.2} \quad (2-67)$$

Another slug frequency correlation was proposed by (Nydal, 1991) based on the fact that slug frequency is only affected slightly by the superficial gas velocity for high superficial liquid velocities. It was further stated that slug frequency strongly correlates to superficial liquid velocity. Below is the proposed correlation:

$$f_s = 0.088 \frac{(V_{SL} + 1.5)^2}{gD} \quad (2-68)$$

Zabaras (1999) proposed a modification to the Gregory and Scott (1969) correlation where the influence of pipe inclination angle was accounted for. About 400 data points obtained in test sections with pipeline inclination angle between 0 - 11°, were the basis of their modified correlation. Pipe with IDs of 0.0254 – 0.2032 m were utilised. The correlation proposed is as follows:

$$f_s = 0.0226 \left[ \frac{V_{SL}}{gD} \left( \frac{19.75}{V_M} + V_M \right) \right]^{1.2} 0.836 + 2.75 \sin \theta \quad (2-69)$$

Shell slug frequency correlation cited in (Zabaras, 1999) was obtained by utilizing data from Heywood and Richardson (1979) study and came up with:

$$f_s = \sqrt{\frac{g}{D}} \times \left[ 0.048 Fr_L^{0.81} + A \left( (Fr_L + Fr_G)^{0.1} - 1.17 Fr_L^{0.064} \right)^2 \right] \quad (2-70)$$

Where  $Fr_{L,G} = V_{SL,SG}/gD$  and  $A = 0.73 Fr_L^{2.34}$

The effect of viscosity on slug flows in horizontal pipes was investigated by (Bahadir Gokcal et al., 2009) by using oil with viscosities ranging from 0.181 to 0.590 Pa.s. An 18.9 m long test section with 0.0508 m pipe ID was used in the experimental investigations. Two dimensionless groupings were used to develop a correlation. The Authors correlate a slug frequency closure model using (Wallis, 1969) dimensionless Froude number for inertia forces and the dimensionless viscosity number for the viscous forces. Thus:

$$f_S = 2.63 \frac{1}{N_F^{0.612}} \frac{V_{SL}}{D} \quad (2-71)$$

Where the dimensionless inverse viscosity number,  $N_F = D^{3/2} \sqrt{\rho_L(\rho_L - \rho_G)g} / \mu_L$

Schulkes (2011) developed a new slug frequency correlation by collating proprietary data from Statoil and several data in literature. The Author obtained data for pipe diameters ranging from 0.019 – 0.1 m, fluid viscosity from 0.001 – 0.590 Pa.s and pipeline inclination from 1 - 80° to the horizontal plane. The most influential functional groupings were deduced from several dimensionless groupings investigated. Slug frequency correlation was proposed as follows:

$$F = \frac{f_S D}{V_M} = \Psi(\alpha) \Phi(Re_{SL}) \quad (2-72)$$

Where

$$\Psi(\alpha) = 0.016\alpha(2 + 3\alpha)$$

$$\Phi(Re_{SL}) = \begin{cases} 12.1 Re_{SL}^{-0.37} & Re_{SL} < 4000 \\ 1 & Re_{SL} \geq 4000 \end{cases}$$

Zhao et al (2013) recently performed experiments in 0.026 and 0.074 m pipe IDs in horizontal pipes with a liquid viscosity ranging from 1.0 – 7.5 Pa.s. It was noted that the effect of gas superficial velocity was not accounted for in (Schulkes, 2011) correlation. They modified the (Schulkes, 2011) correlation to account for the gas superficial velocity and proposed a new correlation as follows:

$$\frac{F}{\Psi(\alpha)} = \begin{cases} 10.836 Re_{SL}^{-0.337} & Re_{SG} \leq 4000 \\ 6.40 Re_{SL}^{-0.141} & Re_{SG} > 4000 \end{cases} \quad \text{for } Re_{SL} < 4000 \quad (2-73)$$

$\Psi(\alpha)$  is defined as in (Schulkes, 2011). The (Zhao et al., 2013) and the (Schulkes, 2011) correlations gave relatively better prediction for high viscosity liquid applications.

Most recently (Archibong, 2015) studied the effect of high effect of viscosity on slug flows in 0.026 m pipe IDs in horizontal pipes with a liquid viscosity ranging from 1.0 – 7.5 Pa.s. He noted that models developed on high viscosity data either have uncertain range of validity or perform poorly when tested against the present data set thus came up with a new correlation given below;

$$\ln F_s = \psi_1 \ln(Fr) - \psi_2 \ln(V_{sgd}) + \psi_3 \ln(\lambda) - \psi_4 \ln(M_R) \quad (2-74)$$

Where

$$Fr = \frac{V_m}{\sqrt{gD}} \quad (2-75)$$

$$V_{sgd} = \frac{V_{sg} \left[ \sqrt{[(\rho_l - \rho_g) / \rho_g]} \right]}{\sqrt{gD}} \quad (2-76)$$

$$M_R = \frac{Re_{sl} \cdot V_{sl}^2}{Re_{sg} \cdot V_{sg}^2} \quad (2-77)$$

$$\lambda = \frac{V_{sl}}{V_M} \quad (2-78)$$

And  $\psi_1$ ,  $\psi_2$ ,  $\psi_3$  and  $\psi_4$  were obtained from his dataset as 0.138, 0.801, 1.661 and 0.277 respectively.

### 2.3.5.3 Slug Translational Velocity, Distribution Parameter and Drift Velocity

This is the velocity of slug units often estimated with closure relationship in two phase flow modelling. It is the sum of the bubble velocity in a stagnant liquid, i.e. the drift velocity,  $V_D$ , and the maximum velocity in the slug body.

Nicklin et al (1962) proposed an equation for the estimation of slug translational velocity as;

$$V_T = C_0 V_m + V_D \quad (2-79)$$

Where

$C_0$ = Distribution parameter

$V_m$ =Mixture velocity

$V_D$ =Drift velocity

Kouba and Jepson (1990) experimentally studied flow characteristics in horizontal slug in the Harwell Laboratory using 0.15 m ID pipeline and proposed an empirical correlation given as;

$$V_T = 1.21(0.1134 + 0.94V_{sl} + V_{sg}) \quad (2-80)$$

Drift velocity and Distribution parameters are both vital closure relationships in the slug translational velocity and drift flux model.

Zuber and Findley (1965) investigated two phase annular and slug flow in pipelines for an air-water system. The in-situ gas velocity showed a strong relationship with the mixture velocity as observed. A new average volumetric liquid holdup was proposed as a function of the distribution parameter,  $C_o$  and the average drift velocity,  $V_D$  thus:

$$C_o = 1.2; \quad V_D = 1.53 \left[ \frac{g\sigma(\rho_L - \rho_G)}{\rho_L^2} \right]^{1/4} \quad (2-81)$$

The following equation was proposed by (Ishii, 1977) for the distribution parameter and drift velocity for an air-water system in the churn-turbulent flow pattern as:

$$C_o = 1.2 - 0.2 \sqrt{\frac{\rho_G}{\rho_L} (1 - \exp(18\alpha_G))} \quad (2-82)$$

$$V_D = (C_o - 1)V_M + \sqrt{2} \left[ \frac{g\sigma(\rho_L - \rho_G)}{\rho_L^2} \right]^{1/4}$$

Pearson et al (1984) proposed the distribution parameter and the drift velocity as shown below:

$$C_o = 1 + 0.796 \exp\left(-0.061\sqrt{(\rho_G/\rho_L)}\right); \quad (2-83)$$

$$V_D = 0.034 \sqrt{(\rho_G/\rho_L)} - 1$$

Bendiksen (1984) investigated single elongated bubbles in flowing liquid at different flow conditions and pipe inclinations and came up with the drift velocity correlation which is widely used. It is given by:

$$V_D = V_D^h \cos \theta + V_D^v \sin \theta \quad (2-84)$$

Benjamin (1968) also proposed another correlation widely used in the industry for drift velocity in horizontal pipes thus:

$$V_D = 0.542\sqrt{gD} \quad (2-85)$$

Fabre and Line (1992) used the liquid Reynolds number and proposed a distribution parameter for slug flow as shown below:

$$C_o = \frac{2.27}{1 + (Re/1000)^2} + \frac{1.2}{1 + (1000/Re)^2} \quad (2-86)$$

Gokcal et al (2009) investigated the effect of liquid viscosity on drift velocity in horizontal and upward inclined pipelines; liquid with viscosities ranging from 0.001 to 0.7 Pa.s were used, varying pipe inclinations from 0 - 90° and 0.0508 m internal diameter. The proposed correlation is given by:

$$V_D = V_D^v (\sin \theta)^{0.7} + V_D^h (\cos \theta)^{1.5} \quad (2-87)$$

Jeyachandra et al (2012) proposed an extension of (Gokcal et al., 2009) work to allow for more pipe inclinations, IDs and liquid viscosities. A set of 0.0508, 0.0762 and 1.524 m Pipe IDs were used and a range of 0 - 90° inclination angles. The drift velocity correlation was proposed as:

$$Fr_\theta = Fr^h \cos \theta + Fr^v \sin \theta \quad (2-88)$$

A closure relationship was developed by (Choi et al., 2012) to estimate liquid holdup using the drift flux model. Data were gotten from literature for pipe ID ranging from 0.0508 – 0.1496 m, liquid viscosity from 0.001 – 0.601 and pipeline inclination from -2 – 90° from the horizontal plane. Synthetic datasets obtained from OLGA, widely used multiphase flow simulator was used to generate data for pipeline inclinations of -10 – 10°, pipe diameter 0.0762 m, and liquid viscosity of 0.001 – 0.002 Pa.s, They proposed a closure relationship for the distribution parameter which was based on (Fabre and Line, 1992) and (Ishii, 1977) as follows:

$$C_o = \frac{2.27}{1 + (Re/1000)^2} + \frac{1.2 - 0.2\sqrt{(\rho_G/\rho_L)}(1 - \exp(18\alpha_G))}{1 + (1000/Re)^2} \quad (2-89)$$

In addition, drift velocity was proposed based on a modification of the (Zuber and Findlay, 1965) model thus:

$$V_D = A \cos \theta + B \left[ \frac{g\sigma(\rho_L - \rho_G)}{\rho_L^2} \right]^{1/4} \sin \theta \quad (2-90)$$

The authors gave the values of A and B as 0.0246 & 1.606 and -0.191 & 12.59 based on his experimental and synthetic database.

Archibong (2015) having reviewed published works, noted that most of the closure relationships were developed from low viscous liquid-gas flows for distribution parameter and drift velocity. Based on his review, he noted that (Gockal et al., 2009), (Jeyachandra et al, 2012) and (Choi et al., 2012) used the highest viscosities, however the maximum value of viscosity in their works were still lesser than 0.7 Pa.s. Based on this premise and the conclusion made by (Gockal et al., 2009) and (Choi et al., 2012) that viscosity was a major factor that influences distribution parameter. He developed a new closure relationship for distribution parameter correlated partly from (Choi, 2012) proposed combination and from his experimental dataset ranging from 0.18 to 8.03 Pa.s in addition to those in the literature. The proposed distribution parameter is given as

$$C_0 = \frac{\Psi_1}{\Psi_2 + \left(\frac{Re}{1000}\right)^2} + \frac{\Psi_3 + \Psi_4 \sqrt{\rho_g/\rho_l (1 - \exp(1 - \exp(-18\alpha_G)))}}{\left(\frac{Re}{1000}\right)^2} \quad (2-91)$$

Where the following parameters  $\Psi_1, \Psi_2, \Psi_3$  and  $\Psi_4$  were respectively obtained as 0.272, 0.236, 0.471 and 17.143. He concluded that the proposed distribution parameter is to be used in combination with the drift velocity correlation developed by (Jeyachandra et al., 2012) stated above.

### 2.3.5.4 Slug Body Length

Brill et al (1981) based on field data obtained from the Alaska Prudhoe Bay field noted that slug lengths can be represented by a log-normal distribution. A slug length correlation based on this data was proposed as a function of pipe diameter and mixture velocity given in the equation below.

$$\ln(L_s) = -3.851 + 0.059 \ln\left(\frac{V_m}{0.3048}\right) + 5.445 \left[ \ln\left(\frac{D}{0.0254}\right) \right]^{0.5} \quad (2-92)$$

Norris (1982) modified the (Brill et al., 1981) slug length by using an expanded data from the same field. He eliminated that mixture velocity in (Brill et al., 1981) having

found that it has no significant effect on the slug length. The proposed correlation is given as:

$$\ln\left(\frac{L_S}{0.3048}\right) = -2.099 + 4.859 \sqrt{\ln\frac{D}{0.0254}} \quad (2-93)$$

Base on the same field data from Alaska Prudhoe Bay (Gordon and Fairhurst, 1987) proposed a slug length correlation for 0.3048 m, 0.4064 m and 0.508 m internal diameter pipes:

$$\ln L_S = -3.287 + 4.859\sqrt{\ln D + 3.673} + 0.059\ln(V_m) \quad (2-94)$$

Again, on addition of data from 0.588m ID pipe (Gordon and Fairhurst, 1987) proposed

$$\ln L_S = -3.287 + 4.859\sqrt{\ln D + 3.673} \quad (2-95)$$

Scott et al (1989)utilized the entire dataset from the Alaska Prudhoe Bay field to develop slug length correlation. The mechanism of slug growth in long and large diameter pipe was considered in their slug length correlation. The proposed correlation is given as:

$$\ln L_S = -26.6 + 28.495 \left[ \ln\left(\frac{D}{0.0254}\right) \right]^{0.1} \quad (2-96)$$

An experimental investigation was conducted by (Al-Safran et al., 2011) on the effect of viscosity on slug length in 0.0508 m ID horizontal pipelines with a viscosity range of 0.181 – 0.589 Pa.s. They noted that increased frequency and reduced slug length were as a result of the viscosity effects on the scooping process in the front and the shedding process in the slug tail. They proposed the slug length for high viscosity liquid-gas flow in horizontal pipelines based on a slug frequency model of (Gockal et al., 2009), thus:

$$\frac{L_S}{D} = 2.63 \left[ \frac{D^{2/3} \sqrt{\rho_L(\rho_L - \rho_G)}}{\mu_L} \right]^{0.321} \quad (2-97)$$

Wang (2012) experimentally studied the effects of high oil viscosity in both horizontal and vertical pipes for which 300 tests was conducted using 0.0525 m ID. Oil viscosities ranging from 0.15 to 0.57 Pa.s was used. A closure relationship for average slug length for all angle of inclination was developed based on an inverse dimensionless viscosity number. The model is given as;

$$L_S = \left\{ 10.1 + \frac{16.8}{1 + \text{Exp}[-3.57 * (\text{Ln}(N_f) - 5.4)]} \right\} \left[ \text{Cos}^2 \theta + \frac{\text{Sin}^2 2\theta}{2} \right] D \quad (2-98)$$

Barnea and Brauner (1985) and (Taitel et al., 1980) simulated the mixing process between the film and slug in order to understand the mechanism of stable slug length formation using a wall jet entering a large reservoir. They noted that a developed slug length requires a distance for a jet to be absorbed by the liquid and by using this approach, they concluded that minimum liquid slug length is 32D and 16D for horizontal and vertical flows respectively. In addition, a model was developed by (Dukler et al., 1985) to predict the minimum stable slug length in slug flow. They concluded that the minimum slug length is of the order of 20D.

### 2.3.6 Summary of Gas-Liquid Two-Phase Flow

Several modelling and experimental studies have been conducted on two phase gas-liquid flows in pipelines, most of which are for low viscous oil-gas flow. However, from the above literature review, it is clear that the available prediction correlations and models do not exhibit any explicit dependency on liquid viscosity. In addition to this, it has been established by (Gokcal, 2008) that slug frequency increases while the slug length decreases when liquid viscosity increases. As a result, this study has focused on the development of new closure models by accounting for viscosity effects to enhance the prediction of slug length and frequency. Table 2-2 below presents the summary of the experimental investigations and predictive closure relationships reviewed in this work focusing on medium and high viscous oil.



**Table 2-2: Review of experimental studies high viscosity oil-gas flow**

Author(s)	Liquid			Gas		Pipe		Parameters Measured	Models/Correlations Proposed
	Type	Viscosity (cP)	Density (kg/m <sup>3</sup> )	Type	ID (m)	Inclination (Degree)	Material		
Al-Safran <i>et al.</i> (2011)	Oil	181-589	-	NA	NA	NA	NA	NA	Slug length
Archibong (2015)	Oil	1000- 7500	916	Air	0.074, 0.0254	0, 30	Acrylic	Flow pattern, slug frequency, holdup, slug velocity,	Distribution parameter, slug liquid holdup, Slug Frequency
Al-Safran <i>et al.</i> (2013)	Oil	1-589	-	Air	0.0508	0	NA	Slug liquid holdup	Slug liquid holdup
Al-Safran <i>et al.</i> (2013)	Oil	587	-	Air	0.0508	0	Acrylic	Slug Frequency	Slug Frequency
Brito <i>et al.</i> , (2013)	oil	10-180	-	Air	0.0508	0	Acrylic	Pressure gradient, flow pattern, translational velocity	Slug Frequency
Choi <i>et al.</i> (2012)	Oil	1-601	-	Air	0.0508 – 0.1496	-100	NA	Pressure Gradient	Drift Velocity
Farsetti <i>et al.</i> (2013)	Oil	900	-	Air	0.0228	0, 5, 10, 15, -5, -15	NA	Slug Frequency Slug Holdup	NA
Foletti (2011)	Oil	896	886	Air	0.022	0	Plexiglas	Pressure Gradient	NA

Gokcal <i>et al.</i> (2010)	Oil	181-590	-	Air	0.0508	0	NA	-	Slug Frequency
Gokcal <i>et al.</i> (2006)	Oil	181-590	-		0.022	0	NA	Flow pattern	NA
Gokcal <i>et al.</i> (2008)	Oil	181-590	-		0.0508	0	NA	Flow pattern, slug frequency, holdup, slug velocity, drift velocity and slug length	Slug frequency
Jeyachandra <i>et al.</i> (2012)	Oil	181, 257, 378, 587	-	Air	0.0508 – 1.5424	0 - 90°.	Acrylic	Drift Velocity	Drift Velocity
Kora <i>et al.</i> (2011)	Oil	181, 257, 387, 587	-	Air	0.0508	0	Acrylic	Slug Liquid Holdup	Slug Liquid Holdup
Schulkes (2011)	Oil	1-590	-	Air	0.019 – 0.1	0 - 80	-		Slug Frequency
Weisman <i>et al.</i> (1986)	glycerol-water	75, 150	-	Air	0.012, 0.025, 0.051	0	-	Flow pattern	NA
Wang (2012)	Oil	15, 28, 57	890	air	0.0508	0, 90	NA	Slug liquid holdup and mean slug length	Slug liquid holdup and mean slug length

Zhao <i>et al.</i> (2013a)	Oil	1000, 7000	916	Air	0.0254, 0.074	0	Acrylic	Flow pattern, pressure gradient, slug frequency, holdup and slug liquid holdup	Interfacial friction factor
Zhao <i>et al.</i> (2013b)	Oil	1000, 3500	916	Air	0.074	0	Acrylic	Slug Frequency	Slug Frequency

## 2.4 Liquid-Liquid Two-Phase Flow

Another frequently encountered flow in process and oil & gas industries is that of two immiscible liquids flowing concurrently in pipelines. This sub-section is aimed towards reviewing previous studies in a view to establish areas that require further work.

### 2.4.1 Flow Patterns in Liquid-Liquid Flow

Two phases of immiscible liquids flowing in pipelines may configure themselves in different geometrical distributions. This arrangements in configuration largely depend on the phases' physical properties, the flow conditions and the flowing area geometry. Two-phase flow of water and low viscous liquid have been investigated by many researchers such as (Angeli and Hewitt, 2000; Lovick and Angeli, 2004; Trallero, 1995).

Trallero (1995) characterised flow patterns as segregated or dispersed based on experimental investigation conducted in a test section with 15.54 m pipe length, and 0.05 m ID. They further characterized segregated flow pattern into stratified and stratified with interfacial mixing as well as dispersed flow patterns into water or oil dominant flow with dispersed second phase i.e. emulsified in the dominant phase. The following diagrams depict the observed flow patterns in their investigations.

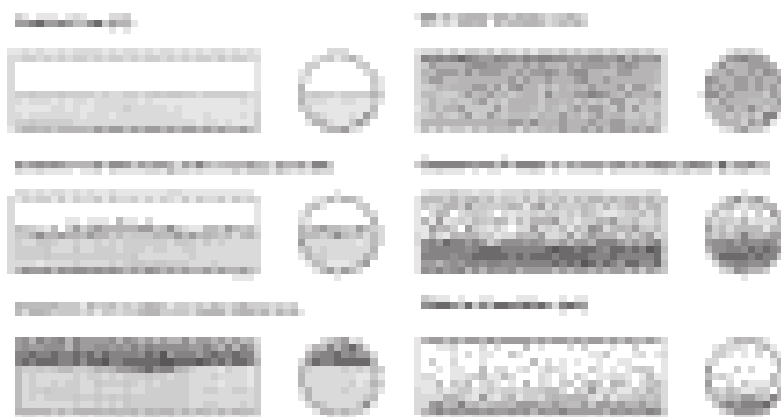


Figure 2-4: Oil-water flow patterns (Trallero 1995)

Rodriguez and Oliemans (2006) used oil with 0.0075 Pa.s viscosity to study on oil-water two-phase flow in an inclined and horizontal test section. A range of -5 - +5° pipe inclinations were used in the study. Similar flow patterns were observed in both studies other than a third separated flow that was also observed; the stratified wavy flow lying between the smooth stratified and the stratified flow with interfacial mixture.

#### **2.4.1.1 Flow Patterns in Viscous Liquid-Liquid Flow**

Water and emulsion are often used to enhance the flow of heavy oil during transportation as it helps to reduce pumping energy. Most of the existing models based on CAF flow do not put the complexities of phase distribution into consideration especially in the Water Assisted Flow region. In the light of this, investigation on the effect of high viscous two-phase liquid-liquid flow become issue of importance.

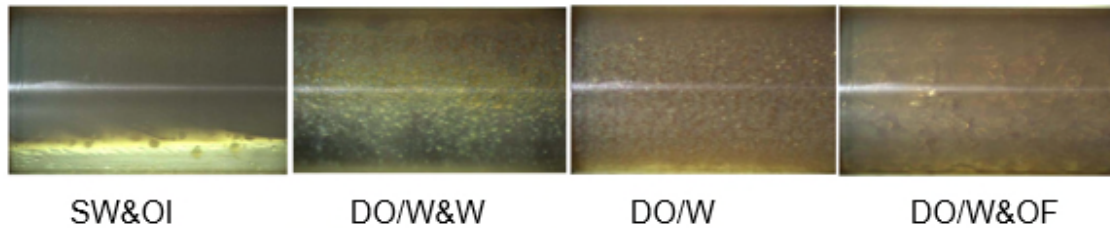
Vuong et al (2009) investigated the flow pattern in high viscosity oil/water flow in horizontal and vertical pipes using a test fluids which comprises refined mineral oil ND 50 with viscosity 0.44 – 0.107 Pa.s and Tulsa City tap water. Important parts of the test section includes stainless steel pipe with U-shape, inclined to the vertical at -2 – 90° range of angles with 44 m length and 0.0525 m ID. From the study, the flow regimes, pressure gradients and water holdup were determine using graduated cylinders, differential pressure transducers and high speed video camera. Four flow regimes were mainly observed in the horizontal flow test. A range of 0.1 – 1 m/s oil and water superficial velocities were utilized for both horizontal and vertical flows.

Different flow patterns were observed in their study as illustrated as Figure 2-6. One of the observation was a flow of oil and water separated into layers in which oil flow at the top and water at the bottom of the pipe. Droplets of oil and waviness were observed at the interfacial boundary known as *Stratified Wavy with Oil Droplets at Interface (SW&OI)*. It was found to occur when superficial velocities of oil and water are low.

Another flow pattern with dispersed oil droplets in a continuous water phase at the top section and free water stream flow at the bottom of the pipe, occur as the

water flowrates increased and the free layer of water eventually disappeared upon further increase in water & oil flowrates. This type of flow regime was referred to as *Dispersion of Oil in Water over a Water Layer (DO/W&W)*. An external phase of water & oil droplets distributed from bottom to the top of the pipe was observed to form a flow regime and it is called *Full Dispersion of Oil in Water (DO/W)*.

Furthermore, capacitance probe was used to observe a combined flow patterns of DO/W and DO/W&W where oil dispersed in continuous water phase as well as thin oil film (This is “probably” related to the pipe wall wettability). A flow regime was named as *Dispersion of Oil in Water and Oil Film (DO/W&OF)*.



**Figure 2-5: Flow Patterns Observed in Vuong et al. (2009) study**

Bannwart et al (2004) investigated the flow patterns in heavy crude oil-water flow system using 488 cP viscosity oil as test fluid in 2.84 cm ID pipe and 5.43 m length. A range of 0.07 – 2.5 m/s and 0.04 – 0.5 m/s superficial velocities of oil and water were also used respectively. Their test was conducted in both in horizontal and vertical section with the following base flow patterns observed in the horizontal section and further illustrated by Figure 2-7 below;

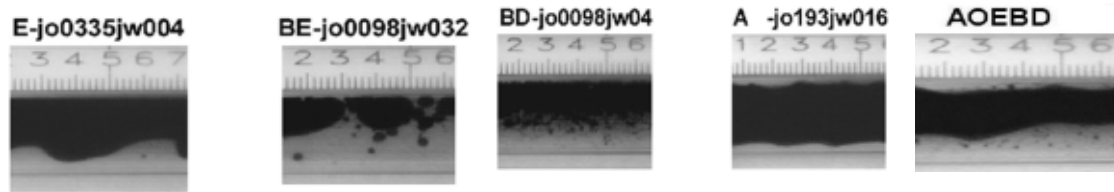
Stratified (E): This occurs in the glass pipe such that the upper walls are kept lubricated by water a fact they noted to be attributed to wettability effects and interfacial phenomena (i.e. the glass wall is oleo-phobic and hydrophilic)

Bubbles ~stratified (BE): This occurs at low flow rates and characterized by packages of coalescent bubbles often considered as an intermittent flow pattern.

Dispersed bubbles (BD): This flow pattern is characterized by bubbles dispersed in the segregated water phase. The bubbles can be either be homogeneously dispersed (BDH) or stratified (BDE) in the water phase.

Annular (A): This flow pattern was observed to be either smooth and centred (AP) or wavy and off centred (AOE).

Other combined flow patterns observed in their study in the horizontal test section are: Stratified + Dispersed + Bubbles (EBD), Wavy + Annular + Stratified + Dispersed bubbles (AOEBD), Stratified bubbles + dispersed bubbles (BEBD) Perfect annular + Dispersed bubbles (APBD)



**Figure 2-6: Flow Patterns Observed in Bannwart et al., (2004)**

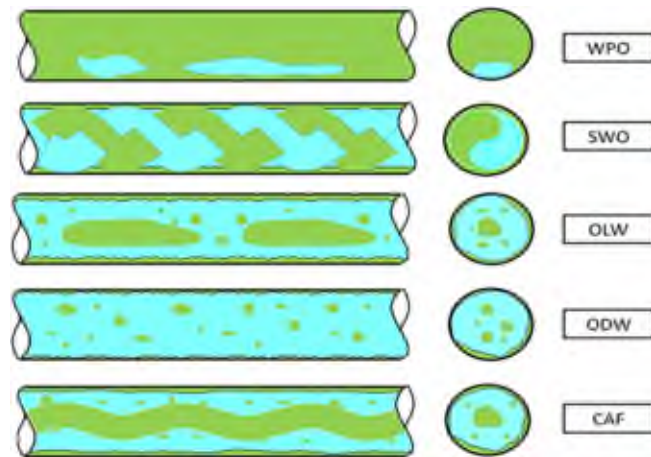
Additionally, (Bannwart et al., 2004) proposed a description for laminar core-laminar annulus flow criterion for liquids that have close densities but different viscosities. The relation below represents fully separated annular flows;

$$\mu_1 > \mu_2 + 0.0005\rho_2 V_{SL} D \quad \text{for} \quad \frac{\rho_2 V_{SL} D}{\mu_2} > 2000 \quad \text{and} \quad \varepsilon > 0.5 \quad (2-99)$$

Where  $\rho_2$  and  $V_{SO}$  are the density and superficial velocity of the annulus fluid respectively,  $D$  is the pipe diameter,  $\varepsilon$  is the core volume fraction,  $\sigma$  is the interfacial tension,  $g$  is the acceleration due to gravity and  $\mu_1$  &  $\mu_2$  are the viscosity of the core and annulus fluid. It was shown that stabilization of core flow is possible in pipe when  $\pi\Delta\rho g D^2 \varepsilon / 4\sigma < 8$  and the peripheral flow effect on the annulus was incorporated as well. It was concluded from the study that the essential requirements for existence of core annular flow with heavy oil viscosity  $> 1.0$  Pa.s is provided by the criteria represented by the equations.

The most interesting part of their investigations was the observation of core annular flow in both pipes and owing to its importance in production and transportation high viscous oil.

Al-Awadi (2011) studied the oil-water two-phase in a 5.5 m pipe length pipe and 0.0254 m ID with a range of 3.5 – 17.0 Pa.s oil viscosity. It was stated that results obtained was in good agreement with (Vuong et al., 2009) and oil fouling was noticed on the pipe wall for all tested flow pattern. The study revealed the following flow patterns; SWO: Spiral motion of Water & Oil, CAF: Core Annular Flow, OLW: Oil Lumps in Water continuous phase, WPO: Water Plugs in Oil continuous phase and ODW: Oil Dispersion in Water continuous phase as illustrated in Figure 2-9 below.



**Figure 2-7: Viscous oil-water flow patterns schematics by (Al-Awadi, 2012)**

Wang et al (2013) conducted a systematic work on the prediction of flow patterns transition of the oil-water two-phase flows using a wide range of oil viscosities for which four flow patterns were observed; stratified, dispersed, core-annular, and intermittent flow. They concluded that stability of the oil-water stratified flow in horizontal pipe is strongly related to oil viscosity, gravity and interfacial tension. For viscous oils, the influence of shear stress becomes much more obvious and can be characterised by ignoring the velocity of the viscous phase while, in dispersed flow, as the viscosity increases, oil droplets become harder to breakup, meaning that the ability of droplets to recover deformation becomes stronger. It is more difficult for o/w dispersed flow to be formed in viscosity oil. Additionally,



core-annular flow tends to occur in a pipe where the two fluids have much different viscosities but relatively close densities. It was also observed that drop entrainment occurs easily in core-annular flow and must be taken into consideration in transition criterion.

## 2.4.2 Two Phase Liquid-Liquid Flow Modelling Studies

The use of empirical, analytical and phenomenological models has become very vital in research & development units as well as industries for multiphase flow behaviour prediction especially for liquid-liquid phase. However, most of these models were developed based on low viscosity liquid-liquid flow considering the fact that very little work has been done on high viscous liquid-liquid flow. A brief review of the liquid-liquid flow models that are widely used in petroleum industries and research areas are presented below.

### 2.4.2.1 Analytical Models

A mechanistic model was developed by (Taitel and Dukler, 1976) for the predicting pressure gradient in oil-gas flow pipelines as reviewed earlier in this chapter. (Hall et al., 1993) utilized this technique to predict the pressure gradient in oil-water flow. The initial momentum balances were treated separately in the two fluids as shown below;

$$-A_W \left( \frac{dP}{dx} \right)_W + \tau_W S_W - \tau_i S_i + A_W \rho_W g \sin \alpha = 0 \quad (2-100)$$

$$-A_O \left( \frac{dP}{dx} \right)_O - \tau_O S_O - \tau_i S_i + A_O \rho_O g \sin \alpha = 0 \quad (2-101)$$

where  $A$ ,  $(dP/dx)$ ,  $\tau$ ,  $\rho$ ,  $\theta$ ,  $S$  and  $g$  respectively represent the area, pressure gradient, shear stress, density, inclination angle, perimeter covered and gravitational acceleration, and the subscripts  $W$ ,  $O$  and  $i$  relates each parameter to the water, oil and oil-water interface respectively. They arrived at a complex model which required iterative computational procedures by specifying several input parameters in order to have a solution.

Brauner(1991) investigated two immiscible liquids and proposed a predictive model for analysing the annular-core flow. The integral momentum equations was

used to derive the model for the annular and core regions with wall and interfacial shear stress expressed in terms of the respective friction factors. The two phase dimensionless pressure gradient obtained is given as;

$$\Phi_{Brauner} = \frac{K_1}{\varphi} \left[ \frac{(K_1\varphi)^2 + \varphi + 1}{(K_1\varphi)^2 + 1} \right] \quad (2-102)$$

$$\varphi = \frac{v_{so}}{v_{sw}} \quad (2-103)$$

$$K_1 = \begin{cases} \frac{0.046 \cdot Re_{s,w} \cdot \mu_w}{16\mu_o} & V_{SG} \leq 5.0m/s \\ \frac{\mu_w}{\mu_o} & V_{SG} \geq 0 \end{cases} \quad (2-104)$$

where  $Re_{s,w} = \rho_w V_{sw} / \mu_w$

Recently (Edomwonyi-Otu and Angeli, 2015)) developed a new interfacial configurations for the (Taitel and Dukler, 1976) model by investigating oil-water flow patterns in test facility of 0.014 m pipe ID. The model was applied to stratified liquid-liquid flow. The new configurational model considered the interfacial waviness and equivalent roughness which resulted in a substantial improvement of pressure gradient prediction when implemented in the two-fluid model. The interfacial equivalent roughness was based on (Rodriguez and Baldani, 2012) model and is given by:

$$f_i = f_k \left[ 1 + C_i \frac{\alpha}{D} \right] \quad (2-105)$$

Where  $C_i$  correction factor is obtained experimentally and given as 50,  $\alpha$  is the interfacial wave amplitude and  $f_k$  is the wall friction factor. The interfacial configurations are given thus:

$$S_o = D \cos^{-1} \left( \frac{2h_w}{D} - 1 \right); \quad S_w = \pi D - S_o; \quad S_i = \beta R; \quad (2-106)$$

$$A_o = 0.5(S_i R - R^2 \sin \beta) + 0.25 D S_o - 2X(2h_w - D); A_w$$

$$= 0.25\pi D^2 - A_o$$

where  $S_o$ ,  $S_w$ ,  $S_i$ ,  $A_o$  and  $A_w$  are the wall wetted perimeter of the oil phase, wall wetted perimeter of water phase, interfacial length, oil phase area and water phase area respectively.

Investigators such as (Chakrabarti et al., 2005)– the Energy Minimization Model and (Ooms et al., 1983)– Hydrodynamic Lubrication Theory developed other forms of mechanistic models. (Chakrabarti et al., 2005) relied on the principle that the parameters of any given system will stabilize to its minimum total energy i.e. kinetic, potential and surface energies, while the second author relied on a principle that allows oil to float and enveloped completely by water in a two phase liquid-liquid flow.

#### 2.4.2.2 Phenomenological Models

In order to develop closure relationships for fully dispersed two phase liquid-liquid flows based on suitably defined principle for the two-phase density, viscosity and velocity, it is quite necessary to make an assumption of homogenous mixture. The closure relationships developed are subsequently used to predict pressure gradient by implementing them in standard single phase flow models. The pressure gradient prediction using the Darcy-Weisbach single phase pressure gradient model is a typical example. The model is given thus:

$$\left(\frac{dP}{dx}\right)_{TP} = f \frac{\rho_M V_M}{2D} \quad (2-107)$$

Where  $(dP/dL)_{TP}$ ,  $f$ ,  $\rho_m$ ,  $U_m$  and  $D$  are two-phase pressure gradient, friction factor, density of the mixture, mixture velocity and pipe diameter respectively.

Arney (1993)proposed a model for concentric core-annular flow that was based on turbulence neglecting waviness of the core. The friction factor of the model is given by;

$$f_i = \begin{cases} \frac{64}{Re_{Arney}} & \text{Laminar Flow} \\ \frac{0.316}{Re_{Arney}^{0.25}} & \text{Turbulent Flow} \end{cases} \quad (2-108)$$

The modified Reynolds number  $Re_{Arney}$  is given by;

$$Re_{Arney} = \frac{\rho_m D V_m}{\mu_w} \left[ 1 + \eta^4 \left( \frac{\mu_w}{\mu_o} - 1 \right) \right] \quad (2-109)$$

Where  $u_m$  the mixture velocity,  $\rho_m$  the mixture density and  $\eta$  are given by;

$$\begin{aligned} V_m &= V_{os} + V_{ws} \\ \rho_m &= 1 - \eta^2 \rho_w + \eta^2 \rho_o \\ \eta &= \sqrt{1 - H_w} \end{aligned} \quad (2-110)$$

The author also developed a correlation for the water holdup,  $H_w$  as follows;

$$H_w = C_w [1 + 0.35(1 - C_w)] \quad (2-111)$$

Where;

$$C_w = \frac{u_{ws}}{u_{ws} + u_{os}}$$

$u_{ws}$  and  $u_{os}$  are the water and oil superficial velocities respectively. The dimensionless pressure gradient  $\phi_{Arney}$  was computed thus;

$$\phi_{Arney} = \frac{\lambda_{Arney} \rho_c u_m^2}{2D} \quad (2-112)$$

#### 2.4.2.3 Empirical Models

A correlation for predicting the pressure gradient in core annular flow was proposed by (Bannwart, 1999), the correlation is given thus:

$$\left(\frac{dP}{dx}\right)_{Bannwart} = \Delta P_w C_w^{-n} \quad (2-113)$$

Where  $n = 0.1$  for oleophilic and  $0.286$  for oleophobic pipe walls.  $\Delta P_w$  is the single phase pressure gradient for water flowing at the mixture velocity,  $V_M$ .

$$\Delta P_w = \frac{f_w \rho_w V_M^2}{2D} \quad (2-114)$$

$$f_w = \frac{0.316}{Re_w^{0.25}} \quad \text{and} \quad Re_{water} = \frac{\rho_w V_M D}{\mu_w}$$

Yusuf et al (2012) *et al.* (2012) obtained experimental dataset from a 0.0254 m pipe ID oil-water test using 0.012 Pa.s viscosity oil for which a pressure gradient correlation was developed. The correlation is given by:

$$\frac{dP}{dx} = 435.1 V_M^2 \quad (2-115)$$

McKibben et al (McKibben, 2000) opined that from experimental investigations conducted in 0.05, 0.1 and 0.2 m pipe IDs, with liquid viscosity ranging from 0.2 – 31.4 Pa.s, existing predictive models are inadequate to predict pressure gradient in viscous oil-water two-phase flow due to the effect of fouling on the pipe wall. They showed that existing models generally under predicted the pressure gradient since most of them were modelled based on Core Annular Flow (CAF) which is difficult to maintain for water cuts and operating conditions of practical importance. Continuous Water-Assisted Flow was used to distinguish this flow pattern from CAF. They expressed the pressure gradient in the pipeline as function of the wall shear stress,  $\tau_w$  and pipe diameter,  $D$  thus

$$-\frac{dP}{dx} = \frac{4\tau_w}{D} \quad (2-116)$$

It was further stated that the wall shear stress depends on a combination of the shear stress due to laminar shearing of heavy oil and shear stress due to the turbulent flow of water. In order to minimize empiricism and simplicity, the shear

stress on the pipe wall was defined as a function of the friction factor of the oil-water mixture. It is given below as:

$$\tau_w = \frac{f_m V_M^2 \rho_m}{2} \quad (2-117)$$

Where  $f_m$ ,  $\rho_m$ , and  $V_M$  are the mixture friction factor, density and mixture velocity respectively.  $\rho_m$  and  $V_M$  are as earlier defined in Equation (2-109) above. It was concluded by (Joseph et al., 1999) that the friction factor of the pipeline flow was mainly dependent on the water friction factor; (McKibben et al., 2013) postulated that other factors such as properties and concentration of the aqueous phase and oil viscosity were as well crucial together with water. A correlation for the mixture friction factor,  $f_m$  was proposed thus:

$$f_m = 15 \cdot Fr^{-0.5} f_w^{1.3} f_o^{0.32} C_w^{-1.2} \quad (2-118)$$

Where Froude number,  $Fr$ , mixture friction factor for the aqueous phase,  $f_w$  and oil friction factor,  $f_o$  are defined by:

$$Fr = \frac{V_M}{\sqrt{gD}} > 0.35; \quad f_w = \frac{1}{\sqrt{16 \log \sqrt{5.7 / \rho_m V_M^2 D}}}; \quad (2-119)$$

$$f_o = \frac{16}{Re} \quad Re = \rho_o V_m D / \mu_w$$

The authors concluded that for high viscous oil-water flow, the correlation gave reasonable estimates of the pressure gradient. The correlations expressed above were valid for the water assisted flow region only, the flow was considered as non-water assisted for  $Fr \leq 0.35$ .

### 2.4.3 Summary of Liquid-Liquid Flow

A concise review of studies related to concurrent flow of water-oil two phase has been presented in this section, the water assisted method is of great advantage in oil transportation for its ability to reduce pressure gradient and pumping requirements. Various models proposed for predicting pressure gradient in some of these studies needs to be validated against independent dataset.

Table 2-3: Review summary for oil-water two-phase flow

Authors	Pipe			Oil		Flow Variables	
	ID (mm)	Material	Orientation (degrees)	Viscosity (cP)	Density (kg/m <sup>3</sup> )	Measured	Models/Correlations
Arney <i>et al.</i> (1993)	15.9	Glass, PVC	0	600, 2700	985	Pressure gradient, holdup	Pressure Gradient
Trallero (1995)	50.1	Acrylic	0	29.6	850	Holdup, flow patterns, and pressure gradients	Flow Pattern Transition
Nadler and Mewes (1997)	59	Perspex	0	22~35	841	Flow Patterns, Phase Inversion	NA
Rodriguez <i>et al.</i> (2006)	82.5	Stainless Steel, Perspex	0, ±1, ±2, -5	7.5, 800	830, 1060	Flow patterns, pressure gradients, and oil/water holdups.	NA
Grassi <i>et al.</i> (2008)	21	Acrylic	0, ±15	533, 653, 800	886	Flow Patterns	NA
Sotgia <i>et al.</i> (2008)	25.4	Acrylic	0	800	885	Flow Patterns	NA

Al-Awadi (2011)	25.4	Perspex	0	3500 - 17000	916	Pressure Gradient, Flow Patterns	Pressure Gradient
McKibben and Gillies (2013)	54.4	Steel	1	622 - 1100	886 - 972	Pressure Gradient, Flow Patterns	Pressure Gradient
Strazza <i>et al.</i> (2011)	21, 22	Plexiglas, glass	-10 ~ 15	900	886	Flow patterns, pressure gradients, oil/water holdups.	-
Vuong <i>et al.</i> (2009)	52.5	Steel	0, 90	304 - 1070	884.4	Flow patterns, holdup, and pressure drops	NA
Yusuf <i>et al.</i> (2012)	25.4	Acrylic	0	12	885	Pressure gradient, flow patterns	Pressure gradient



## **3 EXPERIMENTAL SETUP**

The details description of experimental test facility, experimental design and unit operations employed for this investigation are provided in this chapter. Gas-liquid two phase and liquid- liquid two phase flow experiments were conducted in 0.074m ID and 0.024m ID horizontal test facilities located at Oil and Gas engineering Centre laboratory of Cranfield University. A full description of the main instrumentation (Gamma Densitometer and differential pressure transducers) and their calibration method are presented in addition to the test fluids used and their physical properties. Also presented in the chapter is the basic operating procedure for the test facilities.

### **3.1 Description of One-Inch Test Facility**

The 1-inch experimental test facility has the capability of handling different multiphase flow combinations ranging from two phase to four phase flows namely; air-oil, water-oil water-oil-sand and water-sand-oil-air and vice-versa. The facility is made up of a 0.024m ID horizontal pipeline fabricated from a Perspex pipe with a length of about 5.5m as presented in Figure 3-2. The test facility comprises of the following sub sections: the test fluid/material (air, water, oil and slurry) section at injection point, unit operations equipment section and the instrumentation and data acquisition section.

#### **3.1.1 Fluid Handling Section**

A 0.15 m<sup>3</sup> capacity tank is used for the storage of High viscosity oil which is pumped by a variable speed Progressive Cavity Pump (PCP) into the multiphase flow line through a T-junction. Just before the injection point, a bypass loop is connected to the oil tank for the purpose of ensuring uniform oil temperature is achieved. A Coriolis flow meter (Endress+Hauser Promass 83I DN 50) which gives three outputs: mass flow rate, density and viscosity is also installed before the injection point for oil metering. The HART output of the meter is connected to the data acquisition system for data logging during experimental runs. A schematic of the 1-inch test facility is shown in Figure 3-1 with the detailed descriptions of components are listed in Table 1.

Water is stored in a 0.15 m<sup>3</sup> capacity tank which was made from a plastic material insulated with fibres from the outside. A variable speed Progressive Cavity Pump (PCP) of 2.18 m<sup>3</sup>/hr maximum capacity with a maximum discharge of 10 barg pressure is used for pumping water into the flow line. The flow of water into the line is metered using an electromagnetic meter manufactured by Endress+Hauser, Promag 50P50 D50, with a range of 0 – 2.18 m<sup>3</sup>/hr. The meter has a 4-20mA HART output connected to the data acquisition system (DAS) for data logging during experimental test runs.

A screw compressor manufactured by AtlasCopco® Screw Compressors with maximum capacity of 400 m<sup>3</sup>/hr and maximum discharge pressure of 10 barg receives free air which is compressed before supplying to the test facility. The air from the compressor is first discharged into a 2.5 m<sup>3</sup> air tank before delivery to the test line. This is aimed towards preventing the pulsation of air supply to the test facility. It is worth noting that the test facility is pressure tested to withstand a maximum pressure of 14 barg while the compressed air is fed in to the test line and regulated to a maximum pressure of 7 barg. Filters are installed in the compressor supply lines to ensure the delivery of air free from moisture and debris to aid easy and accurate metering.

### **3.1.2 Unit Operation Equipment Section**

The separator and the temperature regulator (controller) are the two main unit operations equipment been used in the test facility. While the separator is a rectangular shaped tank made from plastic material with viewing windows installed at the sides for liquid levels and separation process monitoring. The multiphase fluid enters the separator where the viewing windows are located, initial separation by gravity takes place in this section, the denser phase settles at the bottom while the dense phase moves to the second section for further separation. The multiphase mixture requires a residence time of at least 18–24 hrs for complete separation into its component phases.

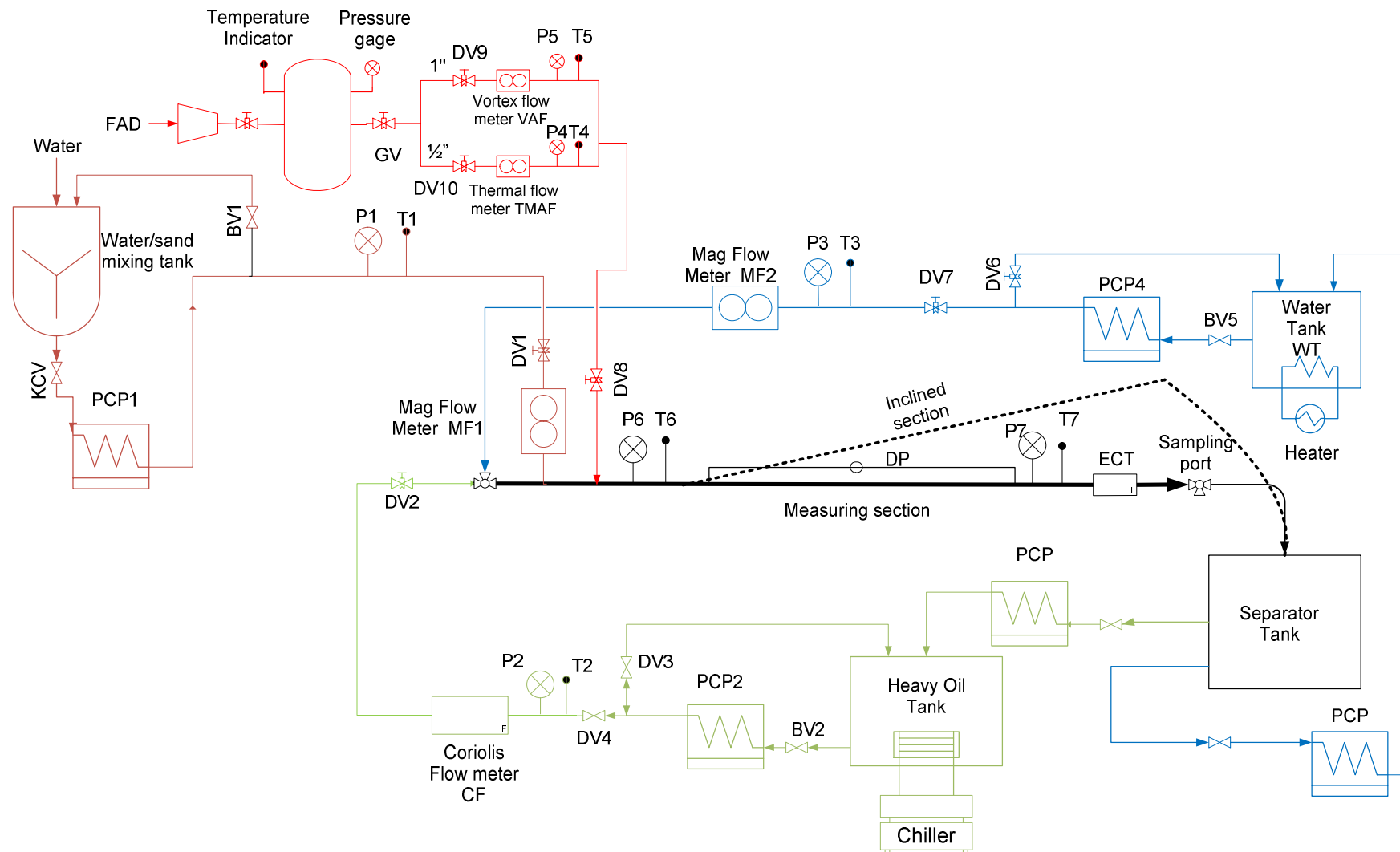


Figure 3-1: The schematic of one-inch test facility

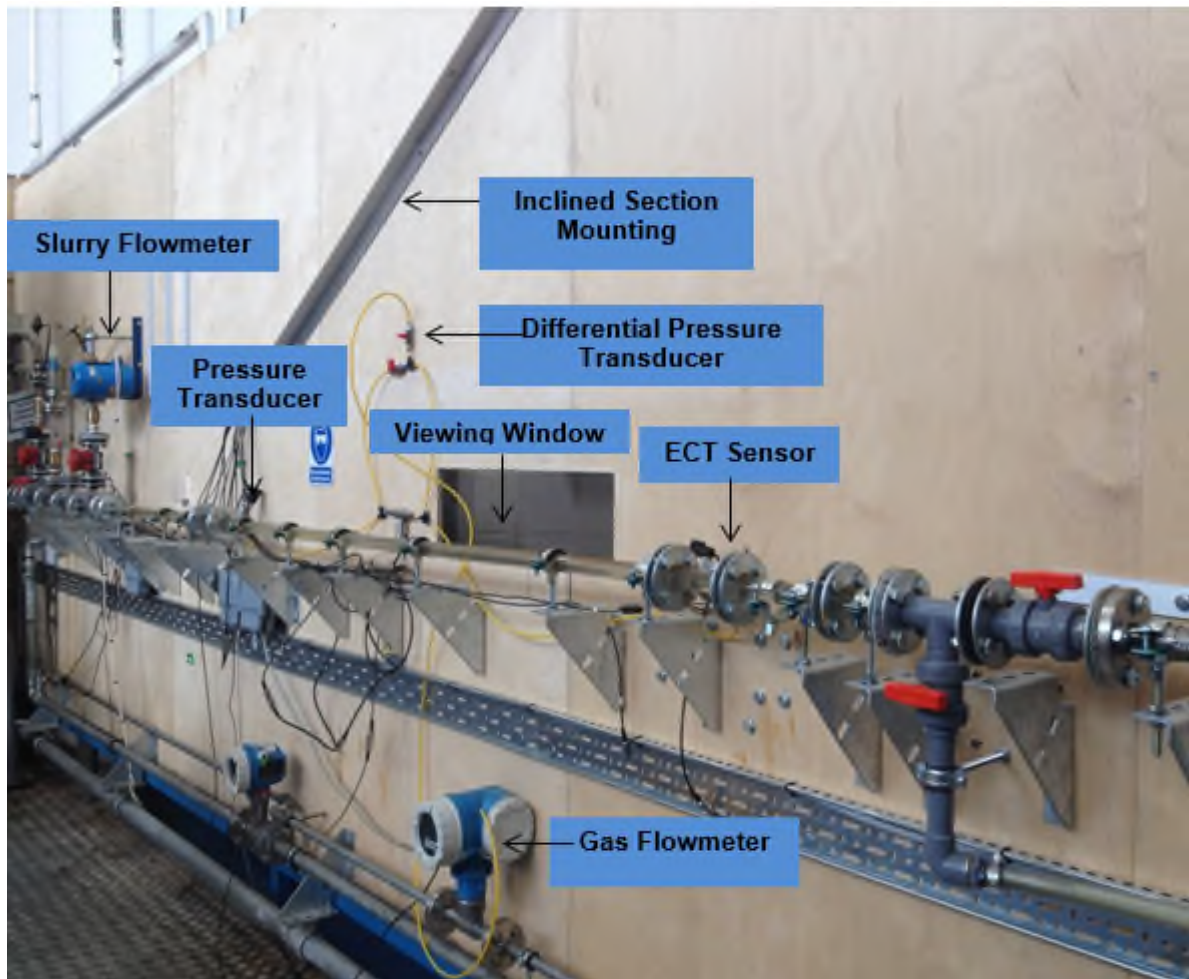


Figure 3-2: Pictorial view of one-inch test facility

**Table 3-1 specification for 1-inch facility**

<b>Abbreviations (Symbols)</b>	<b>Full Name</b>	<b>Description</b>
HOT	Heavy oil tank	0.15 m <sup>3</sup>
WT	Water tank	0.15 m <sup>3</sup>
ST	Separation tank	0.5 m <sup>3</sup>
PCP1	Progressive cavity pump for water/sand (Injection)	Flowrate: 0 ~ 2.18m <sup>3</sup> /h, Temperature: 5 ~ 50 °C, Discharge Pressure: 10 bara, Pressure switch equipped
PCP2	Progressive cavity pump for heavy oil (Injection)	Flowrate: 0 ~ 1.05m <sup>3</sup> /h, Temperature: 5 ~ 50 °C, Discharge Pressure: 10 bara, Pressure switch equipped
PCP3	Progressive cavity pump for heavy oil (Return)	Flowrate: 0 ~ 1.05m <sup>3</sup> /h, Temperature: 5 ~ 50 °C, Discharge Pressure: 10 bara, Pressure switch equipped
PCP4	Progressive cavity pump for Water (Injection)	Flowrate: 0 ~ 2.18m <sup>3</sup> /h, Temperature: 5 ~ 50 °C, Discharge Pressure: 10 bara, Pressure switch equipped
PCP5	Progress cavity pump for Water (Return)	Flowrate: 0 ~ 2.18m <sup>3</sup> /h, Temperature: 5 ~ 50 °C, Discharge Pressure: 10 bara, Pressure switch equipped
MF1	Electromagnetic flow meter for water/sand	Promag 55S50, DN50, Flow rate: 0 to 2.18 m <sup>3</sup> /h, Temperature: 5 ~ 50 °C, Maximum sand volume fraction: 0.15 v/v, 4-20 mA SIL HART output
MF2	Electromagnetic flow meter for water	Promag 50P50, DN50, Flow rate : 0 to 2.18 m <sup>3</sup> /h, Temperature: 5 ~ 50 °C
CF	Coriolis flow meter	Promass 83I50, DN50, Mass flow rate: 0 to 2000kg/h, Density: 0 ~ 1500 kg/m <sup>3</sup> , Viscosity: 1000~10000cP (Newtonian fluid), Temperature: 5 ~ 50 °C
VAF	Vortex air flow meter	Prowirl 72F25 DN 25, Flow rate: 3 to 100 m <sup>3</sup> /h, Maximum pressure: 10bara; Maximum measured error: ±1%
TMAF	Thermal mass air flow meter	T-mass 65F15 DN15, Flow rate: 0 to 3 m <sup>3</sup> /h, Maximum pressure: 10bara
P	Pressure gauge/transducer	GE Druck PMP 1400, 6 Bar g. Total Error Band: ±2%
DP	Differential pressure transducer	GE Druck PMP 1400, -200mbar ~ +200mbar, ±2%FS
Chiller	Thermal fisher temperature control system	Heats or cools down the oil, -5~ +50 °C
FAD	Free air delivery	Supplied from the laboratory compressor, which has a maximum supply capacity of 1275 m <sup>3</sup> /h free air delivery (FAD), Maximum discharge pressure:8 bara



Once complete separation of the phases is achieved, oil is recovered and reused while the waste-water are discharged into the waste-water tank. The temperature control system otherwise known as the chiller as shown in for oil is a refrigerated bath circulator manufactured by Thermal Fisher represented Figure 3-3. Copper coils submerged in the oil tank are connected to the circulator, by running cold or hot glycol in the coils at specific time intervals, the temperature of oil in the tank is thus controlled by heat transfer. The circulator's temperature ranges from 0 to +50 °C, with an accuracy of  $\pm 0.01$  °C. By changing the temperature of the glycol, the liquid contained in the tank is either heated or cooled to a desired temperature over a period of time and thus the viscosity of the liquid contained in the tank changes.

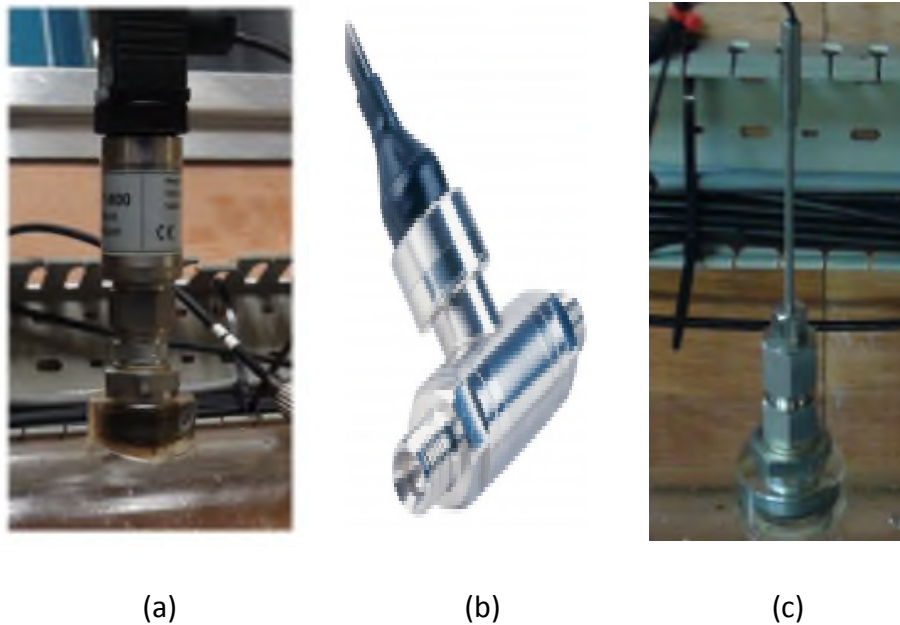


**Figure 3-3 Temperature Regulator for 1-Inch Rig**

### **3.1.3 Instrumentation and Data Acquisition Section**

Static pressure transducers PMP 1400 (two in number) manufactured by GE Druck Limited, with pressure range of 0 – 4 barg and accuracy 0.04% over the full scale is used to obtain the static pressure in the test section, they are placed 83D apart with the first one placed 60D from the last point of injection to ensure full flow development. A Honeywell STD120 differential pressure transducer with minimum pressure drop measurement of 100 Pa and an accuracy of  $\pm 0.05\%$  is used for the measurement of the differential pressure in the flow line. Test fluids

temperature are monitored by means of J-type thermal couples with an accuracy of  $\pm 0.1^{\circ}\text{C}$  placed at different locations along the multiphase flow line. Video recordings to aid visual observations of flow pattern observation are made possible by two high definition, 60GB HDD Sony camcorders, DSCH9 with 16 megapixels. Figure 3-4 and Figure 3-5 gives the pictorial view of the pressure transducers and camera used.



**Figure 3-4: (a) & (b) GE Druck Static and Differential Pressure Transducers (c) Thermocouple**

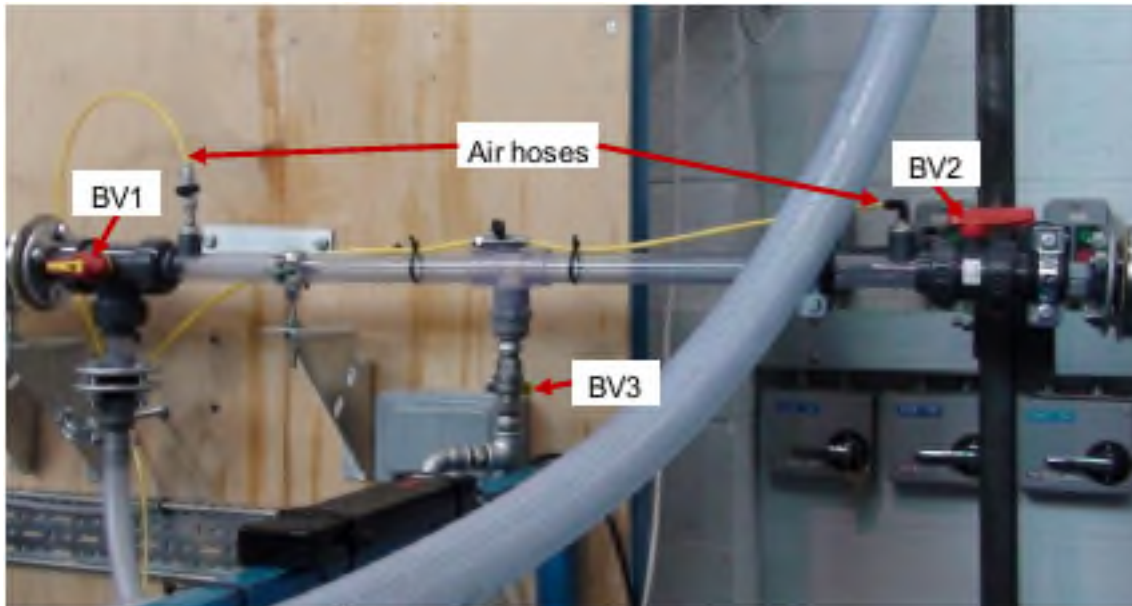


**Figure 3-5: Sony camcorders**

Quick closing valves designed in laboratory using Ball Valves (BV) and located downstream the test/observation area was used for the measurement water holdup. The Ball Valves (BV) (two in number) are placed 40D apart with the



upstream one, BV1 made up of three way T-port ball valve and the downstream one BV2 is a two way straight ball valve. The pictorial view of the water holdup measurement section consisting of two Ball Valves; BV1 and BV2 is shown in Figure 3-6.



**Figure 3-6: Pictorial view of the installed Ball Valves for water holdup measurement**

Data acquired from the flowmeters, differential pressure transducers, pressure transducers and temperature sensors are saved to a Desktop Computer using a Labview® version 8.6.1 based system. The system consists of a National Instruments (NI) USB-6210 connector board interfaces which output signals from the instrumentation using BNC coaxial cables and the desktop computer.

### **3.2 Description of Three-Inch Test Facility**

The test facility is a scaled-up of the one-inch test facility earlier described. It is a once-through facility fabricated from a 3-inch ID Perspex pipe with length of about 17 m. It consists of a vertical and horizontal pipe sections with observation section is placed 150D upstream of the last injection point to ensure full development of flow in the horizontal section. In the vertical section, two observation points are located 100D from the base of the upwards and downwards pipes. The various

sections of the 3-inch test facility similar to those of 1-inch described above are presented below.

### **3.2.1 Test Fluid Handling Section**

#### **3.2.1.1 Air Supply**

Air supply to the 3 inch test facility is from a laboratory compressor manufactured by Anglian Compressors Limited with maximum discharge pressure of 10 barg and maximum capacity of 400 m<sup>3</sup> hr<sup>-1</sup> to which free air is received and compressed before it is been supplied to the test facility. A 2.5 m<sup>3</sup> air tank into which delivery from the compressor is made regulates the air pressure to 7 barg. For safety and accuracy, air supply from the compressor is made to pass through a dryer and filter to ensure supply of moisture and particles free air. This section has two gas flow meters a 0.5-inch (Prowirl 72F15 DN15) vortex flow meter with range of 0~20 m<sup>3</sup>/hr and a 1.5-inch (Prowirl 72F40 DN40) vortex flow meter with range from 0~130 m<sup>3</sup>/hr both manufactured by Endress+Hauser which are used for air metering. A 2 inch steel pipe is used to inject air into the mainline about 150 pipe diameters upstream of the observation sections.

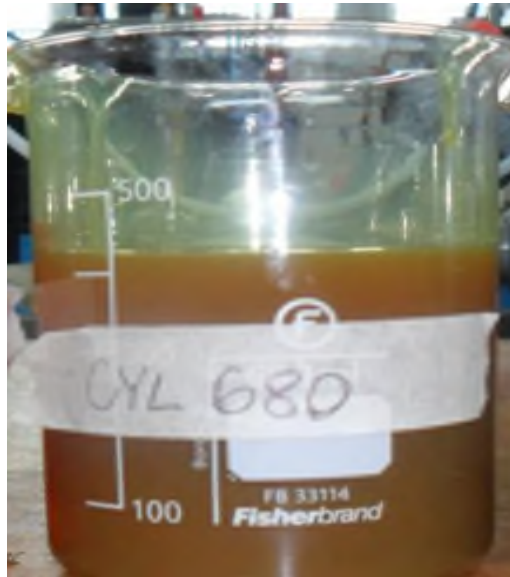
#### **3.2.1.2 Oil Supply**

High viscosity oil is pumped with aid of Progressive Cavity Pump (PCP) with variable speed and maximum capacity of 17 m<sup>3</sup>/hr is stored in a tank of 2 m<sup>3</sup> capacity. A Coriolis flow meter; Promass 831 DN80, of 0~171 m<sup>3</sup>/hr range is used in metering the oil flow. This flow meter with measurement accuracy of 0.1%-0.5% has three outputs; mass flow rate, density and viscosity. Mineral oil manufactured by Total with density of 921 kg/m<sup>3</sup> and viscosity of 680 cP at 40°C was used for the test as showed in Figure 3-7.

#### **3.2.1.3 Water Supply**

Water supply from a tap in the lab is stored in a 2.5 m<sup>3</sup> cylindrical mixing vessel slurry tank. A variable speed progressive cavity pump (PCP) with maximum capacity 2.1 m<sup>3</sup>/hr and a maximum discharge pressure of 10 barg is used to pumped water into the 3 inch test loop. Water flow is metered using an

electromagnetic meter manufactured by Endress+Hauser, Promag 50P80 DN80, with a range of 0 – 21 m<sup>3</sup>/hr.



**Figure 3-7: Mineral oil (CYL 680) used for the study**

### **3.2.2 Unit Operation Equipment Section**

This section is comprised of two main units which are the chiller and the separator. The high viscosity oil temperature is controlled by a chiller system with temperature ranges of (-5°C to +50°C) aimed towards achieving the desired oil viscosity for the experiment. The temperature control system for oil is a refrigerated bath circulator manufactured by Thermal Fisher. The tank is incorporated with submerged steel pipes which are connected to the circulator, and by running cold or hot glycol in the coils at time intervals

The separator is a rectangular shaped tank made from steel metal with viewing windows which allows for liquid level and separation process monitoring. The multiphase fluid enters and fills the separator through a pipe situated at the top of the tank giving room for initial separation by the action of gravity. The fluid collected in the separator is separated in layers with the denser phase settling at the bottom while the less dense phase moves to the upper section for further separation. The mixture of oil, water and air requires a residence time of at least 12~24 hours for complete separation into its component phases. On complete

separation of the phases, oil is recovered for reused while used water is disposed. Figure 3-8 and Figure 3-9 are pictorial view of the separator and the chiller system respectively.



**Figure 3-8: The 3-inch test facility chiller unit**



**Figure 3-9: 3-Inch test facility separator with its viewing window**

### **3.2.3 Instrumentation and Data Acquisition Section**

Mineral oil (CYL680) temperature is measured by means of J-type thermocouples with an accuracy of  $\pm 0.1^{\circ}\text{C}$  placed at different locations while differential pressure transducer manufactured by Honeywell STD120 are installed at the bottom of pipe at 52D downstream, and 171D downstream and upstream of vertical section. High definition, 60GB HDD Sony camcorders, DSCH9 with 16 megapixels are used for video recordings during the test to aid visual observations for the flow patterns.

Data acquired from the flowmeters, differential pressure transducers, pressure transducers and temperature sensors are saved to a Desktop Computer using a Labview® version 8.6.1 based system. The system consists of a National Instruments (NI) USB-6210 connector board interfaces which output signals from the instrumentation using BNC coaxial cables and the desktop computer. The schematics and pictorial view highlighting the various sections of the 3-inch multiphase flow facility are presented in Figure 3-10 and Figure 3-11 respectively in addition to specification for 3-inch test facilities presented in Table 3-2.

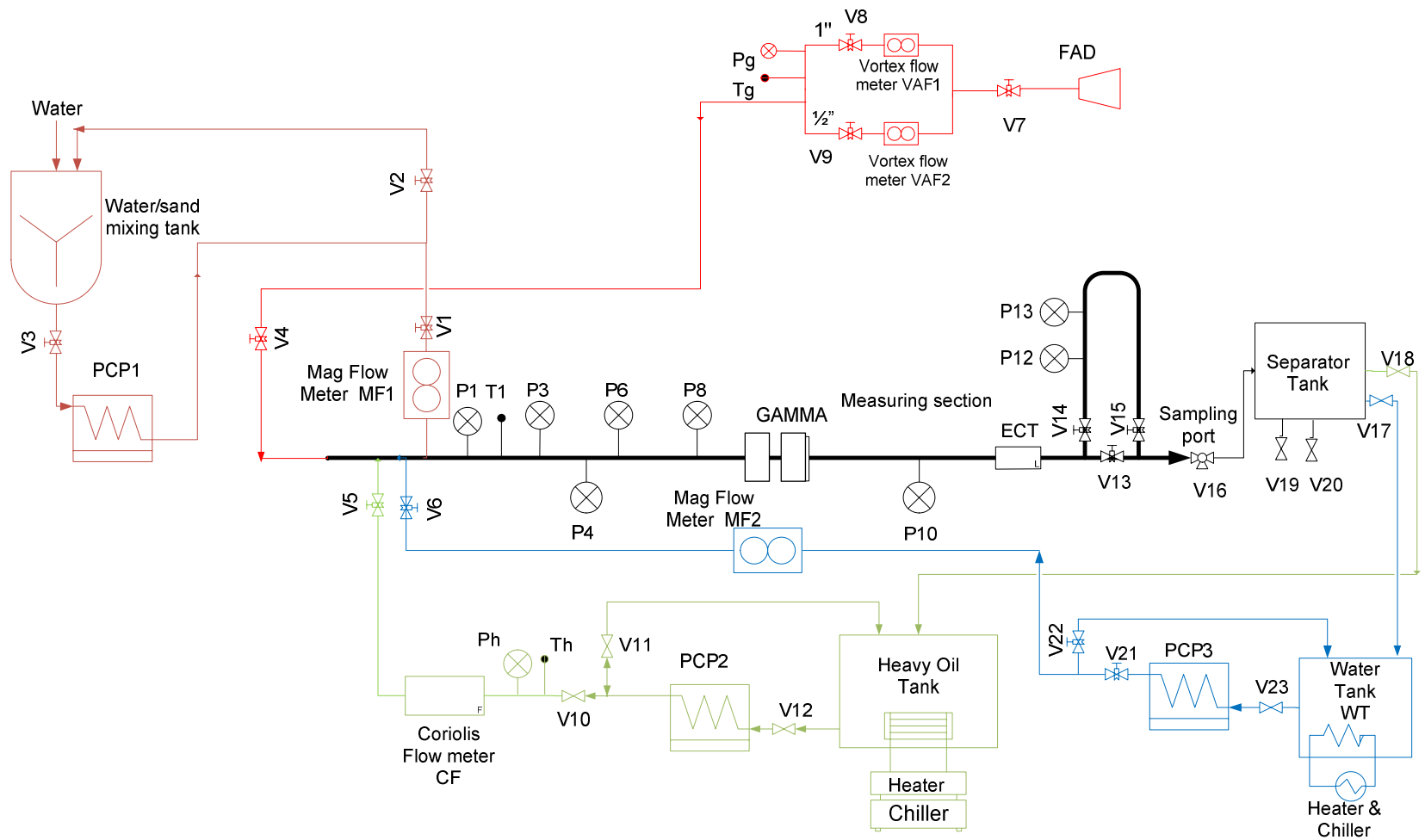


Figure 3-10: 3-inch multiphase flow facility schematics

**Table 3-2: The specification for 3-inch facility**

<b>Abbreviations (Symbols)</b>	<b>Full Name</b>	<b>Description</b>
HOT	Heavy oil tank	2 m <sup>3</sup>
WT	Water tank	2 m <sup>3</sup>
ST	Separation tank	6 m <sup>3</sup>
PCP1	Progressive cavity pump for water/sand (Injection)	Flow rate: 0 ~ 17 m <sup>3</sup> /h
PCP2	Progressive cavity pump for heavy oil (Injection)	Flow rate: 0 ~ 17 m <sup>3</sup> /h
PCP3	Progressive cavity pump for Water (Injection)	Flow rate: 0 ~ 21 m <sup>3</sup> /h
MF1	Electromagnetic flow meter for water/sand	Promag 55S80, DN80, Endress+Hauser
MF2	Electromagnetic flow meter for water	Promag 50P80, DN80, , Endress+Hauser
CF	Coriolis flow meter	Promass 83F80, DN80, Endress+Hauser
VAF1	Vortex air flow meter	Prowirl 72F40 DN 40, Flow rate: 10 to 130 m <sup>3</sup> /h, Endress+Hauser
VAF2	Vortex air flow meter	Prowirl 72F25 DN 25, Flow rate: 0 to 20 m <sup>3</sup> /h, Endress+Hauser
P4,P10	Pressure gauge/transducer	0~4 bar, PMP4010
P1,P3,P6,P8,P12,P13	Pressure gauge/transducer	0~6 bar, PMP1400
ECT	Electrical capacitance tomography	ITS M3000C+3" Sensors
GAMMA	Gamma Densitometer	Neftemer
Heater/Chiller	Temperature Regulator	ICS TAE-evo
FAD	Free air delivery	Supplied from the laboratory compressor, which has a maximum supply capacity of 1275 m <sup>3</sup> /h free air delivery (FAD), Maximum discharge pressure: 8 bara

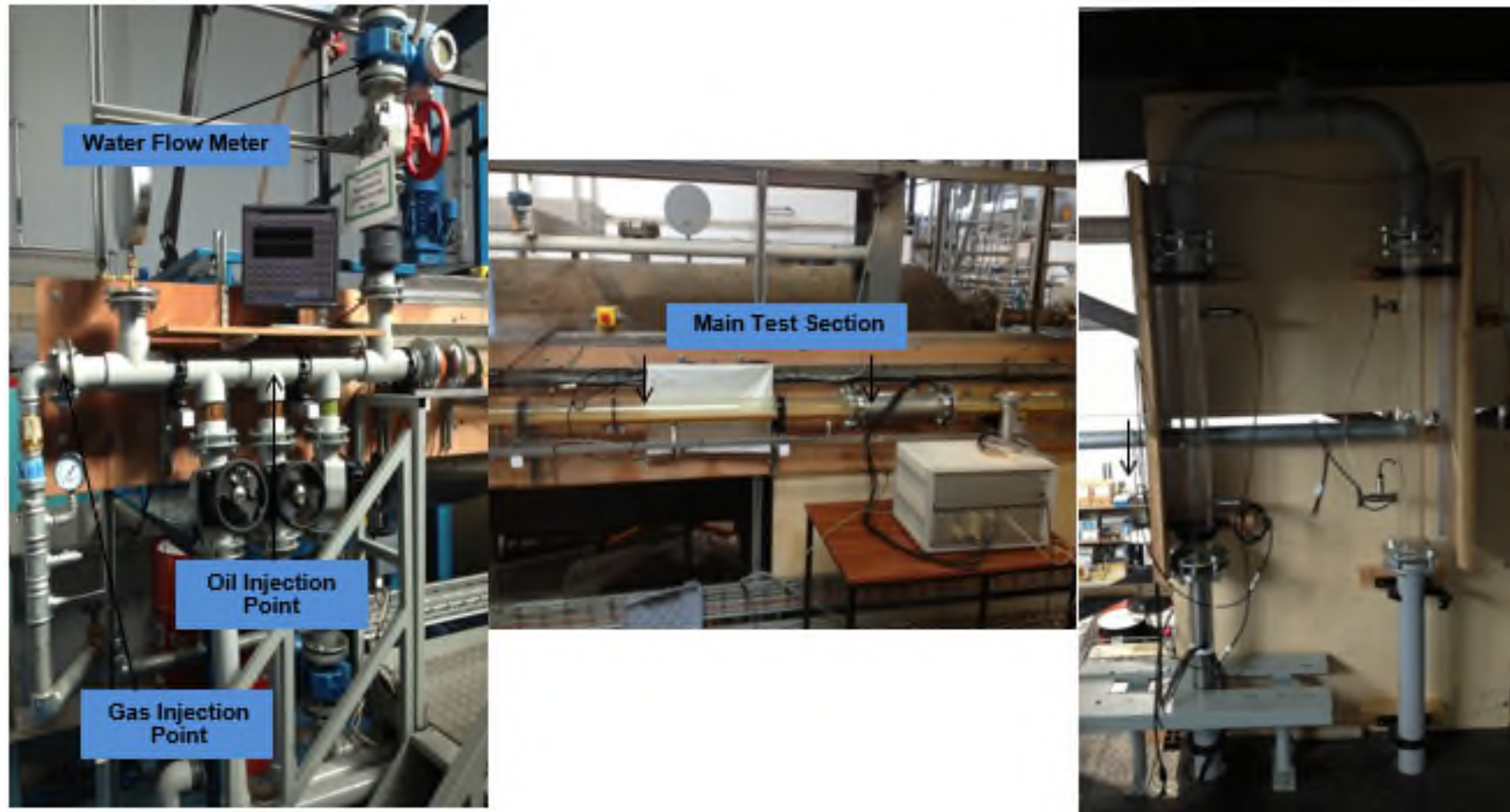


Figure 3-11: Injection and test sections in 3-inch facility (Zhao, 2014)



### 3.2.3.1 Viscosity measurement

Generally viscosity is termed as the measure of resistance of fluid to flow. It is the measure of the gradual fluid deformation by shear or tensile stress caused by internal friction of fluid molecules flowing at different velocities. Though the test liquid (CYL680) used for this investigation were specified by industrial manufacturers; it was necessary however to validate their claims before commencement of experimental runs for the purpose of enabling viscosity variations with temperature for the test matrix. Measurement of the oil's viscosity using Brookfield DV-I™ prime viscometer Figure 3-12 at different temperature was carried out in the laboratory and compared with manufacturer's specifications data shown in Figure 3-13 below.



**Figure 3-12: Brookfield DV-I™ prime viscometer**

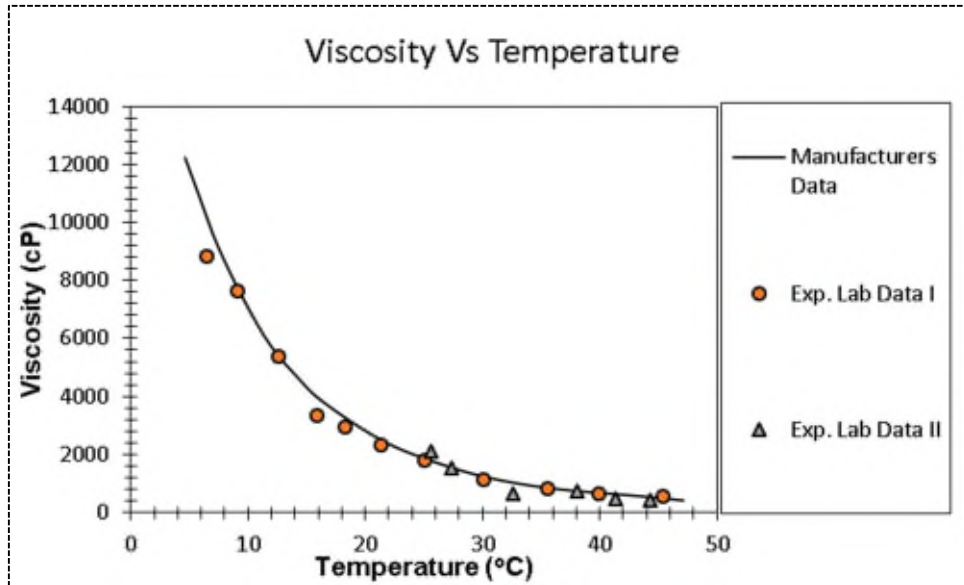


Figure 3-13: Viscosity versus temperature measurement

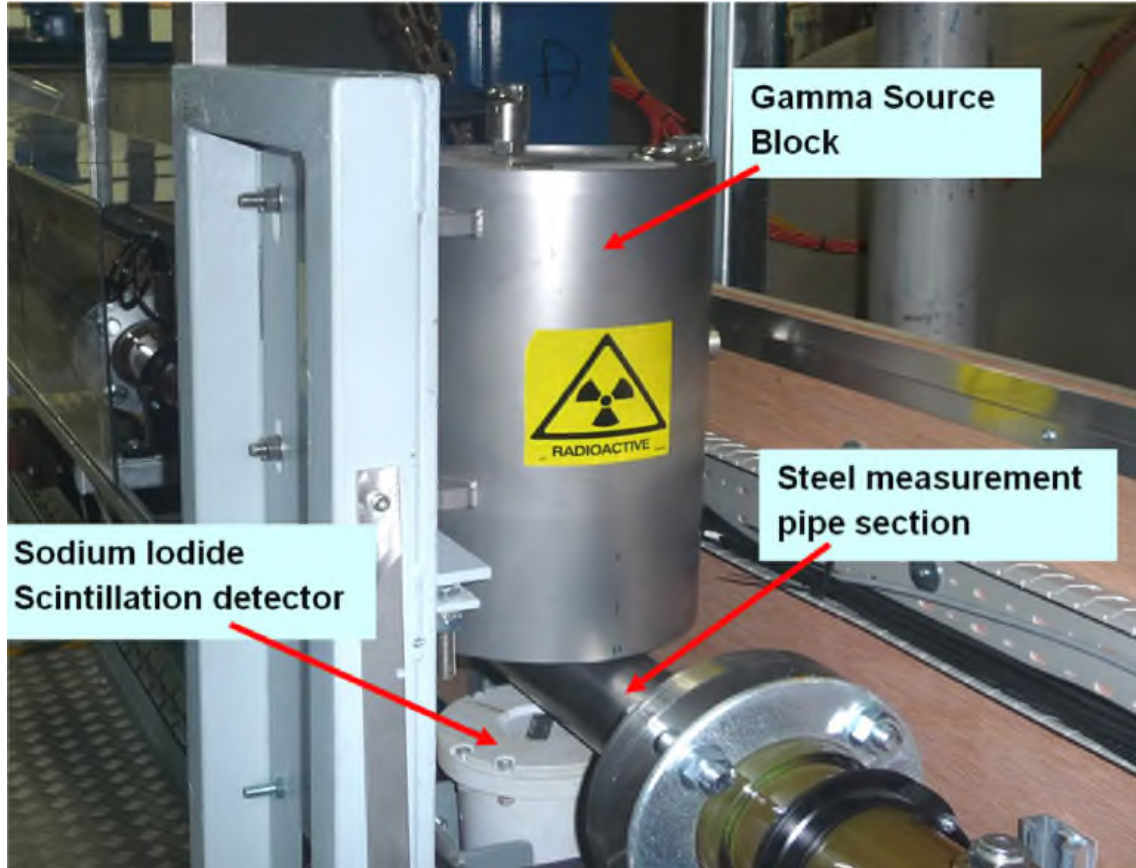
### 3.3 Gamma Densitometer

#### 3.3.1 Basic Concept Gamma Rays

Radiation basically refers to the transfer of energy from one place to another. Radiation detectors are generally referred to as “Dosimeters” in a field of study called dosimetry. A term better explained as the function of an instrument for the measurement of dose. Generally, detectors or dosimeters function in the provision of interpretable data on characteristics of a radiation field or provision of interpretable estimates of the nature and magnitudes of some radiation effects in a medium (Lewis-Van et al., 1980).

In this experimental study, two single-beam gamma densitometer provided by Neftemer Limited which operates in the count mode was used to measure accurately the liquid holdup for two phase air–water and air-oil experiments. The gamma densitometer whose main components are highlighted in Figure 3-14 consists of a single energy source emitting gamma rays at 662 Kev high energy level (hard spectrum) and the soft spectrum, lower energy level with range of 100 ~ 300 Kev. Caesium 137 acquired via a sodium iodide scintillator was used in the study. The energy source is attenuated through a steel wall in the measurement section. A proprietary DAS is used for voltage signal acquisition produced by the

detector, ICP i-7188 programmable logic controller which is used to convert the raw voltage to gamma counts signals (counts are the remainder of the attenuation signals after absorption by the media it passes through).



**Figure 3-14: A gamma densitometer clamped onto the 3-inch multiphase flow test facility**

Before the commencement of experimental data collection for different flow conditions, separate average gamma count values were determined for individual component phases of the working multiphase fluid — 100% heavy oil, 100% water and 100% air— under static conditions. These average gamma photon count values are the calibration results which aids the determination of in-situ chordal phase fractions from the gamma densitometer.

The Beer-Lambert equation represented by (3-1) is used for linear attenuation coefficients computation and hence, the liquid hold up. For an empty pipe, the gamma radiation beam's intensity remains unchanged inside the pipe because of the non-existence of an attenuating media, however; some of the incident beam is attenuated at the entrance and exit of the beams due to the pipe walls.

$$\lambda_L = \left[ \frac{\ln\left(\frac{I_M}{I_A}\right)}{\ln\left(\frac{I_L}{I_A}\right)} \right] \quad (3-1)$$

Where:

$I_M$  = average gamma count obtained from liquid-gas mixture in the pipeline

$I_A$  = average calibration gamma data obtained for empty pipe (i.e. 100% Air)

$I_L$  = average calibration gamma data obtained for pipe containing pure liquid

$\lambda_L$  = Liquid Hold Up

As a non-intrusive investigation instrument used for the measurement of multiphase flow parameters. The gamma densitometer must be calibrated either on-line or static bench test for more accurate result. For the purpose of this experimental investigation, the gamma densitometer count rates for the individual test fluid were determined in static conditions. The process of static calibrations involve a procedure where by the test pipe is filled completely with each of the test fluid (i.e. CYL 680 and Air) and repeated when half-filled mimicking stratified flow with the photon count rates for each are recorded accordingly. The liquid ( $I_L$ ) and gas ( $I_A$ ) are outputted with lower and higher count-rates as can be seen from Figure 3-16 . The lower count rate of for the liquid is attributed to high attenuation. The average error for the static bench test conducted was found to be 10% as illustrated by Figure 3-15 for the Gamma predictions in comparison to the value obtained from a measuring cylinder. The error margin in measure can be credited the beam width whose liquid holdup measurements predict a liquid holdup by length relatively better than liquid holdup by volume considering the fact that it is

single beam gamma densitometer. For this study two gamma densitometers placed 103D and 124D downstream of the last injection point.

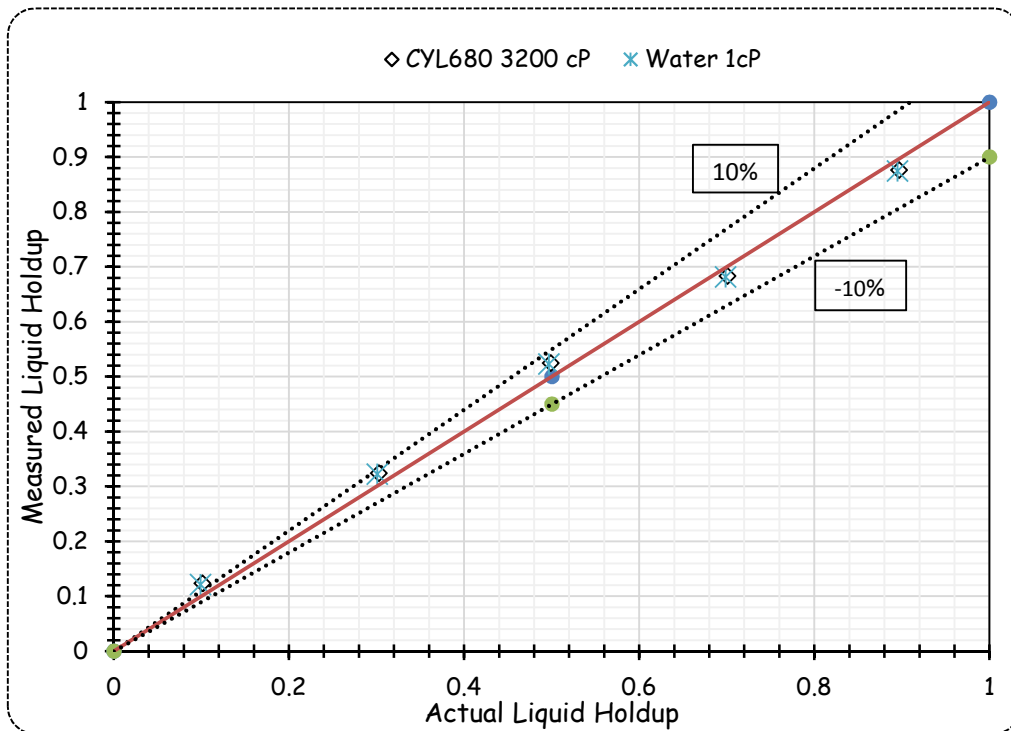


Figure 3-15: Actual liquid holdup versus gamma estimated holdup

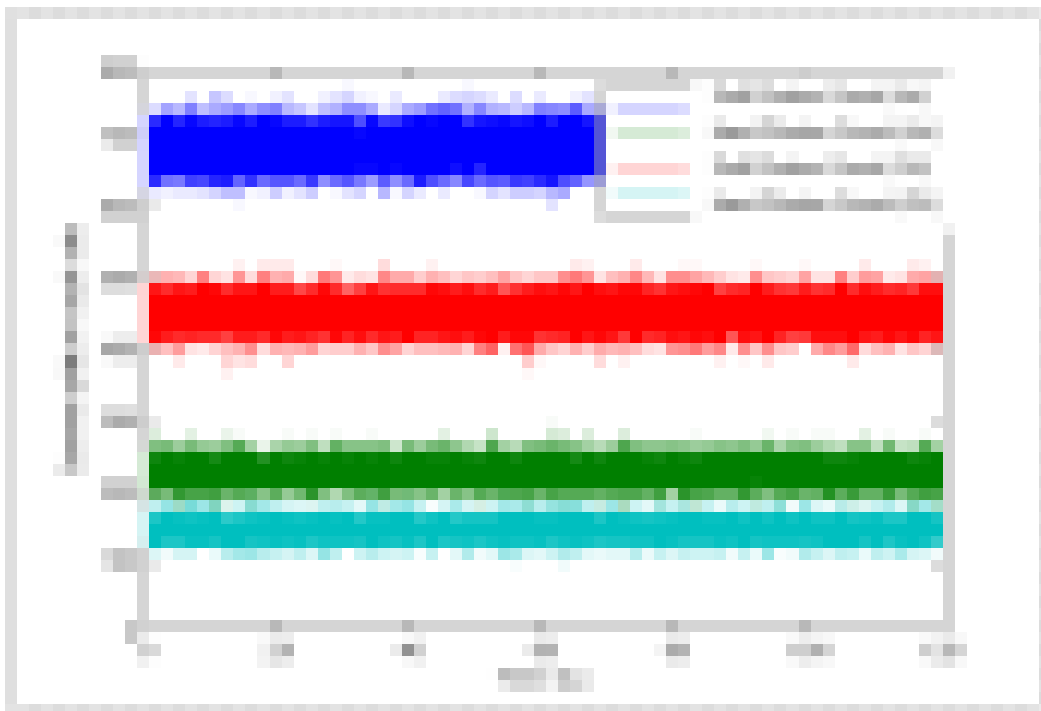
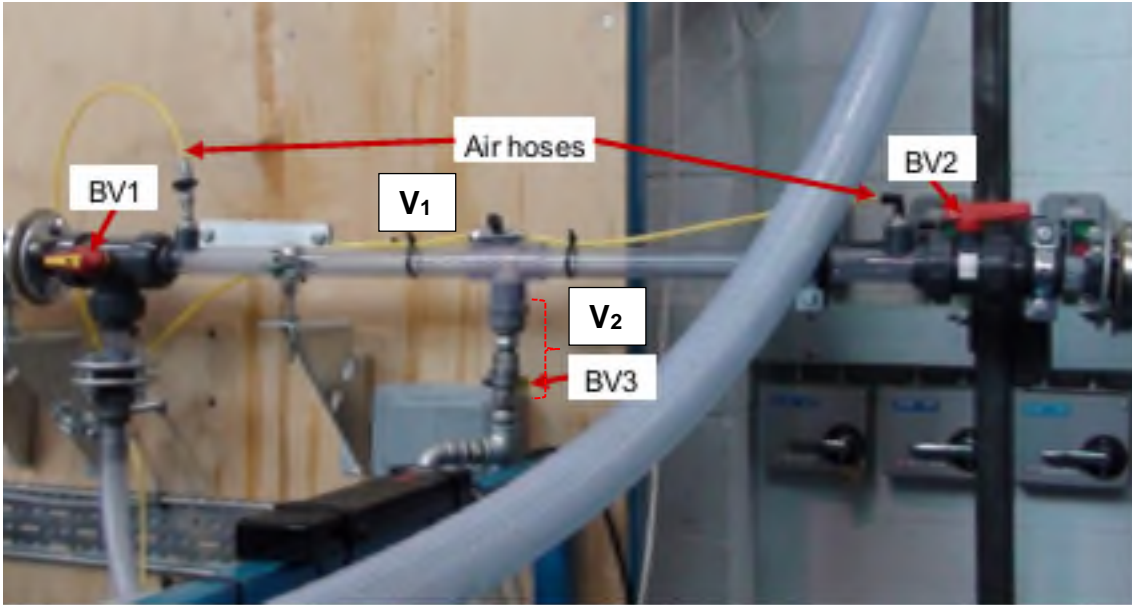


Figure 3-16: Gamma photon count rate for single phase oil and air bench test

The gamma ray detection system outputs measurement in two forms namely; direct rays and scattered rays. While the direct rays is the gamma densitometer hard photon count rate, the scattered rays is the summation of both soft and hard photon count rate. Figure 3-16 below is a plot of gamma densitometer soft and hard count rate for air and oil phases used for this investigation. From the figure, it can be seen that the measurement exhibits some fluctuations, this is normal as radioactive phenomena are random and discrete in their nature. The fluctuations were however taken care of by utilizing the MATLAB signal processing toolbox (smooth filter). It is important to note that average output from normalized photon count rate for both hard and soft count are equal, the gamma hard photon count rate was however utilized for this study

### **3.4 Quick Closing Valves**

The water holdup was measured using the technique of quick-closing valves which works such that once there is a steady flow of the mixture through the flow and upon achieving full flow development, the valves are closed trapping the fluid and thereby diverting the flow via the T-junction. The process of calibration involves running only water through the flow loop with the volume taken as  $V_1$  and  $V_2$  as shown pictorially in Figure 3-17. The volumes of samples obtained for three different water flow rates varied within 10ml as shown in Figure 3-17 (a). The volume obtained for  $V_1$  and  $V_2$  were 538 ml and 28 ml respectively, thus the total volume used for the horizontal section BV1 and BV2 was 510 ml. This volume was as the bases for the calculation of water holdup as explained below.



**Figure 3-17: Quick closing valve section for water holdup measurement**

If the volume of the horizontal sampling section is given by  $V_3$

$$V_3 = V_1 - V_2 \quad (3-2)$$

For water-assisted heavy oil flow, as water is always the continuous phase, the small section in the vertical port line above the valve BV3 is occupied by water. Denoting  $V_4$  as the volume of water collected water for two-phase liquids, the volume of water in horizontal sampling section,  $V_5$  can be estimated by

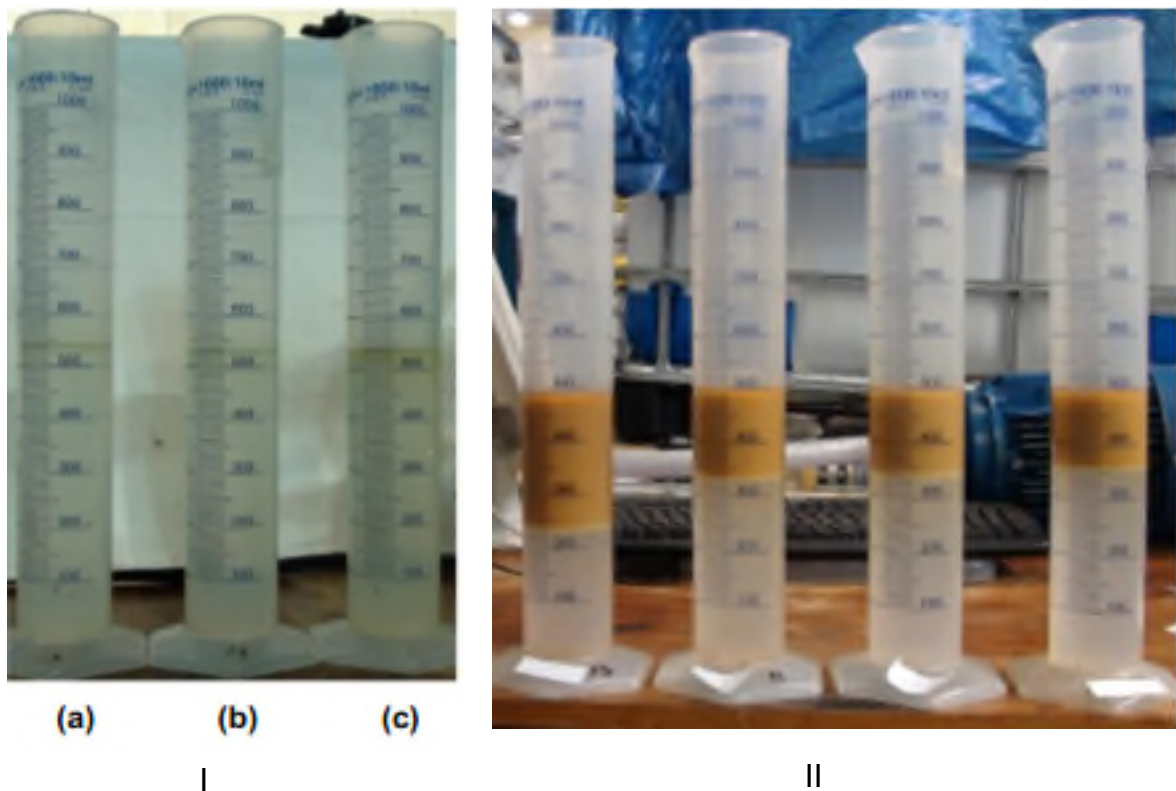
$$V_5 = V_4 - V_2 \quad (3-3)$$

Thus the water holdup,  $H_W$ , can be calculated as

$$H_W = \frac{V_4 - V_2}{V_1 - V_2} \quad (3-4)$$

While the oil holdup can be obtained from

$$H_o = 1 - H_W \quad (3-5)$$



**Figure 3-18: (I) calibration samples collected for the fluid sampling section volume. (a)  $V_{sw}= 0.6$  m/s; (b)  $V_{sw}= 0.8$  m/s; (c)  $V_{sw}= 1.0$  m/s. (II) Collected samples of two-phase flow for different flow conditions**

### **3.5 Test Materials and Matrix**

The section aims towards highlighting test fluids used for experimental investigation and their physical properties which is desirable in aiding the understanding of multiphase flow characteristics.

#### **3.5.1 Test Fluids**

The test fluid used for this investigation includes water and mineral oil with a generic name CYL680 manufactured by Total Limited, UK with physical properties at 25°C given as 917 kg/m<sup>3</sup> and 1.83 Pa.s for density and viscosity respectively. The oil's minimum and maximum viscosity were given as 0.333 and 15.33 Pa.s at temperatures of 2.5 and 50°C respectively. The water was sourced from the tap supplying water to the laboratory while air was used as the gas



phase. A summary of the test fluid and the matrix used for experimental investigation is presented in Table 3-3 below.

**Table 3-3: Summary of test fluid properties**

S/N	Density (kg/m <sup>3</sup> )	Test fluids	Viscosity (cP)	Interfacial tension (25°C, N/m)	Test matrix (m/s)	API gravity
1	1.293	Air	0.017	0.033	0.3-9.0	-
2	≈ 1000	Water	1	0.029	0.06-0.4	-
3	≈ 918	CYL680	1000~6000	0.033	0.06-0.3	22.67

### 3.6 Experimental Procedure

The process for the experimental test starts by visual inspection of the test facility to ensure that the facility and unit operations are in good working condition. The standard operating procedures for the facility are then followed as explained below.

For two phase gas-oil experiment, the test commences by first setting the chiller temperature to achieve a desired viscosity after which the oil in the oil tank is put on recirculation through the oil tank and the test facility bypass/injection section to ensure a uniform viscosity of oil. The oil tank has temperature controller coils mounted on its walls to ensure either heating or cooling of the test liquid. On the inception of any experiments, data is first obtained for a completely empty facility and a single phase filled facility to ensure noise and zero errors in the devices are eliminated during data analysis. During the test proper, oil is first fed into the main test line via a pipe section in series with the main test line. Compressed air is subsequently injected into main test line. The two fluids become mixed and develop along the pipe with varying flow patterns and other flow parameters depending on flow conditions.

Each flow condition is allowed to run for at least 30s and simultaneously logged into the computer via Labview<sup>®</sup> software. Gamma densitometer with sampling frequency of 250 Hz. are logged for each flow condition using proprietary software

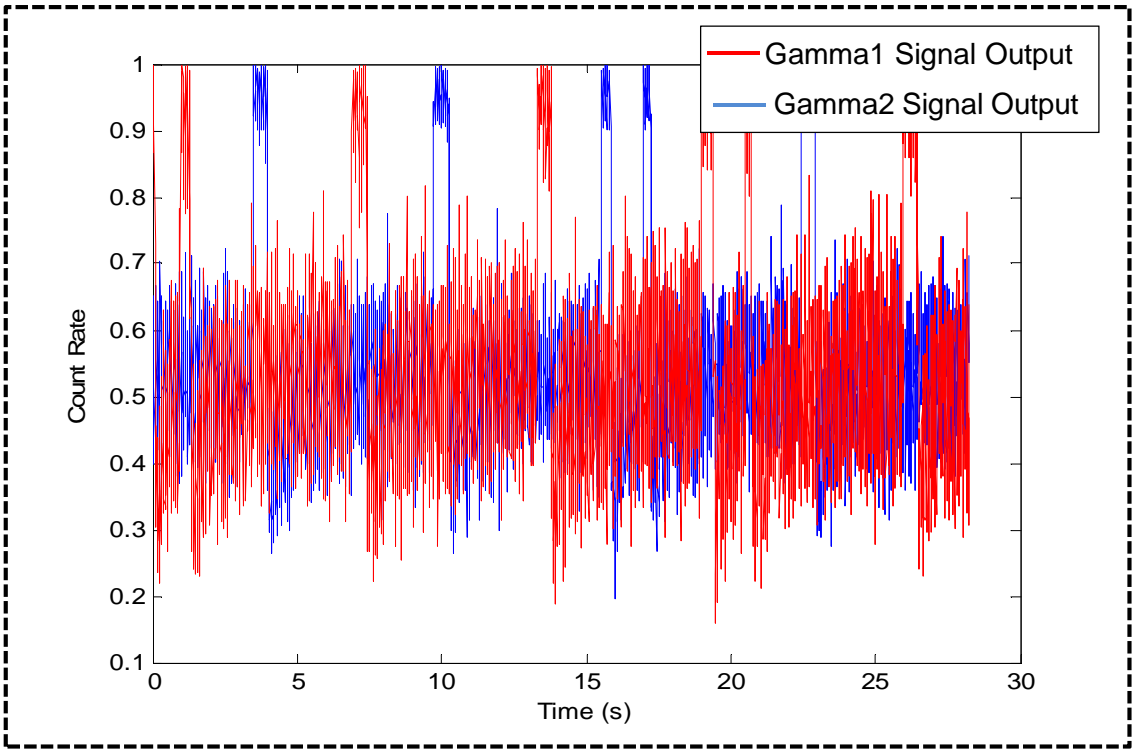
from the device manufacturers while video recordings are also obtained for every flow condition

During each test, the oil is kept at a constant superficial velocity while the gas velocity is fed in from the lowest superficial velocity of about 0.3 m/s to the highest of about 9-10 m/s while. For oil-water flow, similar procedure is followed with the gas being replaced by water and the superficial velocity of water being reduced from the maximum to minimum velocity at constant oil superficial velocity.

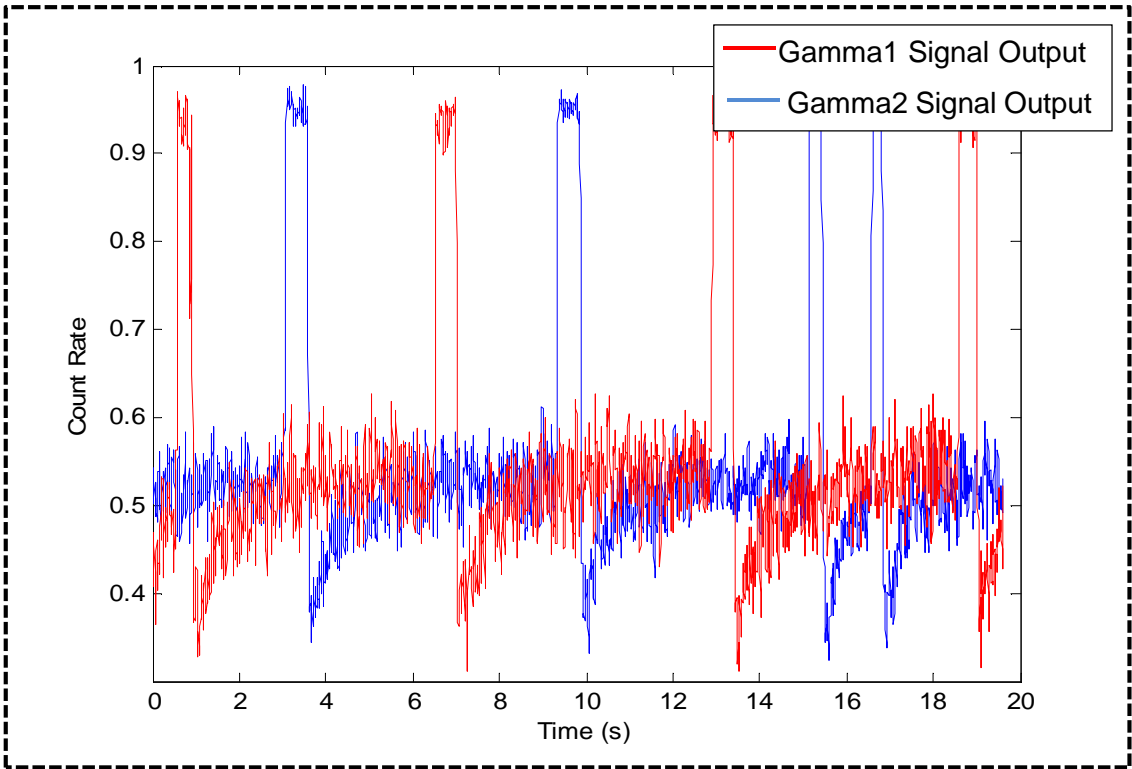
It should be noted that in the event of an emergency, the operator is required to push one of the several emergency shut down buttons available at strategic locations and in so doing; all pumps will be cut off from power supply.

### **3.7 Data Processing**

Noise in signals is an underlying problem related to several areas of research in signal processing and communications. The introduction of noise between the transmitter and receiver distorts the output signal, thus providing an inferior signal quality on the receiving end. It is therefore important to filter the raw output signal to improve data quality. For the purpose of this study, the analysis was conducted by MATLAB to filter the output signals from the gamma densitometer. The “smooth” function was used. It utilizes a moving average filter (average of 8) aimed towards noise reduction. Presented in Figure 3-19 and Figure 3-20 are typical example of raw of signal and filtered signal output from gamma densitometer.



**Figure 3-19: Raw signal output from gamma photon counts**



**Figure 3-20: Sample of a filtered signal output**

### 3.8 Cross-correlation Procedure

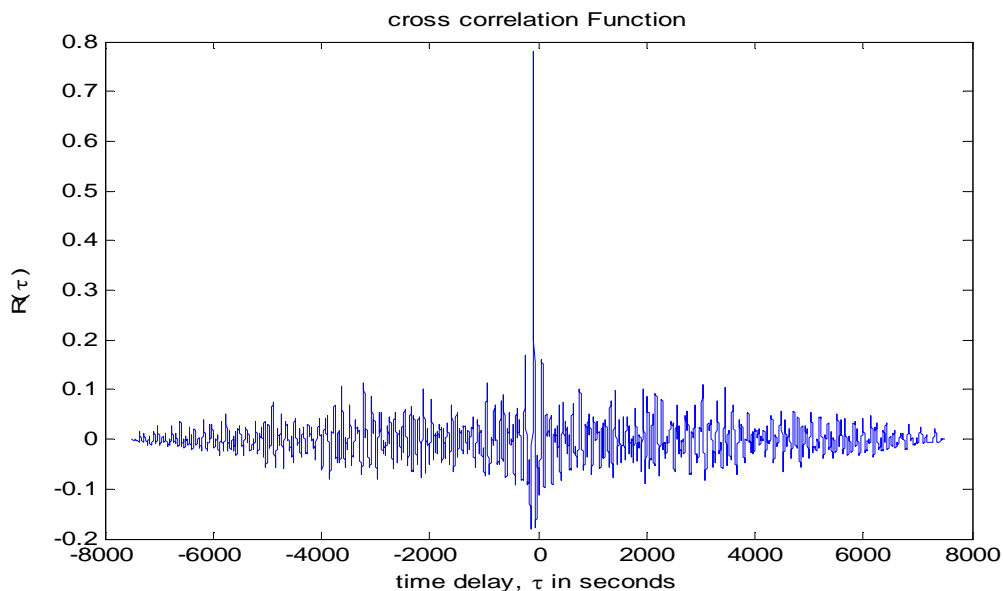
Cross-correlation is a standard method which measures the degree to which two signals correlate with one another with respect to the time displacement that exist between them. The cross-correlation for similar and identical signal tends towards unity or unity and if they are dissimilar the cross-correlation will be closer to zero or zero. Assuming two time series,  $X(t_n)$  and  $Y(t_n)$ , where  $n=0, 1, 2, 3, \dots, N-1$ , then the cross correlation coefficient is defined as;

$$R_{xy}(\tau) = \frac{C_{xy}(\tau)}{\sqrt{C_y(0)C_y(0)}} \quad (3-6)$$

$$C_{xy}(\tau) = \frac{1}{N - \tau} \sum_{n=1}^{N-\tau} X(t_n) Y(\tau + t_n), \quad (3-7)$$

Equation (3-6) and (3-7) are time series data when  $\tau$  is the temporal lag.

The filtered signal output from both gamma densitometer are then used for performing cross-correlation. It is worth noting that a better correlation is achieved if the output if the cross correlation function result tend towards “1” and no correlation if it tends towards “0”. Figure 3-21 is a typical representation a strong correlation between two time series signal output.



**Figure 3-21: Cross-Correlation results between Gamma Densitometer 1 and Gamma Densitometer 2**

### 3.9 Uncertainty Measurements

Uncertainty of a measured value is an interval around that value such that any repetition of the measurement will produce a new result that lies within this interval. Factors responsible for such differences ranges from changes in temperature, humidity etc. Other factors that may affect measurement results are instrument error, skill of the operator and measurement procedure. Uncertainty of each of the measurement values are shown below; for the direct measurements (pressure gradient, viscosity and liquid holdup), the uncertainty in measurement is obtained from the manufacturers' guide upon a repeatability test conducted to ascertain accuracy of values while for the indirect measurements (superficial liquid and gas velocities). Detailed uncertainty analysis and explications are shown in Appendix

**Table 3-4 Uncertainty of measurement**

<b>Measurements</b>	<b>Uncertainty</b>
Superficial liquid velocity	±0.5%
Superficial gas velocity	±2.1%
Liquid viscosity	± 1%
Liquid holdup	± 10%
Pressure drop	± 2%

## **4 LOW VISCOUS GAS LIQUID FLOW IN HORIZONTAL PIPE**

In this chapter, results of two-phase flow experimental investigation conducted in the 3-inch horizontal pipeline earlier described in Chapter 3 are presented. Gas-liquid two phase flow test were carried out with water as the liquid phase and air as the gas phase. Differential pressure transducers were used for the measurement of pressure gradient which permitted the effects of flow rates on flow behaviour to be studied. Hold up time trace obtained from gamma densitometer was analysed and flow characteristic such liquid holdup, slug frequency, slug translational velocity and slug length are reported while flow patterns were determined qualitatively using visual observations and high-definition video recorders. Also results comparisons with prediction models and correlations are reported.

### **4.1 Single Phase Water Test**

The single phase water test was carried out in order validate experimental set-up and instrumentation by way of comparison with established single phase flow correlations, a series of experiments was conducted on the 17m, 3-inch horizontal test facility. The water velocity investigated ranged from 0-1.4 m/s. The result of this investigation as indicated in Figure 4-1 shows that the measured pressure gradient plotted against water velocity increased with increasing water velocity this is expected since pressure gradient is a function of square of flow velocity.

#### **4.1.1 Comparison of measurements with Friction Factor Correlations**

A comparison between experimental measurements of frictional pressure gradient with prediction from Darcy-Weisbach phenomenological equation for pressure gradient correlations (Haaland, Chen, Sawmee and Fang et al., 1981) has been carried out as illustrated in Figure 4-2. The result shows an agreement with measured frictional pressure gradient with an average error margin of 2.3% which is attributed to the measurement uncertainties and flow conditions investigated and this shows the reliability and operational functionality of the experimental setup.

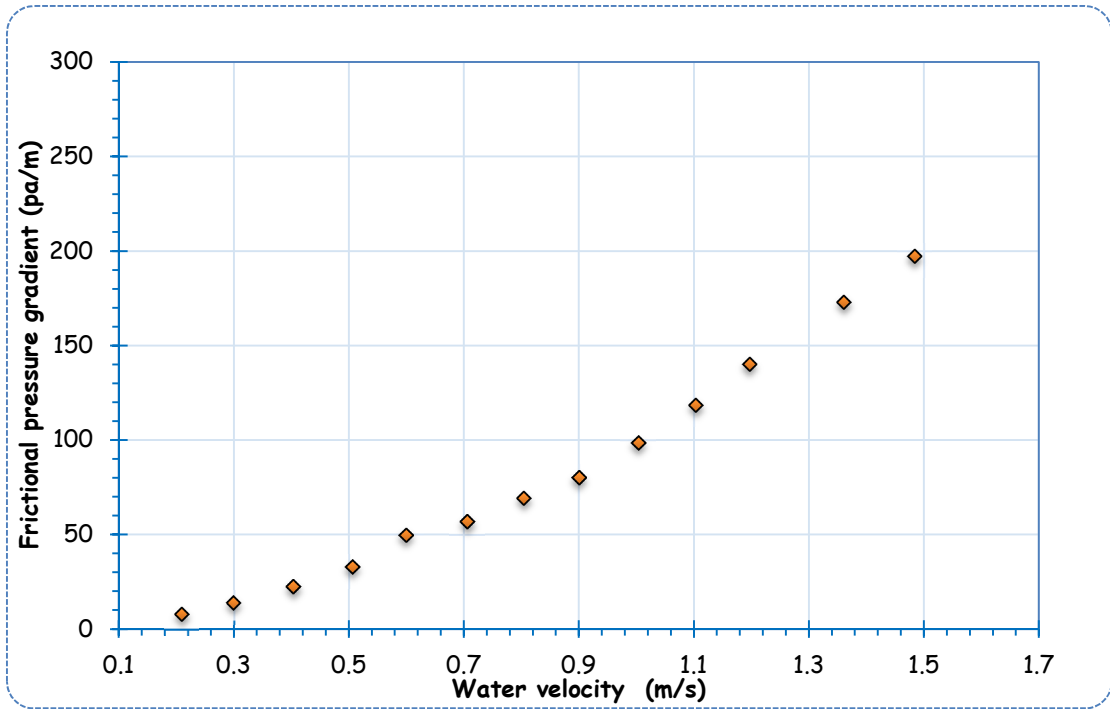


Figure 4-1: Frictional pressure gradient as a function of water velocity.

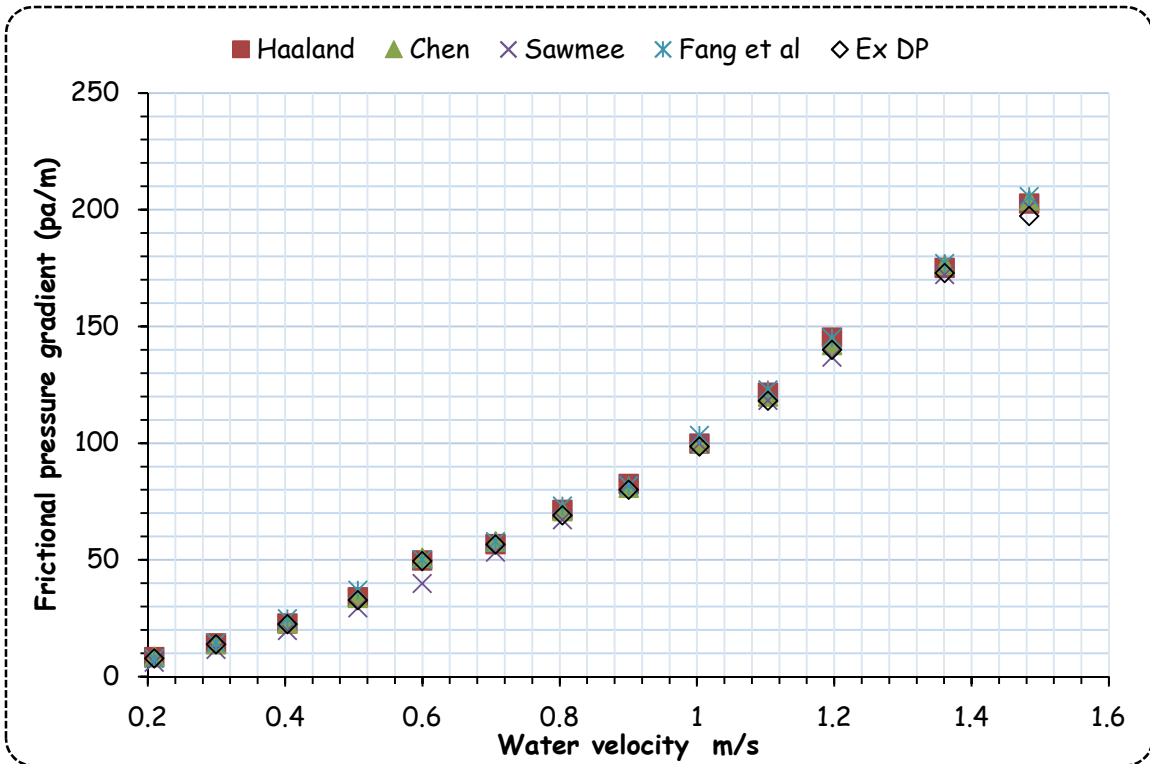


Figure 4-2: Frictional pressure gradient Vs single phase prediction models

## 4.2 Two Phase Air-Water Test

Many industrial processes (i.e. nuclear industry, refrigeration, chemical systems and air conditioning) involves the interaction of two or more phases. The interaction of this phases results in complex mixtures thereby making its knowledge of great interest to facilitate better understanding. Air-water test were investigated in the 3-inch horizontal test facility to benchmark the facility against existing standard and generally accepted flow pattern maps and to examine the facility reliability. Table 4-1 below show the test matrix used for then the experimental investigation.

**Table 4-1: Air-Water Test Matrix**

Pipe Diameter (m)	$V_{sw}$ (m/s)	$V_{sg}$ (m/s)
0.0762	0.1-0.4	0.1-12.00

## 4.3 Flow Pattern Characterization

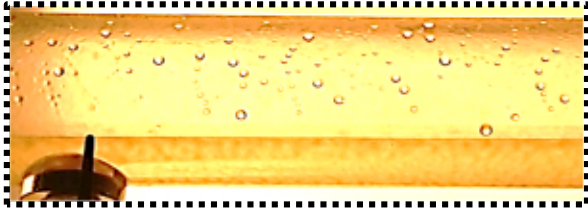


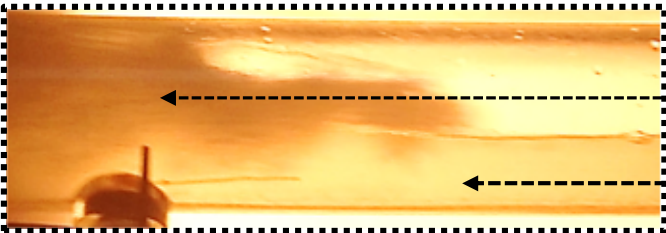
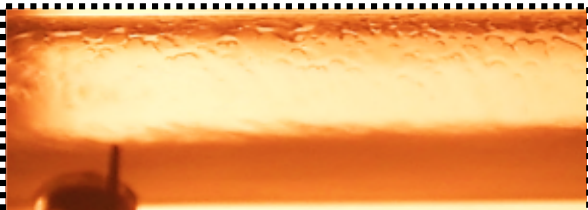
Visual inspections and video recordings were obtained for each flow condition during experiments. Side view recordings were done with a Sony HDR-CX 550 camera, wide-angle, Full HD 1080 was used for the video acquisition with its lens zoomed in (or out) at interval for each test run which lasts for 30 s. The following flow patterns were observed; stratified, stratified wavy, plug and slug flow. Individual description of the flow patterns are presented below.

- *Stratified flow*: this flow pattern as illustrated occurs as the dominant flow pattern at low liquid superficial velocity @  $V_{sw}=0.1$  m/s irrespective of the operating superficial gas velocity. This flow pattern is characterized by complete separation of the two phases such that the less dense phase (gas) occupies the top of the pipe cross-sectional area while the denser phase (liquid) occupies the bottom owing to gravity effects with an undisturbed horizontal interface. This is not surprising as can be seen from the pictorial representation that the liquid height is not high enough to aid transition to another flow regime.

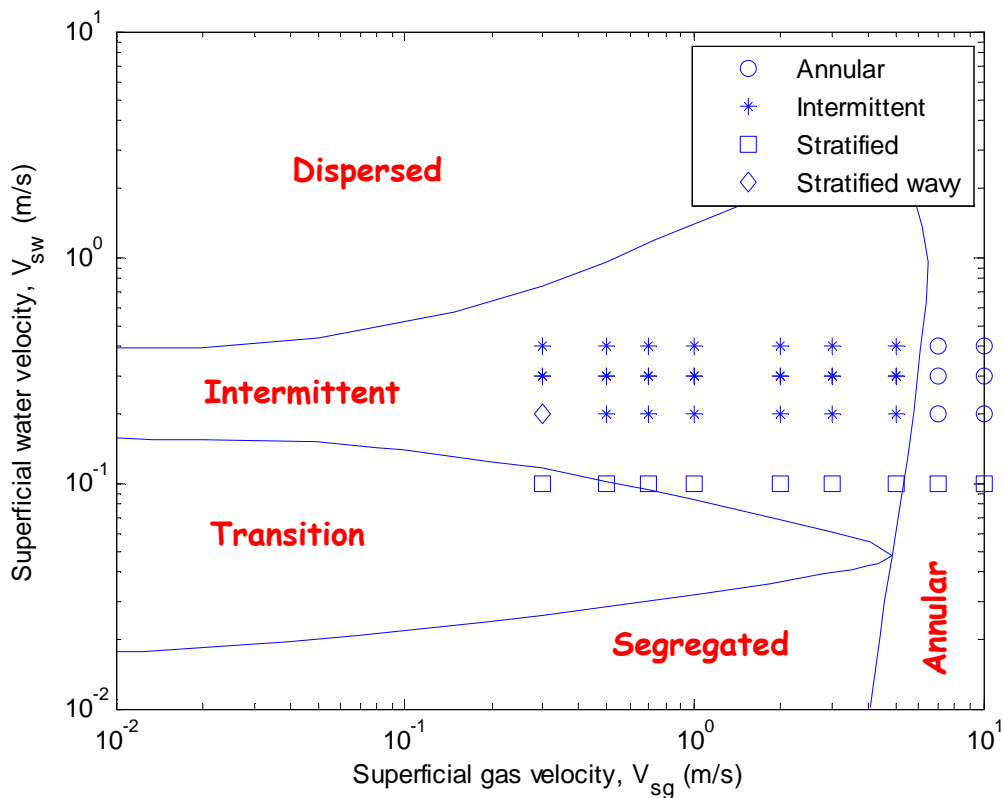


- *Stratified wavy flow*: increasing the superficial gas velocity, provided the liquid height is less than half full will result in the interface becoming disturbed with surface ripples or small amplitudes illustrated in Table 4-2. The wave pattern usually have little or no effect on the pressure fluctuations
- *Plug flow*: At much higher liquid level and lowest gas superficial velocity, this flow regime which is characterized by liquid plugs with no noticeable gas entrainment that are separated by elongated gas bubbles whose diameter are smaller than that of the pipe diameters. The elongated gas bubble is such that the phase flow in strata with bulk of the gas at the top and the liquid film occupying the base of the pipe owing to gravity effects. Its mechanism of formation is as a result of gradual build-up of the liquid level to more than half of the pipe diameter.
- *Slug flow*: With continuous increase in the gas velocity, a point is reached when the elongated bubble becomes similar in size as the pipe diameter moving at higher momentum and shorter liquid body compare to plug flow. Gas entrainment is a characteristic feature of the elongated liquid body in slug flow in comparison with plug flow which has no entrainment.
- *Annular flow*: Further increasing the gas superficial velocity, a point is reached when the liquid holdup in pipe becomes inadequate to form liquid body capable of bridging the top of the pipe of the pipe and this brings about the leftover liquid to be swept to the top section of the pipe forming an annulus liquid round the pipe though thicker at the bottom owing to gravity effects and the gas phase flowing at the core of the pipe. A flow pattern generally term as annular flow. Table 4-2 below gives a pictorial description of the observed flow patterns

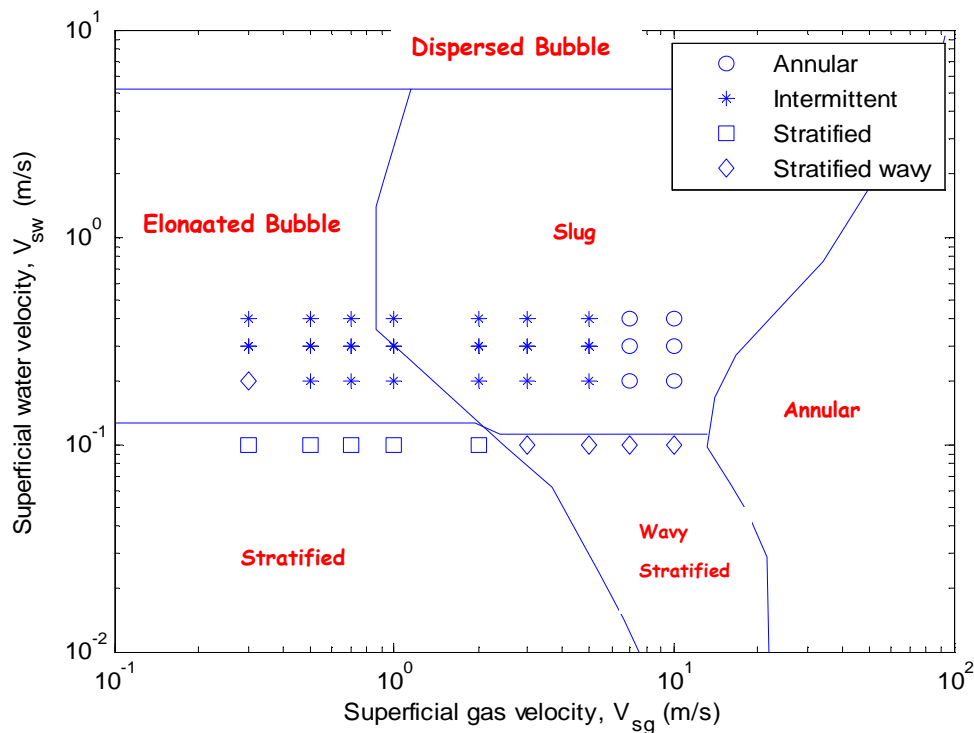
**Table 4-2: Pictorial representation of observed flow patterns**

Superficial Water Velocity $V_{sw}$ (m/s)	Superficial Gas Vel. $V_{sg}$ (m/s)	Side View	Flow Pattern
0.1	0.3 -10		Stratified Flow
0.2- 04	0.3-0.7		Wavy-stratified flow
0.2- 04	0.7-2.0		Plug Flow
0.2- 04	2.0-8.0		Slug Flow
0.2- 04	8.0-10.0		Annular flow

The flow patterns observed in this study are compared with the flow pattern maps of (Beggs and Brill, 1973; Mandhane et al., 1974) as presented in Figure 4-3 and Figure 4-4 below. The choice of Beggs and Brill, 1973 was based on the fact that the flow pattern map was constructed over wide range of flow condition with relatively better correlations and generally acceptable in the industry while Mandhane et al, 1974 was chosen wide acceptability and simplicity. The test result agreed excellently with the Beggs and Brill, 1973 in the intermittent flow region than the Mandhane et al., 1974 flow pattern map with some slight differences in the separated region and this can be the diameter differences confirming the findings of (Weisman et al., 1979) who reported that an increase in pipe diameter moves the transition line from separated to intermittent region towards higher liquid flow rates.



**Figure 4-3 Comparison of air-water test and Beggs & Brill (1973) flow pattern map**

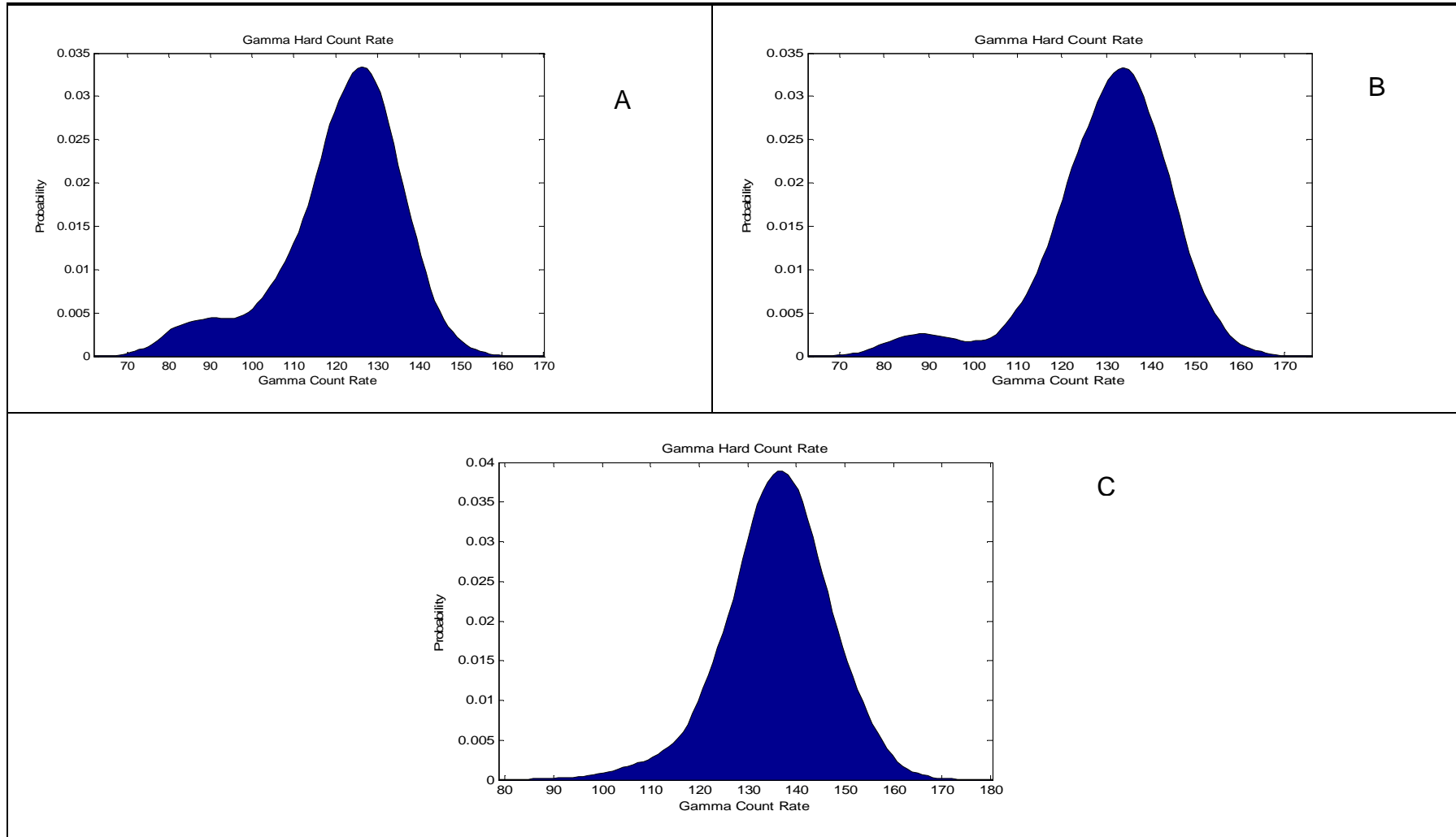


**Figure 4-4: Comparison of air-water test and Mandhane (1974) flow pattern map**

#### **4.4 Flow Pattern Visualization with Gamma Densitometer**

Gamma Densitometer with a sampling frequency of 250 Hz was used to study the phase distribution of air-water two phase flows in 3 inch horizontal pipe. Table 4-3: PMF plots of Air-Water experiment below shows the plots of gamma densitometer hard photon count rate for air-water experimental runs as a validation of visual observation presented above. The PMF structure for figure A and B shows a bi-modal distribution with two peaks. The two peak structure is a qualitative confirmation of visually observed intermittent flow pattern (plug and slow pattern). The peak with the highest photon count rate is indicative of a passing film region while the smaller peak with lower count rate is indicative of a passing slug liquid body through the detector. Figure A which represents plug flow pattern is differentiated from Figure B representing slug pattern by virtue of the dominance of the smaller peak for Figure A as against B attributed due to less entrainment in the liquid body when compared to Figure B characterised by high entrainment in the liquid body. The uni-molar distribution as illustrated by Figure C is indicative of annular flow.

Table 4-3: PMF plots of Air-Water experiment



#### 4.5 Pressure Gradient

The accurate prediction of this key parameter is fundamental to the efficient design of pipelines for oil and gas industry as it gives an estimate for the power requirements for the cost efficient transportation of oil and gas. In this experimental investigation, pressure gradients were measured by means of a differential pressure transducer on the 3-inch facility. The results of two phase pressure gradient obtained for air-water test on the 17 m long 3-inch horizontal pipe as shown in Figure 4-5 indicate an increase in pressure gradient with increasing superficial gas velocities. For example: Figure 1-3 show that at the superficial liquid velocity of 0.29 and 0.385 m/s, the pressure gradient increased from 0.112 to 0.457 kPa/m and 0.135 to 0.624 kPa/m respectively and this is because an increase in water superficial velocity result to an increases in the water content in the pipe which in turn increase the shear in the pipe walls. Similarly, increase in the gas superficial velocity was observed to increase pressure gradient which steepened at higher superficial gas velocities and this can be attributed to increased shear in the pipe walls corresponding to the annular flow region which is characterised by the liquid phase flowing at the pipe wall and the gas phase flowing at the core.

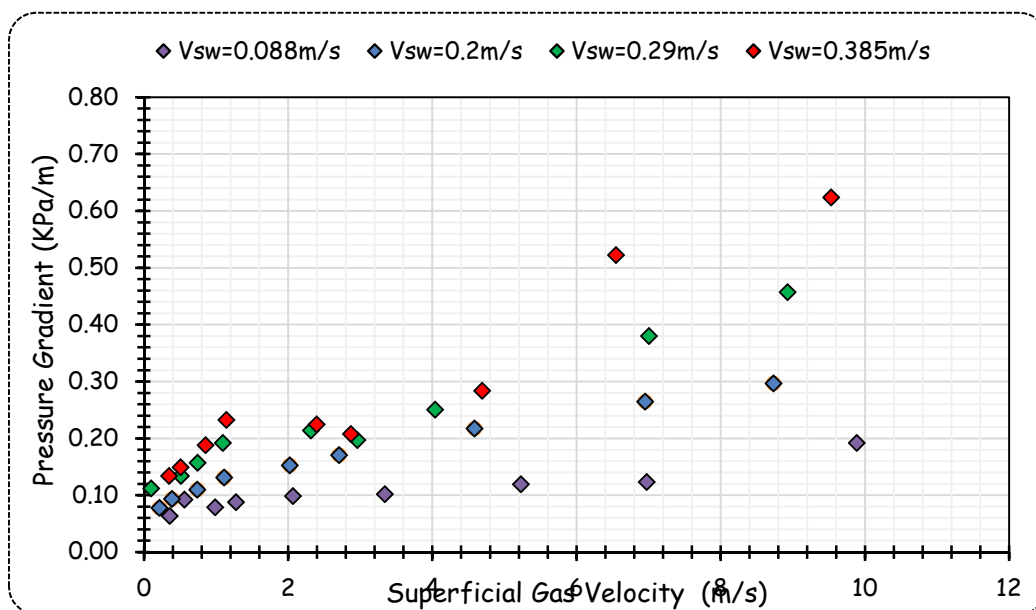


Figure 4-5: Pressure gradient as a function of gas superficial velocities for different superficial water velocities

#### 4.6 Comparison of Measured Pressure Gradient with Predictions Models

The predictions models of the (Beggs and Brill, 1973; Dukler and Hubbard, 1975) for pressure gradient were evaluated against the measured experimental values using statistical analysis i.e. the Average Percentage Error (APE), Average Absolute Percentage Error (AAPE) and Standard Deviation for which results obtained as indicated in Figure 4-6 for both prediction models shows that the Beggs & Brills prediction model performs better with an APE, AAPE and SD of -1.908, 36.57716 and 17.98% respectively against the (Dukler and Hubbard, 1975) model with an APE, AAPE and SD of 27.56, 53.66512 and 30.29% respectively.

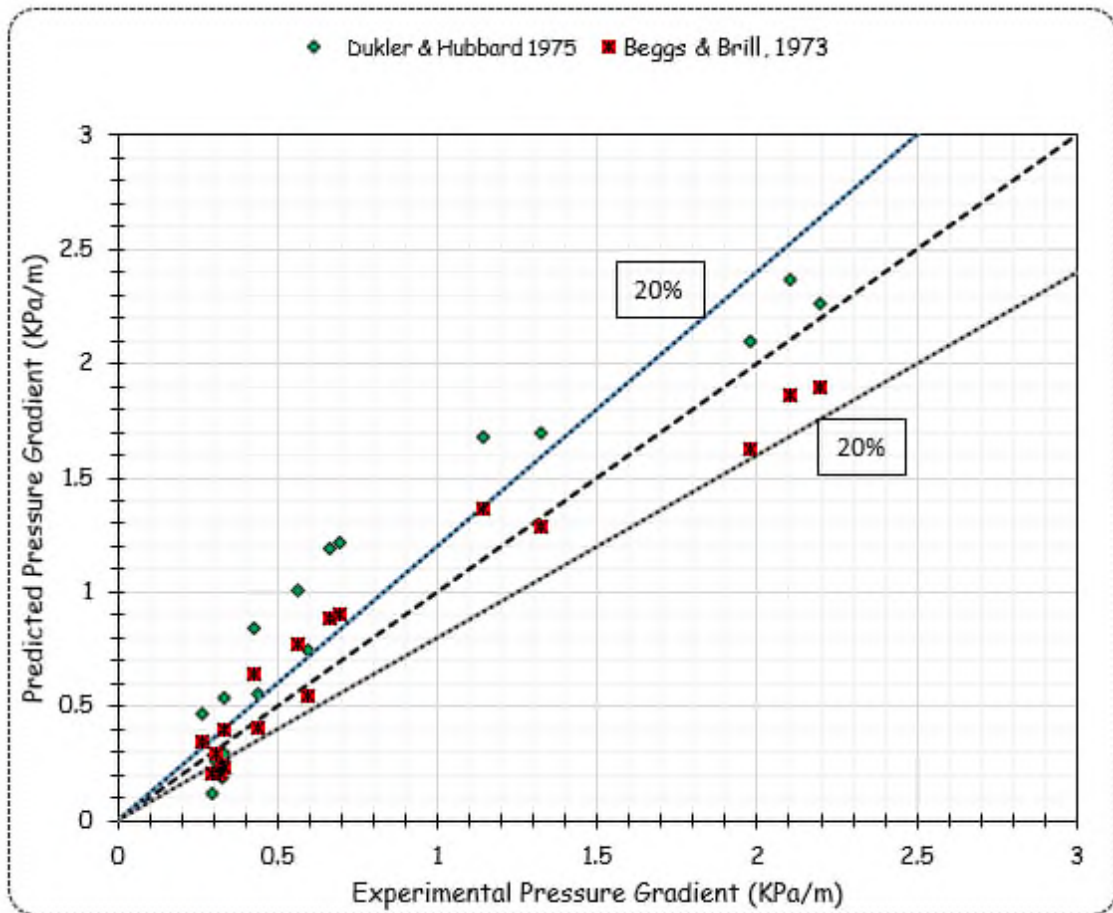
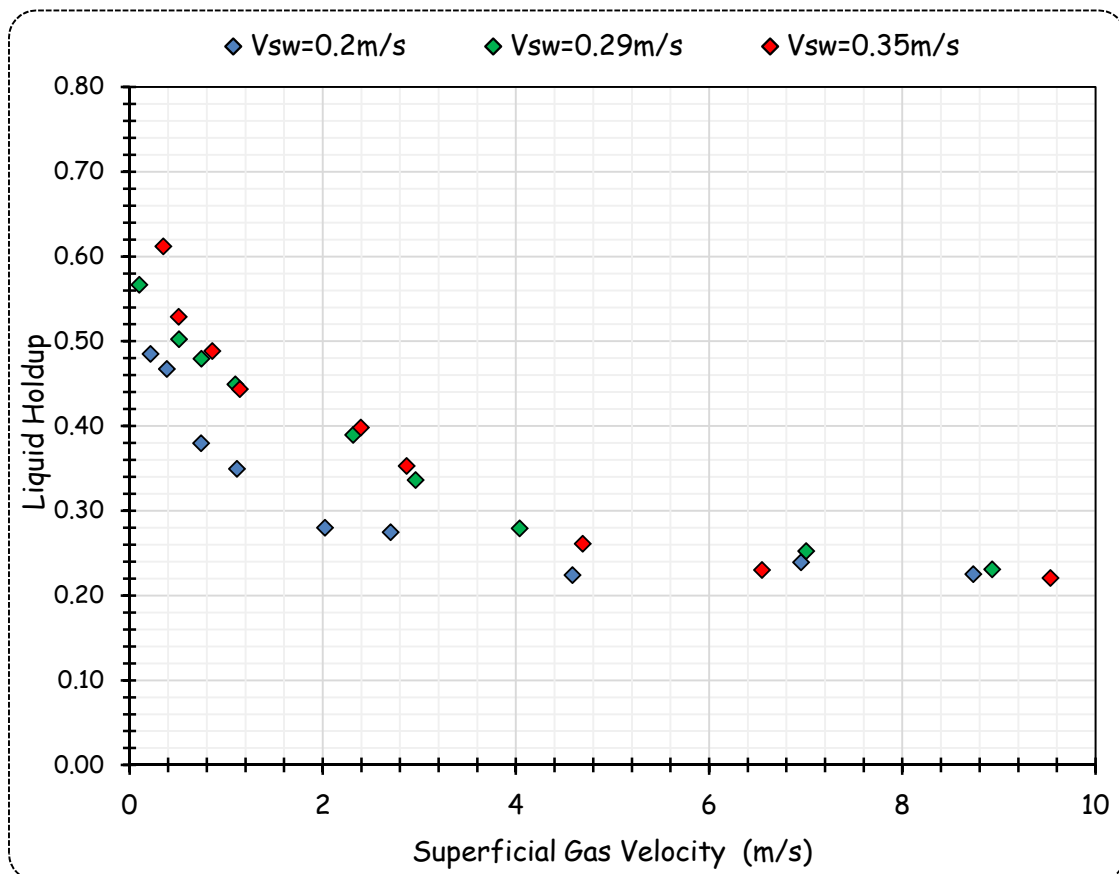


Figure 4-6: Pressure Gradient Prediction as a Function Experimental Measurement

## 4.7 Liquid Holdup

Liquid holdup plays a very vital role in the oil and gas industry as its accurate prediction is crucial to the effective prediction of many two phase flow calculations and in most cases serve as the starting point of this predictive models. The experimental liquid hold was computed from gamma densitometer photon count using the Beer-Lambert logarithmic equation explained in subsection 3.3.1.

The result of the liquid holdup as presented in Figure 4-7 shows that the time averaged liquid holdup measurement obtained for a period of 30 sec exhibits a general decreasing trend for liquid holdup value as the gas superficial velocity increases. An increase in the gas superficial velocity brings about more of the gas phase occupying the total cross sectional area of the pipe analogous to reduction of the liquid holdup in the cross sectional area of the pipe.



**Figure 4-7: Measured Liquid Holdup versus Superficial Gas Velocity**



A comparison of the measured liquid holdup against liquid holdup prediction models found in the literature was conducted. The drift flux models used for the comparison are; (Ishii, 1977; Kataoka and Ishii, 1939; Maley and Jepson, 1998; Pearson et al., 1984; Ros, 1961; Sonnenburg, 1989; Zuber and Findlay, 1965) The accuracy of the models was measured by the Average Percentage Error (APE), Average Absolute Percentage Error (AAPE) and Standard Deviation (SD) for which the result obtained as shown in Figure 4-7 indicates that the Jowitt et al. 1984 drift flux model outperformed all the model tested and this can be attributed to the fact that the model accounted for the fluid properties of phase involved unlike the others. Presented in Table 4-4 is the performance comparison for liquid hold up predictions

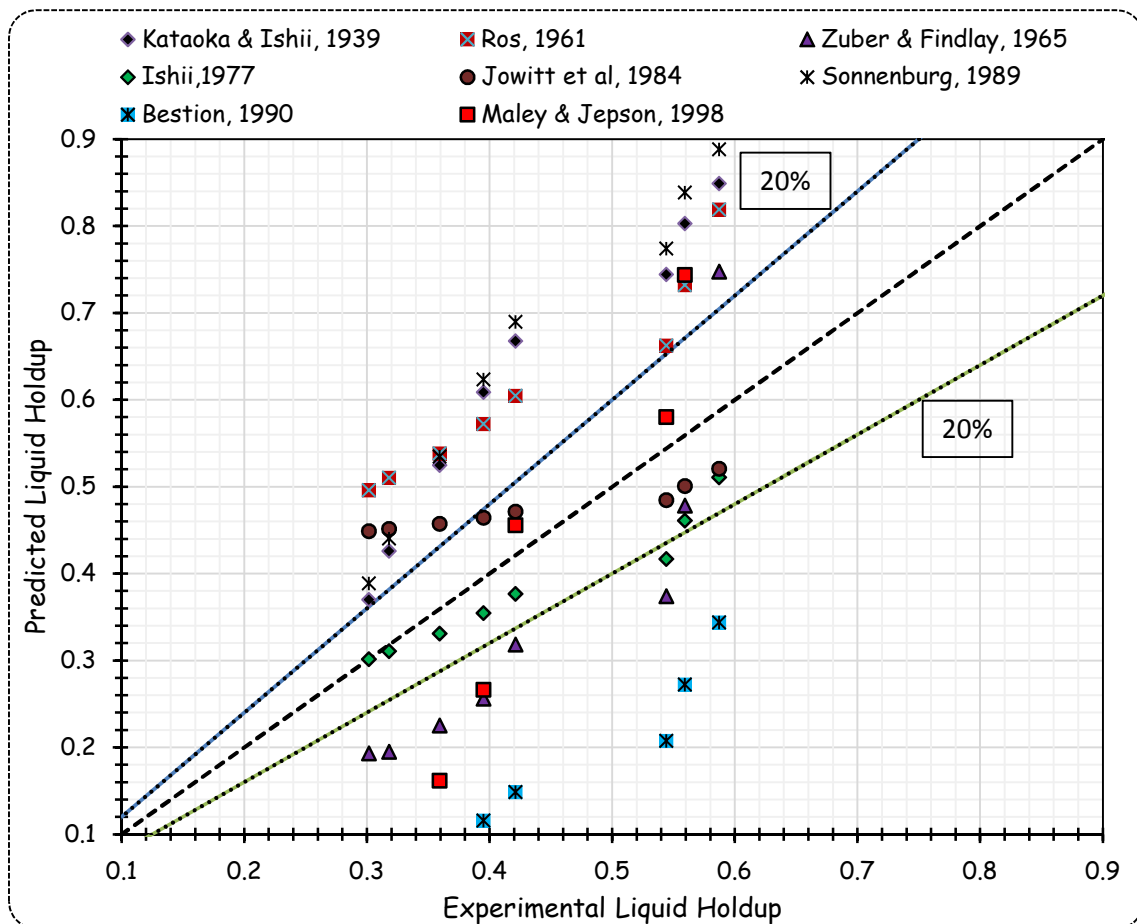


Figure 4-8 Comparison of measured liquid holdup and prediction models.

**Table 4-4 Evaluation of Liquid Holdup correlations using Statistics**

PREDICTION METHOD	APE	AAPE	SD
KATAOKA AND ISHII (1939)	42.57	30.61	10.64
ROS (1961)	21.45	21.45	15.84
ZUBER & FINDLAY (1965)	-32.37	41.48	17.11
ISHII (1977)	-24.64	24.64	10.63
JOWITT et al (1984)	-5.96	5.96	0.65
SONNENBURG (1989)	26.86	33.36	21.31
BESTION (1990)	-69.82	69.82	19.79
MALEY & JEPSON (1998)	-22.05	52.40	30.65

## 4.8 Slug Translational Velocity

Slug translational velocity is one of the closure parameters that is often used as input parameter for most slug flow models. It was experimentally estimated by dividing the distance between the two gamma densitometer by the time lag obtained from cross correlation of the signal output as described in sub-section 3.8 above. Figure 4-9 below shows a plot of measured slug translational velocity versus mixture velocity which indicates a linear tendency with an increase in slug translational velocity as mixture velocity increases for all the flow conditions investigated. The flow coefficient was found to be 1.19 which is consistent with the findings of (Carpintero Rogero 2009; Romero et al. 2012; Pan 2010 and Lu 2015 ).

### 4.8.1 Evaluation of Slug Translational Velocity Prediction Models

Measured slug translational velocity in this study were compared prediction models in the literature. The models whose performance were evaluated include (Nicklin et al. 1962; Gregory & Scott 1969; Hubbard 1965; Kouba & Jepson 1990 and Nicholson et al. 1978). The performance evaluation as presented in Figure 4-10 and Table 4-5 shows that Nicklin et al. 1962 and Nicholson et al. 1978 shows a better a agreement with the present data as compared to others and this can be attributed to the fact that they both accounted for drift velocity which (Nicholson et al. 1978 and Bendiksen 1984) have shown to exist in horizontal cases and can even even exceed the vertical case value.

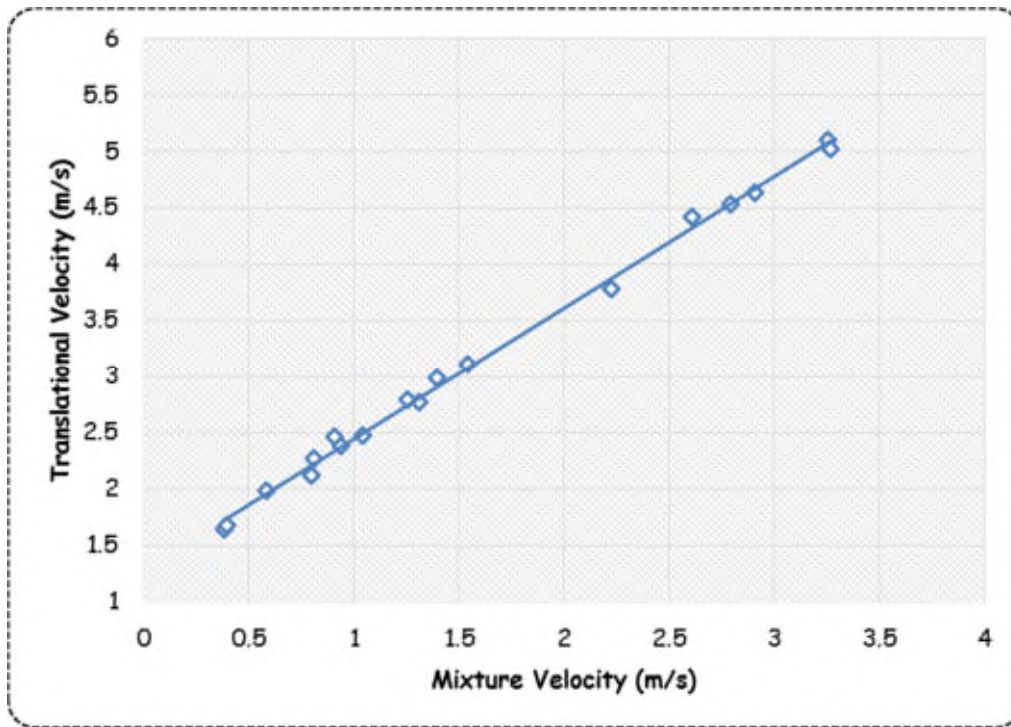


Figure 4-9: Slug translational velocity plotted as a function of mixture velocity

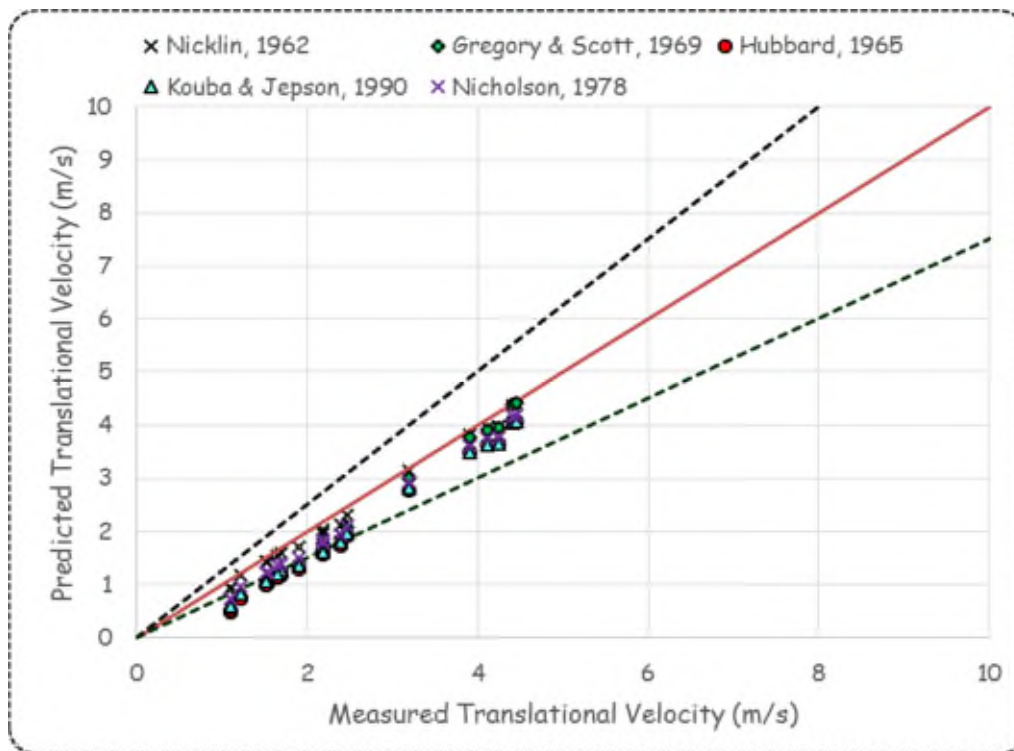


Figure 4-10: Comparison between measured data and prediction models

**Table 4-5: Performance evaluation of prediction models for present data**

Prediction Models	APE	AAPE	SD
Nicklin, 1962	-6.58	6.58	4.31
Gregory and Scott 1969	-20.92	20.92	15.81
Hubbard, 1965	-26.78	26.78	14.64
Kouba & Jepson, 1990	-23.36	23.36	11.50
Nicholson et al, 1978	-16.57	16.57	8.07

#### 4.9 Slug Body length

This closure parameter is another primary variable in slug flow modelling. It was estimated by multiplying the translational velocity by the time lag for the flow conditions investigated. The result shows the measured slug length is approximately 24-36D with an with a mean length of 30.6D and agrees with the work of (Pan, 2010) who observed an approximate length of 20-40D and a mean length of 30D for air-water and 24D for 4cP oil-air experiment in a 0.075 m ID pipe as presented in Figure 4-11 showing measured of slug length plotted as a function of mixture velocity. It is worth noting that experimental observations according the works of (Barnea and Brauner, 1985; Dukler and Hubbard, 1975; Fabre and Line, 1992; Nicholson et al., 1978) for air-water systems in upward vertical and horizontal flows suggest that the average stable liquid slug length is relatively insensitive to the gas and liquid flow rates and depends mainly on the pipe diameter. They also concluded that average slug length has been observed to be about 15—40D. Figure 4-12 below is a plot of lognormal distribution of measured slug length which agrees with the experimental data plotted used using Easy-Fit software 3.6 conforming to the findings of (Nydal et al., 1992) who measured the statistical distributions of some slug characteristics in air-water two phase flow in horizontal pipeline and noted that the cumulative probability density function of measured slug length fits a log-normal distribution in addition to been right-skewed.

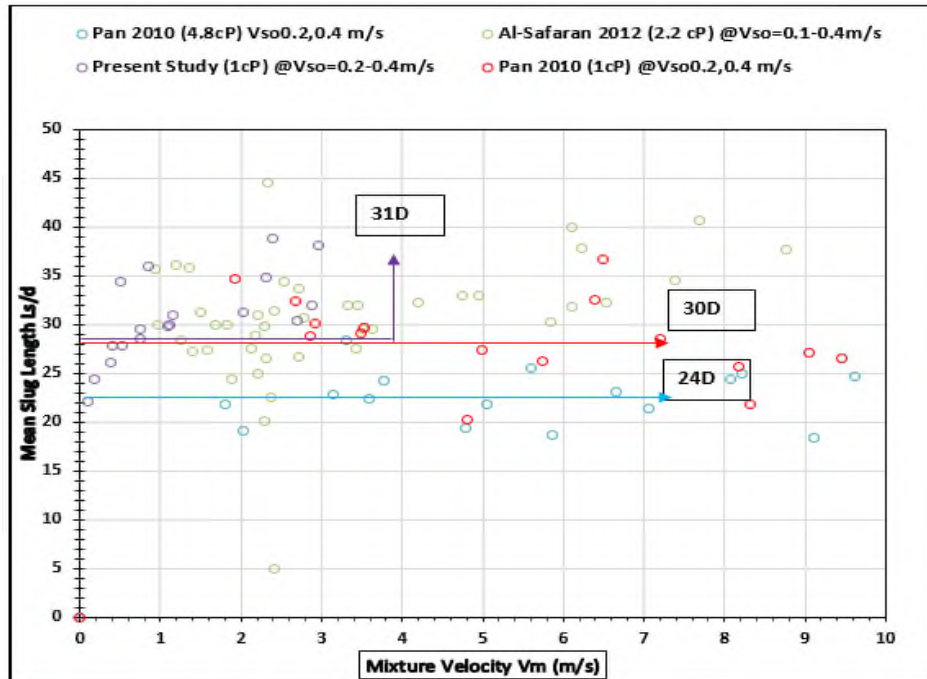


Figure 4-11: Slug length as a function of mixture velocity

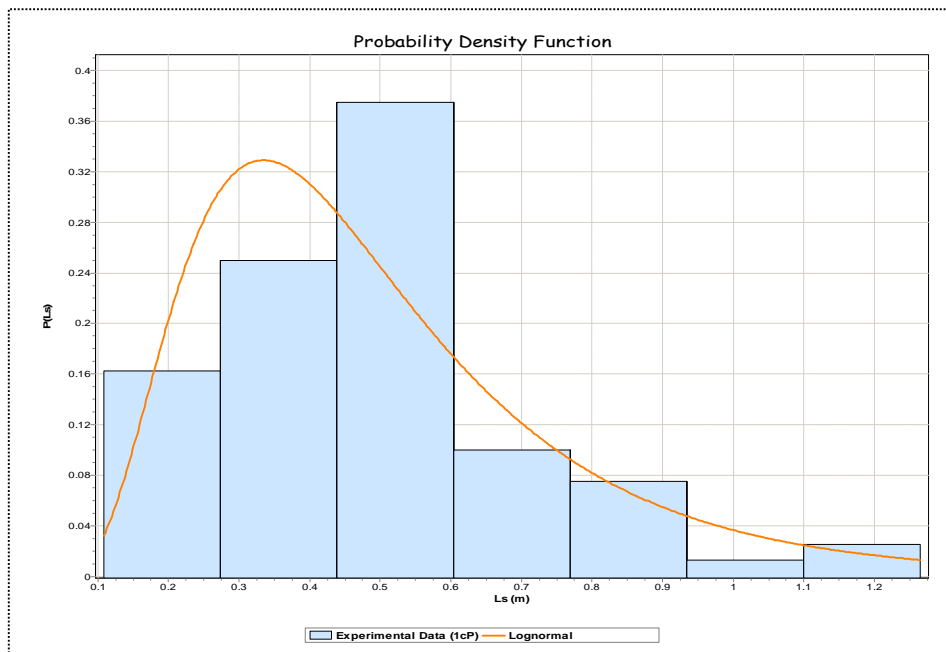


Figure 4-12: Slug length distribution and log-normal fits for flow conditions investigated ( $V_{sg}=0.3-7$  m/s and  $V_{sw}=0.2-0.4$  m/s)

### 4.9.1 Comparison with Prediction Models

The measured slug body length were compared with available slug body length predictions models in the literature. Those whose performance were evaluated as shown in Table 4-6 below include (Brill et al., 1981; Gordon and Fairhurst, 1987; Norris, 1982; Scott et al., 1989). The prediction models of Norris 1982 and Brill et al. 1981 are closer and performed better when compared to Gordon & Fairhurst 1987; Scott et al. 1989 and this is not not suprising since Norris, 1982 is a modified version of Brill et al. 1981 by the exclusuion of mixture velocity term which was found to be negligeable. Gordon & Fairhurst 1987 and Scott et al. 1989 exhibited very high descrepancy, this can be attributed to the fact that both correlations were regressed from very large large-diameter oil and gas transportation pipelines where there is the possibility long terrain-induced slugs.

**Table 4-6: Evaluation of slug length prediction against present data**

Prediction Models	APE	AAPE	SD
Norris, 1990	-78.07	78.07	3.31
Brill et al, 1981	-70.90	70.90	3.43
Gordon and Fairhurst (a) 1987	4109.47	4109.47	495.63
Gordon and Fairhurst (b), 1987	26587.48	26587.48	10845.97
Scott et al. (1989).	811.99	811.99	137.48

### 4.10 Chapter Summary

Single phase water and two-phase air-water flow in 0.0742m ID horizontal pipe are reported in this. Frictional pressure gradient for single phase water was measured and tested against friction factor correlations for single phase flow available in the literature. Those tested include; Haaland, Chen, Sawmee and Fang et al., 1981. Results obtained from comparison shows agreement with the prediction models with error margin of 2.3% indicating the reliability of the test facility.

Pressure gradient and liquid hold up analysis were carried for two phase air-water test with obtained data from the 0.074m ID horizontal test facility. Flow patterns

for the experiments conducted were monitored in addition to measurement of slug translational velocity and slug body length. The flow patterns observed were stratified, wavy-stratified, plug, slug and annular flows. A comparison of observed flow patterns with flow pattern maps (Beggs and Brill, 1973; Mandhane et al., 1974) in the literatures shows a good agreement for the dominating flow pattern (plug and slug flow pattern).

Measured slug translational velocity plotted as a function of mixture velocity shows an increase in the translational velocity with increasing mixture velocity conforming to the findings of earlier researchers. Also measured was the slug body length which was found to be 24-36D with a mean length of 30.6D. The obtained result is in agreement with the postulation of (Dukler and Hubbard, 1975) and the findings of (Pan, 2010). Conclusively, this chapter generally demonstrates the reliability of the test facility used.

## **5 HIGH VISCOUS OIL-GAS FLOW IN HORIZONTAL PIPELINE**

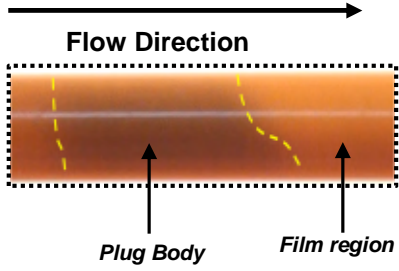
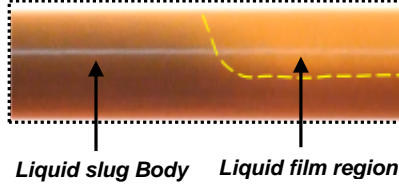

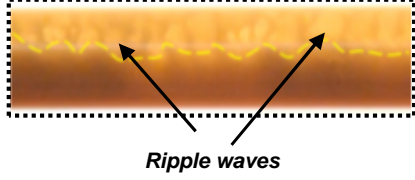
Non-conventional resources in the oil and gas industry, (i.e. high viscous oil) have become a subject of increasing interest hence the need for further investigation. As part of this research work, high viscous liquid-gas flows were conducted at the Oil and Gas Engineering Centre of Cranfield University. This chapter elucidates the observations from experimental investigations carried out in the 3-inch high viscosity multiphase flow facility by way of discussions of results. Liquid viscosities studied ranged from 1.0 – 5.5 Pa.s. Instantaneous time trace of the liquid holdup and pressure gradient were measured using gamma densitometer and differential pressure transducers respectively. Flow pattern characterization was done with the aid of visual observations and video camera recordings. In addition, output signal from gamma densitometer was analysed for the determination of liquid holdup, slug holdup, slug frequency, slug translational velocity and length. Performances evaluation of existing predictive models/correlations were carried out highlighting the effects of liquid viscosities.

### **5.1 Flow pattern Characterization**

Flow patterns play a very important role in two phase flows with each regime exhibiting certain hydrodynamics behaviours. To date, there are no uniform procedure for describing and classifying flow patterns as they are subjective to the researcher's observation. For the present study, the designation of flow patterns observed in the high viscous oil-gas test were interpretation of visual observation via viewing section along the flow line and analysis of video recordings and Probability Mass Function (PMF) plots from the Gamma Densitometer instantaneous time varying liquid holdup time traces. The flows patterns identified in this study are: plug, slug, pseudo slug and wavy annular flows. Table 5-1 depicts the representative images (i.e. side view), time series and PMF plots of the observed flow patterns for high viscosity oil-gas flow experiment.



**Table 5-1 Representative video images and flow condition**

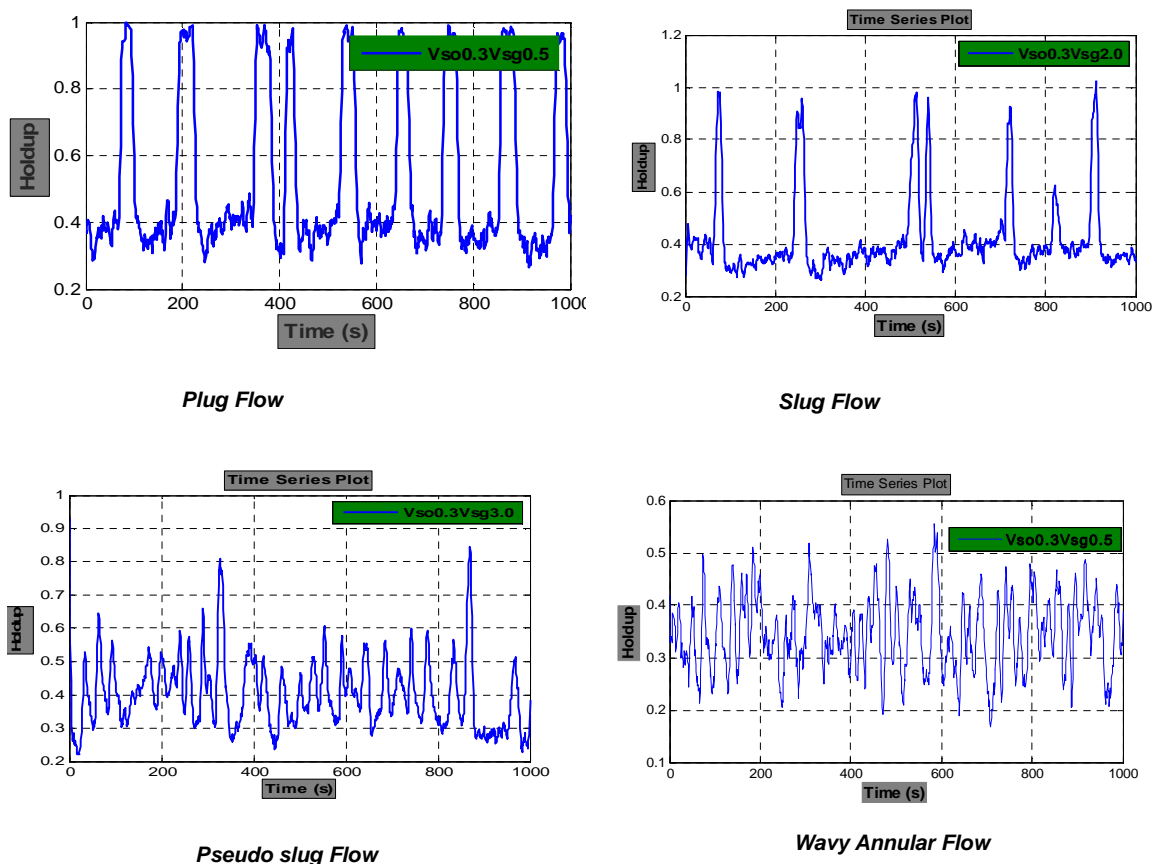
Nomenclature	Flow Condition	Video image
Plug Flow	$V_{so} 0.3\text{m/s}$ , $V_{sg} 0.3\text{-}0.7\text{m/s}$	
Slug Flow	$V_{so} 0.3\text{m/s}$ , $V_{sg} 0.7\text{-}3.0\text{ m/s}$	
Pseudo Slug Flow	$V_{so} 0.3\text{m/s}$ $V_{sg} 3.0\text{-}5.0\text{ m/s}$	
Wavy Annular Flow	$V_{so} 0.3\text{m/s}$ $V_{sg} 5.0\text{-}9.0\text{ m/s}$	

- Plug Flow:** This flow regime occurs relatively at low flow velocity and is usually characterized by the intermittent flow of two distinct units; one which comprises of a stratified less dense gas phase and a denser liquid phase flowing at the top and bottom of the pipe respectively. A second unit with more or less faster moving elongated liquid body flowing intermittently with variations owing to changes in flow condition. A thick coating of oil is also observed on the pipe walls with the passage of the liquid body which becomes even thicker as the superficial oil velocity increases in attribution to increased oil content in the flow line. Increase in the viscosity of oil

results in slower draining time which in turns results in slower draining speed and consequently the thicker coatings.

- **Slug Flow:** With increase in the superficial velocity of gas, slug flow which is similar to plug flow is observed but with liquid body shorter compared to plug flow. This flow pattern is also characterized by a liquid film and a liquid slug body which are more energetic and turbulent relative to plug flow. Oil coatings on the walls of the pipe similar to those of plug flow were observed but with gas entrainments in the coatings owing to turbulence. Higher frequency and shorter slug length are the distinguishing features of slug flow in high viscosity liquids as revealed by the works of (Al-safran et al., 2011) and confirmed by this study.
- **Pseudo Slug:** With the further increase in the gas superficial velocity a pseudo slug flow pattern representing a transition between slug and annular flow is observed. This flow pattern is characterized by a relatively rough gas-oil interphase. Liquid phase is infrequently swept from the bottom of the pipe and bridges the gas phase as in the case of the elongated liquid body in slug flow. However, the liquid phase is less energetic with very low liquid holdup and the bridge is partial. Pseudo slug flow pattern gives a representative feature reflecting the mechanism of slug deformation.
- **Wavy Annular Flow:** This flow pattern occurs at a relatively much higher gas superficial velocity. The increase in the momentum of the gas phase results in increase in energy dissipation along the interface such that oil is swept to the top of the pipe forming a ring layer around the walls of the pipe with most of the gas phase travelling at the core though some were observed to be entrained in the oil. The oil layer at the bottom of the pipe was observed to be wavy and thicker than that of the top owing to gravity and density effects as depicted in Table 5-1 above.

The Neftemer Gamma densitometer used for this study offers the count rate of the mixture based on the density of the phases present in the pipe section. Plots of normalized photon count rate as a function of time were analysed for which four different patterns were deduced as presented in Figure 5-1



**Figure 5-1 Gamma Densitometer Liquid Holdup Time series**

The plots as showed above offer some extent some measure of objectiveness for the characterization of oil-gas flows under different operating conditions. The instantaneous time-series graphs displays the variations of liquid holdup time series as a function of time. The temporal variations as displayed in the graphs are as a result of mixture density fluctuations occurring in the oil-gas flows. The crest and troughs appearance in the waveform of the time varying gamma-count signals presented in the time-series plot are suggestive of the dominating flow regime (plug/slug flow).

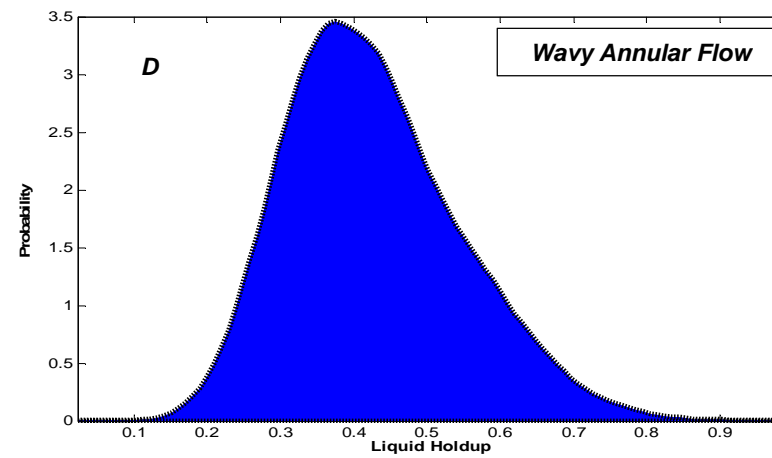
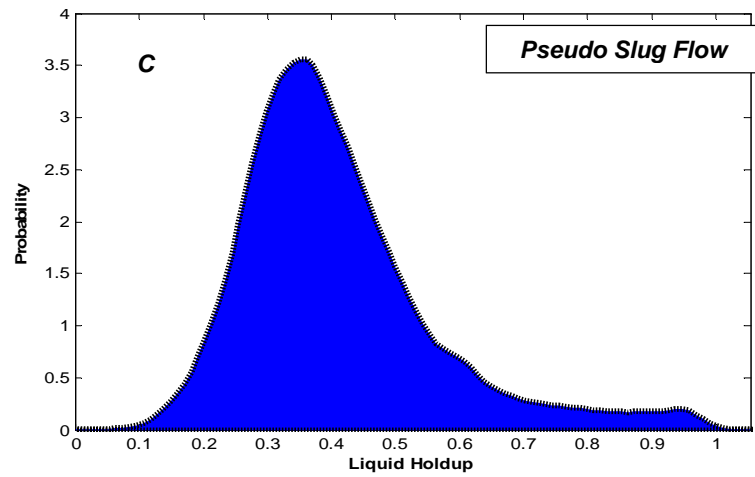
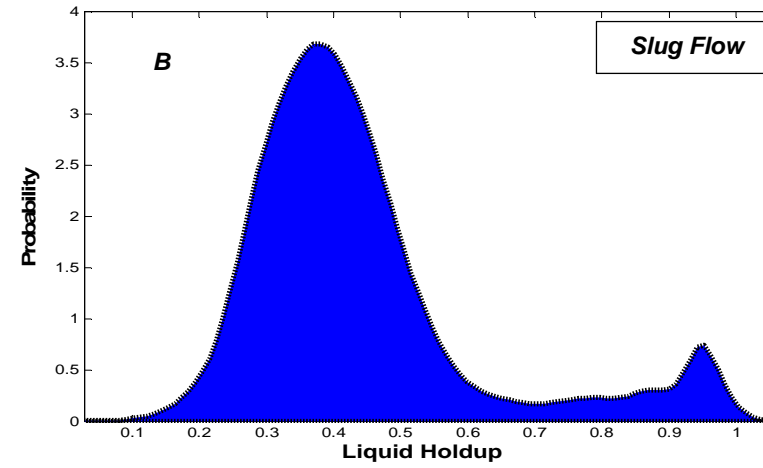
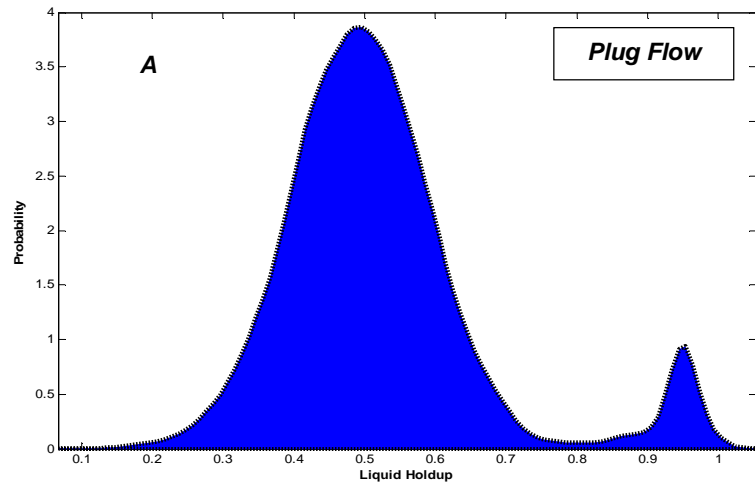
- *Plug Flow:* Intermittent fluctuation was observed from the time varying liquid holdup for this flow pattern from a trough value of 0.4 to a crest value of 1. The crest values are suggestive of the liquid film in the plug region while the trough value are indicative of an elongated plug liquid body.

- *Slug Flow*: The time series plot for this flow pattern was observed to be similar to that of plug flow except that crest values were less than 1 owing to gas entrainment in the elongated body in addition to lower average of value for the liquid film attributed to increased input gas fraction in the pipe.
- *Pseudo Slug*: Pseudo-slug flow regime exhibited a maximum amplitude value of 0.8 for less frequently occurring crest and a more frequent interfacial wave.
- *Wavy Annular Flow*: Wavy annular flow was observed to almost share similar features with that of pseudo-slug though there were no observable crest but rather a continuous wavy interface. Pseudo-slug also accounts for a relatively higher average liquid holdup than wavy annular flows.

To further validate the observations from using video camera and time-series signal waveform plots of gamma densitometer count rate for flow pattern identification, a statistical analysis of the time-series measurement was done using Probability Mass Function (PMF) of the “hard” count gamma as presented in Figure 5-2. (Alagbe, 2013; Arubi, 2011; Blaney, 2008 and Hernandez, 2007) are some of the researchers that have used PMF for the identification of gas-liquid flow patterns. PMF offers the probability of each value of a discrete random variable often expressed as

$$P(X = x) = f(x) \text{ for all } x \quad \text{Where } x \text{ in this case is liquid holdup} \quad (5-1)$$

As can be seen in Figure 5-2 A and B, a PMF plot exhibiting two peaks is usually an indicator that the slug flow regime is the prevailing flow regime within the measurement pipe section. A shorter peak is representative of flow of liquid slug body while the taller peak is suggestive of passage of gas pockets (i.e. liquid film region) however, plug flow was distinguished from slug flow by virtue of the dominance of the liquid film region in plug flow compared to slug flow which can be attributed to increased gas entrainment in slug flow. Pseudo slug exhibited features of both slug and annular flow with a gradual levelling of the smaller peak confirming a transition between slug and annular flow. Wavy annular flow exhibited a characteristic single peaks.



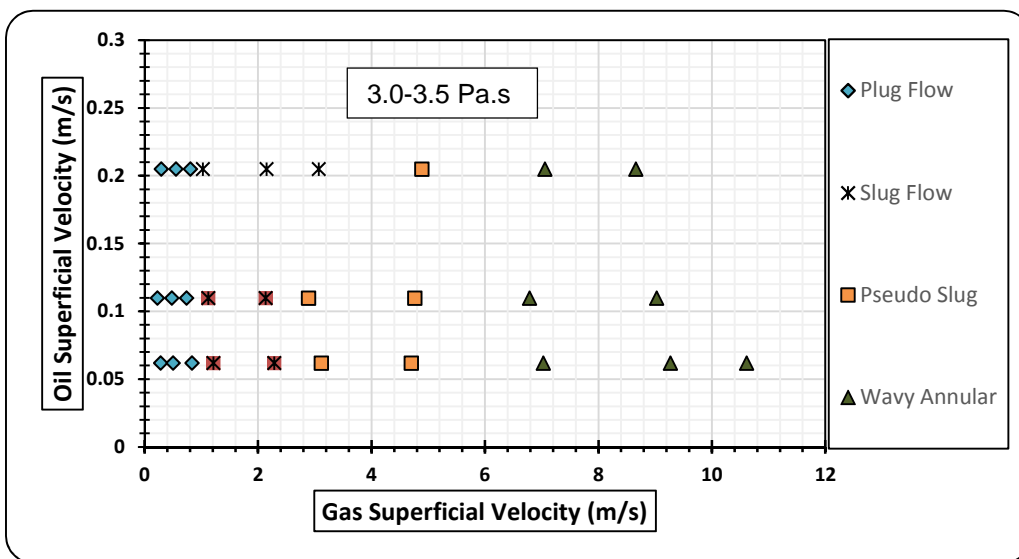
**Figure 5-2 Probability Mass Function (PMF) of Gamma Densitometer Liquid Holdup Time Series**

## 5.2 Flow Regime Map

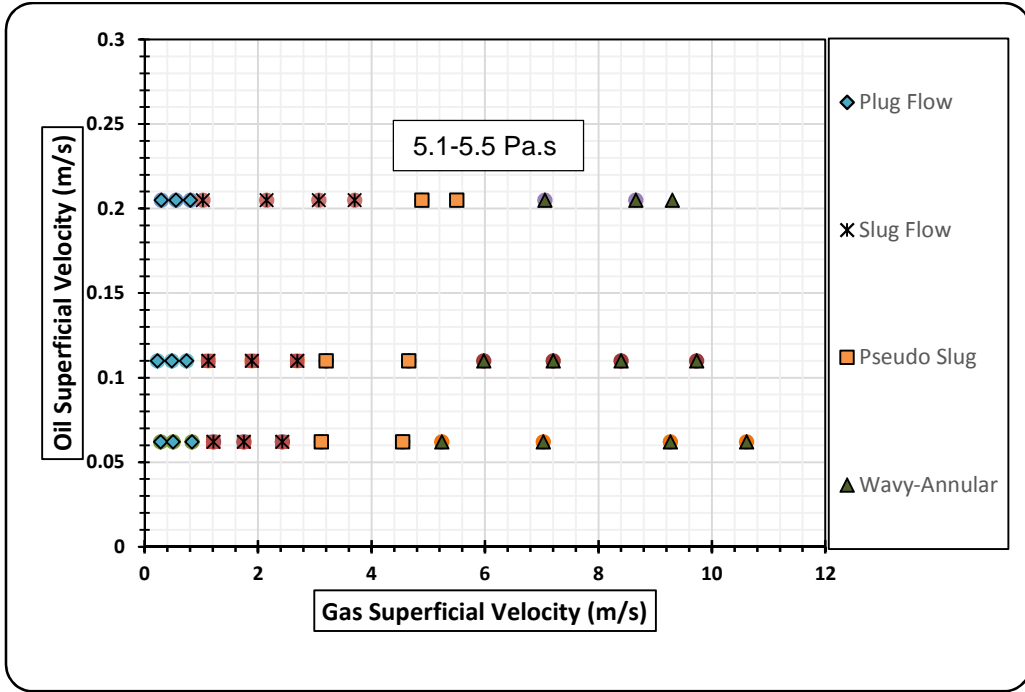
Flow pattern maps are means by which local flow patterns are presented as a function of gas and liquid velocities. Generally, there are plots of two-dimensional graphs showing separate areas corresponding to different flow patterns defined transition criteria. Undoubtedly, no universally accepted flow pattern map has been developed however, a number of flow patterns maps have been proposed by early researchers and widely used in the oil and gas industry some of which are; (Beggs and Brill, 1973; Hewitt and Roberts, 1969).

Flow pattern maps have been constructed based on experimental observations in this study using superficial velocities of oil and gas as ordinate and abscissa respectively. Figure 5-3 (a) and (b) are flow regime maps highlighting the effects of liquid viscosity on oil-gas two phase flow. As can be seen, flow pattern changes from intermittent region (i.e. plug and slug) to transition region (i.e. pseudo-slug) and then to separated flow region (i.e. annular flow pattern). Plug flow is observed from experimental observations within the range of superficial velocity of oil and superficial gas velocities of 0.3-1.0 m/s. Slug flow pattern is then observed as the gas phase gains more kinetic energy owing to increase in superficial gas velocity. Entrainment of droplets from the elongated liquid body occurs with increasing turbulence and this eventually leads to breaking up the liquid body into shorter ones. It is worth noting here that, the range of liquid viscosity range investigated showed that the intermittent region (i.e. plug flow and slug flow) dominates the flow map and even become amplified as the viscosity of liquid increases conforming to the findings of (Archibong, 2015; Brito et al., 2013; Gokcal, 2008; Zhao, 2014; Zhao et al., 2015) and this can be attributed to the increase in shear in the pipe walls owing to viscosity effects. The intermittent flow region is also amplified as the superficial velocity of liquid increases credited to increased liquid height which enhances the formation of slug. With further increase in the gas phase resulting in reduction of the liquid fraction translates into insufficient liquid height to aid slug formation thereby initiating the transition from slug flow to annular flow (i.e. pseudo-slug) and occurs generally at 3-5 m/s superficial velocity of gas with the appearance of rolling waves at the interphase. In Figure 5-3 (c), a

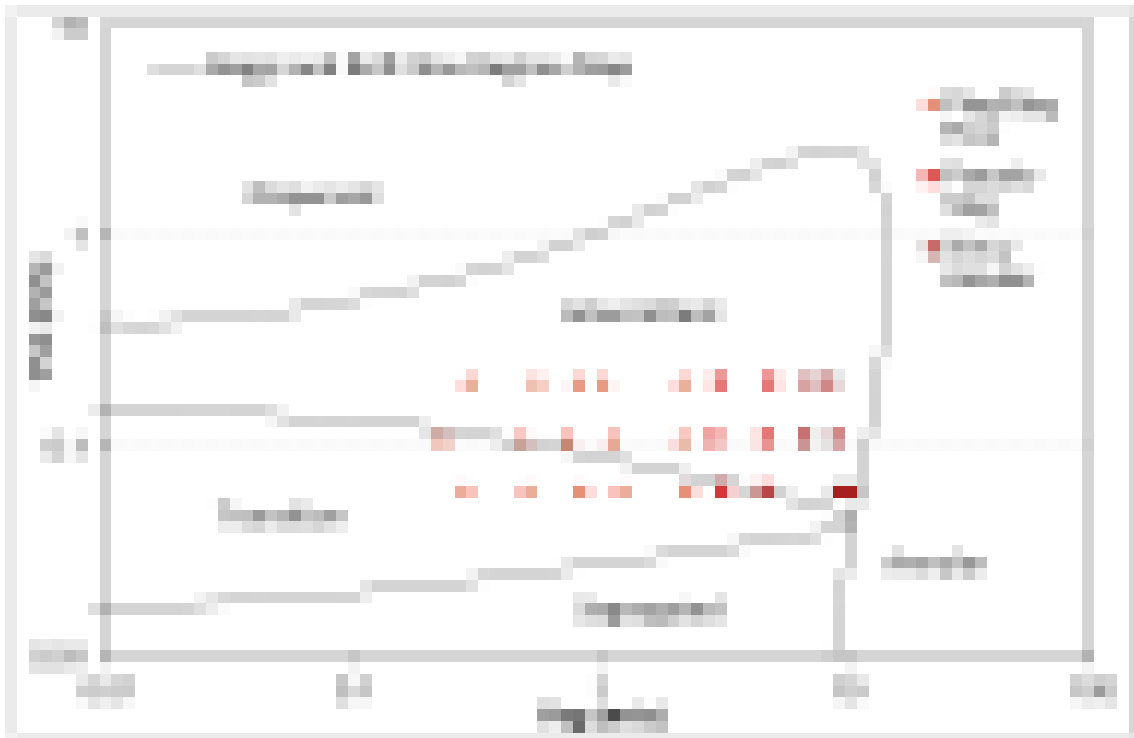
comparison of observed flow against the prediction of flow regime map proposed by Beggs and Brill (1973) is presented. As can be seen, the Beggs and Brill (1973) flow pattern map shows some discrepancies in the prediction of the flow regimes for this experimental investigation. The transition from intermittent to annular flow is over predicted by the map. This could be due to diameter difference as Beggs and Brill used 1-inch and 1.5-inch diameter pipes and viscosity effects. In Figure 5-4 a comparison of the flow pattern map for this study with that of (Taitel and Dukler, 1976) shows an agreement in terms of non-existence of the stratified pattern region, the map however under predicted the annular flow region.



(a)



(b)



(c)

Figure 5-3: Flow Pattern Map for Gas-Liquid Two phase Flow



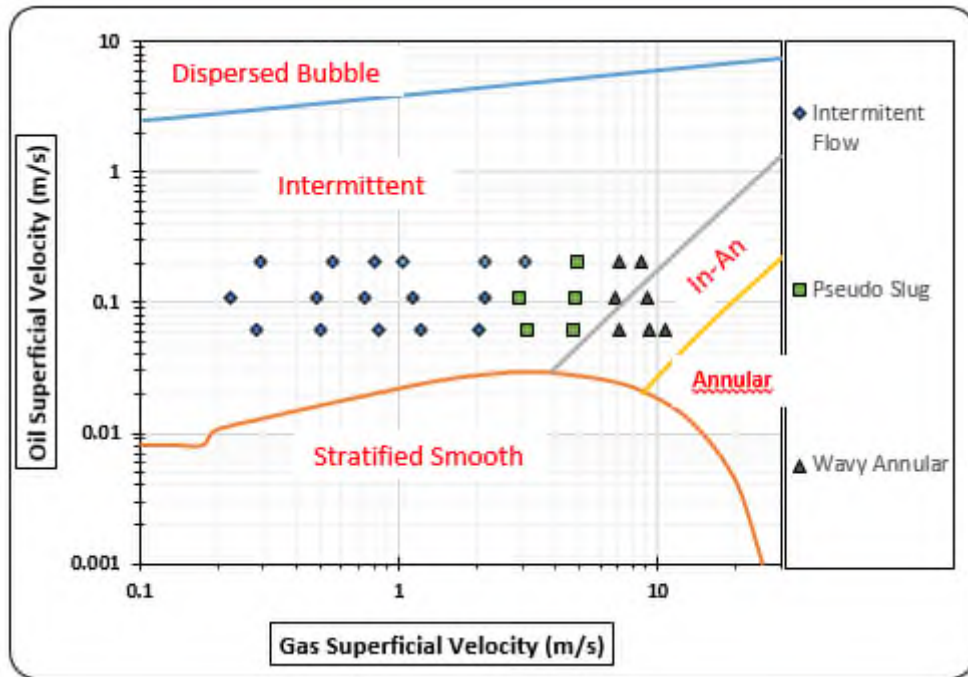


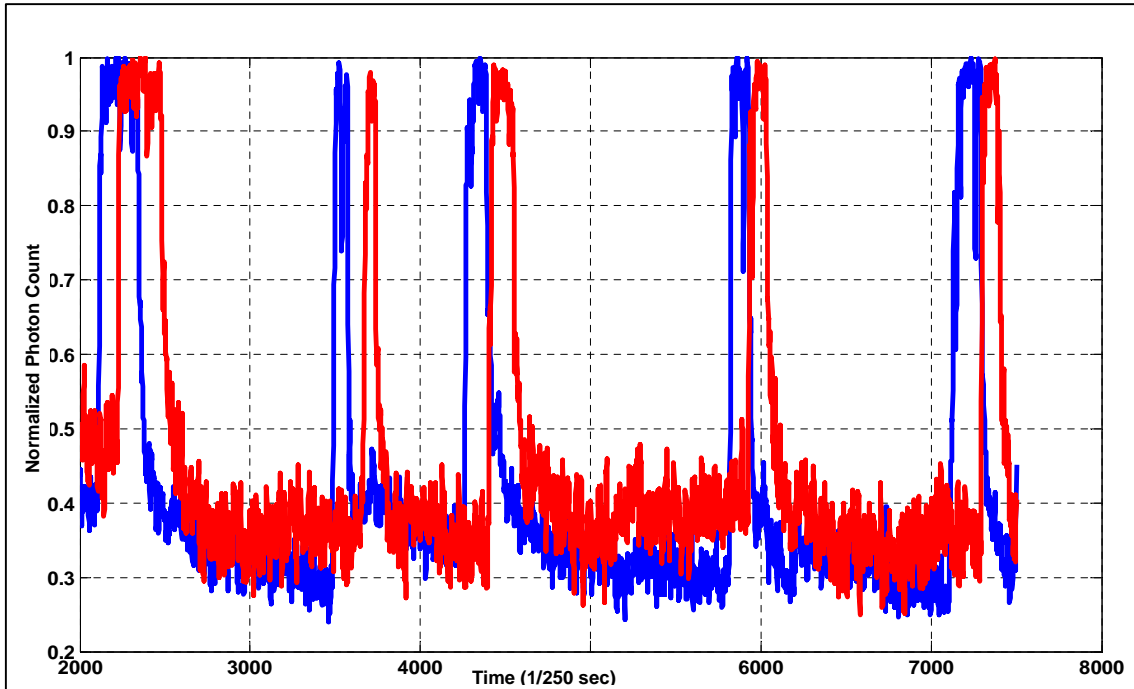
Figure 5-4 Comparison of Flow Pattern Map with Taitel and Dukler (1976).

### 5.3 Liquid Holdup

In this section, the analysis and interpretation of liquid holdup result obtained from Gamma Densitometer time series photon count rate. It is a vital hydrodynamic parameter needed for accurate design and safe operation of unit operation equipment such as slug catchers, separators as well as transportation pipelines. Liquid holdup which is known as the in-situ volume fraction of a particular phase over the total mixture in a test section of specific length is a major determinant for flow patterns, pressure gradient amongst others and are usually the starting point for many prediction models in the literatures.

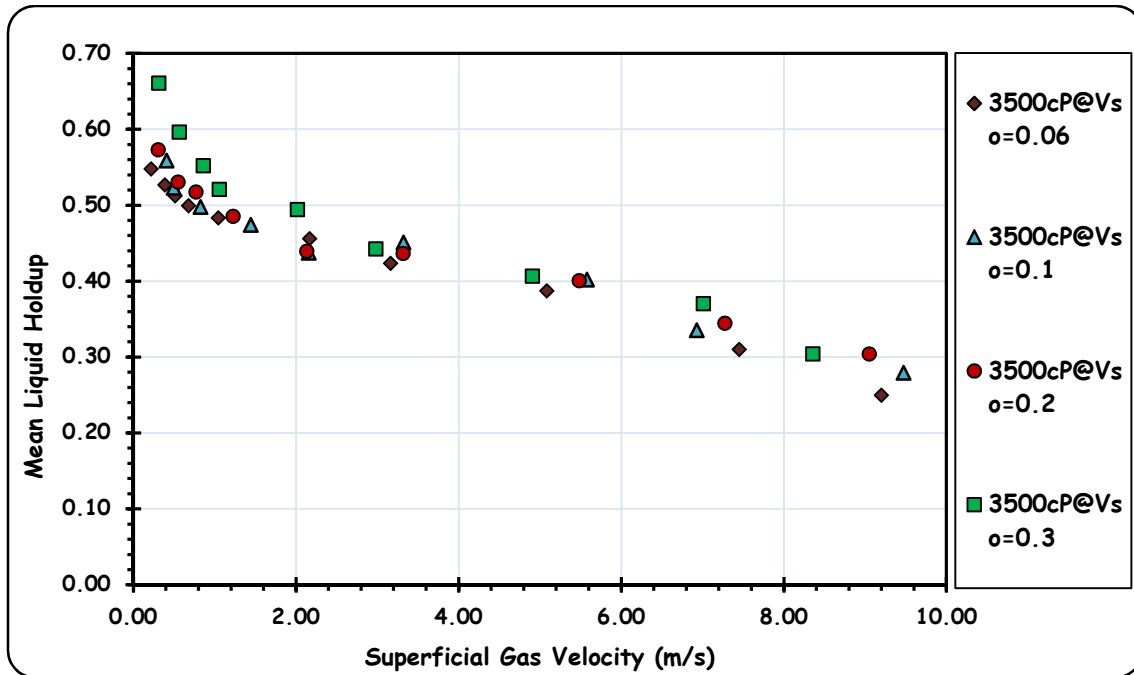
The mean liquid holdup is the point of interest of time varying liquid holdup. As a result, from the obtained liquid hold time series Figure 5-5, if  $\delta_m$  is the instantaneous volumetric fraction of the phase- $m$  (where  $m$  is either the liquid or gas phase) existing at a point in time within the steel pipe cross sectional area of the gamma densitometer, then the mean volumetric phase fraction over a time duration ( $T$ ) recorded can be estimated for each test flow condition. Assuming  $N$  is the number of recorded data over the test period. Then the average volumetric fraction over the total time series range  $\delta_m$  can be estimated by:

$$\bar{\delta}_m = \frac{1}{T} \int_T \delta_m dt = \frac{1}{N} \sum_{n=1}^{n=N} \delta_m \quad (5-2)$$



**Figure 5-5: A typical time varying instantaneous liquid holdup time trace derived from the gamma densitometer.**

Figure 5-6 below illustrates the mean liquid holdup obtained as a function of gas superficial velocity. As can be seen in general, the average liquid holdup decreases with increasing superficial gas velocity and this is credited to the gas phase occupying more volume fraction in the cross-sectional area of the pipe thus reducing the liquid content. Also an increase in the superficial liquid velocity result to an increase in the liquid holdup and this can be attributed to increased liquid height. The liquid hold up trend observed agrees with the findings of (Archibong, 2015; Brito et al., 2014; Gokcal, 2008; and Zhao, 2014).



**Figure 5-6: Measured mean liquid holdup as function of liquid superficial velocity for different liquid superficial velocities.**

### 5.3.1 Viscosity Effects on Mean Liquid Holdup

As expected, the plot of obtained liquid holdup from gamma densitometer as a function of increasing superficial gas velocity as represented in Figure 5-7 at a fixed superficial liquid velocity leads to relatively slight increase in the average liquid holdup and can be attributed to the increased viscous drag in the pipe wall due to viscosity effects. Another interesting trend that can be observed from Figure 5-7 is the fact the mean liquid holdup changes with flow pattern. Observation shows that this value is relatively higher plug and slug flow region vis-à-vis the pseudo slug and annular flow region.

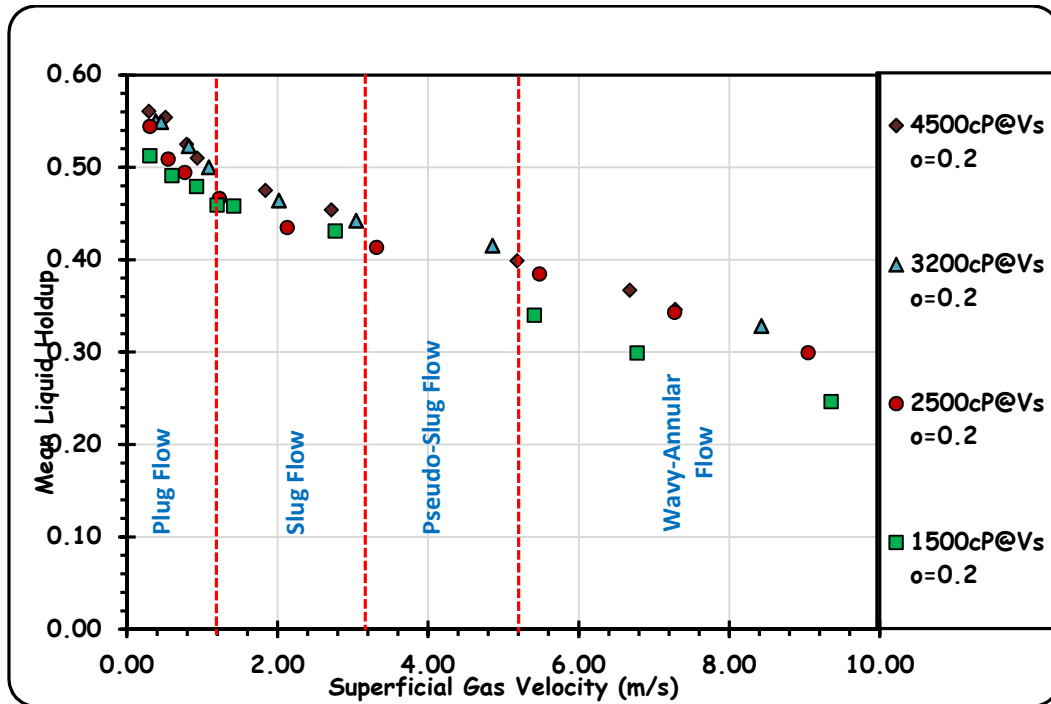


Figure 5-7: Measured mean liquid holdup as function of liquid superficial velocity for different liquid viscosities.

### 5.3.2 Comparisons Against Liquid Holdup Prediction Models

The few correlations for the prediction of liquid holdup that exist in the literature were tested with the present experimental data. Two categories of these models were identified. In the first category, two fluid models for which the models of (Beggs and Brill, 1973; Xiao et al., 1990) were considered while the drift flux prediction models of (Bestion, 1990; Choi et al., 2012 and Zuber and Findlay, 1965) were considered in the second category. While the choice of (Beggs and Brill, 1973) prediction model is based on the fact that it is widely used and acceptable for the calculation of liquid holdup in the petroleum industry, (Choi et al., 2012) was chosen because a relative higher viscosity liquid was used for the study. Results of comparison shown in below Figure 5-8 indicates that all the models tested predicted the present data with different degree of discrepancies and this can be attributed to the fact that there were all developed from observation of low viscous liquids though the (Xiao et al., 1990) model performed better when compared to others probably because it accounted for some characteristic features of slug flow bearing in mind that slug flow is the dominant

flow pattern. Three statistical error evaluators namely: average percentage relative error ( $\varepsilon_1$ ), average absolute percentage relative error ( $\varepsilon_2$ ) and standard deviation were used to test the performance of the prediction models as shown in Table 5-2: Statistical evaluation of prediction models with respect to experimental liquid holdup values

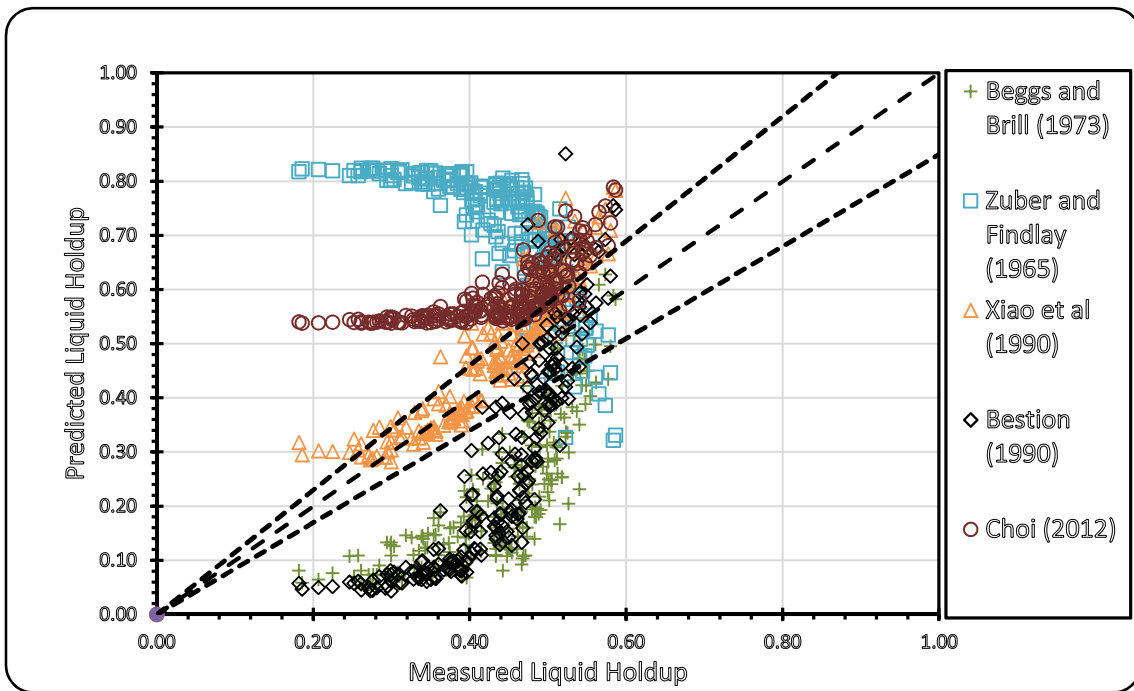


Figure 5-8 Comparison of experimental measured liquid holdup versus predicted mean liquid holdup

Table 5-2: Statistical evaluation of prediction models with respect to experimental liquid holdup values

Correlations	$\varepsilon_1$	$\varepsilon_2$	$\varepsilon_3$
Zuber and Findlay 1965	74.43	77.73	65.47
Beggs & Brill 1973	-50.45	50.69	21.27
Xiao et al 1990	12.96	14.34	13.15
Bestion 1990	-39.44	45.19	35.45
Choi 2012	39.84	39.84	28.03

## 5.4 Pressure Gradient

The importance of Pressure gradient in the oil and gas industry cannot be overemphasized as it is the foremost variable for the accurate design of pipelines for transportation and the chief determinant for pumping power requirements. In this experimental investigation, pressure gradients were measured by means of a differential pressure transducer with two tapings placed 17D apart and positioned 184D downstream point of injection of the 3-inch horizontal multiphase flow facility located at the Oil and Gas Engineering Laboratory in Cranfield University. Experimental datasets were obtained at a sampling rate of 250Hz for all the experiments conducted.

From the plot of pressure gradient against superficial gas velocity as shown in Figure 5-9 to Figure 5-11, it can be seen that the measured pressure gradient is strongly dependent on the observed flow patterns. On a general note, pressure gradient increases with increasing superficial gas velocity at a fixed liquid superficial velocity and this is expected considering the fact the pressure gradient is directly proportional to the square of flow velocity. Pressure gradient in the intermittent flow region exhibits persistence stable trend with some cases of initial slight decrease or increase at the lower flow condition. The slight increase is probably attributed to the effect of oil shear thinning. This brings about reduction in the pressure drop by reducing shear between the two phases, and pressure gradient increases with increase in mixture velocity. The slight decrease afterwards can be attributed to the reduction of the multiphase flow effective viscosity which occurs within a limited range the increasing effect of mixture velocity becomes the driving of pressure gradient.

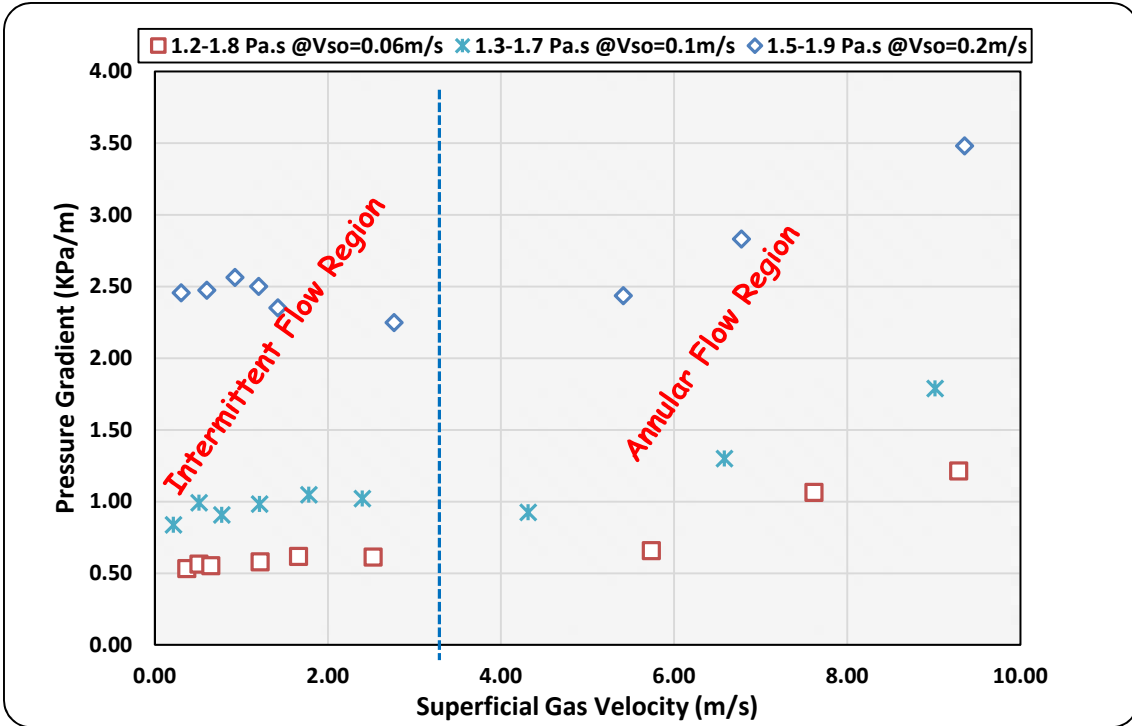
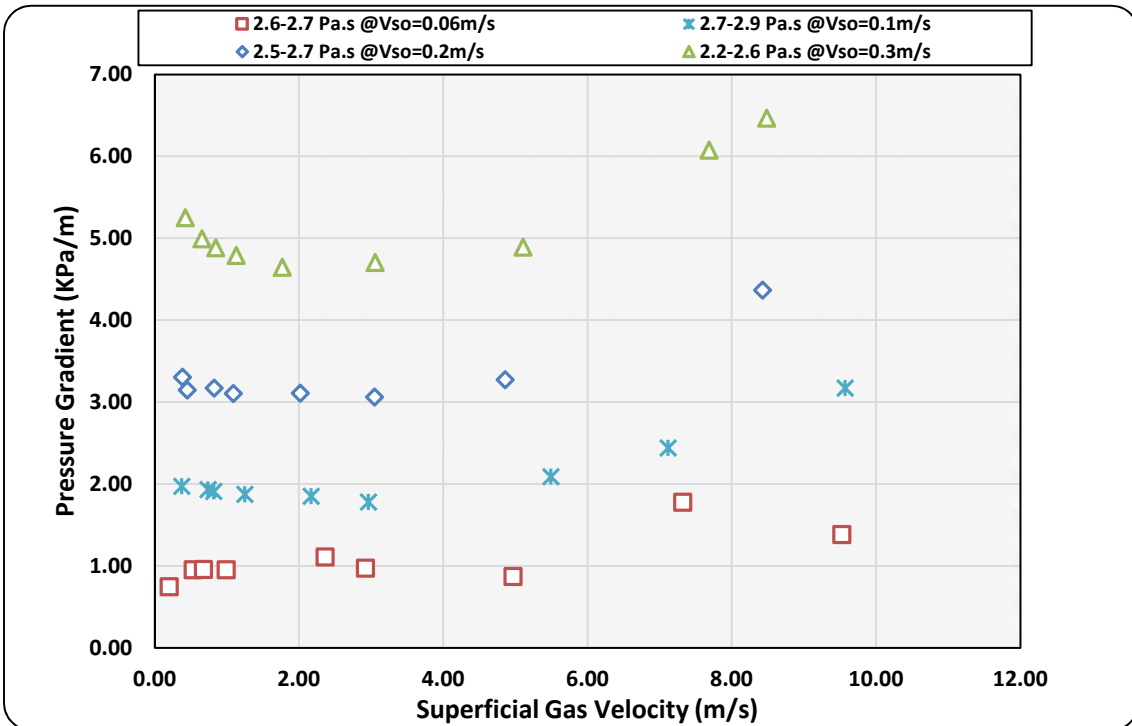


Figure 5-9: Pressure gradient versus gas superficial velocity for viscosity range (1.2-1.5 Pa.s)



(a)

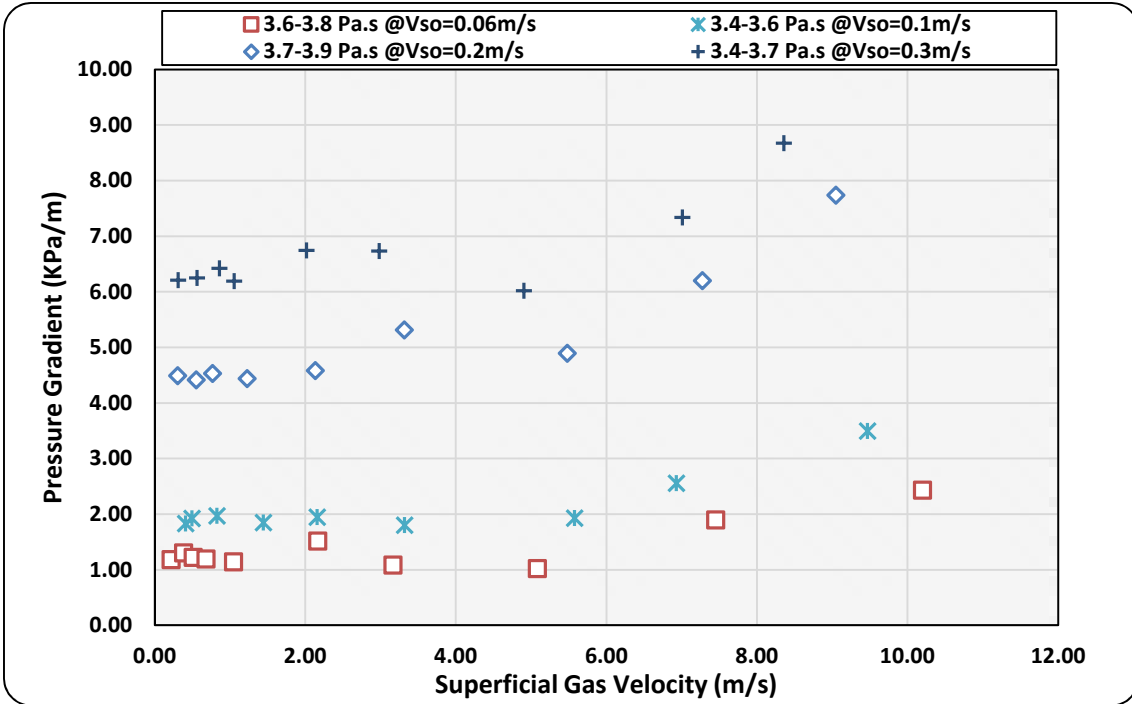


Figure 5-10: Pressure gradient versus gas superficial velocity for viscosity range (a) 2.2-2.9 Pa.s, (b) 3.4-3.9 Pa.s.

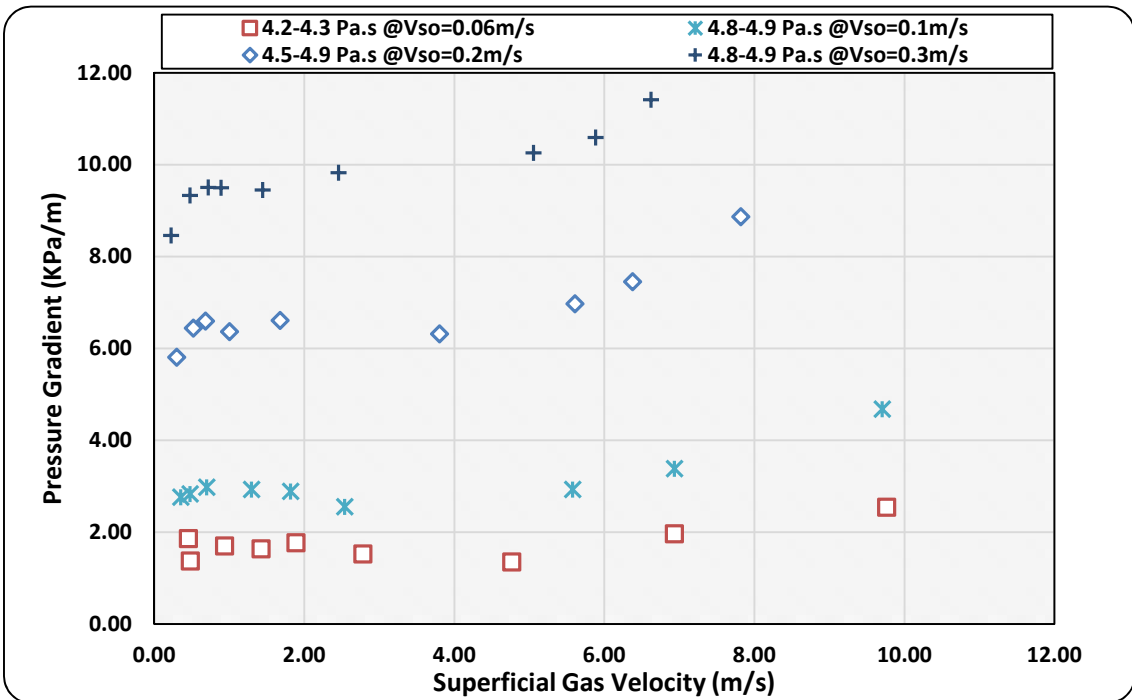


Figure 5-11: Pressure gradient versus gas superficial velocity for viscosity range (4.2-5.0 Pa.s)



### 5.4.1 Viscosity Effects on Pressure Gradient

A plot of pressure gradient as a function of superficial gas velocity as shown in Figure 5-12 similarly exhibits the similar increasing trend as that discussed in 5.4 for superficial oil velocity of 0.2m/s and 1.0-5.5 Pa.s range of viscosity investigated. From the results obtained, it can be seen that measured pressure gradient generally increase with increase in oil viscosity and increase in superficial velocity of oil ascribed to increase in shearing in the test line as a result of viscosity increase. Increasing viscous shear on the pipe walls results in corresponding increase in frictional pressure losses.

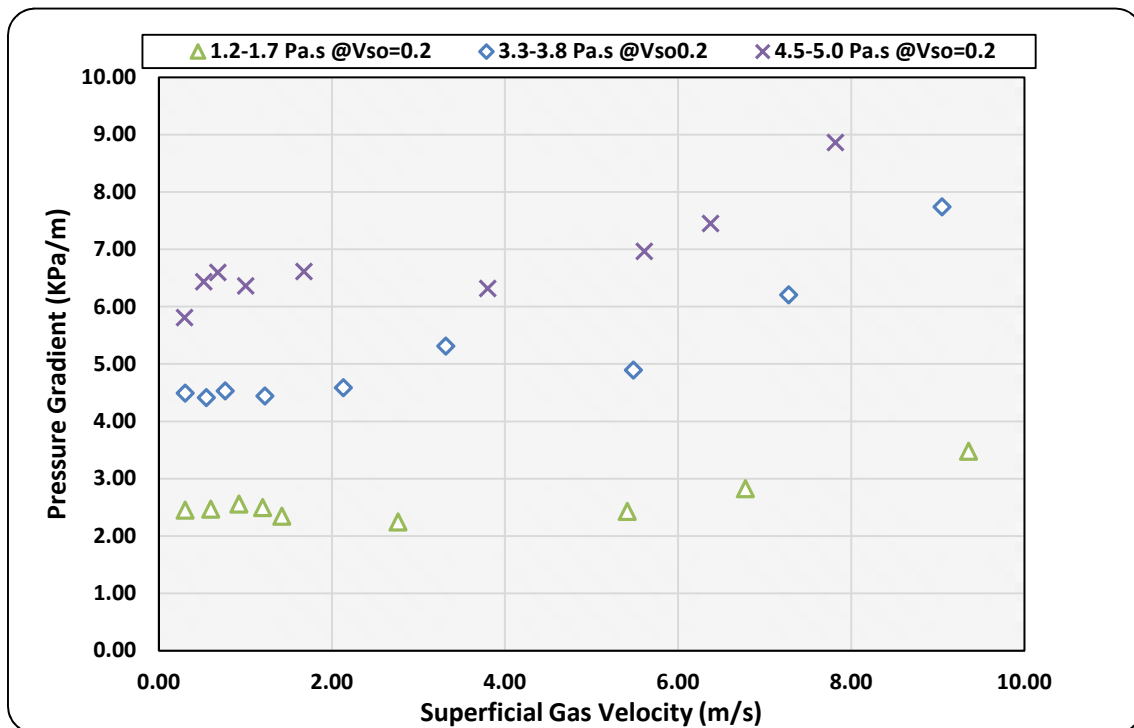


Figure 5-12: Pressure gradient as a function of gas superficial velocity for different viscosities

### 5.4.2 Comparisons with previous pressure gradient data

A comparison of present experimental data for high viscosity oil with the data from (Gokcal, 2008) are shown in Figure 5-13 and Figure 5-14. (Gokcal, 2008) investigated high viscosity oil-gas two phase for oil viscosity ranging from 0.181-0.587 Pa.s. The comparison shows that the new data exhibit a general increasing

trend to that in conformity to the findings of (Gokcal, 2008) when the viscosity of oil and superficial oil velocity increases. (Archibong, 2015; Brito et al., 2013; Farsetti et al., 2014; Foletti et al., 2011; Khaledi et al., 2014; Zhao, 2014) have all reported similar trend for pressure gradient as viscosity increases. The reason for comparing with present result with (Gokcal, 2008) which was obtained from 2 inch internal diameter pipe is to highlight the effects of liquid viscosities.

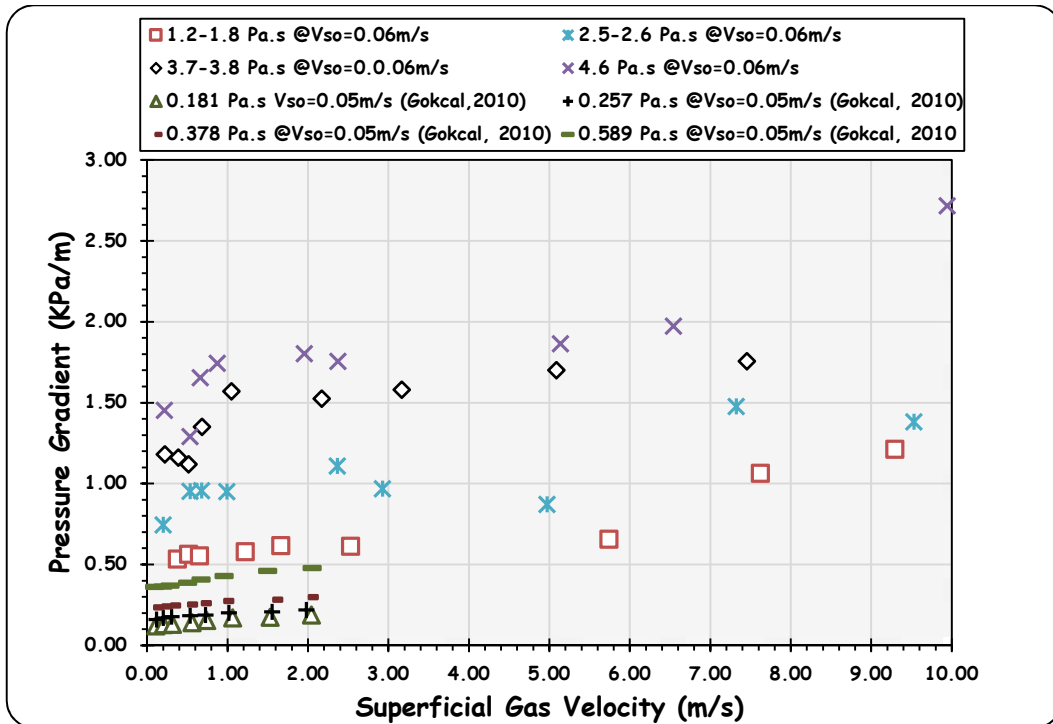


Figure 5-13: Comparison of the present data with Gokcal (2008) data.

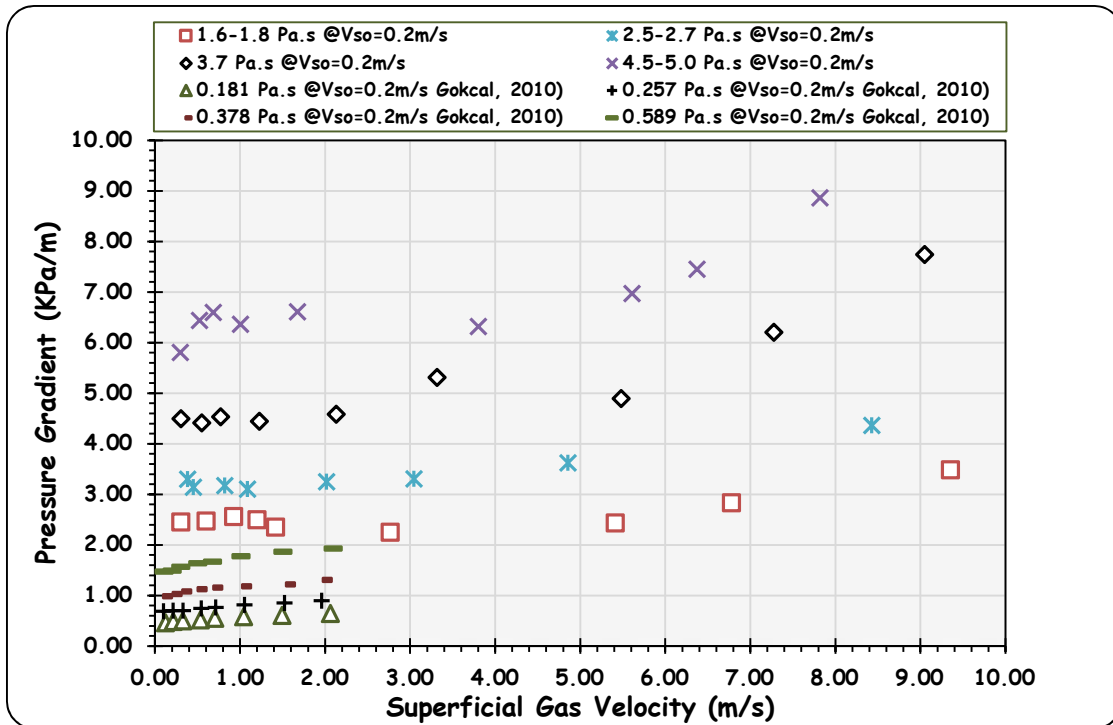


Figure 5-14: Comparison of the present data with Gokcal (2008) data.

### 5.4.3 Comparisons with prediction methods

Considering the very importance of pressure gradient in the oil and gas industry, several research effort have being made in this area and still ongoing to enhance the accurate prediction of prediction in pipelines. Attempt is made in this section to compare some result of some of the widely used pressure gradient prediction model (Beggs and Brill, 1973; Xiao et al., 1990). As can be seen in Figure 5-15 and Figure 5-16. At low oil viscosities and low oil flow rate the Beggs and Brill, 1973 prediction models tends to considerably agree with the measured pressure gradient. However, as oil viscosity and flowrate increases, the discrepancy becomes significant owing increase in viscous drag around the pipe walls as the liquid heigth increases.

Interestingly, the Beggs and Brill, 1973 modified by the integration of liquid holdup model proposed by Xiao et al., 1990 performed better than the original model at higher liquid flow rate and viscosity. The improvement observed could probably as a result of the input from the liquid hold considering the fact that the liquid holdup model has some inherent features of slug flow pattern which happens to

the the dominating flow pattern observed for high viscosdty liquid liquid as earlier discussed. The tested models consistently over-predicted the present data as illustraed in Figure 5-17 hence the need for more robust model that can accout for the increase viscosity effects largely responsible for the increase in pressure gradient

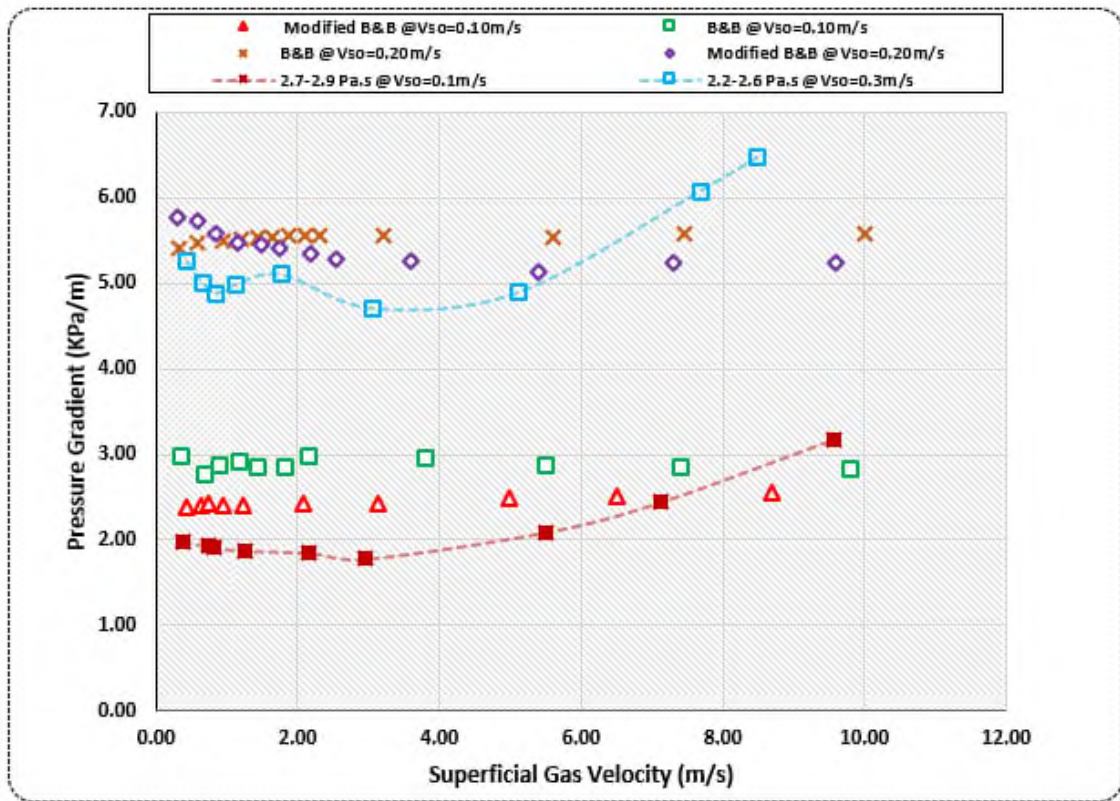


Figure 5-15: Comparison of measured pressure gradient with model predictions.

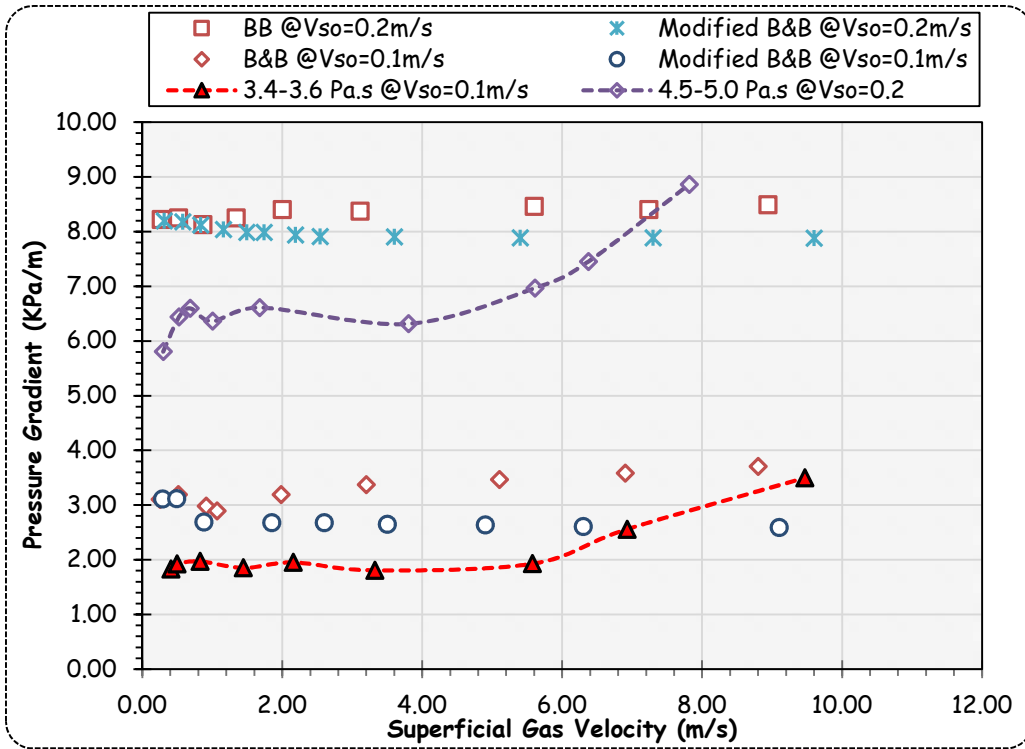


Figure 5-16: Comparison of measured pressure gradient with model predictions

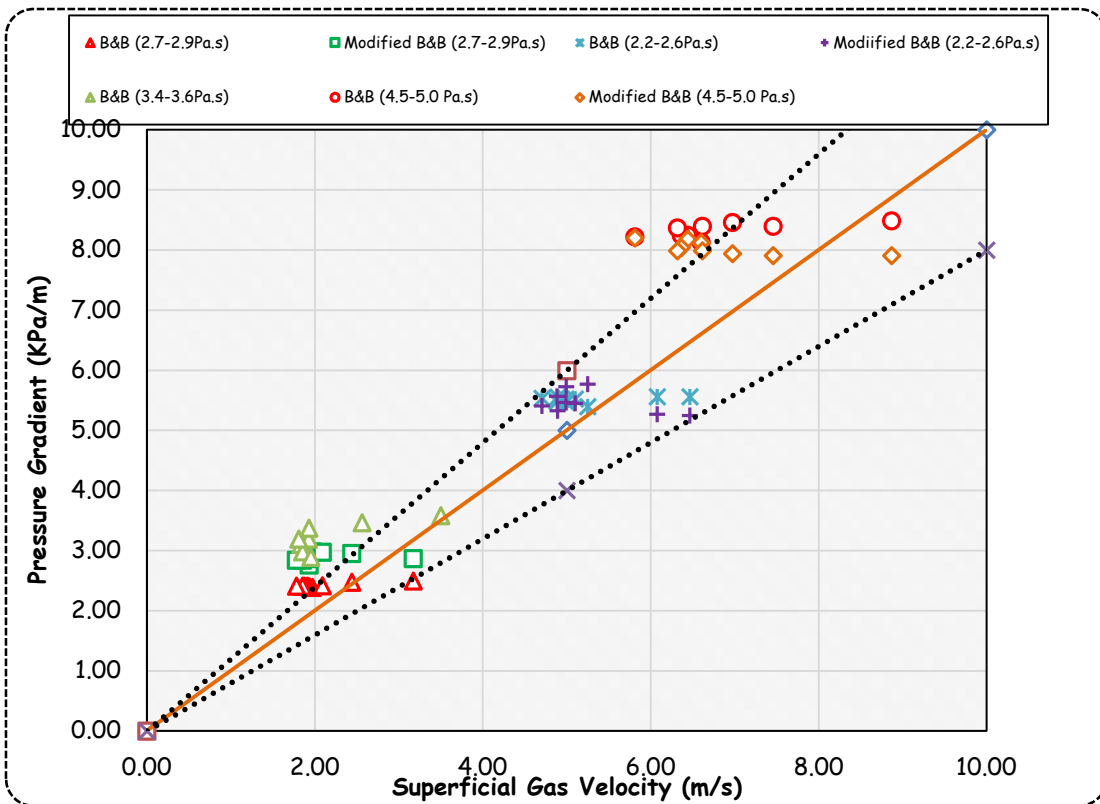


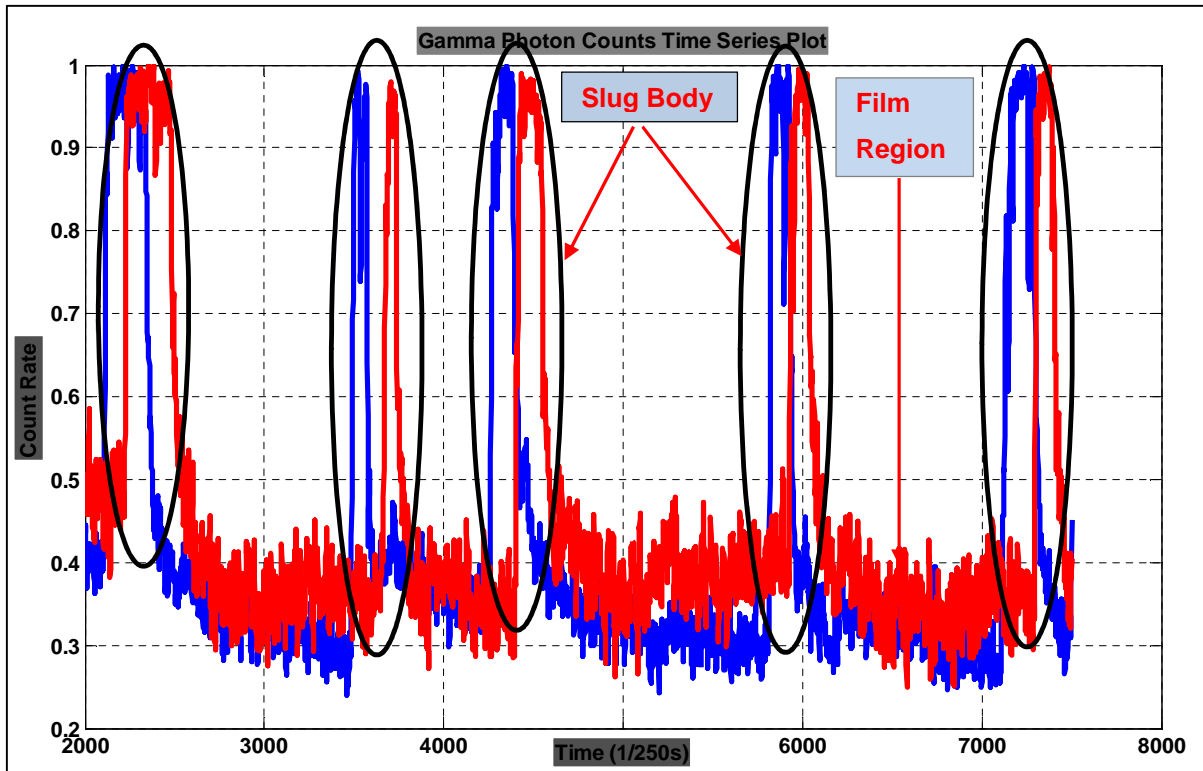
Figure 5-17: Measured pressure gradient versus model predictions

## 5.5 Slug Body Holdup

One of the critical parameters which forms an integral part of slug flow models is the liquid volume fraction in the slug body in other words known as slug body holdup. Investigation have shown that this very important parameter is affected by flow variables such as fluid properties, gas and liquid flowrates and pipe orientation. Time series waveform plots represented in Figure 5-18 illustrating crests and troughs which are suggestive of passage of liquid slug body and film region of a slug cell unit respectively. Slug body holdup estimation involves defining a liquid holdup threshold thereby eliminating the classification of slug holdup from travelling waves. It is worth noting here that different researchers have in the course of their investigation defined distinct threshold values as in the case of (Manolis et al., 1995) who estimated threshold as 2/3 of the value predicted by (Gregory et al., 1978) slug body holdup prediction correlation. (Nydal, 1991; Perez, 2007) adopted values ranging between 0.70-0.75. conversely in this investigation the method used recently by (Zhao, 2014) which adopted an average value relative to the variable liquid holdups at different flow conditions; an approach considered very useful bearing in mind that the mean liquid holdup in the film region of the slug unit in high viscosity liquid two phase flow may sometimes be higher than a particular threshold

$$x_{th} = \frac{1}{2} [\max(x_k) + \min(x_k)] \quad (5-3)$$

Where  $x_k$  time series liquid holdup values obtained from normalization of the gamma densitometer count rate. The slug body holdup is then estimated as the average of the time varying normalized count rate exceeding the threshold.

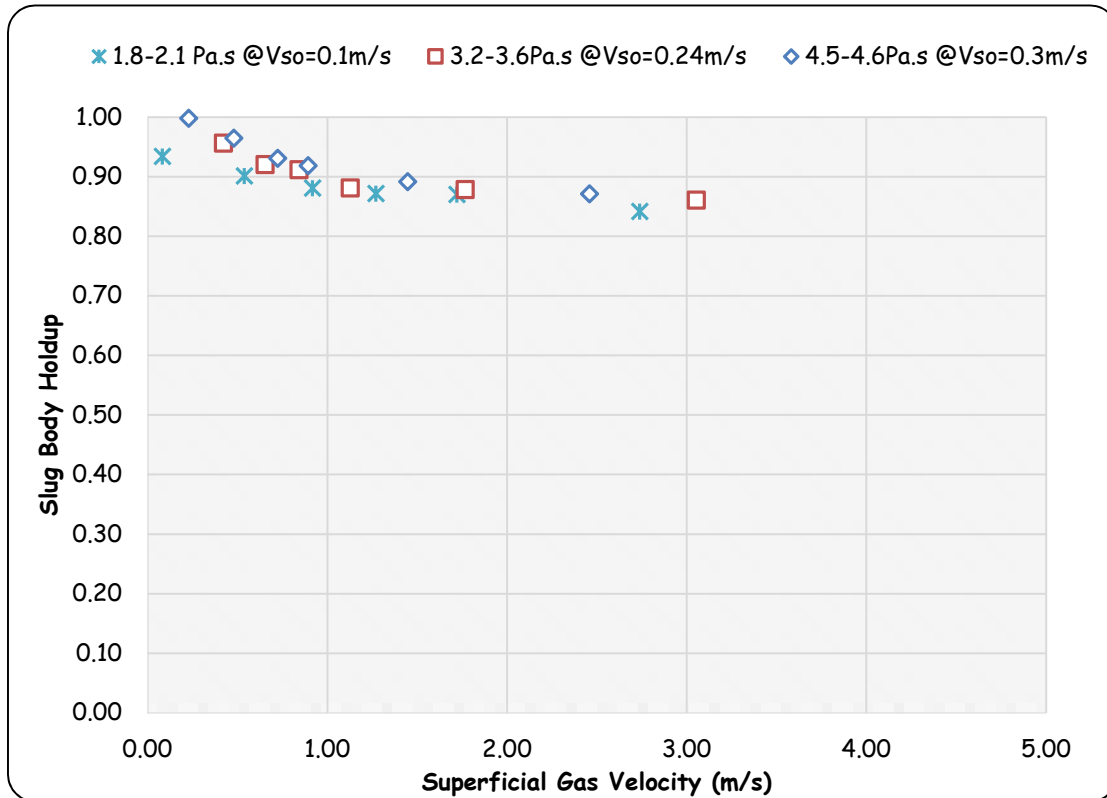


**Figure 5-18: A typical gamma densitometer time series liquid holdup plot.**

Presented in Figure 5-19 - Figure 5-20 below is the measured slug body holdup as a function of gas superficial velocity. For all the flow conditions investigated, slug holdup generally decrease with increasing superficial gas velocity similar to the trend observed for liquid hold up. It can be seen that the decrease at low superficial gas velocities (i.e. less than 1 m/s) is small and corresponding to the plug flow region as illustrated in the flow pattern map earlier discussed. Plug flow is characterised by negligible gas entrainment in comparison to slug flow which explains the reason for the slight decrease. Expectedly, a relatively slight increase in the slug body holdup is observed when the oil superficial velocity is increased, this is as a result of increase in the liquid content in the pipe. The results obtained are consistent with those obtained by (Al-Safran, 2009a; Brito et al., 2014; Kora et al., 2011; Nadler and Mewes, 1995) and most recently the findings of (Archibong, 2015; Zhao et al., 2015).

The effects of liquid viscosity on slug holdup are presented in Figure 5-21 and Figure 5-22. The results shows an increase in slug holdup as viscosity of liquid

increases, this can be attributed to increase in shearing on the pipe walls owing increase in oil viscosity.



**Figure 5-19: Measured slug body holdup as a function of superficial gas velocities for different viscosities**



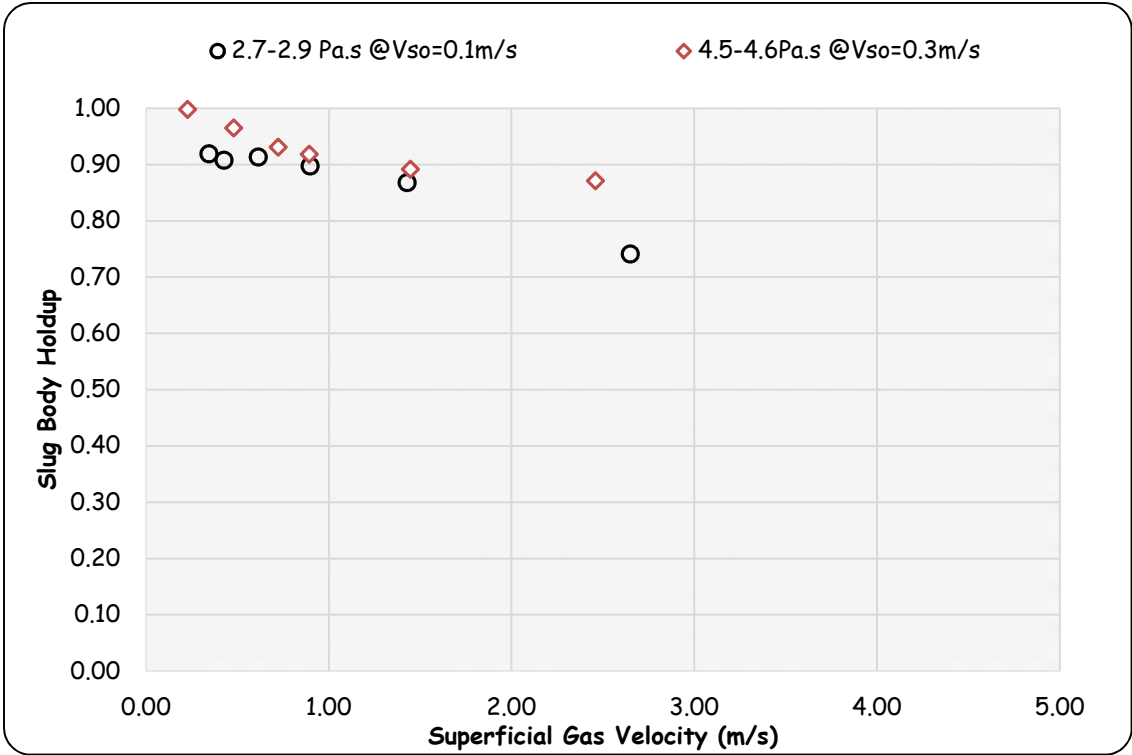


Figure 5-20: Measured slug body holdup as a function of superficial gas velocities for different superficial liquid velocity

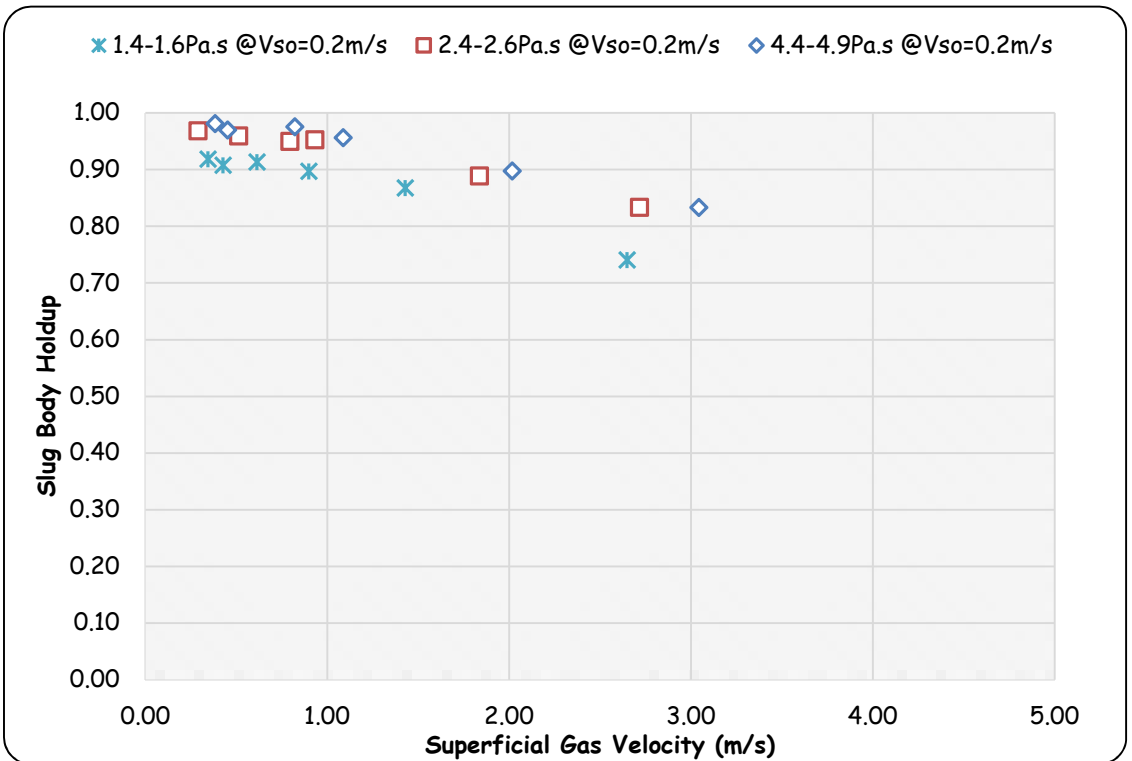
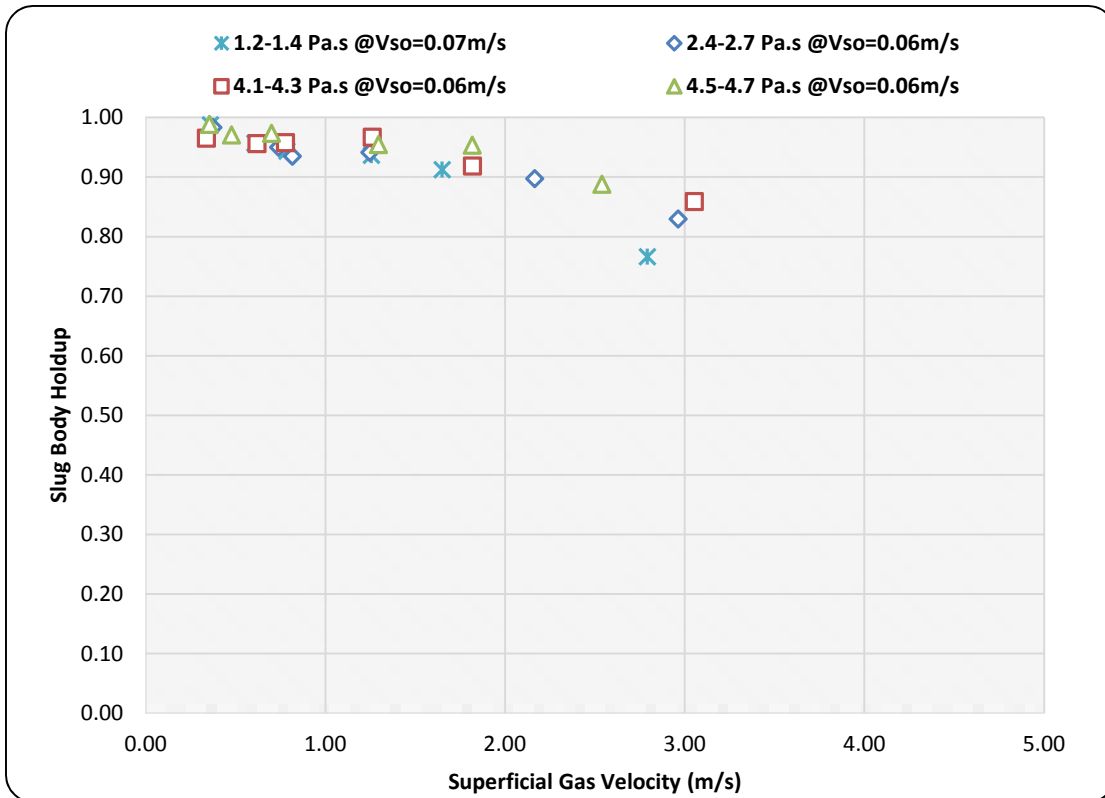


Figure 5-21: Liquid viscosity effects on slug body holdup



**Figure 5-22: Liquid viscosity effects on slug body holdup for different viscosities**

### 5.5.1 Slug Liquid Holdup Prediction Models Evaluation.

A comparison was carried out between the measured slug holdup and existing prediction models in the literature. The performance of the following models (Abdul-Majeed, 2000; Al-Safran, 2009a; Archibong, 2015; Gomez et al., 2000; Gregory et al., 1978; Kora et al., 2011; Malnes, 1982) were assessed as illustrated in Figure 5-23. It is worth noting that other than the prediction models of (Al-Safran, 2009; Kora et al., 2011 and Archibong, 2015) the rest were developed from and validated against low viscosity liquid data. Results shows that all the models tested over-predicted and in some cases under prediction of the present slug holdup data with different magnitude. (Al-Safran, 2009) had the best performance with some over predictions attributable to the viscosity difference in the oil used while (Abdul-Majeed, 2000) showed the farthest prediction. It is suprising to see the (Archibong, 2015) model consistently over predicting the present data considering the fact that the same fluid properties

was involved, this could probably be as a result of diameter effect since his data was sourced from the 1 inch multiphase flow test facility.

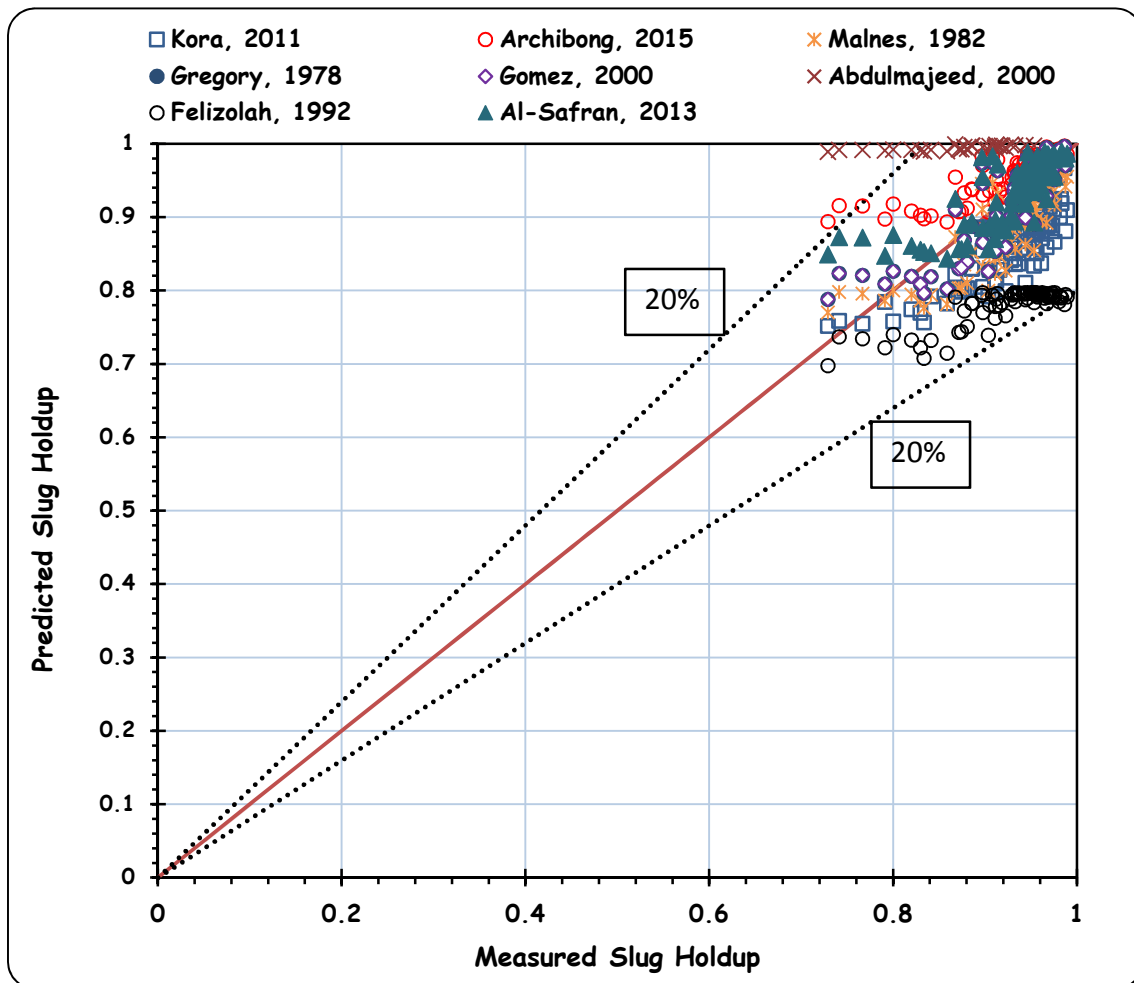


Figure 5-23: Prediction of slug holdup as function of measured slug holdup

## 5.6 Slug Frequency

Slug frequency being one of the most critical feature of the slug structure is required as an input for most slug flow models and is commonly defined as the number of slugs that transverses through the cross-sectional area of a pipe at a given point in time. Inaccurate prediction of this parameter can cause potential damage to pipeline structure due to vibrations as a result they are useful in the estimation of the fatigue life of pipeline. In this experimental study, slug frequency was obtained from liquid holdup time series plot illustrated in Figure 5-5. By simply counting the liquid slug peaks within a measured time period of 30 sec for all the flow conditions investigated. It is also worth noting that the results obtained

were validated by taking counts of the slug passing through the facility's viewing window over the time taken and also by analysis of the video recordings.

From Figure 5-24 - Figure 5-26 below, measured slug frequency is plotted against superficial gas velocities for different liquid velocities. As can be seen from the graph, slug frequency generally decrease with increasing superficial gas velocity within the range of liquid velocities investigated. This can be explained by the fact that an increase in the gas phase within the pipe cross-sectional area results in the creation of interfacial waves, a point is reached when the gas phase supresses the liquid holdup which brings about diminution of the slug body and hence the decrease in slug frequency. However an increase in the liquid velocity which result in increasing the liquid film height which enhances slug formation.

Figure 5-27 was plotted to examine the effects of liquid viscosities on the measured slug frequency for the given set of flow conditions investigated. Result of the plot shows that slug frequency increases with an increase in oil viscosity. This is justified by the fact that an increase in oil viscosity result in increasing the liquid height owing to increase in resistance to flow. The findings in this experimental investigation conforms with the trend observed by (Bahadir Gokcal et al., 2009; Okezue, 2013; Zhao et al., 2013) . From this observation, it can be concluded that slug frequency has strong dependence on liquid viscosity. Conversely, most existing closure relationships for slug frequency available in the literature do not reflect this feature thereby necessitating the development of new closure model taking into account the effects of viscosity on slug frequency. This is discussed in detail in the next chapter.

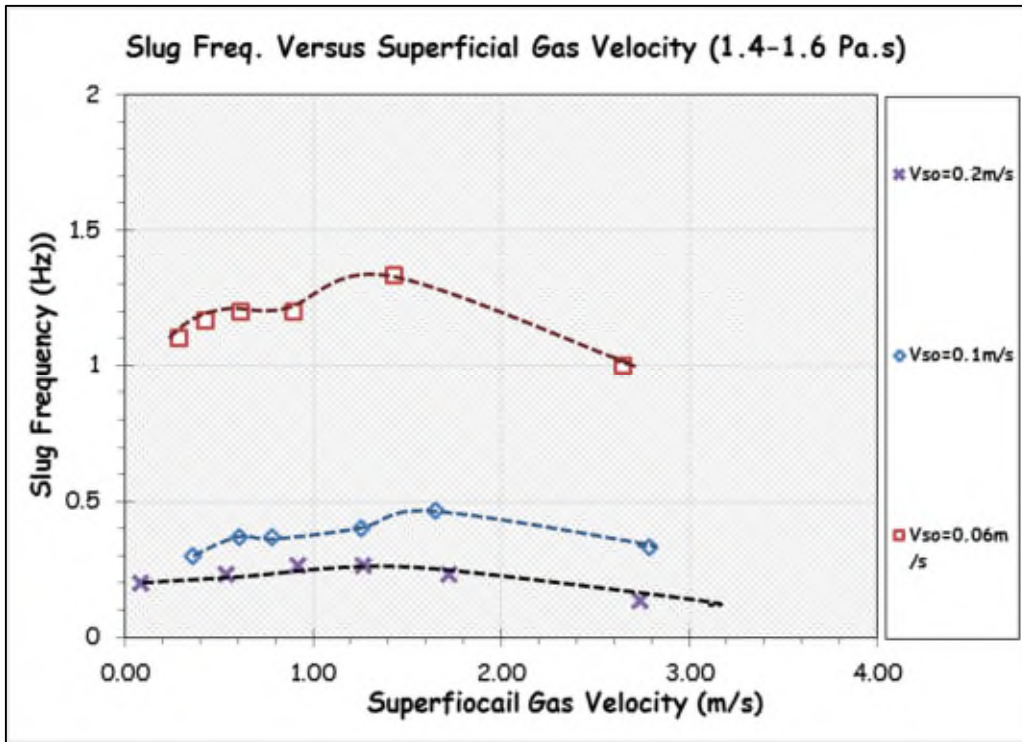


Figure 5-24: Slug frequency vs. gas superficial velocity

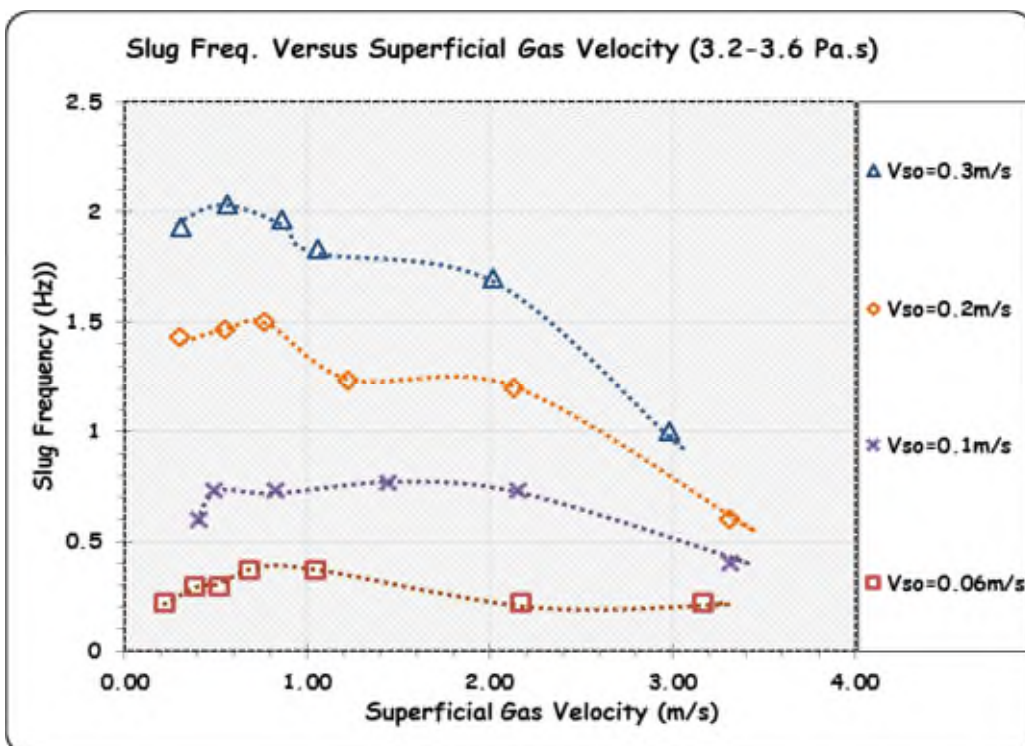


Figure 5-25: Slug frequency vs. gas superficial velocity

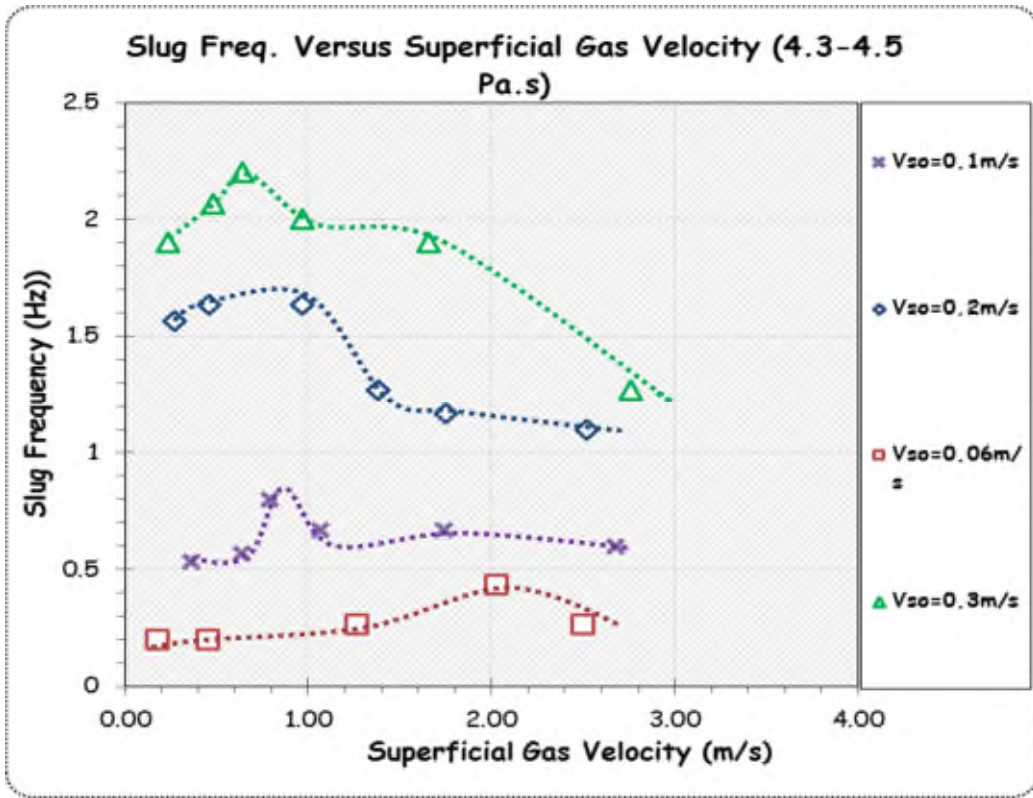


Figure 5-26: Slug frequency vs. gas superficial velocity

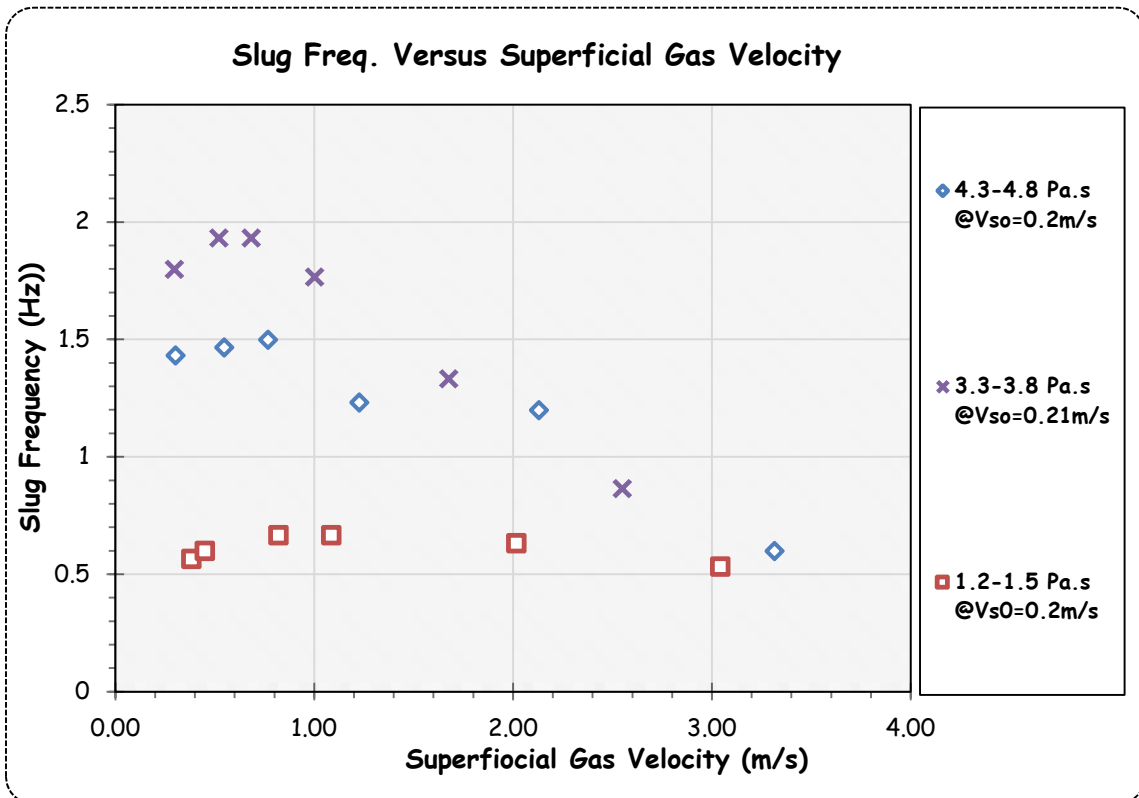
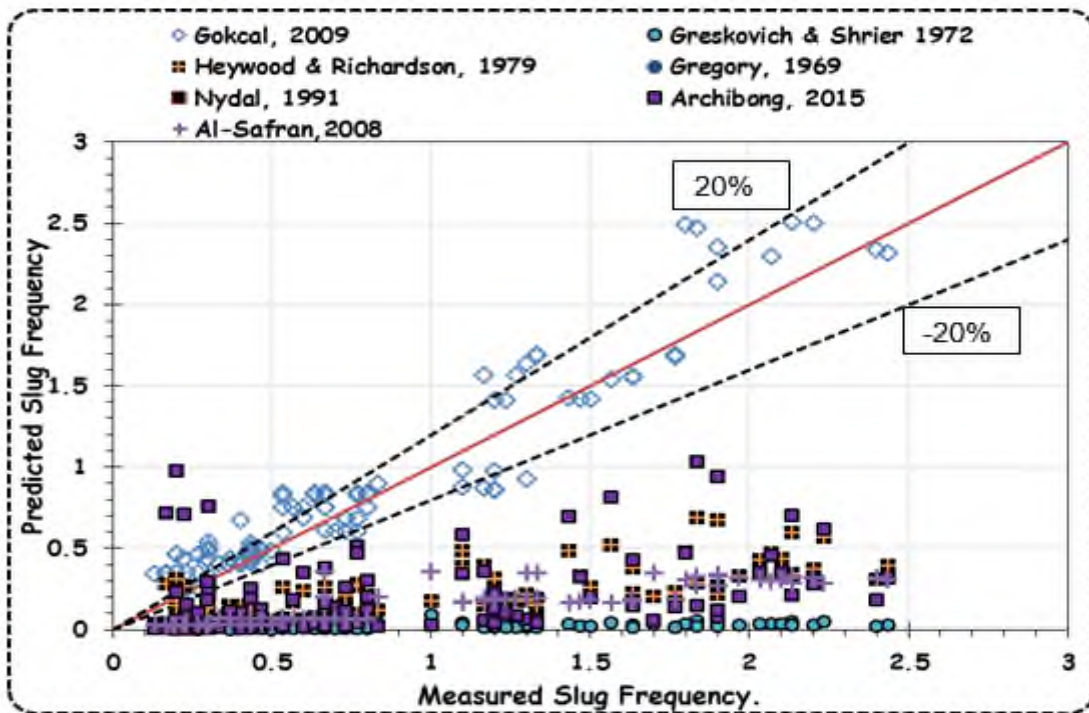


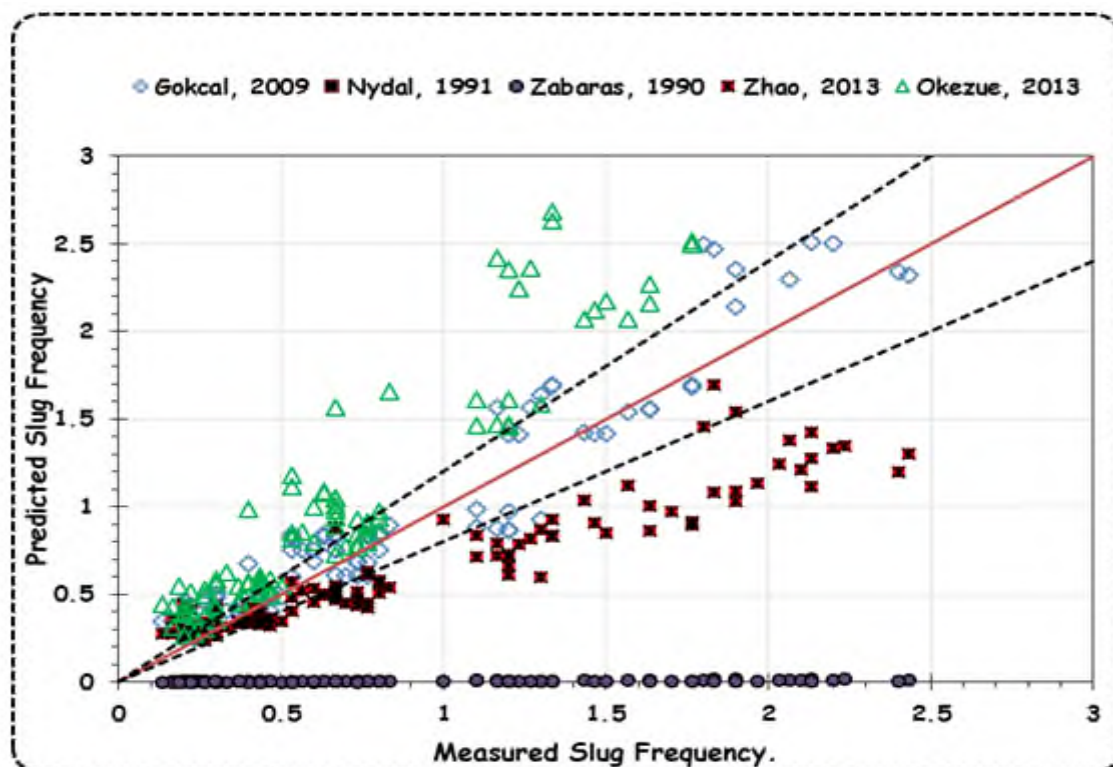
Figure 5-27: Slug frequency vs. gas superficial velocity for diff. viscosities

### **5.6.1 Comparison of slug frequency against prediction models**

Performance evaluation of existing slug frequency models have been carried out against the measured slug frequency data and result presented in Figure 5-28. Models whose performance evaluation were assessed include: (Al-Safran, 2009b; Archibong, 2015; Bahadir Gokcal et al., 2009; Gregory and Scott, 1969; Greskovich and Shrier, 1972; Heywood and Richardson, 1979; Nydal, 1991; Okezue, 2013; Zabararas, 1999; Zhao et al., 2013). Based on the magnitude of error characteristics, none of all the prediction models tested is generally satisfactory. Five of the methods (Gregory and Scott, 1969; Greskovich and Shrier, 1972; Heywood and Richardson, 1979; Nydal, 1991; Zabararas, 1999) exhibited almost equivalent predictions with huge discrepancy, this is expected as they were all developed and validated using conventional data source which does not account for viscosity effects on slug frequency for which experimental observation from this study has established the strong dependence of slug frequency on liquid viscosity. The medium viscosities used by Gokcal et al., 2009 and Al-Safran, 2009b could be the reason for their poor performance. The prediction by (Zhao et al., 2013) which had satisfactory prediction at lower flow velocity and consistent underprediction at higher superficial gas velocities despite using the same facility can be hinged on instrumentation limitation (i.e. ECT used by (Zhao et al., 2013) has a low sampling frequency when compared to Gamma densitometer used in this study). For Archibong, 2015, scaling and inclination effects could be responsible for its poor performance while (Okezue, 2013) had a limited data base. Individual statistical evaluation performance is further discussed in sub-section 6.1.1 of Chapter 6.



(a)



(b)

Figure 5-28a and b: Measured slug frequency versus prediction models



## 5.7 Slug Translational Velocity

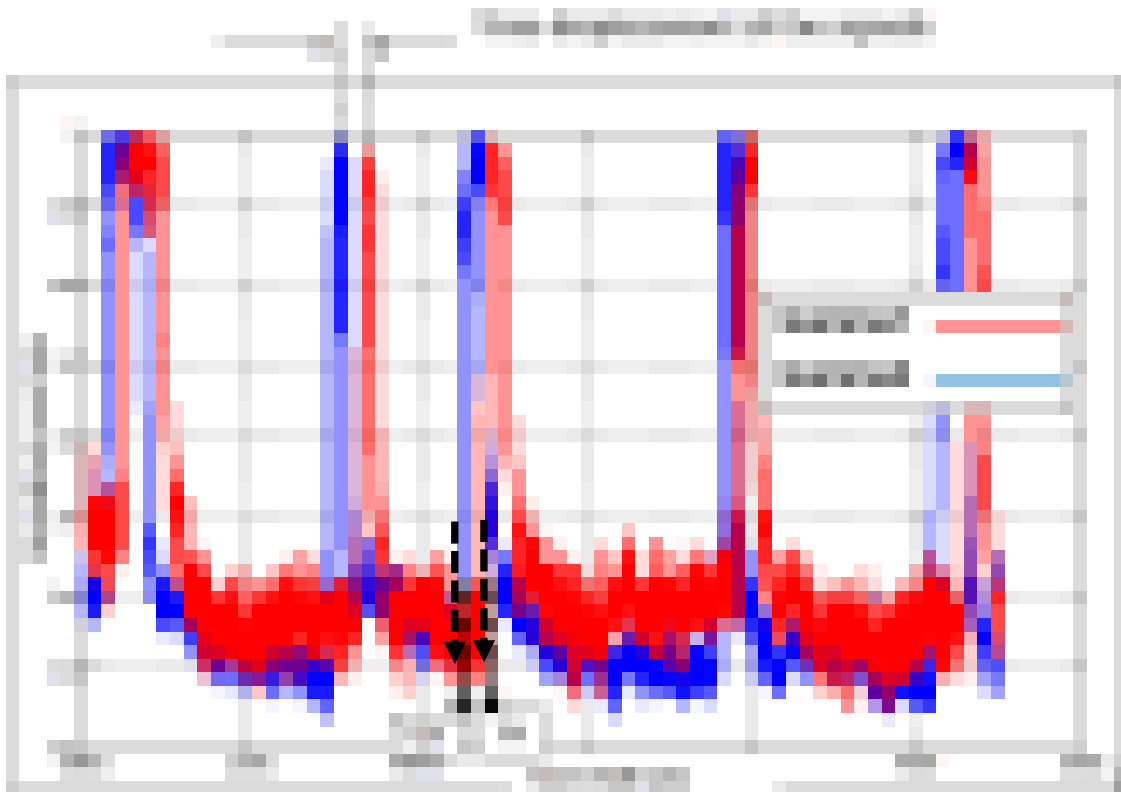
Translational velocity, the velocity of slug units is usually estimated by superimposing the sum of bubble velocity in a stagnant liquid (i.e. drift velocity;  $V_d$ ) and the mixture velocity in the slug body by using equation (5-4) first proposed by (Nicklin et al., 1962).

$$V_T = C_o V_m + V_d \quad (5-4)$$

Where  $C_o$ = distribution parameter is defined as the constant that measures the influence of mixture velocity  $V_m$  in a bubble velocity. Its value is dependent upon the liquid velocity profile in the slug zone and assume values estimated from experiment (the ratio of maximum velocity to the mean velocity of fully developed velocity profile) according to the flow type. It is approximately 1.2 for turbulent flows and 2 for laminar flow.  $V_T$  and  $V_d$  are translational and drift velocity respectively.

Translational velocity been a fundamental variable, is very useful in the determination of other slug flow parameters and commonly used as an input parameter in both transient (King, 1998) and steady-state (Taitel and Barnea, 1990) slug flow models. It is the assumption of most steady-state flow models that the slug front and tail velocities are the same. In this experimental study, only the slug front velocity was measured assuming negligible difference between the slug front and tail.

The holdup time traces obtained from two gamma densitometers positioned at 103D and 124D downstream of the oil injection point were used for the slug translational velocity data collection. This is achieved by carrying out a cross-correlation using a MATLAB signal processing toolbox as earlier described in Chapter 3.



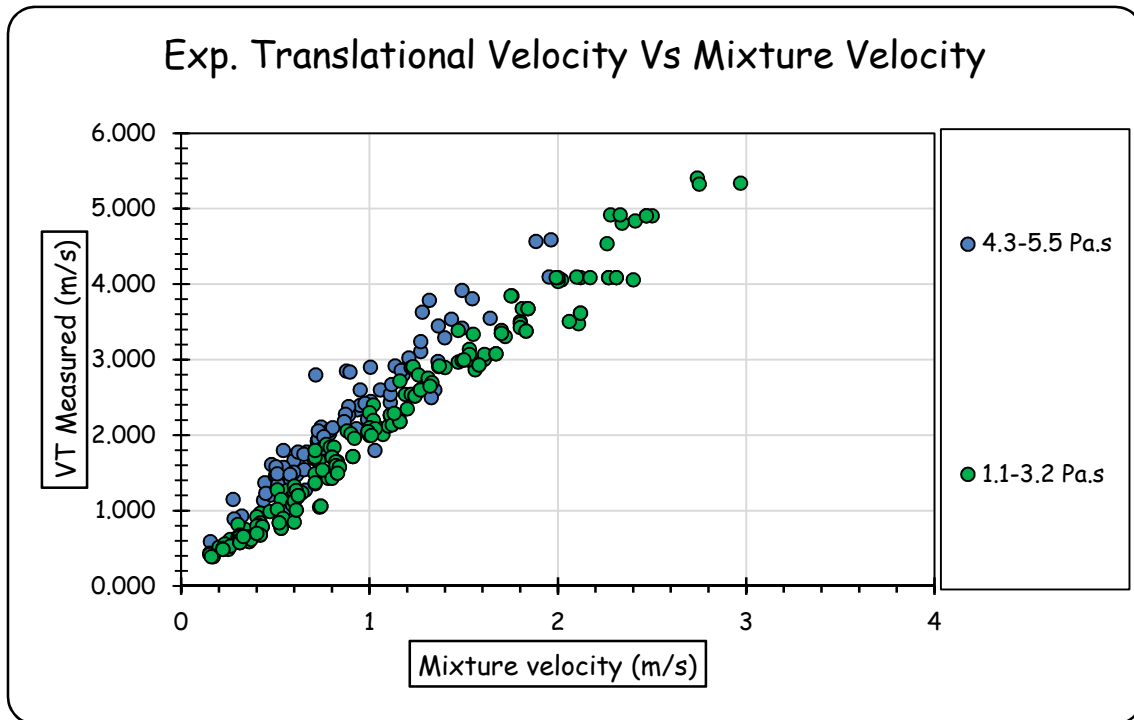
**Figure 5-29: Liquid holdup time trace for the two Gamma densitometer used.**

From Figure 5-29 above, If the distance between the two gamma densitometers is represented by  $\Delta l_{Gamma}$  and assuming the arrival times of the slug front at first and second gamma densitometers are denoted by  $T_1$  and  $T_2$  respectively, obtained by virtue of the passage of a slug body through the cross sectional area of the pipe where the gamma detectors are located. Then the translational velocity is given by;

$$V_T = \frac{\Delta l_{Gamma}}{T_1 - T_2} \quad (5-5)$$

Figure 5-30 shows a plot of measured translational velocity as a function of mixture velocity. The result illustrates a linear relationship between the experimental translational velocity and mixture velocity for different viscosities. Expectedly, the measured translational velocity increases with increasing mixture velocity with the slope of the graph found to be 2.1. The obtained slope represents the flow coefficient  $C_o$  as expressed in the translational velocity equation (5-4). The result also shows that an increase in liquid viscosity slightly affects the flow

coefficient  $C_o$  can be concluded that the experiments conducted are in the laminar flow region as widely reported the literature. It is worth noting here that the value of  $C_o$  obtained in this investigation is in the range of values estimated by the prediction models of Archibong, 2015 and Choi et al., 2012 who both carried out investigation using high viscous oil.



**Figure 5-30: Measured translational velocity as a function mixture velocity**

### 5.7.1 Comparison with Prediction Models

A comparison between measured and predicted translational velocity was carried out and presented in Figure 5-31. The models whose performance evaluation was carried out include; (Benjamin, 1968; Choi et al., 2012; Hubbard, 1965; Jepson, 1989; B C Jeyachandra et al., 2012; Kouba, 1986; Nicklin et al., 1962). While Nicklin et al. 1962 model was based on slug flow in vertical pipes, Hubbard 1965 proposed a one-dimensional model in which the liquid film preceding the slug was accelerated to the velocity of the liquid in the slug and assumed that there is no pressure drop across the mixing length. (Kouba, 1986) proposed an empirical correlation developed from data obtained from downwardly inclined pipe, Jeyachandra et al. 2012 model was developed based on data acquired from

0.0508m ID pipe for oil of viscosity 0.22 Pa.s ; Choi et al. 2012 is a drift flux model developed based on data from 0.0508 m ID pipe and other data sourced from the literature. The illustration from Figure 5-34 shows that all the prediction model grossly underpredicted the present data except for the prediction model of Choi et al., 2012 which performed relatively well and this not far fetched from the fact that the effects of liquid viscosity in the flow coefficient was accounted for. A comprehensive statistical evaluation performance of these models is presented in section 6.3 where this data set was used for the development of a closure relationship.

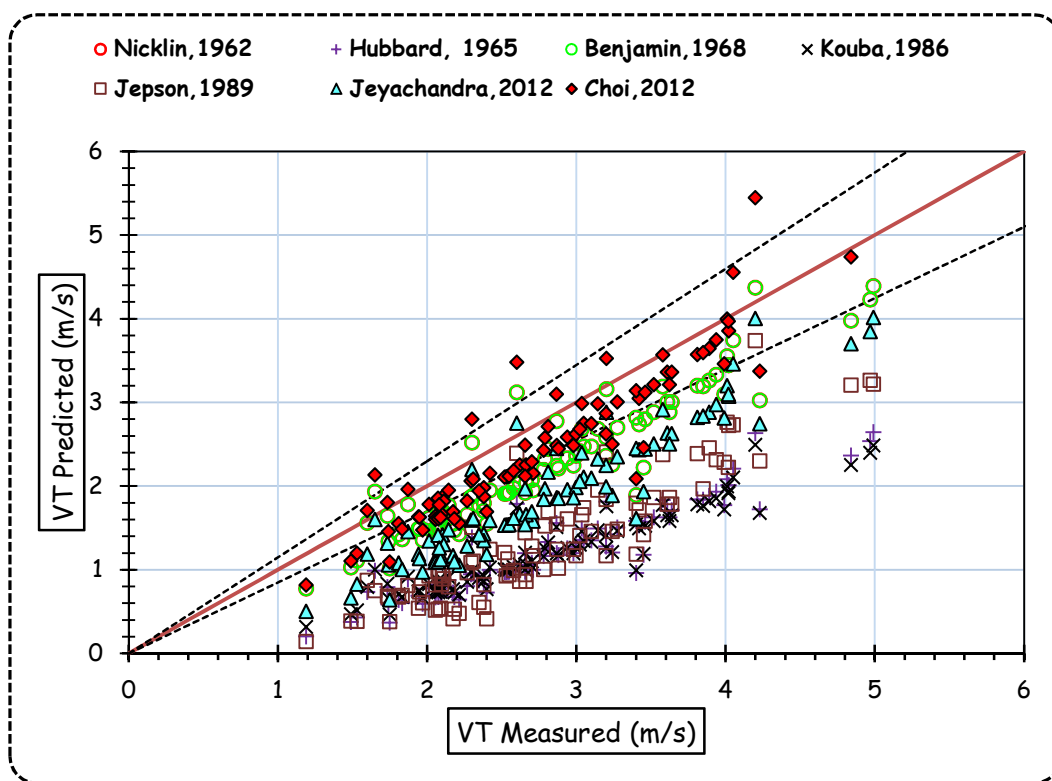


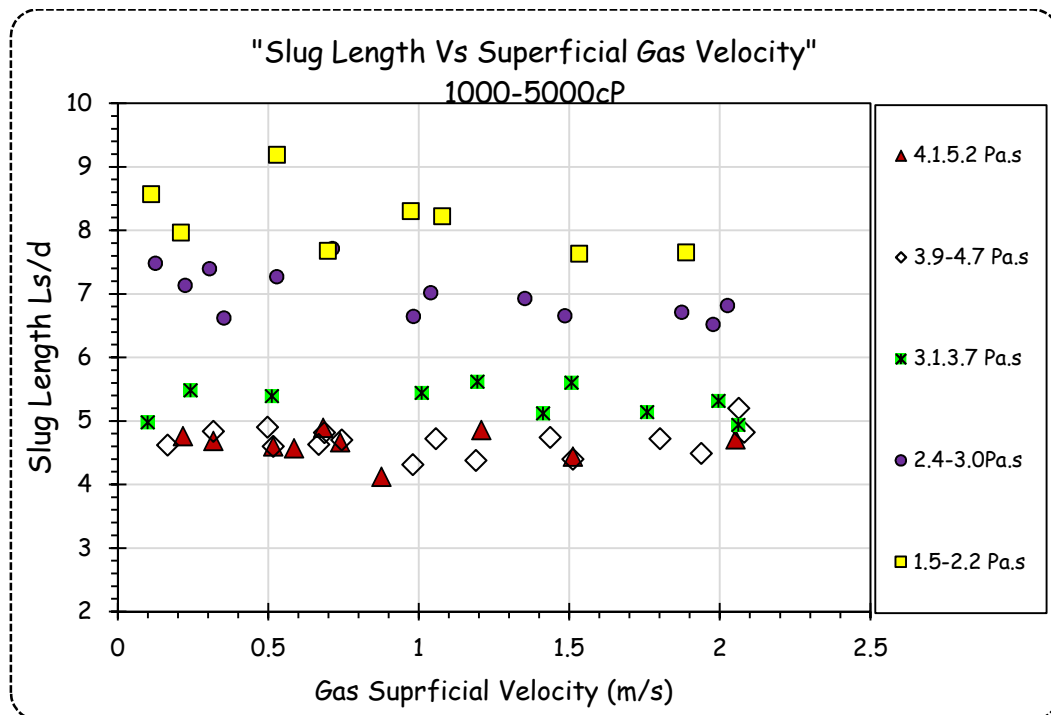
Figure 5-31: Comparison between measured and predicted translational velocity

## 5.8 Slug Body Length

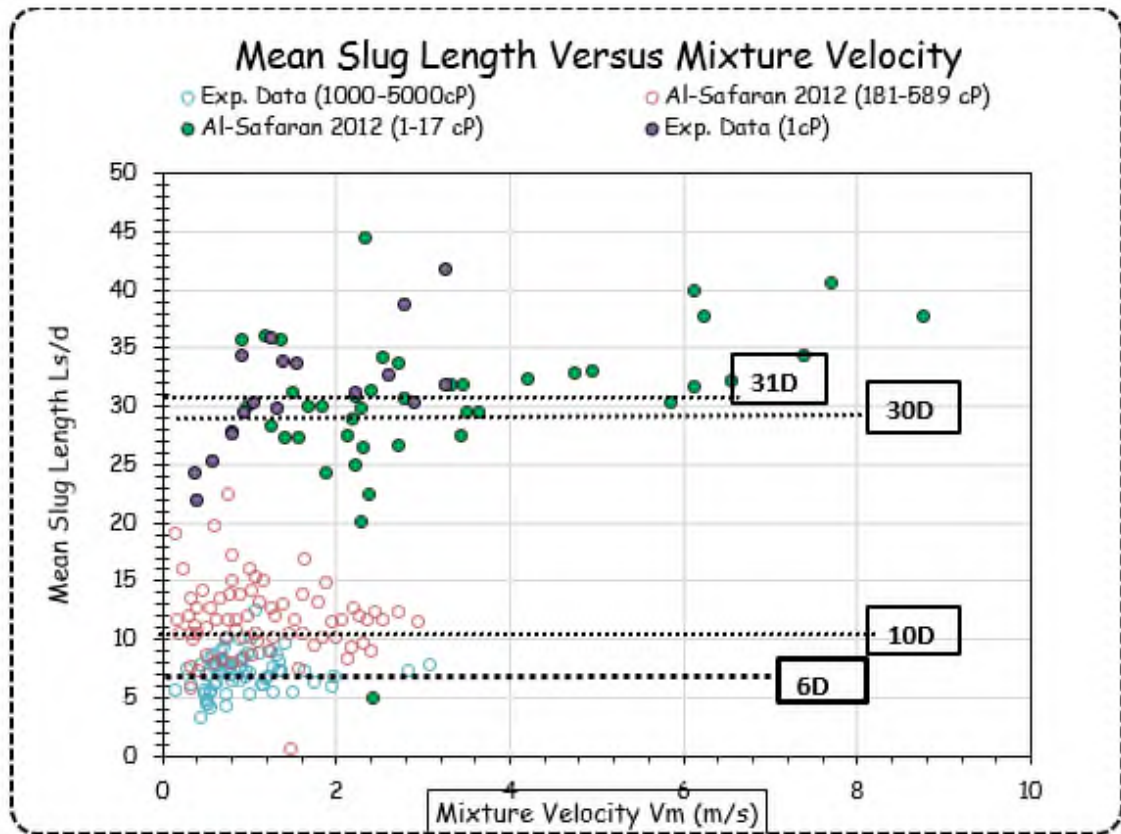
Slug body length is another crucial variable in slug flow modelling. Slug frequency and length are two quantities that are strongly interrelated. Slug body length can be estimated by multiplication of the time difference as the slug body passes the two gamma densitometer by the velocity of the slug. The velocity of

the slug body is determined by the cross correlation of the data set obtained from the two gamma densitometer as described in sub section 3.8.

Figure 5-32 is a plot of measured mean slug as a function as a function of gas superficial velocity for oil superficial velocities  $\sim$  (0.06~0.3 m/s). It shows strong dependence of slug length on liquid viscosity as slug body length decreased with increase in liquid viscosity. The measured slug body length was in the range of 4-9D with an of average length of 6D as against 8-14D, 12-24D, 12-30D, 12-24D and 15-20D for (Al-safran et al., 2011; Dukler and Hubbard, 1975; Nicholson et al., 1978; Nydal et al., 1992) respectively. A comparison of mean slug length of this study and (Al-safran et al., 2011) is presented in Figure 5-33. Most researchers (Gokcal, 2008; Hernandez, 2007; Pan, 2010) unanimously reported that slug body length are generally insensitive to flow conditions (i.e. changes in gas superficial velocity and liquid superficial velocity). This has been confirmed by this study as can be seen illustrated in Figure 5-32 where there is an irregular nature of the data relative to the uncertainties of time of passage of the slug body.

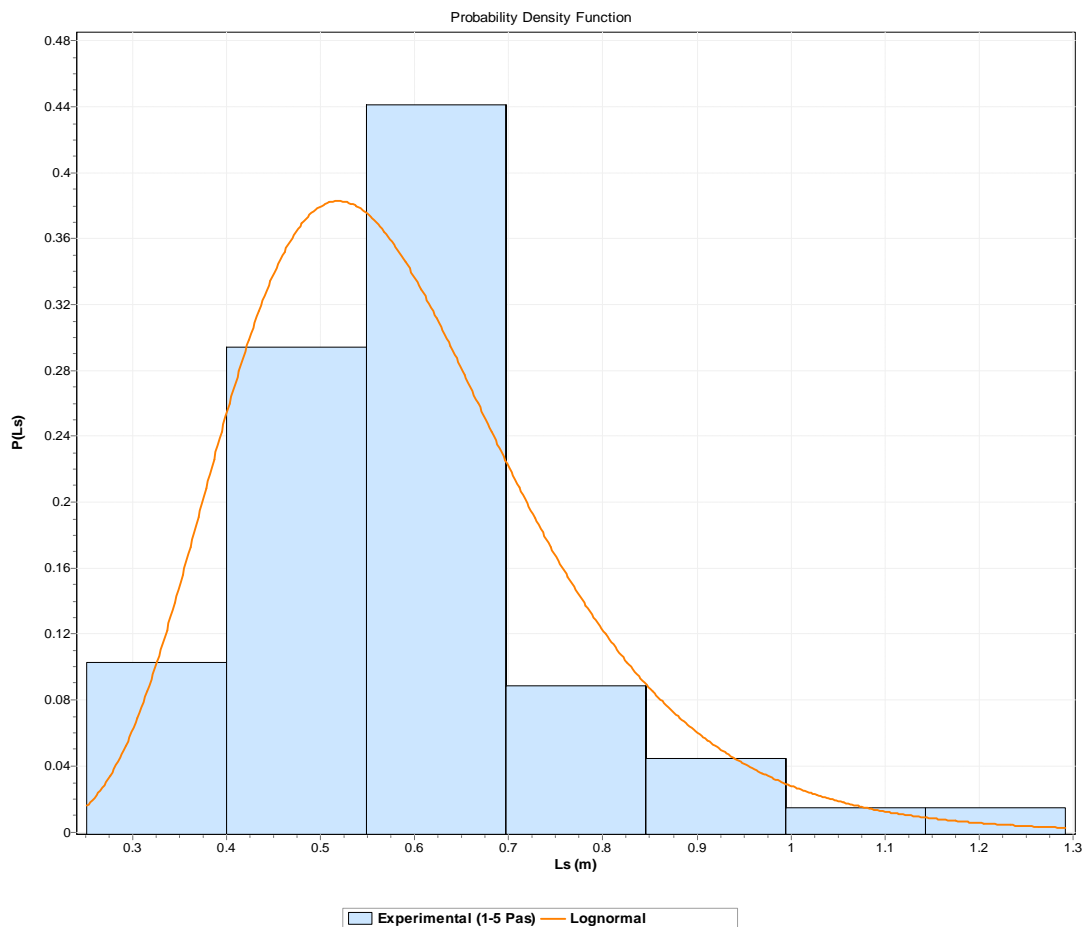


**Figure 5-32: Measured slug length versus superficial gas velocity for different superficial liquid velocity  $V_{sl}=0.06-0.3\text{m/s}$**



**Figure 5-33 Mean Slug Length as a Function of Mixture Velocity**

The liquid slug length data are generally described by positively skewed distributions (i.e. log-normal distribution) according to (Gokcal, 2008; Nydal et al., 1992; Van Hout et al., 2001). In view of this, Easy Fit software 3.0 was used to determine the mean and standard deviation of the Log-Normal distribution. Presented in Figure 5-34 is the comparison between experimental result and Log-Normal distribution which exhibited a good match.



**Figure 5-34: Comparison of experimental result for slug length and Log-Normal distribution**

## 5.9 Chapter Summary

High viscosity liquid and gas flow experiments conducted in 3-inch horizontal pipes are reported in this chapter. Four flow patterns; plug flow, slug flow, pseudo slug flow and annular flow were observed. The characteristics effects of increased liquid viscosity, liquid and gas phase on flow behaviour were observed. Experimental data collected include; mean liquid holdup, slug liquid holdup, pressure gradient, slug frequency, slug length and slug translational velocity. The finding are made are summarized as:

- Intermittent flow pattern (slug and plug) were found to be the dominating flow pattern

- The measured liquid holdup exhibited a decreasing trend as the gas superficial velocity increases. The effects of increase liquid viscosity and liquid content on the mean liquid holdup were found to be slight.
- Measured pressure gradient increased with increase in gas superficial velocity at constant liquid superficial velocity. Similar increase in measured pressure gradient was observed at fixed gas superficial velocity and increasing superficial oil velocity. Additionally, increased oil viscosity also increased the measured pressure gradient at similar superficial oil and gas velocities.
- Slug frequency was found to have strong dependency on liquid viscosity with an increasing trend. Performance evaluation of most existing prediction models against present data revealed wide discrepancies attributed unaccounted liquid viscosity effects in the models.
- Slug body length was also found to have strong dependency on liquid viscosity but unlike slug frequency which increases with increase in viscosity, slug length was observed to decrease when liquid viscosity increases though insensitive to changes in the flow condition. A minimum length of 32D has been proposed by researchers like (Barnea and Brauner, 1985; Taitel et al., 1980) for liquid slug body length in horizontal pipeline. It was however found that the slug body lengths were much shorter than 32D. The mean slug length were approximately found to be 6D within the range of experimental conditions investigated.
- Slug liquid holdup was observed to increase slightly as viscosity increases. Model prediction by (Al-Safran, Kora and Sarica, 2015; Gregory, Nicholson and Aziz, 1978; Kora et al., 2011a) showed good agreement with measured liquid holdup for the flow conditions tested.



## **6 HIGH VISCOSITY LIQUID-GAS SLUG FLOW MODELLING STUDY**

There is an overwhelming amount of research on prediction models which are expected to provide reliable predictions of flow characteristics. Some of the earlier predictive models (Beggs and Brill, 1973; Dukler et al., 1964) for gas-liquid two phase flow in pipeline have shown acceptable performance but are however constrained to some predefined limits.

Flow regimes generally occur in gas liquid two-phase flow and investigations have shown that slug flow is the dominant and most complex flow pattern occurring in the petroleum industry. The understanding of slug flow characteristics i.e., its velocity, frequency and slug length in addition to other variables are of paramount importance in the design of petroleum pipelines, sizing of receiving vessels and pre-processing equipment. The velocity of slug flow unit cell Figure 6-1 for instance, defines the instantaneous gas and liquid flow rate to be delivered to a receiving vessel; the length of the liquid slug correlates strongly with the pressure drop.

Available prediction models in the literatures for the prediction of slug flow characteristics relied mostly for development and comparison, on data bases generated from oil viscosities less than 1 Pa.s in addition to being carried out on small-scale laboratory facilities i.e. 0.025m internal pipe diameters. It is therefore, necessary to develop a model which could account for higher viscosities above 1.0 Pa.s.

In this chapter, empirical correlation for the prediction of four characteristics features (i.e. slug frequency, slug length, slug translational velocity and slug liquid holdup) of slug flow are proposed based on experimental data acquired for high viscosity liquid in the range of 1.0~5.5 Pa.s . The proposed correlations will assist in minimizing the huge discrepancies observed when existing prediction models built from low viscosity data are used thereby enhancing the design of pipeline and receiving vessels.

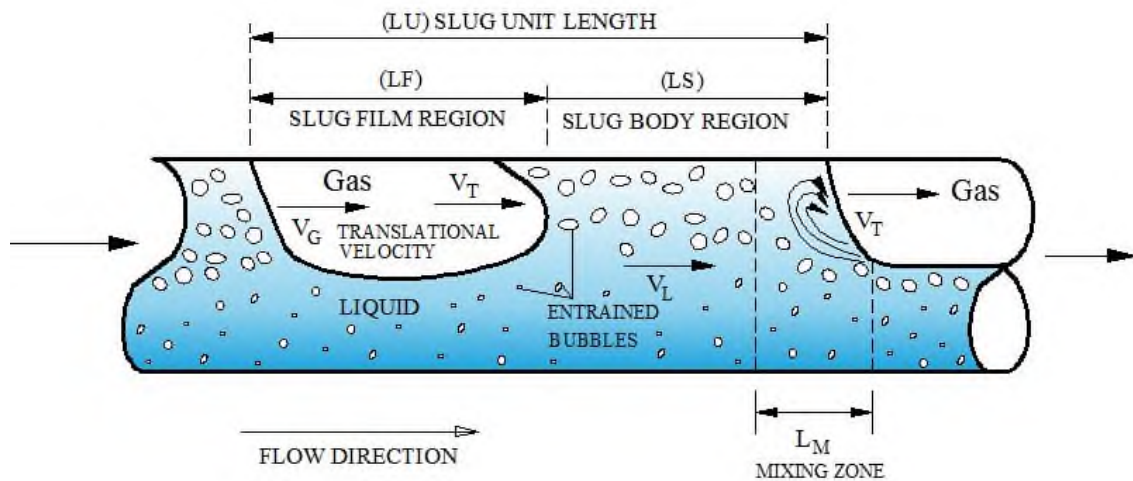


Figure 6-1 Slug Flow Unit Cell

## 6.1 Slug Frequency

Slug frequency models compared with experimental results obtained showed some discrepancies. Most of the models in literature relied on data from low viscosity liquid-gas experiment, those developed on high viscous dataset such as (Archibong, 2015) relied on data obtained wholly from a 1 inch pipeline. It has been experimentally observed in this study and reported by some researchers (Gokcal et al., 2006; Zhao, 2014) that liquid viscosity enhances slug flow region and thus slug frequency. Therefore a development of a model that will account for the effect of viscosity, relatively large pipe diameter and dimensional consistency becomes important.

From experimental observations of the hydrodynamic behaviour of slug flow and several published works, the following functional parameters were deduced to strongly correlate slug frequency,  $F_s$

$$f_s = f(V_{so}, V_{sg}, V_m, \mu_l, \mu_g, g, D, \rho_l, \rho_g) \quad (6-1)$$

Performing dimensional analysis on equation 6-1 by way of application of the Buckingham Pi-theorem followed by a non-dimensional groupings yielded the following dimensionless groups: Mixture Reynolds number, mixture Froude number and Viscosity number.

$$f_s = f(Re_m, Fr_m, N_\mu) \quad (6-2)$$

Reynolds number defined as  $\frac{\rho_m V_m D}{\mu_L}$  are used to study fluids as they flow. Its use as candidates for correlation is normal as they capture inertia changes prompted by changes in fluid superficial velocities relative to viscous forces. In addition Reynolds number provides information necessary to categorise flow into laminar or turbulent flow. It should be noted that  $\mu_L$  was used because  $\mu_L \gg \mu_g$  thus  $\mu_g$  negligible. Froude number represented by  $\frac{V_m}{\sqrt{gD}}$  is a dimensionless quantity which is used in hydrodynamics study to indicate the influence of gravity on fluid motion, and viscosity number  $N_\mu$  given by  $\frac{V_m \mu_L}{gD^2(\rho_L - \rho_g)}$  to introduce viscosity effects. Froude number is the ratio of inertial forces of pressure driven gas/liquid flow to the force to separate the liquid from the gas while viscosity number on the other hand which is the ratio of Froude number to the Reynolds number. Upon correlation of the acquired experimental dataset with those from the literature (Gokcal, 2008) a general non- linear regression for slug frequency in high viscosity oil-gas two-phase flow is proposed as;

$$f_s = 1.283 Fr_m^{-0.207} N_\mu^{0.5129} Re_m^{0.0589} \quad (6-3)$$

### 6.1.1 Evaluation and comparison of Proposed Slug Frequency Prediction Model

Statistical performance evaluation of the proposed correlation with other prediction models found in the literature was carried out against present data set. The results of some of the selected prediction models as presented in Figure 6-2 and Table 6-1 exhibited different magnitude of prediction. The proposed correlation out-performed the prediction models of (Gokcal et al., 2009 and Zabaras, 1999) this is not surprising as the liquid viscosities investigated in this study are quite higher than those (Gokcal et al., 2009 and Zabaras, 1999). And as for the correlations developed by (Okezue, 2013), (Zhao et al., 2013) and (Archibong, 2015) despite using the same facility as the data source, their poor

performance can be attributed to the fact that (Okezue, 2013) had a limited data base, and instrumentation limitation in the case of (Y Zhao et al., 2013) and diameter effect for (Archibong, 2015).

Also when the proposed correlation was compared against existing prediction models using published data of dataset (Gokcal, 2008) as illustrated in Figure 6-3 and Table 6-2, a similar trend as that of the present data represented in Figure 6-2 and Table 6-1 was observed. In all, the error margin between the measured slug frequencies result and model prediction becomes more significant with increase in Reynolds number thus highlighting the sensitivity of the proposed model to change in liquid viscosity. It is worth noting here that since intermittent flow pattern was the dominant flow pattern observed for this investigation, it can be concluded that the proposed correlation model will give good prediction result in the laminar flow region.

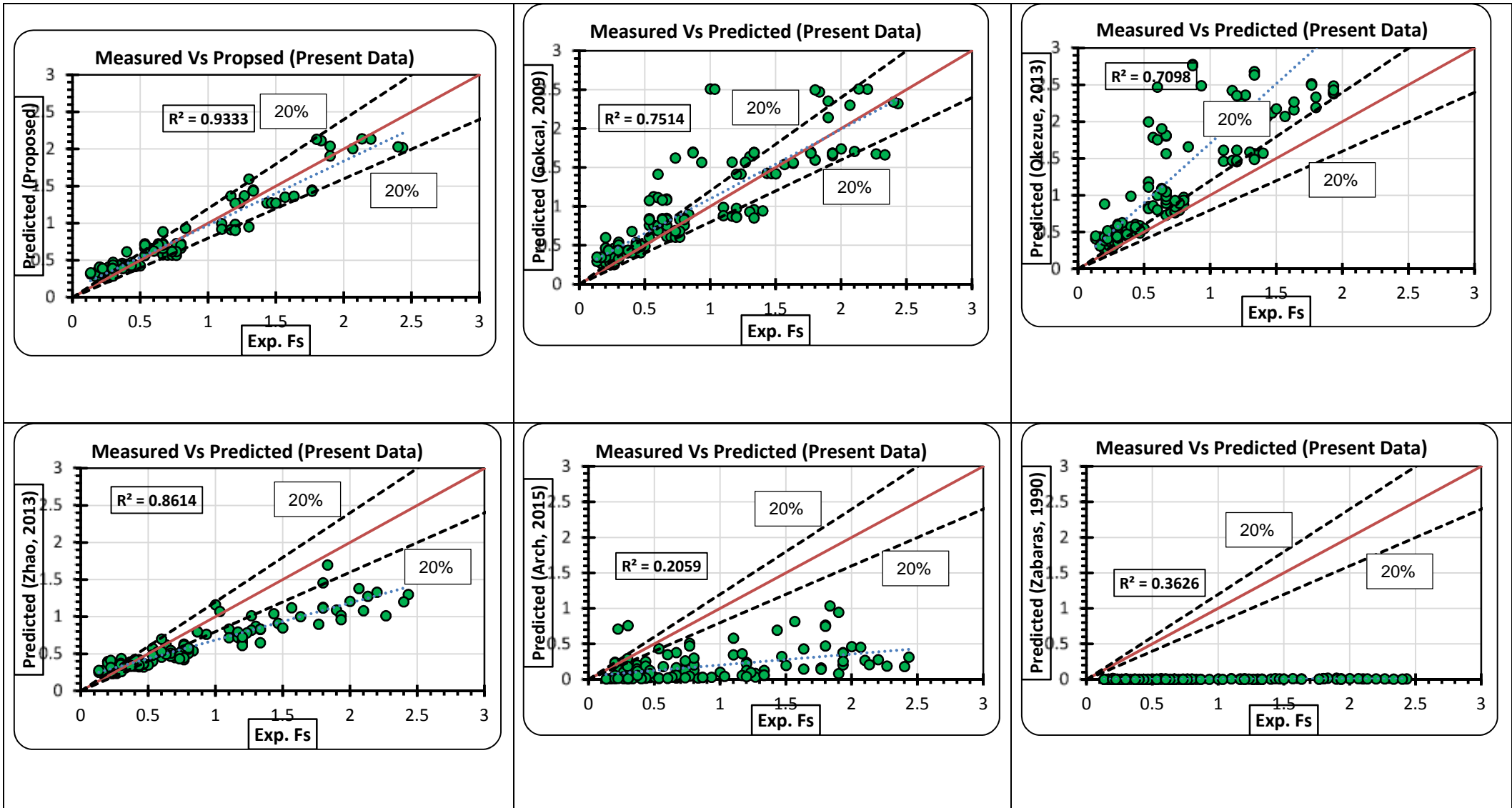


Figure 6-2 Cross-plot of measured slug frequency against predicted for present data set.

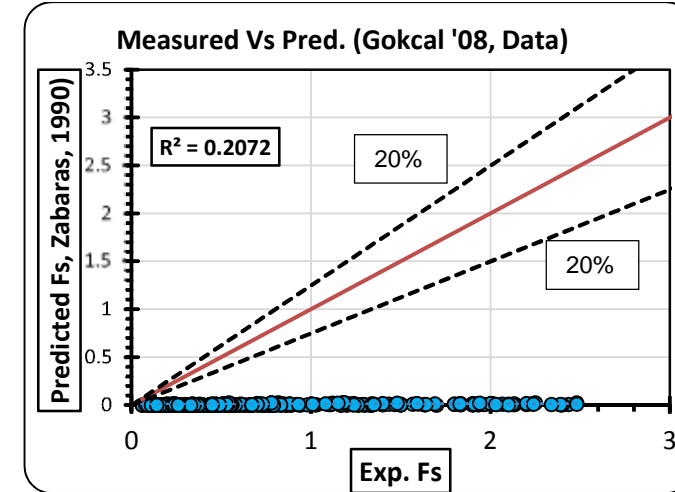
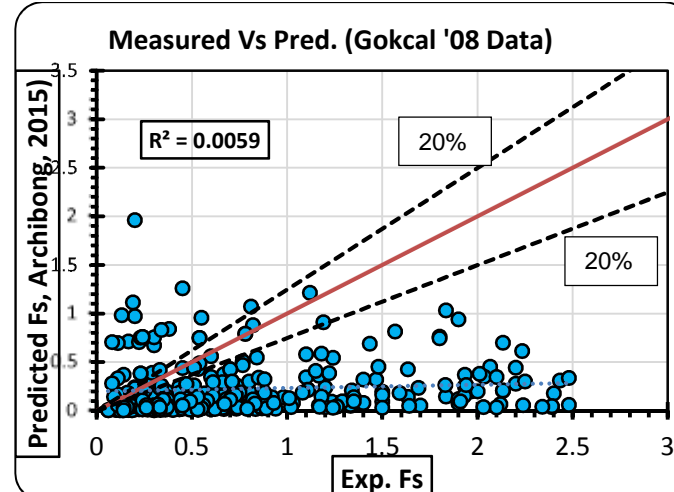
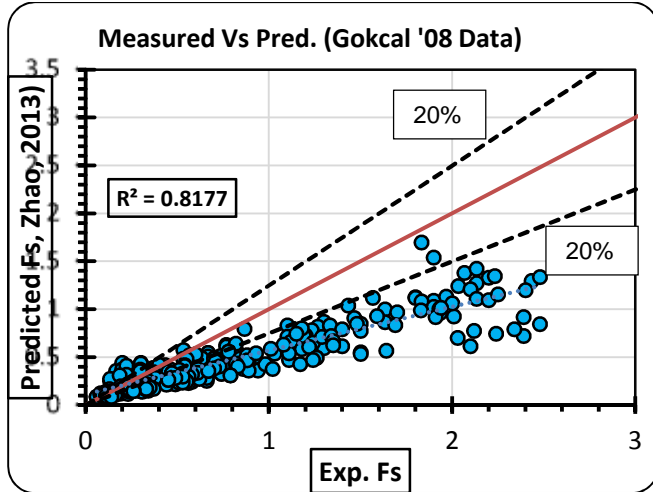
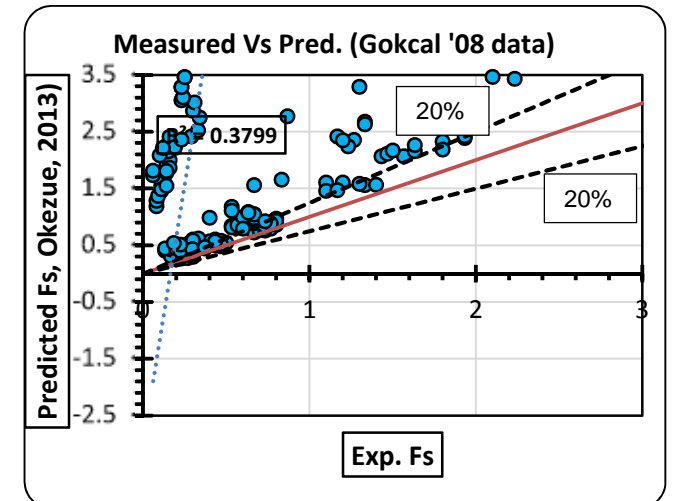
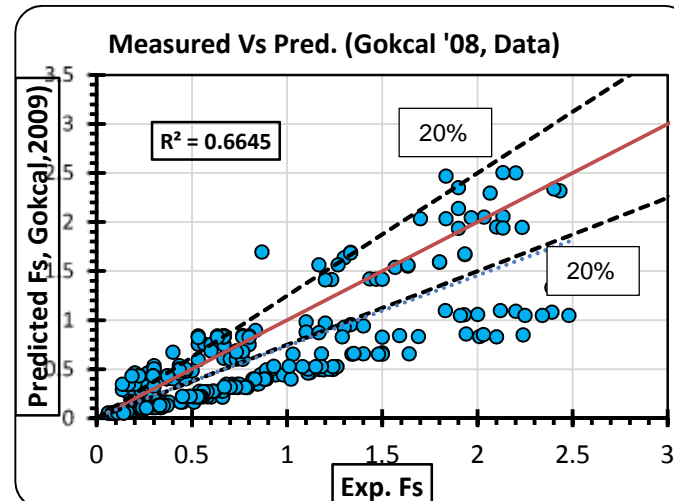
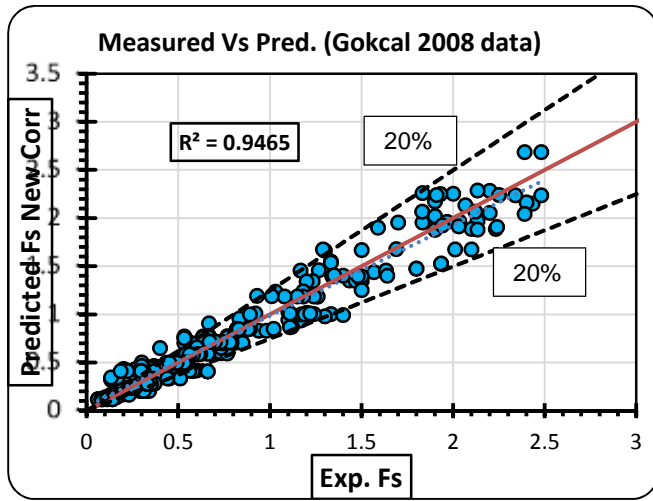


Figure 6-3 Cross-plot of measured slug frequency versus predicted (Gokcal, 2008 dataset)

**Table 6-1 Performance evaluation of proposed model against existing prediction models (Present data)**

	Gregory 1969	Henwood & Richardson 1971	Greskovich & Shrier 1972	Zabaras, 1990	Nydal 1991	Al- Safran (2008)	Gokcal, 2009	Okezue 2013	Zhao 2013	Archibong, 2015	Proposed
$\epsilon_1$	-88.248	-64.520	-85.936	-87.825	-87.991	-76.182	20.756	60.086	-12.499	-58.416	11.001
$\epsilon_2$	88.248	66.778	85.936	87.825	87.991	76.182	26.282	60.086	28.809	75.715	21.139
$\epsilon_3$	11.050	24.339	11.037	11.009	11.020	11.133	38.132	59.807	33.927	67.140	34.240
$\epsilon_4$	-0.805	-0.629	-0.788	-0.802	-0.804	-0.691	0.094	0.573	-0.238	-0.628	0.006
$\epsilon_5$	0.805	0.633	0.788	0.802	0.804	0.691	0.158	0.573	0.275	0.664	0.133
$\epsilon_6$	1.050	0.509	0.596	0.601	0.604	0.515	0.223	0.701	0.313	0.571	0.204

**Table 6-2 Performance evaluation of proposed model against existing prediction models (Gokcal, '08 data)**

	Gregory 1969	Henwood & Richardson 1971	Greskovich & Shrier 1972	Zabaras, 1990	Nydal 1991	Al- Safran (2008)	Gokcal, 2009	Okezue 2013	Zhao 2013	Archibong, 2015	Proposed
$\epsilon_1$	-57.464	-18.831	-54.237	-56.663	-57.242	-40.386	-30.727	1122.291	-22.320	-21.302	-0.909
$\epsilon_2$	57.464	33.882	54.237	56.663	57.242	40.386	30.727	1122.291	24.347	53.061	7.402
$\epsilon_3$	32.235	48.646	30.640	31.807	32.112	25.162	18.383	847.812	21.330	95.102	14.448
$\epsilon_4$	-0.443	-0.232	-0.422	-0.439	-0.442	-0.281	-0.238	10.634	-0.215	-0.211	-0.014
$\epsilon_5$	0.443	0.262	0.422	0.439	0.442	0.281	0.238	10.634	0.217	0.211	0.047
$\epsilon_6$	0.518	0.405	0.496	0.515	0.518	0.298	0.275	16.725	0.307	0.216	0.091

## 6.2 Slug Body length

Accurate prediction of slug body length under intermittent flow conditions are most important for two reasons; firstly, all the mechanistic models available in the literature for the prediction of slug characteristics feature such as (Cook and Behnia, 2000; Dukler and Hubbard, 1975) requires an estimate of slug body length as an input parameter for the calculation of pressure drop and liquid holdup. Secondly and most importantly the knowledge of maximum possible slug body length, since the design of slug catchers depends solely on the longest encountered slug and not necessarily on the average one.

Experimental investigation and review of existing literatures indicates that slugs are less aerated and more frequent for high viscosity liquid thus resulting in shorter slugs when compared to those of low viscosity oils hence the need for an improvement in the existing prediction models. Therefore, it has become imperative to develop new correlation to account for this difference.

Slug body length and slug frequency are interrelated and are often used interchangeably (Al-safran et al., 2011; Barnea and Taitel, 1993). The following functional parameters of hydrodynamic slug flow from experimental observations and existing published works were deduced to strongly correlate slug body length similar to those of slug frequency:

$$\frac{L_s}{D} = f(\rho_m, V_m, D, \mu_L, g) \quad (6-4)$$

Repeating the procedure used for slug frequency as noted in sub section 6.1 above yielded the following dimensionless groups: Mixture Reynolds number, mixture Froude number and Viscosity number.

$$\frac{L_s}{D} = f(Re_m, Fr_m, N_\mu) \quad (6-5)$$



A general non-linear relationship for the slug body length in high viscosity oil-gas two-phase flow is proposed (6-6), after correlation of the experimental dataset with those obtained from literature.

$$\frac{L_s}{D} = 3.35 Fr_m^{0.03} N_\mu^{-0.2} Re_m^{0.1} \quad (6-6)$$

### 6.2.1 Validation of Proposed Correlation

Performance of the proposed slug length prediction model was examined against selected slug length correlations in the literature. Correlations whose predictive performance were evaluated include; (Al-safran et al., 2011; Brill et al., 1981; Norris, 1982; Scott et al., 1989; Wang, 2012). Results presented in Table 6-3 shows that all the existing prediction correlations found in the literature over-predict the average slug length with huge discrepancy. The correlations of (Brill et al., 1981; Norris, 1982; Scott et al., 1989) over predict obtained experimental data with very wide error margin owing to the fact that were developed from Prudhoe Bay large diameter data while the (Al-safran et al., 2013; Wang, 2012) over predicted as a result of viscosity effects. In summary, the comparative analysis reveals the need for a slug length prediction correlation in a higher liquid viscosity flow conditions.

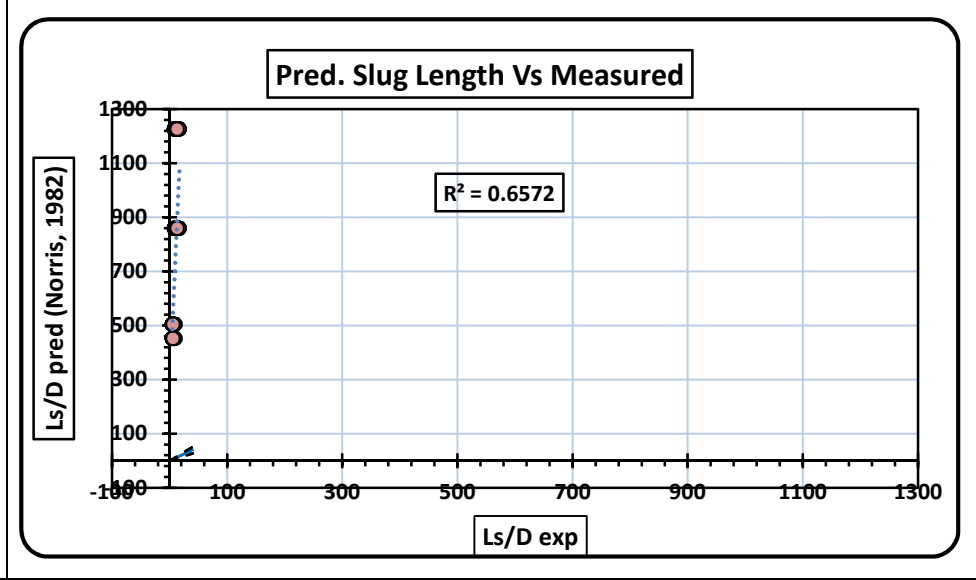
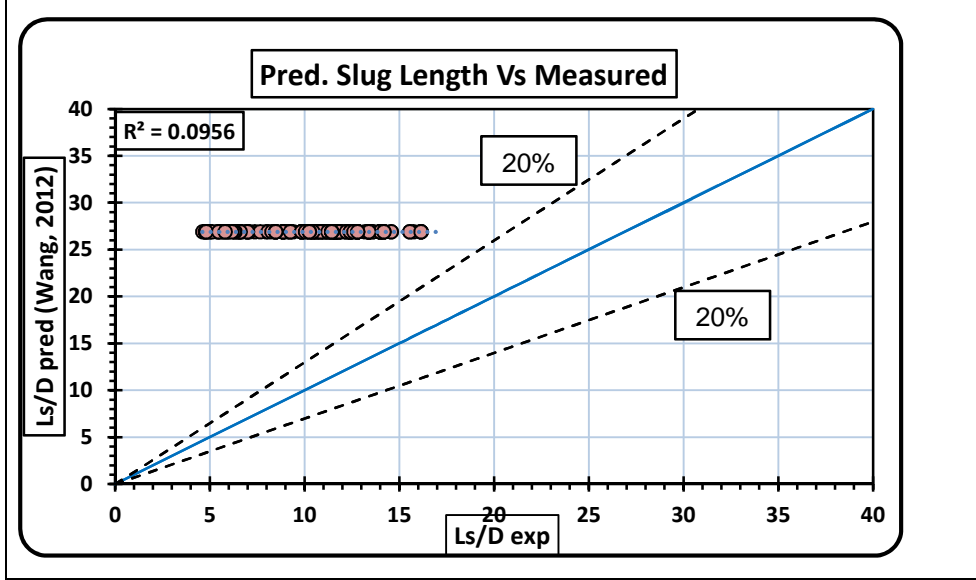
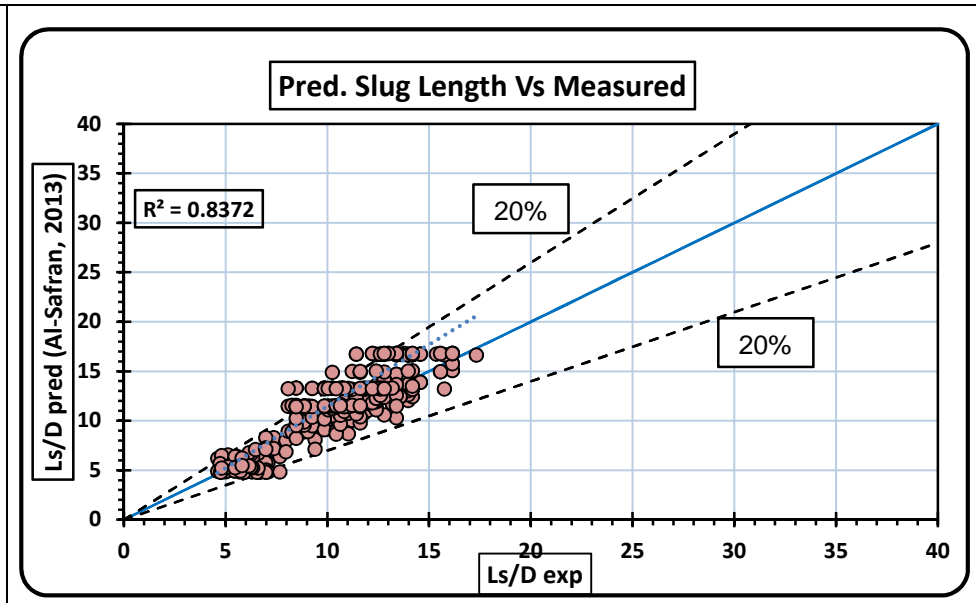
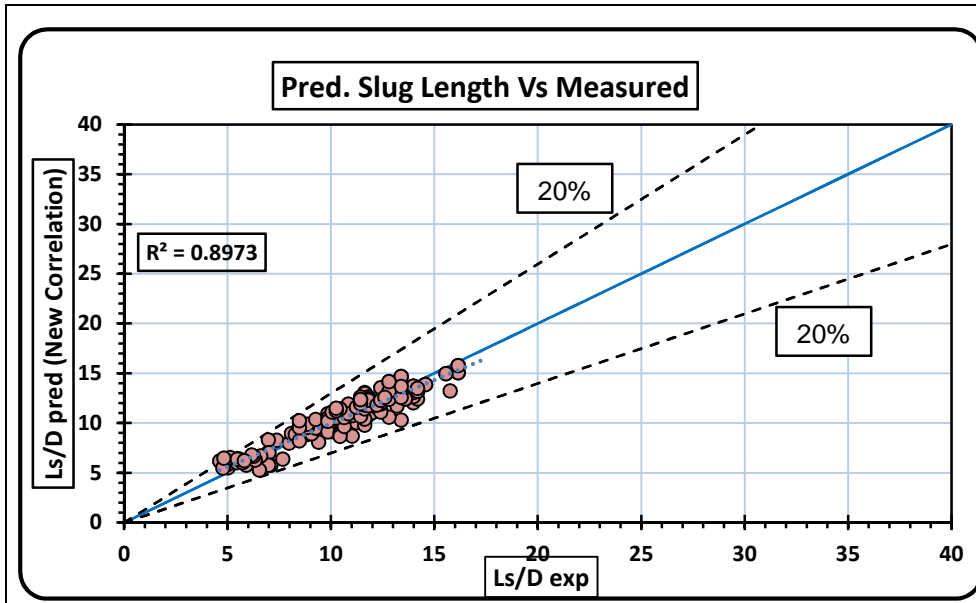


Figure 6-4 Cross-plot of predictive model predictions against experimental measurement.

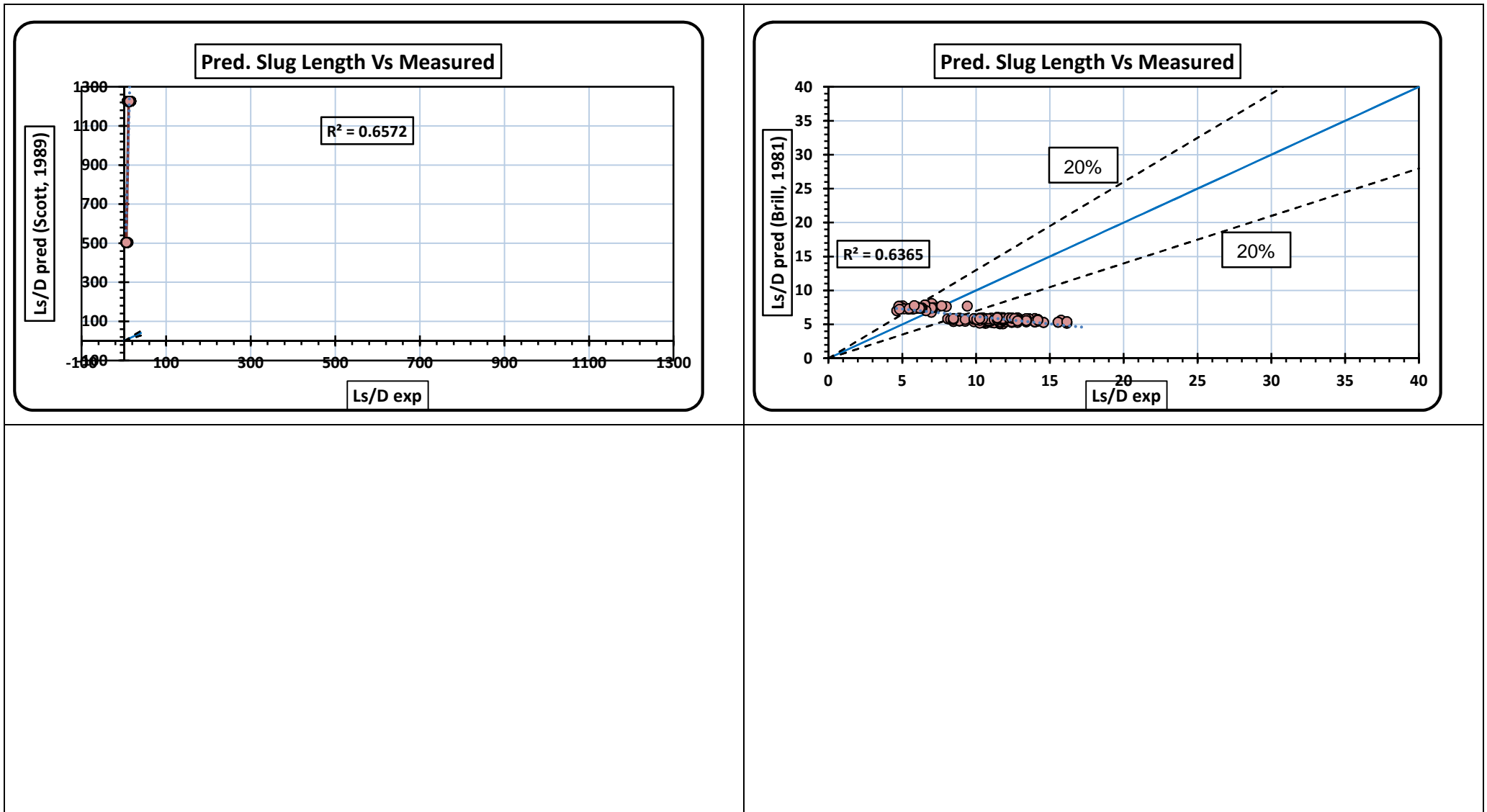


Figure 6-5 Cross-plot of predictive model predictions against experimental measurement.

**Table 6-3 Statistical evaluation of slug length predictive models**

	New Corr	Brill, 1981	Norris, 1982	Scott 1989	Wang 2012	Al-Safran et al, 2013
$\epsilon_1$	0.517391	-34.1318	7401.188	10088.98	181.3125	14.4496
$\epsilon_2$	8.468193	46.13764	7401.188	10088.98	181.3125	20.30533
$\epsilon_3$	10.6204	34.29429	1238.391	1888.901	104.2071	18.50914
$\epsilon_4$	-0.15192	-4.55236	761.5418	1061.032	16.29675	2.736121
$\epsilon_5$	1.505312	5.205357	761.5418	1061.032	16.29675	2.09782
$\epsilon_6$	1.892089	3.638863	165.4363	295.3714	2.976471	2.064682

### 6.3 Slug Translational Velocity

One of the key closure relationships for two-phase flow modelling is translational velocity; velocity of slugs. Existing models found in the literatures have shown significant performance for application in high viscosity applications within predefined limits. It therefore becomes imperative to extend this limits since their accurate prediction is essential in the design of some unit operation equipment.

A correlation i.e. equation (6-7) based on experiment was first proposed by (Nicklin et al., 1962) to predict the velocity of Taylor bubble in vertical slug flow but have largely been applied for all pipe inclination by most researchers in recent times

$$V_T = C_o V_m + V_d \quad (6-7)$$

Where

$V_T$  = Translational Velocity

$V_m$  = Mixture velocity

$V_d$  = Drift velocity

The coefficient  $C_o$  which depends on the liquid velocity profile in the slug region is defined as the weighted velocity/liquid fraction distribution parameter. Its value was found to be close to 1.2 for fully developed turbulent flow and approaching 2 for laminar flow. Previous studies have shown that for low viscosity liquids, the distribution parameter  $C_o$  ranges between  $1.0 < C_o < 1.2$ . However, (Wallis, 1969) noted that the value of  $C_o$  can even be higher than 2 for fully developed laminar flow though it was stated in his work that the exact behaviour was to be determined. This has been confirmed by the works of (Gokcal, 2008) who suggested a larger distribution

parameter. (Choi et al. 2012) proposed  $C_o = 2.27$  for relatively high viscosity oils from equation (6-8). (Lacy, 2012) also suggested 2.3 for  $C_o$  and most recently 2.26 by (Archibong, 2015).

$$C_o = \frac{2}{1 + (Re/1000)^2} + \frac{1.2 - 0.2\sqrt{\rho_G/\rho_L}(1 - \exp(-18\alpha_G))}{1 + (1000/Re)^2} \quad (6-8)$$

Drift velocity acts in the same direction as the mixture velocity thereby is known to contribute to the magnitude of the translational velocity. It is defined as the velocity of the phase relative to a surface moving at a mixture velocity. It is generally estimated using the equation .....

$$V_d = C_1\sqrt{gD} \quad (6-9)$$

Where  $C_1$  is the constant to evaluate the drift velocity first estimated as 0.542 by (Benjamin, 1968). The experimental work of (Gokcal, 2008) showed that drift velocity can be affected by high liquid viscosity which was not taken into account by (Benjamin, 1968) during the estimation of  $C_1$ . This lead to the work of (B C Jeyachandra et al., 2012) who proposed a new correlation equation (6-10)Based on experiments for different oil viscosities ranging from 0.1-0.58 Pa.s.

$$V_d = 0.53\exp(-13.7Ar^{-0.6}Eo^{-0.1}) \quad (6-10)$$

The proposed translational velocity  $V_T$  is thus correlated from the experimental dataset for this study ranging from 1.5 to 5.5 Pa.s and (Gokcal, 2008) dataset ranging from 0.108 to 0.587 Pa.s. By utilization of the sum of squares regression method, the error margin in prediction between the proposed correlation and that of the experimental data is obtained, afterwards minimized by way of fine-tuning  $C_1$  to obtain an optimum local solution. The new optimum solution obtained for  $C_1$  based on the present data set for high viscosity oil ranging 1.5-5.5 Pa.s is 0.79.

Substituting the newly optimized value for  $C_1$  into equation (6-9) and then re-subtitling both equations (6-8) and (6-9) into equation (6-7) with the introduction of viscosity number into the final expression so as to account for the limited viscosity in (Choi et al., 2012) yields the slug translational velocity thus;

$$V_T = (C_o + N_\mu)V_m + 0.79\sqrt{gD} \quad (6-11)$$

Where  $N_\mu$  is the viscosity number given by

$$N_\mu = \frac{V_m \mu_L}{gD^2(\rho_l - \rho_g)} \quad (6-12)$$

Similarly, a non-linear regression correlation is developed using the present dataset. Based on observations from experimental investigation of the behavior of hydrodynamic slug flow and several existing published works, the following functional parameters were deduced to strongly correlate slug translational velocity  $V_T$ ;

$$V_T = F(gD, V_{sl}, V_{sg}, \mu, \rho_g, \rho_l) \quad (6-13)$$

A non-dimensional groupings of equation (6-13) yielded the following dimensionless groups:

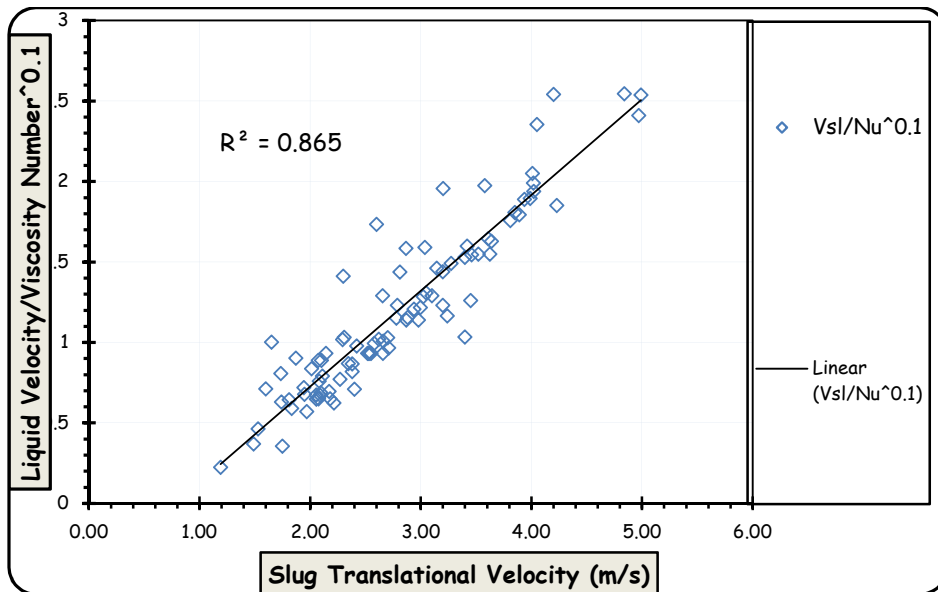
$$V_T = F(gD, C_o V_m, N_\mu V_{sl}) \quad (6-14)$$

A partial correlation was done for each of the groupings by using regression of each dimensionless group against the measured translational velocity. The preliminary analysis showed that equation (6-15) exhibited the best and most significant correlation with the measured slug translational velocity as presented in Figure 6-6.

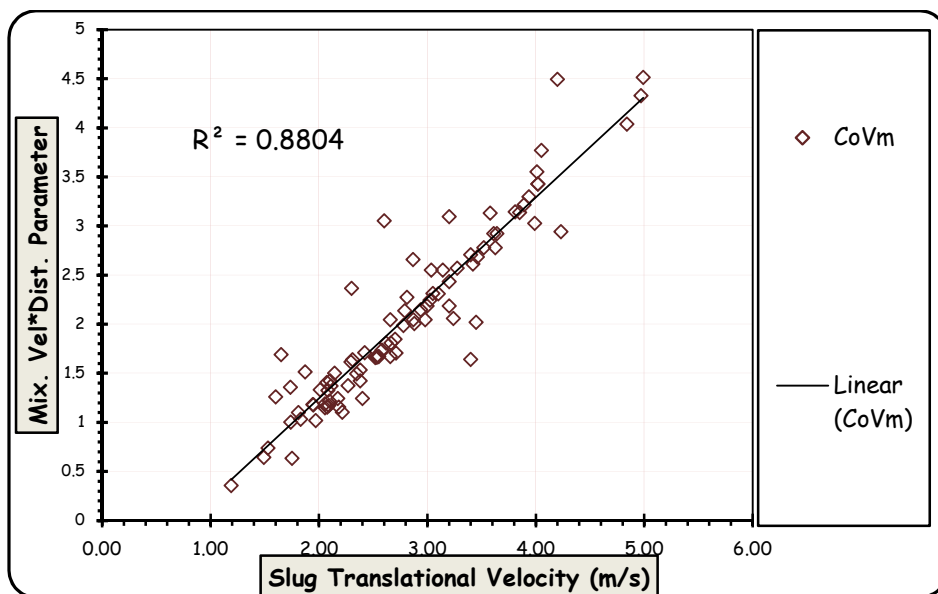
$$V_T = F\left(gD, C_o V_m, \frac{V_{sl}}{N_\mu^{0.1}}\right) \quad (6-15)$$

Upon correlation of the obtained experimental dataset, a general non-linear relationship for the slug translational velocity in high viscosity oil-gas two-phase flow was proposed thus:

$$V_T = C_o V_m + 1.18 \sqrt{gD} - 0.24 \frac{V_{sl}}{N_\mu^{0.1}} \quad (6-16)$$



(a)



(b)

Figure 6-6 a, b: Partial correlation of the dimensionless groupings of equation.

### 6.3.1 Calculation Method

The slug translational velocity for two phase flow high viscosity liquid gas flow can be calculated as follows

1. Calculate (Choi et al., 2012) distribution parameter  $C_o$  using equation (6-8)
2. Drift velocity  $V_d$  is calculated from equation (6-9) using the obtained optimized value for  $C_1$  as 0.79
3. Calculate viscosity number using equation (6-12)
4. Slug translational velocity is finally calculated by solving equation (6-11).

### 6.3.2 Model validation and comparison

Statistical performance evaluation and the validation of the proposed slug translational velocity correlation on an on (Gokcal, 2008) data set not used in its development. The dataset is for liquid viscosity of 0.181-0.587 Pa.s for a range of data similar to those investigated in this study. It is worth noting that the correlation for slug translational velocity developed in this study needs to be further tested against a more a wider range dataset to make it more robust.

Figure 6-7 shows a cross plot of translational velocity of slug body from present data and that of (Gokcal, 2008) data against the proposed prediction models. The results shows over prediction for most of the data points but within the range of 10% and 20% for the present data and (Gokcal, 2008) data respectively. The over prediction can be attributed to the contribution of drift velocity to slug translational velocity which investigation from the works of (Gokcal, 2008; B C Jeyachandra et al., 2012) have indicated generally increase with the increase in liquid viscosity.

A comparison was carried out between the prediction of the proposed correlation and the predictions of existing models for slug translational velocity. Seven correlations were used for the comparison, namely; (Benjamin, 1968; Hubbard, 1965; Jepson, 1989; B C Jeyachandra et al., 2012; Kouba, 1986; Nicklin et al., 1962) and (Choi et al., 2012). Table 6-4 and Figure 6-8 shows the comparison result which reveals that all existing correlations under-predict translational velocity with different magnitudes.



**Table 6-4 Proposed and existing correlation comparison**

	<b>Nicklin, 1962</b>	<b>Hubbard, 1965</b>	<b>Benjamin, 1968</b>	<b>Kouba, 1986</b>	<b>Jepson 1989</b>	<b>Jeyachandra, 2009</b>	<b>Choi, 2012</b>	<b>Pred. (Regres)</b>	<b>Pred. Corr.</b>
	-19.85	-58.20	-19.85	-57.63	-54.32	-33.22	-7.67	9.01	-0.31
<b>£1</b>	20.96	58.20	20.96	57.63	54.32	33.35	17.79	10.76	8.05
<b>£2</b>	10.61	8.64	10.61	6.95	14.96	12.16	31.31	12.41	6.55
<b>£3</b>	-0.54	-1.59	-1.59	-1.59	-1.44	-0.88	-0.11	0.23	0.00
<b>£4</b>	0.56	1.59	1.59	1.59	1.44	0.89	0.54	0.28	0.21
<b>£5</b>	0.29	0.38	0.38	0.42	0.35	0.29	1.43	0.31	0.26

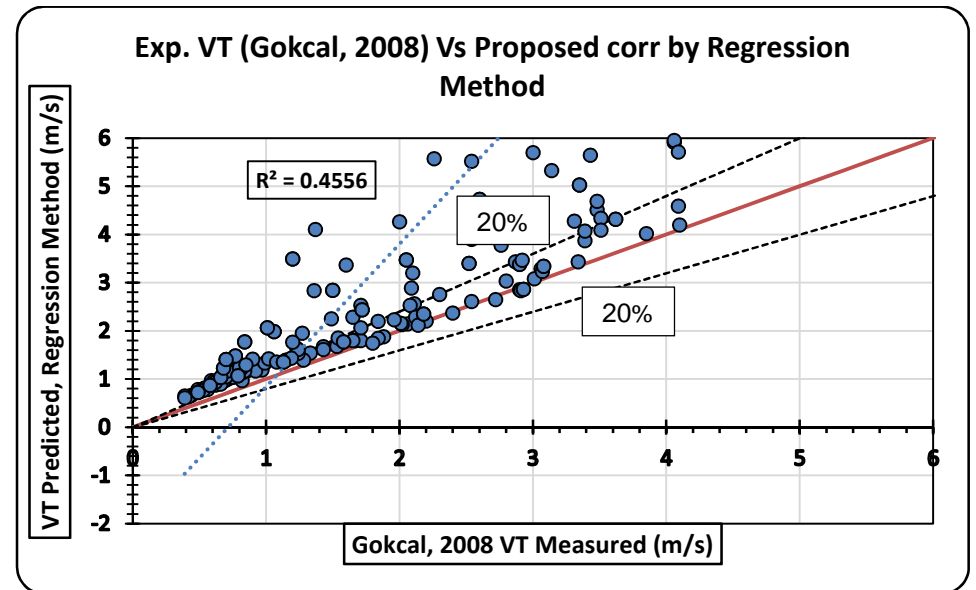
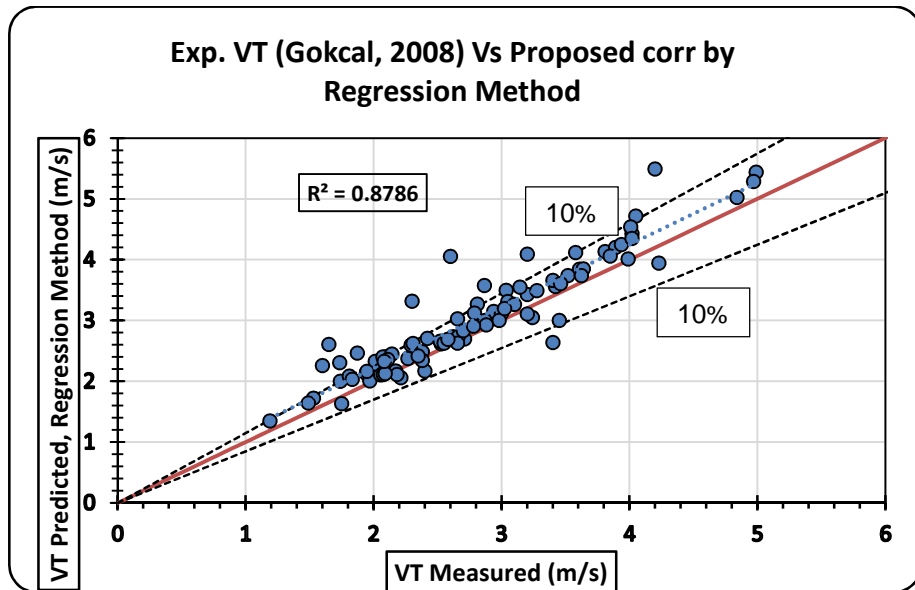
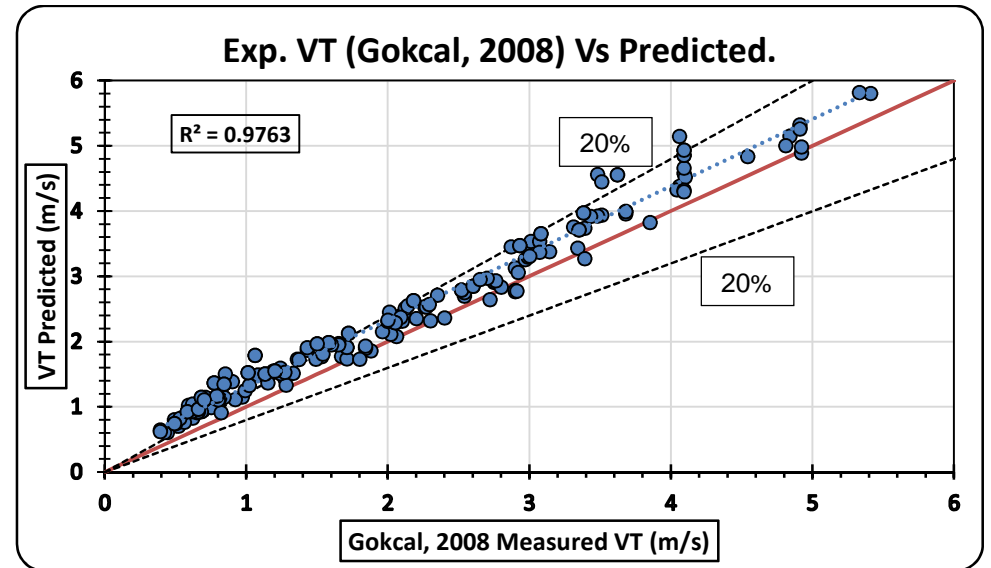
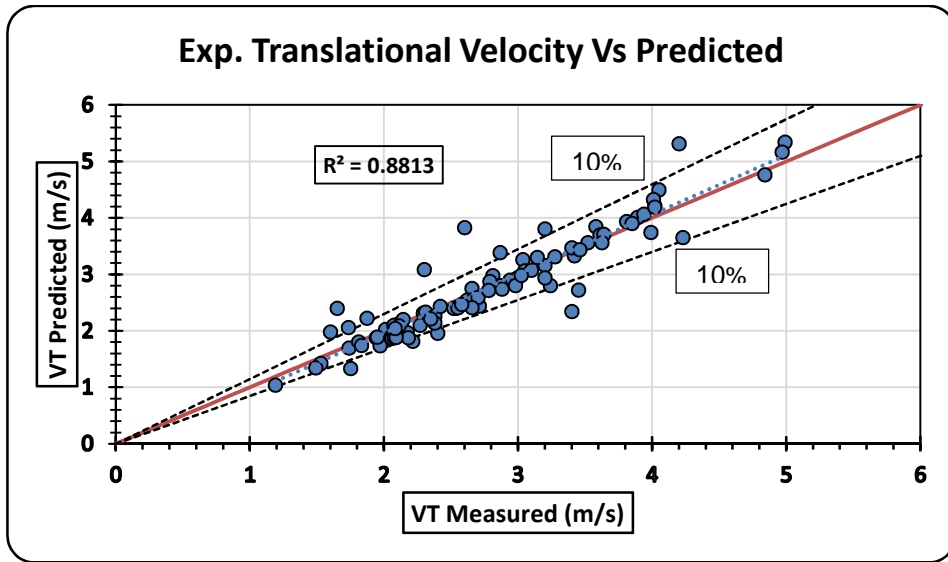


Figure 6-7 Cross-plot of model prediction vs. measurement from experiment from (Gokcal, 2008).

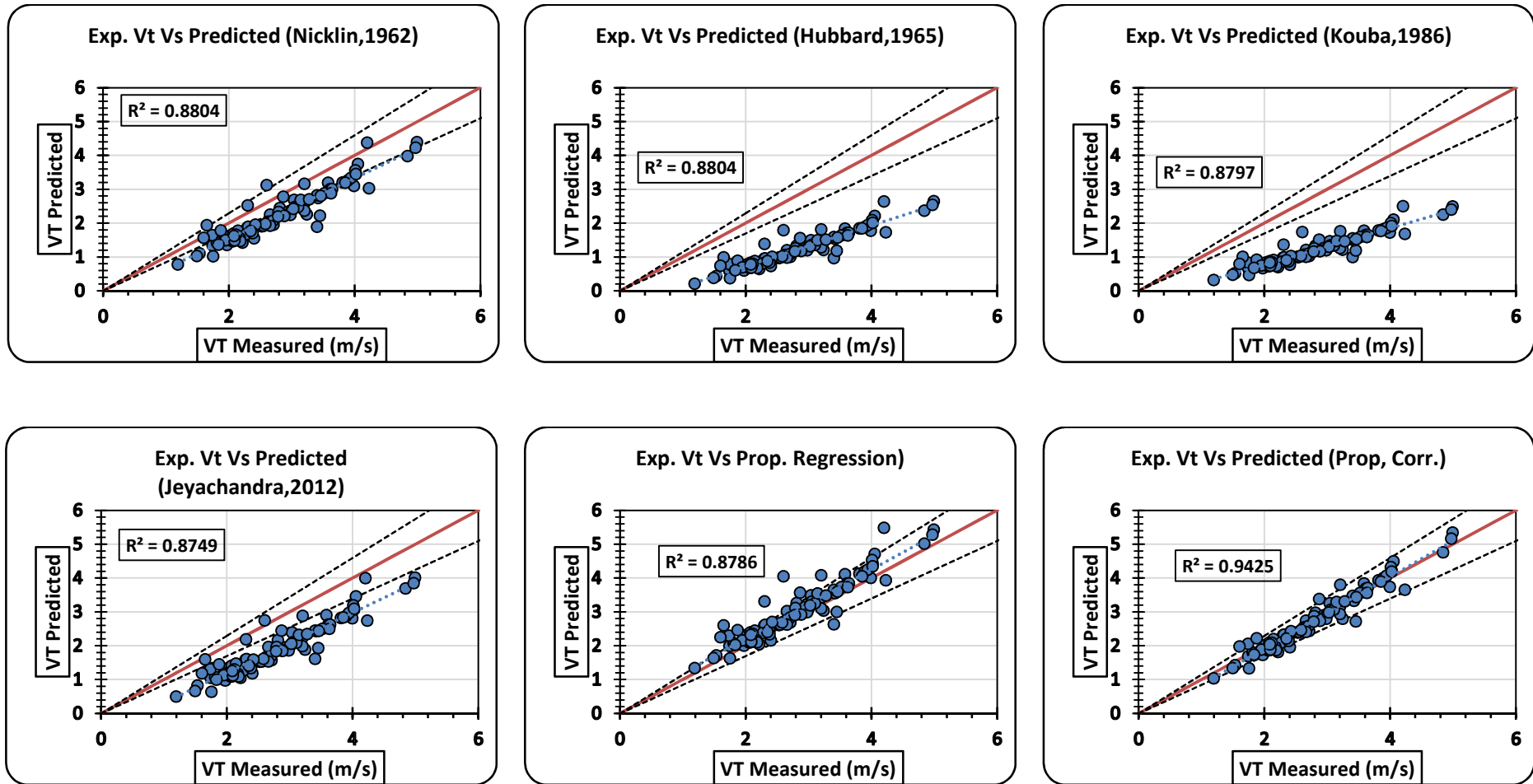


Figure 6-8 Plot of comparison between model predictions and proposed models for present study

## 6.4 Evaluation of Proposed Correlation

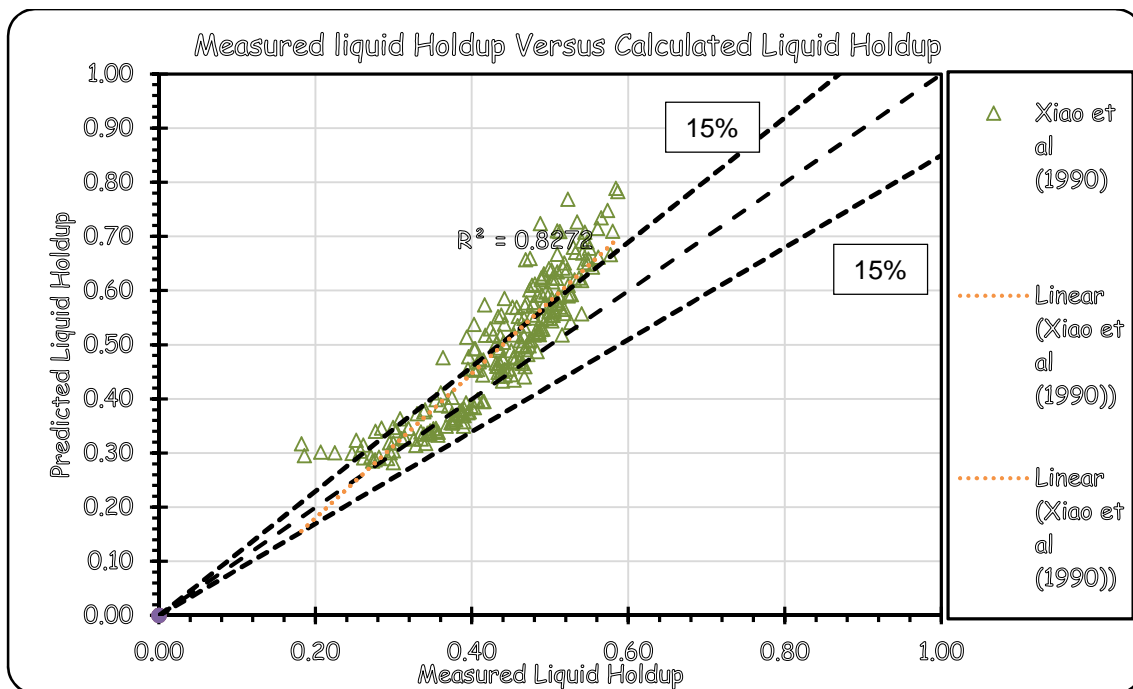
Liquid holdup been an essential parameter associated with multiphase flow is a very important factor to consider when designing oil and gas transportation pipelines and unit operation equipment such as separator and slug catchers since it plays a chief role in the determination of pressure gradient and flow pattern. Its accurate predictions is the key to safe design specs. However, the complexities associated with the distribution of phases considering the wide range of fluid properties encountered in the petroleum industry makes this prediction difficult as such the performance of existing prediction correlations are characteristically inadequate in terms range of application and accuracy.

Several empirical prediction correlations and mechanistic models have been proposed in recent times for liquid holdup, some of which are general in application while others are limited to a narrow range of flow conditions. Investigation have shown that most of these models becomes inconsistent once flow conditions changes thereby making it an onerous task to selecting the most appropriate and accurate prediction correlations.

In order test the performance of the prediction correlation for slug translational velocity proposed in this investigation, an attempt is made in this section by substituting the correlation into the model proposed by (Xiao et al., 1990) for the prediction of two phase flow liquid hold up in the slug flow region as presented equation (6-17) below.

$$E_l = \frac{V_t E_s + V_b(1 - E_s) - V_{sg}}{V_t} \quad (6-17)$$

A plot showing the comparison of experimental data against the (Xiao et al., 1990) prediction model as represented by equation (6-17) is presented in Figure 6-9 below.



**Figure 6-9: Performance of Xiao et al (1990) model using present data.**

As can be seen in Figure 6-9 above, (Xiao et al., 1990) produced over-prediction of high viscosity liquid holdup data. This can be attributed to the fact that the closure relationships used in the (Xiao et al., 1990) model were developed on account of experimental data from low viscous liquids. The (Xiao et al., 1990) model was however modified by inputting the correlation for translational velocity developed in this study and the correlation for slug liquid holdup developed by (Archibong, 2015) for oil viscosity ranging from 0.7 Pa.s-7.0 Pa.s. Figure 6-10 below shows a plot of measured liquid holdup against prediction by modified (Xiao et al., 1990) which shows an improvement in the prediction of the measured liquid holdup. The result can further be improved by tuning the velocity of the dispersed bubble  $V_b$  in the slug body with high viscosity data as this parameter was not measured in this study. Similarly, **Error! Reference source not found.** to **Error! Reference source not found.** shows a cross plot of measured liquid hold versus the prediction models of Choi et al (2012); Bestion (1990); Zuber and Findlay (1965); and Beggs and Brill (1973) respectively. The plots shows that all the tested prediction models predicted the present data with different magnitudes. For instance the (Choi et al., 2012) consistently over-predicted the data while (Beggs and Brill and 1973; Bestion, 1990 and Zuber & Findlay, 1965) under predicted the result obtained. Statistical performance evaluation of all the predictive models accessed are presented in Table 6-5.

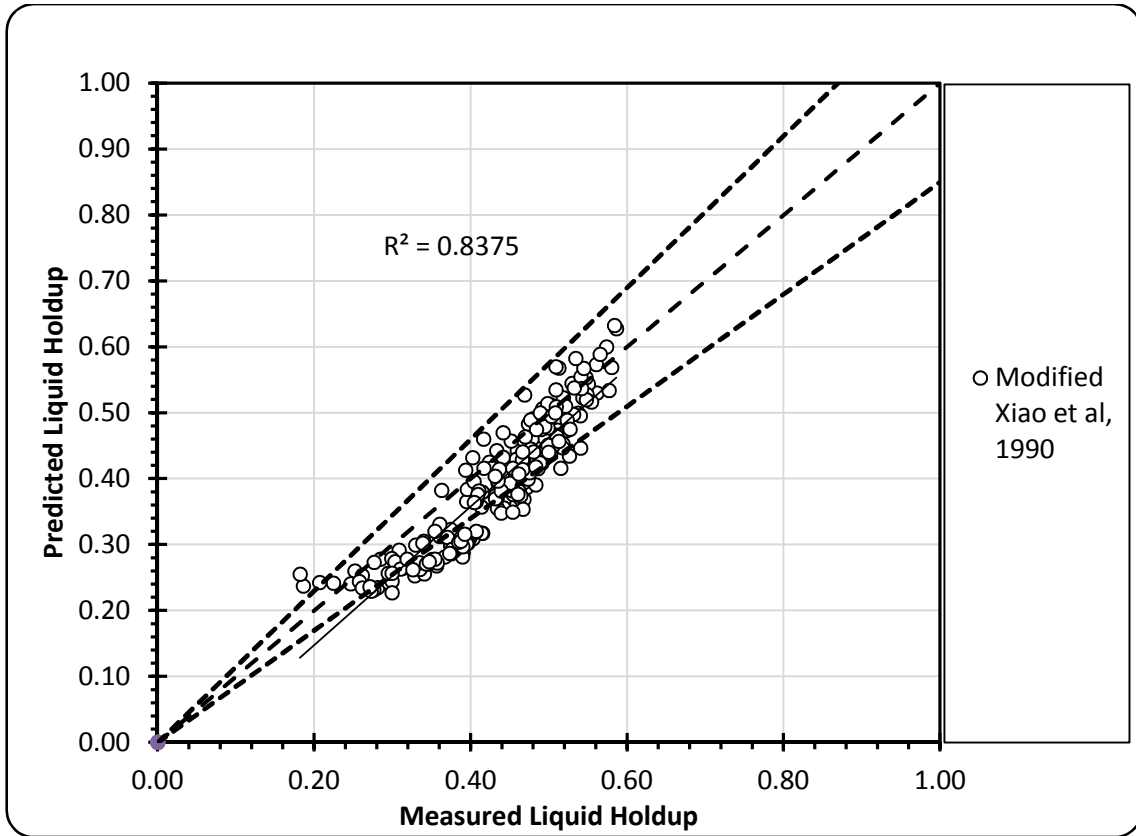


Figure 6-10: Cross-plot of present data against (Modified Xiao, 1990) Prop Corr.

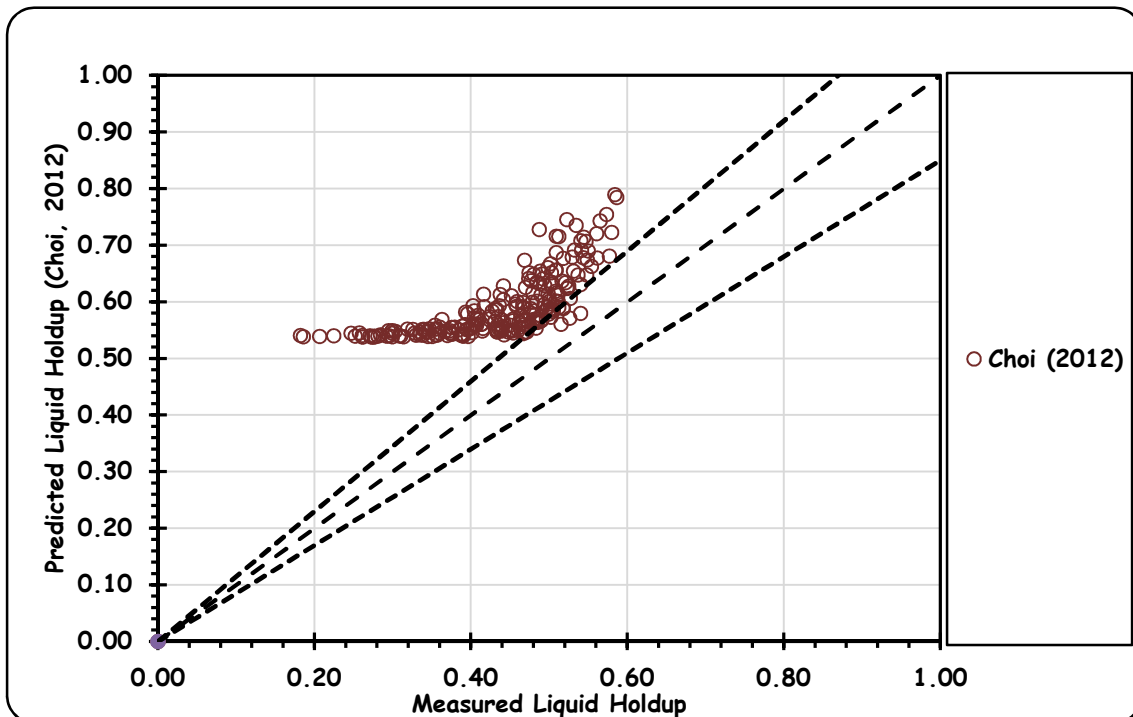


Figure 6-11: Cross-plot of present data against (Choi, 2012) prediction model

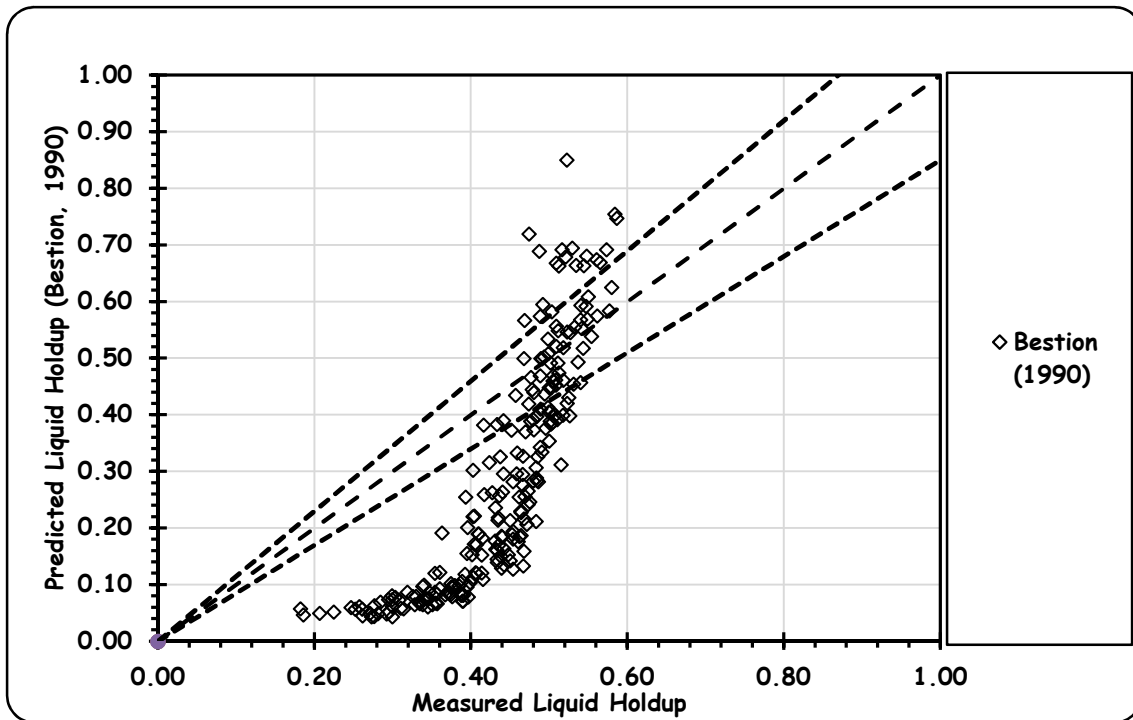


Figure 6-12: Cross-plot of present data against (Bestion, 1990) prediction model

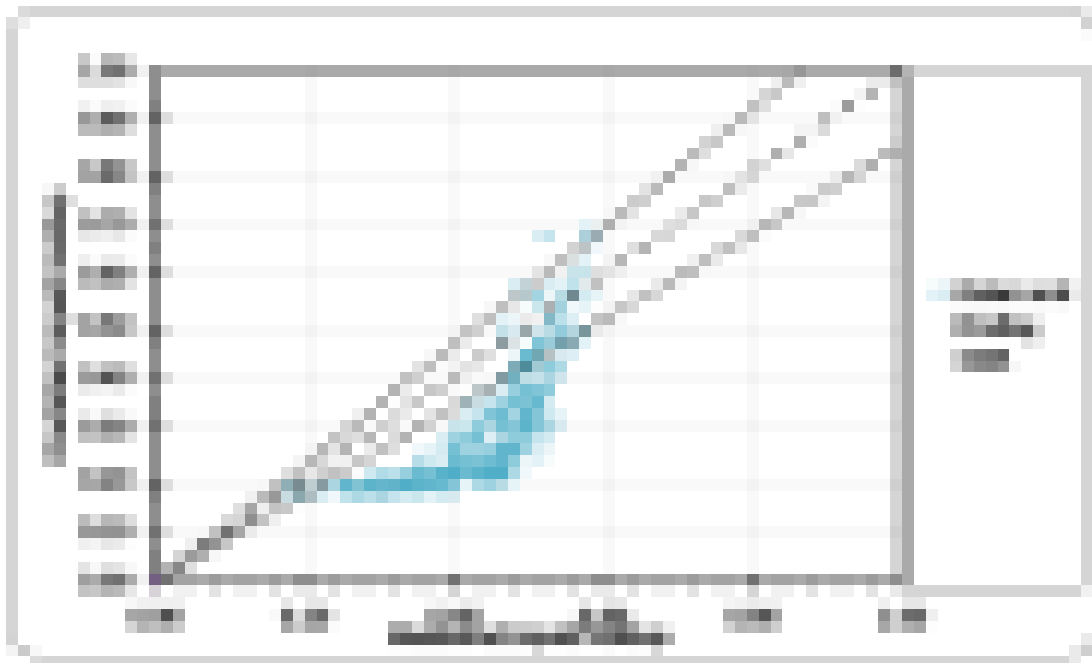


Figure 6-13: Cross-plot of present data against (Zuber and Findlay, 1965) prediction model

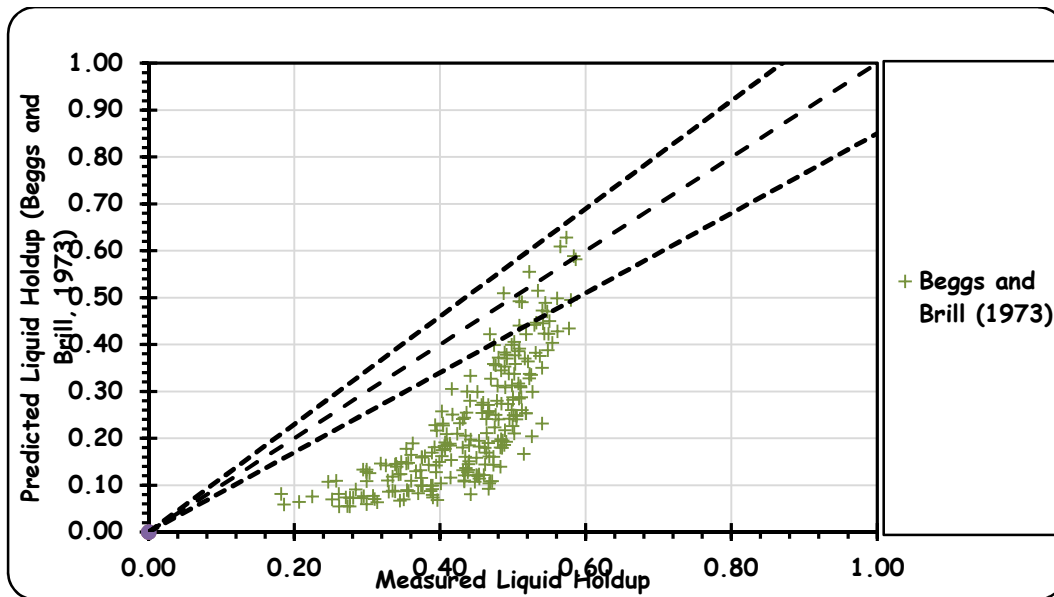


Figure 6-14: Cross-plot of present data against (Beggs & Brill, 1973) model.

Table 6-5: Statistical performance evaluation of proposed correlation in comparison to models in the literature

Correlations	Zuber and Findlay 1965	Beggs & Brill 1973	Xiao et al 1990	Bestion 1990	Choi 2012	Modified Xiao et al, 1990
$\epsilon_1$	75.263	-50.7177	13.00431	-39.7769	40.2563	-4.90375
$\epsilon_2$	78.56138	50.96201	14.38188	45.52704	40.2563	9.072531
$\epsilon_3$	65.94302	21.28471	13.15429	35.5417	28.2865	8.985974

## 6.5 Chapter Summary

Experimental data for two phase high viscosity oil-gas flow carried in the 3-inch internal diameter horizontal pipe facility located in the oil and gas engineering centre lab of Cranfield University have been used to modify existing closure relationships for accurate prediction of high viscosity two phase flow hydrodynamics parameters having observed from the result of experimental investigation presented in Chapter 5 that increase liquid viscosity has effects on these parameter which were not accounted for by most existing correlations found in the literature. In summary, the following were achieved in this chapter.



- A new predictive correlation with improved performance for slug frequency is proposed. The proposed correlation was compared with existing prediction models and evaluated against independent dataset (Gokcal, 2008). Result showed improved performance by the proposed correlation in comparison to others.
- Slug length prediction model was also proposed using the current data and that of (Gokcal, 2008) for high viscosity oils. The proposed slug length correlation in comparison to existing highlighted the discrepancies associated with existing models in the literature built on the basis of conventional oils data base.
- A correlation taking into account the effects of viscosity have been proposed for slug translational velocity. Statistical performance evaluation of the correlations showed improved performance when compared those in the literature.
- The (Xiao et al., 1990) model was modified by inputting translational velocity  $V_T$  and slug liquid holdup  $H_{LS}$  developed from high viscosity data which resulted to an improvement in the prediction compared to those in the literature.

Conclusively, the correlations proposed in this study will be helpful in the oil and gas industry applications. For example, slug frequency, slug length and the modified liquid holdup correlation will be of useful in the design of pipeline design and sizing of separators. They can be used by process control engineers to achieve optimal production by implementing them in their slug control philosophies.



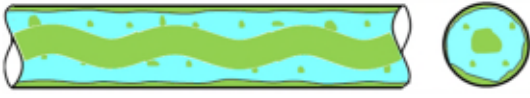
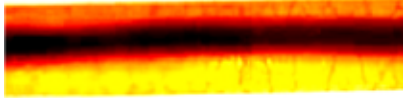
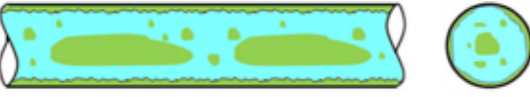

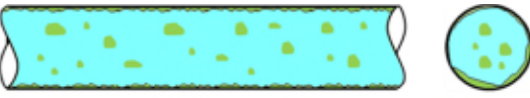
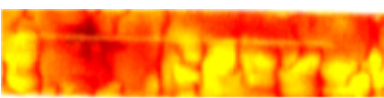
## 7 OIL–WATER TWO–PHASE FLOW

In this chapter, experimental study performed in the 1 inch multiphase flow facility for oil-water two-phase flow is presented. Results include the flow pattern visualization, water cut, oil holdup and pressure gradient measurements. Discussions of these results are also presented. The chapter is divided into sub-sections based on these visualizations and measurements.

### 7.1 Flow Pattern Visualization

Flow pattern visualization constitute the still image capturing and high definition video recordings throughout the different superficial oil and water velocities investigated in this study respectively. On the basis of the video recordings, static images and visual inspection, different flow patterns were identified at different flow conditions and subsequently named.

**Table 7-1: Flow Patterns in High Viscosity Oil-Water Two-Phase Flow**

Artistic Impression (Al Awadi, 2011)	Visual Image
	
Rivulet Flow (RIV)	
	
Core Annular Flow (CAF)	
	
Oil Plug in Water Flow	
	
Dispersed Flow	

In general, four flow patterns were observed in this study, namely; Rivulet, Core Annular, Plug and Dispersed Flow. Table 7-1, shows the artistic impressions and the images captured for different flow patterns visualized.

For oil viscosity of 3.3 Pa.s, at the lowest superficial oil and water superficial velocities, rivulet flow was identified. When oil superficial velocity is kept constant with the water superficial velocity increased, the flow changes to plug flow. Additional increase in water superficial velocity resulted in dispersed flow. At high superficial velocities of oil and constant water superficial velocity, core annular flow is observed. Also, at high superficial velocities of oil and water, core annular flow dominated the flow patterns in the study.

### **7.1.1 Flow Pattern Map**

Flow pattern map of high viscous oil-water two-phase flow obtained in this experimental study is shown in Figure 7-1 and Figure 7-2. The map is constructed in such a way that the superficial velocities of oil and water correspond to the x and y axis respectively.

In this study, the focus was on water dominant flow patterns, this is due to the recent interest in water assisted heavy oil transportation. The main reason for the adoption of this method of transporting produced and pre-processed high viscous crude oil is to reduce the pressure gradient and thus minimize the pumping requirement for transport. At  $V_{so} = 0.06$  m/s and  $V_{sw} = 0.04$  m/s flow pattern observed was a spiral flow of oil and water. At the same  $V_{so}$  and with increased  $V_{sw} = 0.1$  m/s, the flow pattern changed to plug flow. This transition from rivulet to plug flow is due to the increased water content in the pipeline. Increase in water content result in increased lubrication of the pipe walls. With the total mixture velocity  $V_m = (V_{so} + V_{sw})$  of the flow increasing, the turbulence in flow also increases and leads to the breakup of the oil spiral into large globules of oil. With the  $V_{so}$  remaining unchanged and  $V_{sw} = 0.2$  m/s the mixture velocity and the water content in the pipe increases resulting in a further breakup of the formerly large oil globules into a much smaller oil droplets dispersed in a continuous water flow.

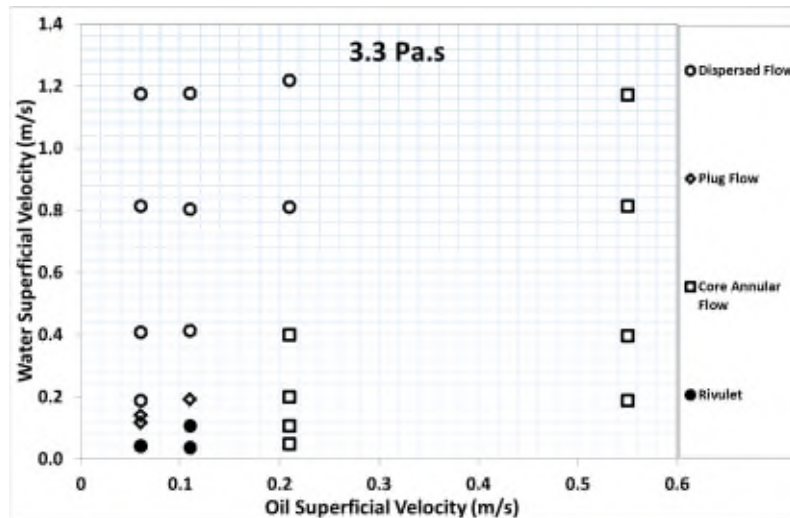


Figure 7-1: Oil-Water Two-Phase Flow (Oil Viscosity = 3.3 Pa.s)

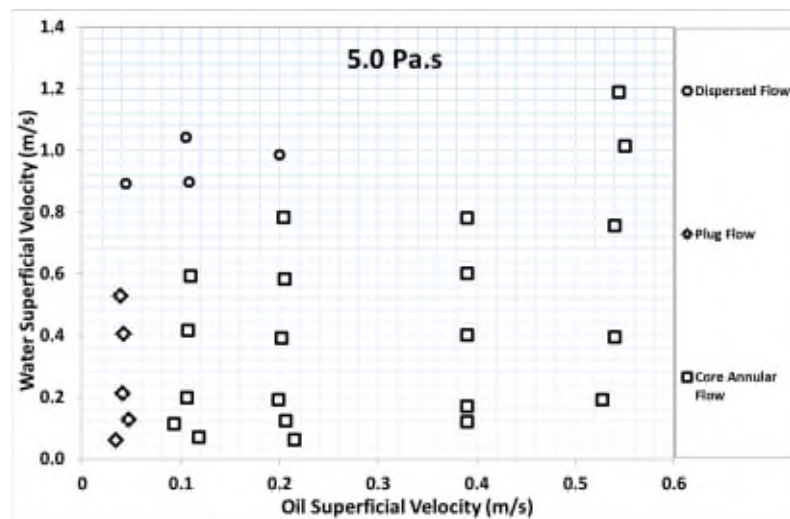


Figure 7-2: Oil-Water Two-Phase Flow (Oil Viscosity = 5.0 Pa.s)

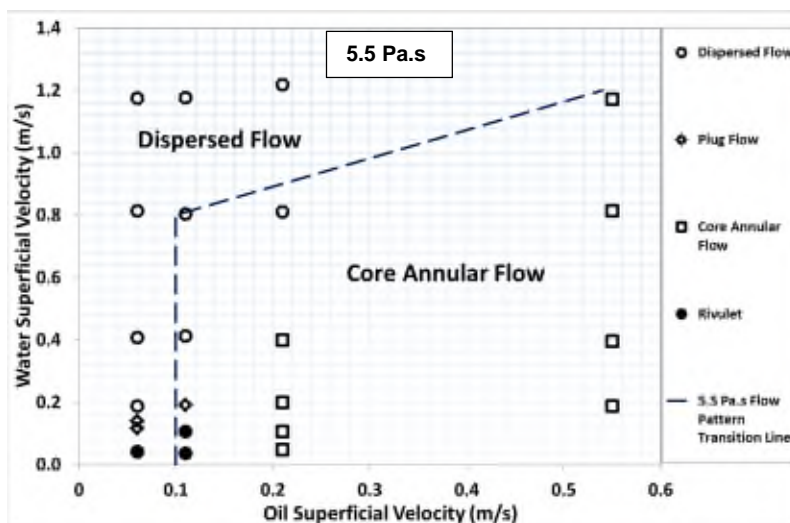


Figure 7-3: Effect of increasing oil viscosity in Oil-Water Two-Phase Flow

Accordingly, for  $V_{sw} = 0.004 \text{ m/s}$  and  $V_{so} = 0.06 \text{ m/s}$  as earlier stated, rivulet flow is observed. However, when  $V_{so}$  is increased to  $0.21 \text{ m/s}$ , the flow pattern changed to core annular flow. An increase in the oil content in the line as a result of  $V_{so}$  being increased leads to more oil content in the pipe. Increased oil content leads to the rivulet flow transitioning to core annular flow. This flow pattern is seen to have a wholly oil core with water enveloping this core. Increasing the oil superficial velocity increased the core size and its undulation becomes more pronounced.

For the  $5.0 \text{ Pa}\cdot\text{s}$ , oil viscosity, similar flow behaviour were observed, however, it is important to state that and as shown in Figure 7:2 the transition from one flow pattern to the next occurred at different oil and water superficial velocities. It is also observed that at higher oil superficial velocities, core annular flow was dominant. On the other hand, increasing the water superficial velocity tended to encourage the dispersed and plug flow patterns. At high water and oil superficial velocities, core annular flow was also dominant. From observations, the explanation to this observation may be as a result of increased oil content in the line which increases the oil holdup and therefore the mass which leads to it being relatively more stable.

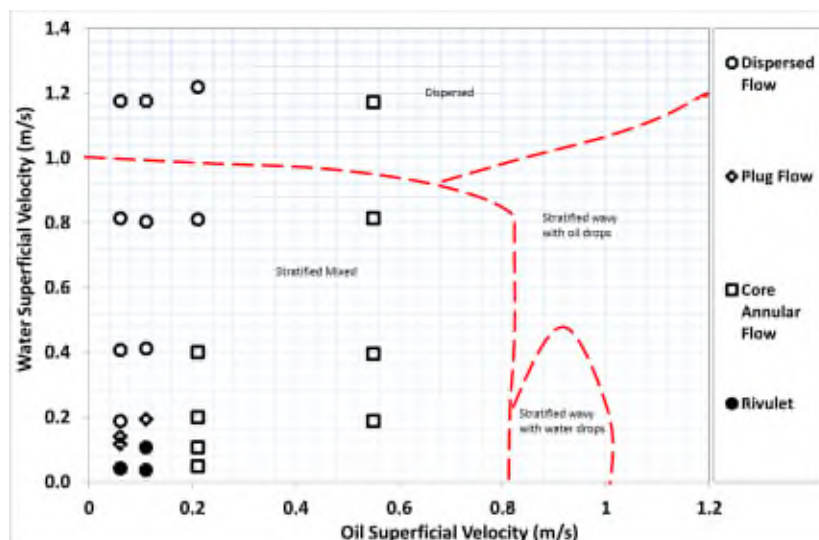
Viscosity effect on the flow pattern can be seen in Figure 7-3 the core annular flow pattern is the dominant flow pattern when the oil viscosity increased from  $3.3 \text{ Pa}\cdot\text{s}$  to  $5.0 \text{ Pa}\cdot\text{s}$ . It is observed that the transition to the core annular flow pattern happens at relatively lower superficial velocities of oil and water when compared to the  $3.3 \text{ Pa}\cdot\text{s}$  flow patterns. It therefore can be inferred that an increased oil viscosity and/or increase in oil superficial velocity will increase the likelihood of core annular flow while an increase in the oil superficial velocity will see a shift into the dispersed and plug flow dominance.

### **7.1.2 Comparison of Flow Patterns in this Study with Flow Patterns observed for Low Viscous Liquid –Liquid Flow**

Flow pattern maps observed in this study were compared with flow patterns in the study of (Sugimoto and Mazza, 2015), this study was selected for comparison because of its similarity with the present study. The flow conditions and pipe geometry used in the study were similar to the facility used in the present study.

Figure 7-4 below shows the flow pattern obtained in the present study (for oil viscosity of  $3300 \text{ cP}$ ) superimposed on flow pattern map in the (Sugimoto and Mazza, 2015)

study. The study was conducted using kerosene and water with viscosities of 1.1 and 1 cP respectively. Results indicates that while the stratified mixed flow was observed in the (Sugimoto and Mazza, 2015) for low superficial kerosene and water velocities, the Rivulet, core annular, plug and dispersed flow were observed in the present study. At the highest superficial water velocity and relatively low oil superficial velocities, dispersed flow was observed for both studies. However, at similar conditions differing only with the increase in oil superficial velocity, CAF was observed in the high viscosity study while dispersed flow was still observed for the low viscosity kerosene-water study. Conclusively as earlier stated, it shows that increased oil viscosity increases the CAF flow region when comparing two different viscosities in the high viscosity (>100 cP) region as well as comparison between the low viscous (<100 cP) and high viscous regions.



**Figure 7-4 Comparison of Flow Pattern obtained in this study with the Flow Pattern Map of Sugimoto and Mazza (2015).**

## 7.2 Oil Holdup

Oil holdup was measured in this study as described in the experimental setup. It is an important parameter that is required as an input closure relationship variable in most mechanistic models for pressure gradient prediction and flow pattern transition. Together with flow pattern, the oil holdup is a major determinant of the pressure gradient.

Oil holdup plotted in x and y axes graphs as a function of the water superficial velocity for different oil superficial velocity studied. In general, the liquid holdup measured reduced with increase in water superficial velocity. When water superficial velocity is increase, the water cut (water fraction) in the pipe increases. As an example for the 3.3 Pa.s, oil viscosity as shown in Figure 7-5 and at an unchanged  $V_{so} = 0.06$  m/s the oil holdup measured is about 63%, a reduction in oil holdup to about 7.3% is observed as  $V_{sw} = 1.2$  m/s. Similar behaviour are observed for all the flow conditions studied. For an unchanged water superficial velocity, it is noted that the oil holdup increased. Again, from the same plot, when  $V_{sw} = 0.4$  m/s oil holdup measured increased from 24% to 54% for their respective oil superficial velocities of 0.06 m/s and 0.05 m/s. Similar data trend are observed for the 5.5 Pa.s plot in Figure 7-6.

Figure 7-7 is used to illustrate the effect of oil viscosity on the measured oil holdup. It is seen that an increase in oil viscosity from 3.3 Pa.s to 5.0 Pa.s slightly increases the oil holdup. This maybe as a result of the increase shear in flow and therefore, and increase resistance to flow.

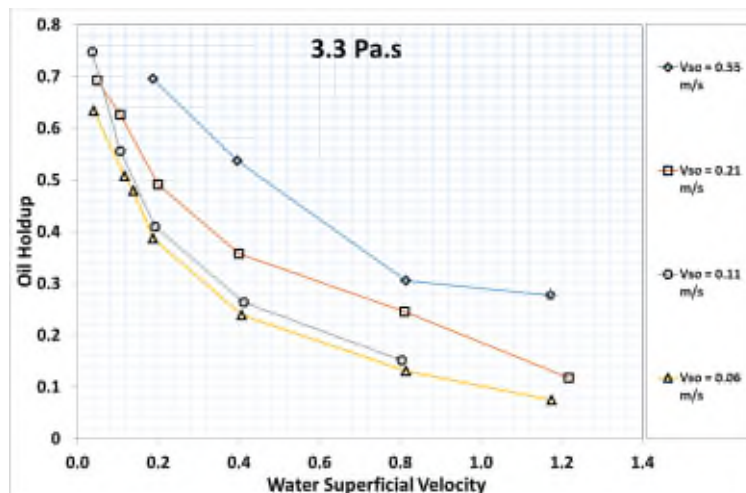


Figure 7-5: Oil Holdup as a function of Water Superficial Velocity,  $\mu_o = 3.3$  Pa.s

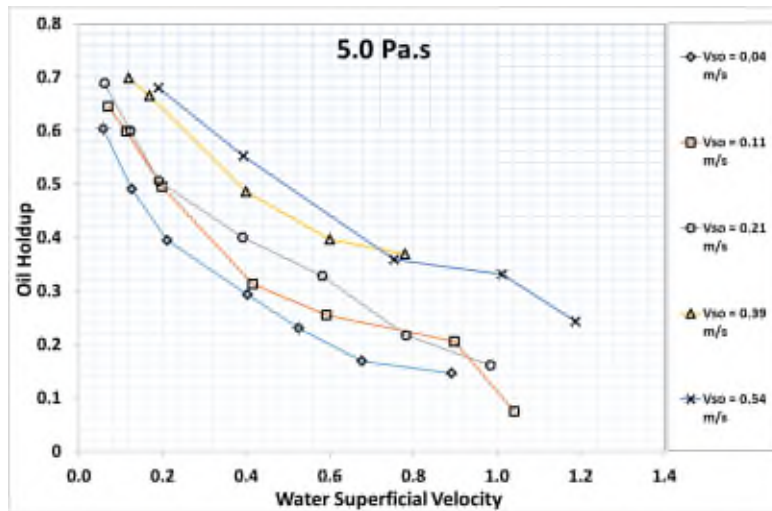


Figure 7-6: Oil Holdup as a function of Water Superficial Velocity,  $\mu_o = 5.0 Pa.s$

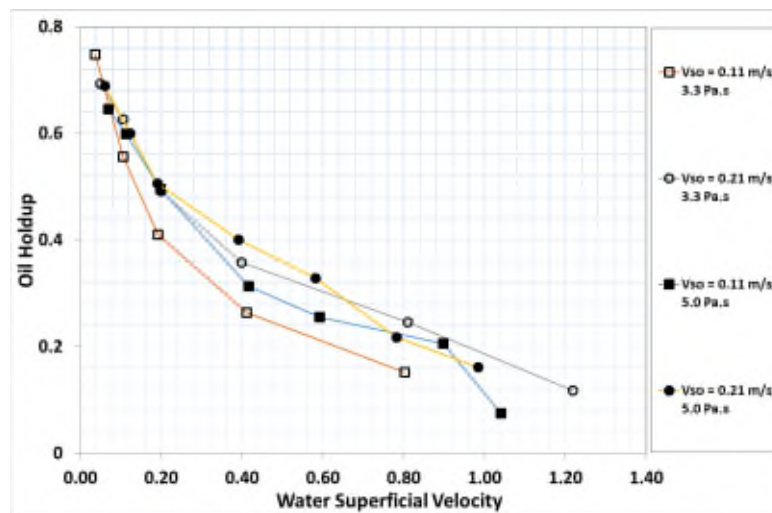


Figure 7-7: Oil Holdup as a function of Water Superficial Velocity

### 7.3 Water Holdup

Water holdup,  $H_w (= 1 - H_o)$  is an important parameter that is also required in mechanistic and empirical models for oil-water two phase flow. Overall, as can be seen in Figure 7-8 below, water holdup behaviour was contrary to that of oil holdup. At an unchanged oil superficial velocity, measured water holdup increased proportionately with water superficial velocity. At an unchanged water superficial velocity, measured water holdup reduced with increase in oil superficial velocity.



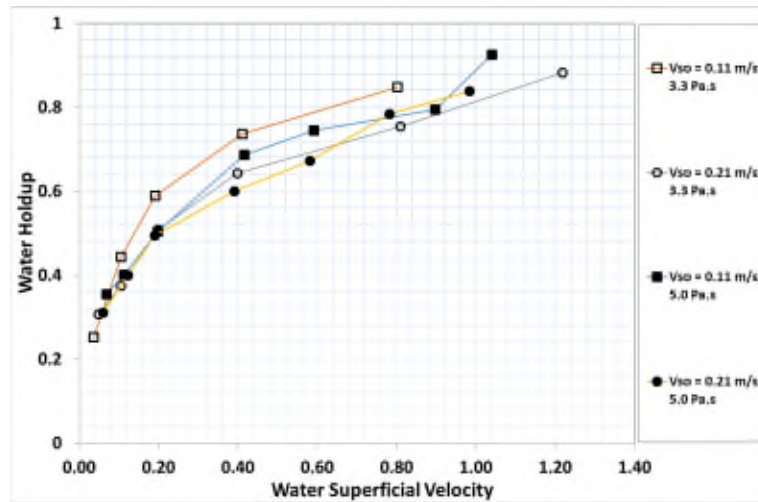


Figure 7-8: Water Holdup as a function of Water Superficial Velocity

### 7.3.1 Comparison of Predictive Models with Experimental Results

Water holdup measurements were compared with predictive models developed by four researchers namely: (Arney et al., 1993; Bannwart, 2001, 1998; Oliemans et al., 1987). Figure 7-9 below, shows that the four models mostly over predicted the water holdup in the experiments with (Oliemans, 1987) model under predicting a few flow conditions. The inaccuracy in prediction may be as a result of the dataset and experimental investigations used in developing these models. In particular, the oil viscosities used in the present experiments is far higher than those in the aforementioned models.

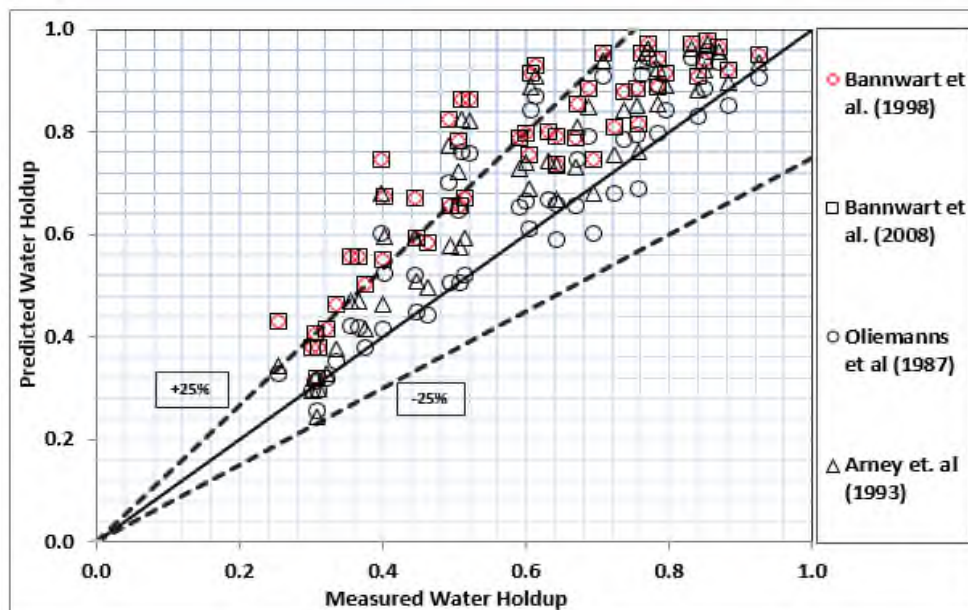


Figure 7-9: Comparison of measured water holdup with predictive models

### 7.3.2 Water Holdup and Water Cut

In some oil-water experiments, water holdup are often, not measured, when this happens, water cut is used as indication of the water fraction in the pipe. Water cut,  $W_C (= V_{SW}/(V_{SW} + V_{SO}))$  will be examined in this section to investigate how it varies from the water holdup estimates in high viscous oil-water flow.

Figure 7-10 shows a plot of measured water holdup as a function of water cut. Results indicate that water cut estimated the water holdup value to within 15% of the actual measured water content in the line. This means that water cut may be used as a good first approximation of water holdup in the absence of data for the measured water holdup in highly viscous oil-water two-phase flow. It is important to state that the water cut gave relatively accurate water holdup compared to the four models earlier investigated in this study.

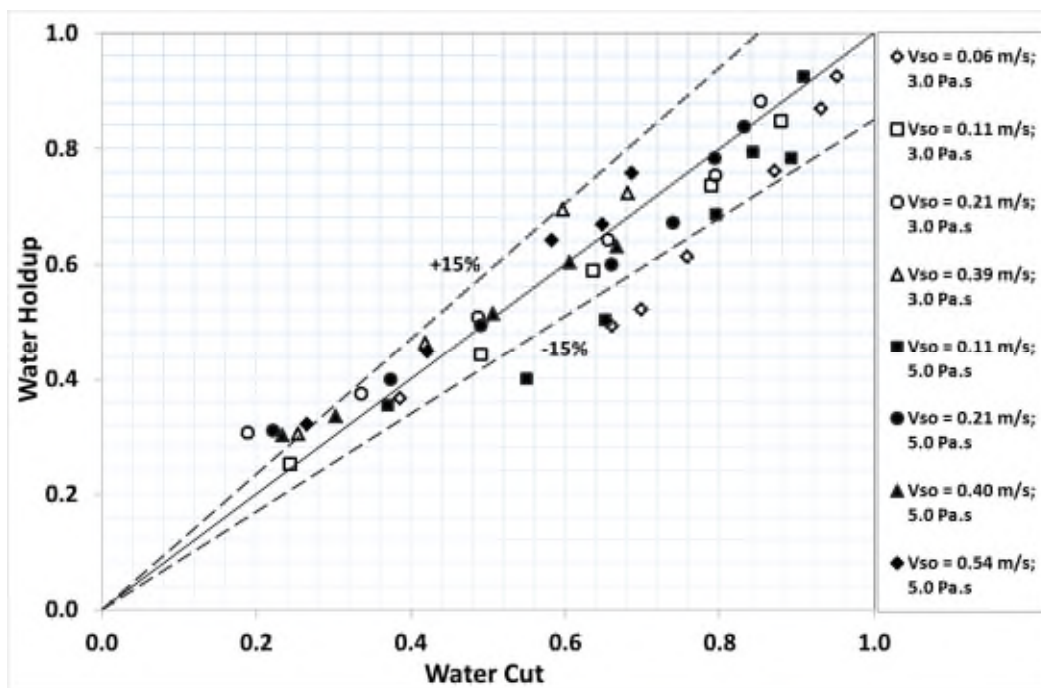


Figure 7-10: Water Holdup as a Function of Water Cut

### 7.4 Pressure Drop

Pressure drop obtained in this study were found to depend strongly on the flow rate and the flow patterns as was observed in studies by (Vuong et al., 2009). As it can be seen in Figure 7-11 pressure drop was highest in the very low water superficial velocities at  $\mu_o = 3.3$  Pa.s. Below  $V_{sw} = 0.0034$  m/s and an unchanged  $V_{sw} = 0.006$  m/s,

pressure drop was measured to be 10.5 kPa/m. Pressure drop reduced drastically at  $V_{sw} = 0.041$  m/s to 6.65 kPa/m. This large reduction is associated with the flow pattern where the flow was less oil dominating. Increased water fraction in the line helped reduce the shear and lubricated the pipe walls leading to a reduction in resistance to flow and the pressure drop. It is seen that beyond this transition to the water dominant flow (Dispersed and Plug Flows), pressure drop increased with increase in  $V_{sw}$ . This happens because the water fraction in the pipe has reached its maximum lubricating efficiency and thereby acts to further fragment the oil, with some of this dispersed oil wetting the pipe wall and thereby increasing pressure drop. In addition, the increase in water superficial velocity increases the turbulence in flow which leads to an increase in pressure drop.

For an unchanged  $V_{sw}$  pressure drop increased with increase in  $V_{so}$ . This leads to an increase in oil holdup in the pipe which has an effect of increasing the shear in the pipe walls, thereby leading to increased resistance to flow. It is important to further highlight the impact of flow pattern on pressure drop as depicted in Figure 7-12. Pressure drop increased marginally in the core annular flow region for  $V_{sw} \geq 0.4$  m/s for all the oil  $V_{so}$  investigated.

Oil viscosity impact on the pressure drop is shown in Figure 7-13. It is seen that the pressure drop increased with increase in oil viscosity below the water dominant region. However, for flow patterns in the water dominant region, oil viscosity had a relatively insignificant effect on the pressure drop.

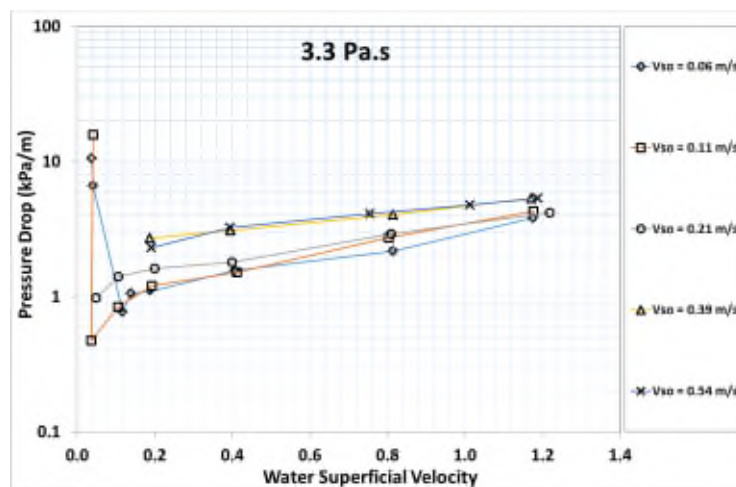


Figure 7-11: Pressure Drop versus Water Superficial Velocity  $\mu_o = 3.3$  Pa.s

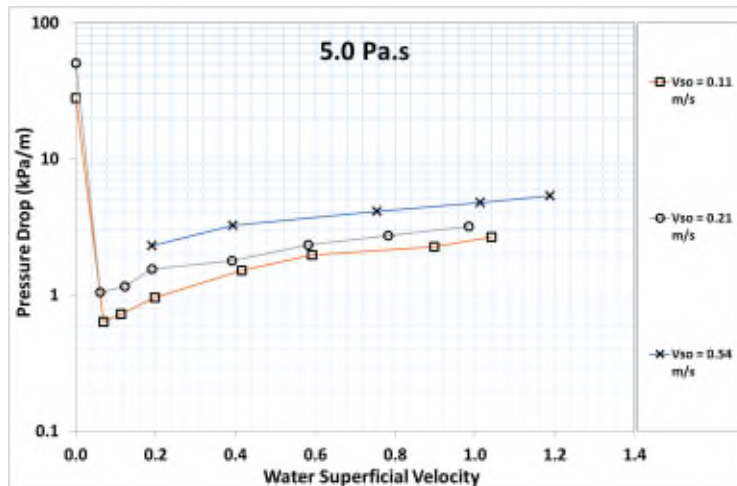


Figure 7-12: Pressure Drop versus Water Superficial Velocity  $\mu_o = 5.0 \text{ Pa}\cdot\text{s}$

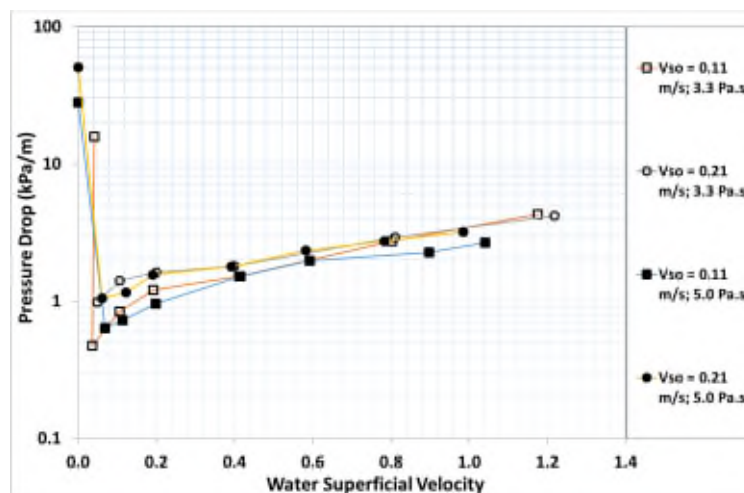


Figure 7-13: Pressure Drop versus Water Superficial Velocity  $\mu_o = 5.0 \text{ Pa}\cdot\text{s}$

## 7.5 Conclusion

Experiments on high viscosity oil-water two-phase flow have been conducted. New experimental dataset have reported. The following conclusion can be drawn from the study:

1. New flow pattern maps have been established for high viscous oil-water two-phase flow in horizontal pipe with ID = 0.0254 m. In general, four flow patterns were observed namely; rivulet, core annular, plug and dispersed flows. High water superficial velocity favoured the dispersed and plugs flow patterns while

high oil superficial velocity favoured core annular flow. These conclusions were also made by (Archibong, 2015).

2. Oil holdup was found to decrease with increase in water superficial velocity and increased with increase in oil superficial velocity. On the other hand, water holdup increased in increase in water superficial velocity while it decreased with increase in oil superficial velocity.
3. A comparative analysis of the measured water holdup with four predictive models showed an over prediction of experimentally measured water holdup by more than 25%. Additionally, an analysis of the water cut and the measured water holdup shows that the water cut was within 15% of the measured holdup. This implies that the water cut gave a better prediction than the predictive water holdup models and may be used as a good first approximation in predictive models for pressure gradient or in practical applications for high viscosity oil-water flows.
4. The maximum pressure drop occurred at the oil dominant flow pattern and in the single phase oil flow. It was also found that below oil superficial velocity of 0.4 m/s, pressure drop decreased with increase in water superficial velocity. Beyond this critical water superficial velocity, pressure drop increased with increase in water superficial velocity.

## 8 CONCLUSIONS AND RECOMMENDATION

This chapter highlights the summary and conclusions drawn from the experimental investigation involving gas-liquid and liquid-liquid two phase flows in horizontal pipelines. The effects of liquid viscosities on oil-gas and oil-water two phase flow characteristics were respectively studied by means of 3-inch and 1-inch ID horizontal pipelines for varying oil viscosities. The applicability of existing models and correlations found in the literatures to the experimental dataset for high viscosity liquids was studied. Most of the prediction tools assessed exhibited discrepancies attributed essentially to the effects of high viscosity which was not accounted for in their development. This discrepancies were addressed by modification of the existing models and correlations to account for the effects of liquid viscosities on the flow parameters studied. A validation of the proposed correlations was done by comparative analysis on the few high viscosity study in literature.

### 8.1 Conclusions

#### 8.1.1 Air-Water Two Phase Flow

- Five flow patterns were identified for the air-water two phase flow in the 3-inch horizontal test facility. The observed flow patterns are; stratified, wavy-stratified, intermittent flow (plug and slug), and annular flow. Comparison of the flow pattern for air-water test with the prediction by flow pattern maps by (Beggs and Brill, 1973) and (Mandhane et al., 1974) shows (Beggs and Brill., 1973) exhibited a better prediction.
- Pressure gradient obtained in the air-water test was plotted as function of gas superficial velocity results showed a gradual increase in pressure gradient with increase in gas superficial velocity at similar water superficial velocity. An increase in pressure gradient was also observed with increase in water superficial velocity at similar gas superficial velocity. Also, comparison of experimental measurement with prediction models showed that the (Beggs and Brill, 1973) produced better prediction than the (Dukler and Hubbard, 1975) model.

- Measured slug translational velocity plotted as a function of mixture velocity shows an increase in the translational velocity with increasing mixture velocity in a linear relationship conforming to the findings of earlier researchers. The slope of the linear relationship was found to be 1.19. This slope represents the flow coefficient  $C_o$  in the translational velocity equation proposed by (Nicklin et al., 1962).
- Also measured was the slug body length which was found to be 24-36D with a mean length of 30.6D. The obtained result is in agreement with the postulation of (Dukler and Hubbard, 1975) and the findings of (Pan, 2010).

### 8.1.2 High Viscous Oil-Gas Flow

- The flow patterns identified for this study are: plug flow, slug flow, pseudo-slug flow and wavy annular flow. The intermittent flow pattern comprising of the plug and slug flow region were found to be the dominating flow patterns.
- The measured liquid holdup was found to decrease with an increase in gas superficial velocity at a constant superficial liquid velocity. Also, analysis of experimental data revealed an increase in the mean liquid holdup when the viscosity of the liquid is increased.
- Slug translational velocity was found to increase with increasing mixture velocity. The flow coefficient  $C_o$  for all the experiment conducted was found to be almost 2.1 showing that all the experiments were in the laminar flow region.
- Measured slug body length was found to decrease with the increase in the viscosity of liquid. Researchers like (Barnea and Brauner, 1985; Taitel et al., 1980) proposed 32D as the minimum liquid slug length. It was however found that the slug body lengths were much shorter than 32D. The mean slug length were approximately found to be 6D within the range of experimental investigation.
- Prediction models and correlations for slug frequency, slug translational velocity and slug length available in the literature were evaluated against the

experimental dataset for this investigation. This study and others mentioned have revealed that slug flow characteristics have strong dependency on liquid viscosity and this effect was not accounted for in most of the prediction tools hence their poor performance. New correlations based on this data and those from (Gokcal, 2008) have been proposed with improved performance for the prediction of these slug flow parameters

### **8.1.3 High Viscous Oil-Water Flow**

- New flow pattern maps have been established for high viscous oil-water two-phase flow in horizontal pipe with ID = 0.0254 m. In general, four flow patterns were observed namely; rivulet, core annular, plug and dispersed flows. High water superficial velocity favoured the dispersed and plugs flow patterns while high oil superficial velocity favoured core annular flow. These conclusions were also made by (Archibong, 2015).
- Oil holdup was found to decrease with increase in water superficial velocity and increased with increase in oil superficial velocity. On the other hand, water holdup increased in increase in water superficial velocity while it decreased with increase in oil superficial velocity.
- A comparative analysis of the measured water holdup with four predictive models showed an over prediction of experimentally measured water holdup by more than 25%. Additionally, an analysis of the water cut and the measured water holdup shows that the water cut was within 15% of the measured holdup. This implies that the water cut gave a better prediction than the predictive water holdup models and may be used as a good first approximation in predictive

## **8.2 Recommendations for Further Work**

Hydrodynamics of slug flow, principally on heavy oil, is still a very fertile area. Investigation has shown there huge gap which have not been investigated in full detail. This experimental investigation have revealed a number of possible directions for further investigation. Presented in this section are the possible areas for future experimental, modelling and simulation work to be carried out.



- Nonexistence of detailed slug flow data for high viscosity oil-gas system for other pipe inclination pipes. The 3-inch facility can be modified by incorporating other angle of inclination operated as there is a strong effect of inclination on flow behaviour. In particular, the effect of pipe inclination on slug body length needs to be investigated.
- Gamma densitometer was used for this experimental investigation, it is recommended that other instrumentations (i.e. Electrical Capacitance Tomography) be used for investigation in a view to compare the outputs from both measuring instruments.
- The proposed correlations can be further verified against field data and implemented in commercial software like OLGA for validation of results obtained.
- The review of literature has shown that very few works exist for oil viscosity in the range of 0.5-7.0 Pa.s. Based on this premise, further work is recommended for experimental investigation above the mentioned viscosity range as this could be valuable to the oil and gas industry.
- Drift velocity has been found to play a significant role in the slug translational velocities. This was not investigated in this study owing to instrumentation limitation as such recommended for further study.
- Experimental investigation has shown that mean slug body length decreases with increase in liquid viscosity. There is a need to improve the existing models or develop new models that will take into account the effects of much higher liquid viscosities.
- Most hydrodynamic models depend on empirical correlations like slug translational velocity, slug length and slug frequency for prediction of pressure gradient. These correlations should be replaced by mechanistic models.

## REFERENCES

- Abdul-Majeed, G.H., 2000. Liquid slug holdup in horizontal and slightly inclined two-phase slug flow. *J. Pet. Sci. Eng.* 27, 27–32.
- Al Awadi, H., 2011. *Multiphase Characteristics of High Viscosity Oil* (PhD Thesis). Cranfield University, United Kingdom.
- Alagbe, S.O., 2013. *Experimental and Numerical Investigation of High Viscosity Oil-Based Multiphase Flows* (PhD Thesis). Cranfield University, United Kingdom, United Kingdom.
- Al-Safran, E., 2009a. Prediction of Slug Liquid Holdup in Horizontal Pipes. *J. Energy Resour. Technol.* 131, 023001.
- Al-Safran, E., 2009b. Investigation and prediction of slug frequency in gas/liquid horizontal pipe flow. *J. Pet. Sci. Eng.* 69, 143–155.
- Al-safran, E., Gokcal, B., Sarica, C., 2011. High Viscosity Liquid Effect on Two-Phase Slug Length in Horizontal Pipes. In: *15th International Conference on Multiphase Production Technology*,. BHR Group, Cannes, France, pp. 257–276.
- Al-Safran, E., Kora, C., Sarica, C., 2015. Prediction of slug liquid holdup in high viscosity liquid and gas two-phase flow in horizontal pipes. *J. Pet. Sci. Eng.* 133, 566–575.
- Al-safran, E.M., Gokcal, B., Sarica, C., 2013. Investigation and Prediction of High-Viscosity Liquid Effect on Two-Phase Slug Length in Horizontal Pipelines. *SPE Prod. Oper.* 28, 12–14.
- Al-safran, Kora, C., Sarica, C., 2013. Prediction of liquid volume fraction in slugs in two-phase horizontal pipe flow with high viscosity liquid. In: *International Conference on Multiphase Production Technology*,. BHR Group, Cannes, France, pp. 415–428.
- Angeli, P., Hewitt, G., 2000. Flow structure in horizontal oil–water flow. *Int. J. Multiph. Flow* 26, 1117–1140.
- Archibong, A., 2015. *Viscous Multiphase Flow Characteristics in Pipelines* (PhD Thesis). Cranfield University, United Kingdom, United Kingdom.

- Arney, M.S., Bai, R., Guevara, E., Joseph, D.D., Liu, K., 1993. Friction factor and holdup studies for lubricated pipelining—I. Experiments and correlations. *Int. J. Multiph. Flow* 19, 1061–1076.
- Arubi, T., 2011. *Multiphase Flow Measurement Using Gamma-Based Techniques* (Phd Thesis). Cranfield University, United Kingdom, United Kingdom.
- Baker, O., 1954. Simultaneous Flow of Oil and Gas. *Oil Gas* 53, 185–195.
- Bannwart, A.C., 1998. Wavespeed and volumetric fraction in core annular flow. *Int. J. Multiph. Flow* 24, 961–974.
- Bannwart, A.C., 2001. Modeling aspects of oil–water core–annular flows. *J. Pet. Sci. Eng.* 32, 127–143.
- Bannwart, A.C., Rodriguez, O.M.H., de Carvalho, C.H.M., Wang, I.S., Vara, R.M.O., 2004. Flow Patterns in Heavy Crude Oil-Water Flow. *J. Energy Resour. Technol.* 126, 184.
- Barnea, D., Brauner, N., 1985. Holdup of the liquid slug in two phase intermittent flow. *Int. J. Multiph. Flow* 11, 43–49.
- Barnea, D., Taitel, Y., 1993. A model for slug length distribution in gas-liquid slug flow. *Int. J. Multiph. Flow* 19, 829–838.
- Beggs, D.H., Brill, J.P., 1973. A Study of Two-Phase Flow in Inclined Pipes. *J. Pet. Technol.* 25, 607–617.
- Bendiksen, K.H., 1984. An experimental investigation of the motion of long bubbles in inclined tubes. *Int. J. Multiph. Flow* 10, 467–483.
- Benjamin, B., 1968. Gravity currents and related phenomena. *J. Fluid Mech* 31, 209–248.
- Bestion, D., 1990. The physical closure laws in the CATHARE code. *Nucl. Eng. Des.* 124, 229–245.
- Blaney, S., 2008. *Gamma Radiation Methods for Clamp-On Multiphase Flow Metering* (Phd Thesis). Cranfield University, United Kingdom, United Kingdom.
- Brennen, C.E., 2005. *Fundamentals of Multiphase Flows*. Cambridge University

Press.

- Brill, J.P., Schmidt, Z., Coberly, W.A., Herring, J.D., Moore, D.W., 1981. Analysis of Two-Phase Tests in Large-Diameter Flow Lines in Prudhoe Bay Field. Soc. Pet. Eng. 21.
- Brito, R., Pereyra, E., Sarica, C., 2013. Effect of Medium Oil Viscosity on Two-Phase Oil-Gas Flow Behavior in Horizontal Pipes. In: Offshore Technology Conference. Offshore Technology Conference, Houston, Texas, USA, p. 285.
- Brito, R., Pereyra, E., Sarica, C., 2014. Experimental study to characterize slug flow for medium oil viscosities in horizontal pipes. In: 9th North American Conference on Multiphase Technology. BHR Group, Banff, Canada, pp. 403–417.
- Carpintero Rogero, E., 2009. Experimental Investigation of Developing Plug and Slug Flows (PhD Thesis). Technische Universität München, Germany, Germany.
- Chakrabarti, D.P., Das, G., Ray, S., 2005. Pressure Drop in Liquid-liquid Two Phase Horizontal Flow: Experiment and Prediction. Chem. Eng. Technol. 28, 1003–1009.
- Chisholm, D., 1967. A theoretical basis for the Lockhart-Martinelli correlation for two-phase flow. Int. J. Heat Mass Transf. 10, 1767–1778.
- Choi, J., Pereyra, E., Sarica, C., Park, C., Kang, J., 2012. An Efficient Drift-Flux Closure Relationship to Estimate Liquid Holdups of Gas-Liquid Two-Phase Flow in Pipes. Energies 5, 5294–5306.
- Cook, M., Behnia, M., 2000. Slug length prediction in near horizontal gas-liquid intermittent flow. Chem. Eng. Sci. 55, 2009–2018.
- Dukler, A.E., Hubbard, M.G., 1975. A Model for Gas-Liquid Slug Flow in Horizontal and Near Horizontal Tubes. Ind. Eng. Chem. Fundam. 14, 337–347.
- Dukler, A.E., Wicks, M., Cleveland, R.G., 1964. Frictional pressure drop in two-phase flow: A. A comparison of existing correlations for pressure loss and holdup. AIChE J. 10, 38–43.
- Edomwonyi-Otu, L.C., Angeli, P., 2015. Pressure drop and holdup predictions in horizontal oil–water flows for curved and wavy interfaces. Chem. Eng. Res. Des. 93, 55–65.

- Fabre, J., Line, A., 1992. Modeling of Two-Phase Slug Flow. *Annu. Rev. Fluid Mech.* 24, 21–46.
- Falcone, G., Hewitt, G.F., Alimonti, C., 2009. *Multiphase Flow Metering Principles and Applications*, First. ed. Elsevier Ltd, Great Britain.
- Farsetti, S., Farisè, S., Poesio, P., 2014. Experimental investigation of high viscosity oil–air intermittent flow. *Exp. Therm. Fluid Sci.* 57, 285–292.
- Felizola, H., 1992. *Slug Flow in Extended Reach Directional Wells (PhD Thesis)*. University of Tulsa, USA.
- Foletti, C., Farisè, S., Grassi, B., Strazza, D., Lancini, M., Poesio, P., 2011. Experimental investigation on two-phase air/high-viscosity-oil flow in a horizontal pipe. *Chem. Eng. Sci.* 66, 5968–5975.
- Gokcal, B., 2008. *An Experimental and Theoretical Investigation of Slug Flow for High Oil Viscosity in Horizontal Pipes (PhD Thesis)*. The University Tulsa, USA, USA.
- Gokcal, B., Al-Sarkhi, A., Sarica, C., Alsafran, E.M., 2009. Prediction of Slug Frequency for High Viscosity Oils in Horizontal Pipes. In: *SPE Annual Technical Conference and Exhibition*. Society of Petroleum Engineers, New Orleans, Louisiana, USA.
- Gokcal, B., Al-Sarkhi, A.S., Sarica, C., 2009. Effects of High Oil Viscosity on Drift Velocity for Horizontal and Upward Inclined Pipes. In: *Presentation at the 2008 SPE Annual Technical Conference and Exhibition*. Society of Petroleum Engineers, Denver, Colorado, pp. 32–40.
- Gokcal, B., Wang, Q., Zhang, H., Sarica, C., 2006. Effects of High Oil Viscosity on Oil / Gas Flow Behavior in Horizontal Pipes. In: *SPE Annual Technical Conference and Exhibition*. Society of Petroleum Engineers, San Antonio, Texas, U.S.A.
- Gomez, L., Shoham, O., Taitel, Y., 2000. Prediction of slug liquid holdup: horizontal to upward vertical flow. *Int. J. Multiph. Flow* 26, 517–521.
- Gordon, I.C., Fairhurst, P.C., 1987. Multi-phase Pipeline and Equipment Design for Marginal and Deep Water Field Development. In: *3rd International Multiphase Flow Conference*. BHR, The Hague, Netherland, pp. 1–12.

- Gregory, G. a., Scott, D.S., 1969. Correlation of liquid slug velocity and frequency in horizontal cocurrent gas-liquid slug flow. *AIChE J.* 15, 933–935.
- Gregory, G.A., Nicholson, M.K., Aziz, K., 1978. Correlation of the liquid volume fraction in the slug for horizontal gas-liquid slug flow. *Int. J. Multiph. Flow* 4, 33–39.
- Greskovich, E.J., Shrier, A.L., 1972. Slug Frequency in Horizontal Gas-Liquid Slug Flow. *Ind. Eng. Chem. Process Des. Dev.* 11, 317–318.
- Hall, A.R.W., Hewitt, G.F., Fisher, S.A., 1993. An experimental investigation of the effects of the water phase in the multiphase flow of oil, water and gas. In: 6th International Conference on Multi Phase Production, BHR Group, Cannes, France.
- Hernandez, P.V., 2007. Gas-liquid two-phase flow in inclined pipes (PhD Thesis). University of Nottingham.
- Hewitt, G.F., 1982. Gas-liquid two phase flows. In: Hetsroni (Ed.), *Handbook of Multiphase Systems*. Hemisphere Publishing Corp.
- Hewitt, G.F., Roberts, D.N., 1969. Studies of two-phase flow patterns by simultaneous x-ray and flash photography. Chemical Engineering Division, Atomic Energy Research Establishment; Available from H.M. Stationery Office, Harwell, England; [London].
- Heywood, N.I., Richardson, J.F., 1979. Slug flow of air—water mixtures in a horizontal pipe: Determination of liquid holdup by  $\gamma$ -ray absorption. *Chem. Eng. Sci.* 34, 17–30.
- Hubbard, M.G., 1965. An Analysis of Horizontal Gas-liquid Slug Flow (PhD Thesis). University of Houston, Houston, USA.
- Ishii, M., 1977. One-dimensional drift-flux model and constitutive equations for relative motion between phases in various two-phase flow regimes. Lemont, IL, USA.
- Jepson, W.P., 1989. Modelling the transition to slug flow in horizontal conduit. *Can. J. Chem. Eng.* 67, 731–740.
- Jeyachandra, B.C., Gokcal, B., Al-Sarkhi, A., Serica, C., Sharma, A.K., 2012. Drift-Velocity Closure Relationships for Slug Two-Phase High-Viscosity Oil Flow in

Pipes. Soc. Pet. Eng. 17, 593–601.

Jeyachandra, B.C., Sarica, C., Zhang, H., Pereyra, E., 2012. Inclination Effects on Flow Characteristics of High Viscosity Oil / Gas Two- Phase Flow. In: SPE Annual Technical Conference and Exhibition. Society of Petroleum Engineers, San Antonio, Texas, USA.

Kataoka, I., Ishii, M., 1939. Drift flux model for large diameter pipe and new correlation for pool void fraction. Int. J. Heat Mass Transf. 30, 1927–1939.

Khaledi, H. a., Smith, I.E., Unander, T.E., Nossen, J., 2014. Investigation of two-phase flow pattern, liquid holdup and pressure drop in viscous oil–gas flow. Int. J. Multiph. Flow 67, 37–51.

King, M.J.S., 1998. Experimental and modelling studies of transient slug flow. Imperial College London.

Kora, C., Sarica, C., Zhang, H., Al-Sarkhi, A., Al-Safran, E., 2011. Effects of High Oil Viscosity on Slug Liquid Holdup in Horizontal Pipes. In: Canadian Unconventional Resources Conference. Society of Petroleum Engineers, Alberta, Canada.

Kouba, G.E., 1986. Horizontal slug flow modeling and metering. University. of Tulsa, Tulsa.

Kouba, G.E., Jepson, W.P., 1990. The Flow of Slugs in Horizontal, Two-Phase Pipelines. J. Energy Resour. Technol. 112, 20–24.

Lacy, C.E., 2012. Applicability of Slug Flow Models to Heavy Oils. In: SPE Heavy Oil Conference. Society of Petroleum Engineers, Calgary, Alberta, Canada, pp. 12–14.

Lewis-Van, C.S., Arthur, C., Eisenhauer, C., 1980. Structure shielding against fallout gamma rays from nuclear detonations. Center for Radiation Research, United States, Urbana-Champaign.

Lockhart, R.W., Martinelli, R.C., 1949. Proposed correlation of data for isothermal two-phase, two-component flow in pipes. Chem. Eng. Prog. 45, 39–48.

Lovick, J., Angeli, P., 2004. Experimental studies on the dual continuous flow pattern in oil–water flows. Int. J. Multiph. Flow 30, 139–157.

- Lu, M., 2015. Experimental and computational study of two-phase slug flow (PhD Thesis). Imperial College London.
- Maley, L.C., Jepson, W., 1998. Liquid Holdup in Large-Diameter Horizontal Multiphase Pipelines. *J. Energy Resour. Technol.* ASME 120.
- Malnes, D., 1983. Slug Flow in Vertical, Horizontal and Inclined Pipes, IFE KR E: Institutt for Energiteknikk. Institute for Energy Technology, Norway.
- Mandhane, J.M., Gregory, G.A., Aziz, K., 1974. A flow pattern map for gas—liquid flow in horizontal pipes. *Int. J. Multiph. Flow* 1, 537–553.
- Manolis, I.G., Mendes-Tatsis, M.A., Hewitt, G.F., 1995. The Effect of Pressure on Slug Frequency in Two-Phase Horizontal Flow. In: 2nd International Conference on Multiphase Flow. Elsevier, Kyoto, Japan, pp. 347–354.
- Márquez, J., Trujillo, J., 2010. Overview: Slug-Flow Characterization for Heavy-Oil Fields. In: Proceeding of SPE Latin American and Caribbean Petroleum Engineering Conference. Society of Petroleum Engineers, Lima, Peru, pp. 1–3.
- Mckibben, 2000. A Laboratory Investigation of Horizontal Well Heavy Oil-Water Flows. *Can. J. Chem. Eng.* 78, 743–751.
- Nadler, M., Mewes, D., 1995. Effects of The Liquid Viscosity on The Phase Distributions in Horizontal Gas-Liquid Slug Flow. *Int. J. Multiph. Flow* 21, 253–266.
- Nicholson, M.K., Aziz, K., Gregory, G.A., 1978. Intermittent two phase flow in horizontal pipes: Predictive models. *Can. J. Chem. Eng.* 56, 653–663.
- Nicklin, D., Wilkes, J., Davidson, J., 1962. Two Phase Flow in Vertical tubes. *Trans. Inst. Chem. Eng.* 40, 61–68.
- Norris, L., 1982. Correlation of Prudhoe Bay Liquid Slug Lengths and Holdups During Including 1981 Large Diameter Flowline Tests. Houston, Texas.
- Nydal, O.J., 1991. An Experimental Investigation on Slug Flow. University of Oslo.
- Nydal, O.J., Pintus, S., Andreussi, P., 1992. Statistical characterization of slug flow in horizontal pipes. *Int. J. Multiph. Flow* 18, 439–453.



- Okezue, C.N., 2013. Application of the gamma radiation method in analysing the effect of liquid viscosity and flow variables on slug frequency in high viscosity oil-gas horizontal flow. In: C.A. Brebbia, Vorobief, P. (Eds.), 8th International Conference on Computational and Experimental Methods in Multiphase and Complex Flow. València, Spain, pp. 447–461.
- Oliemans, R.V.A., Ooms, G., Wu, H.L., Duijvestijn, A., 1987. Core-annular oil/water flow: the turbulent-lubricating-film model and measurements in a 5 cm pipe loop. *Int. J. Multiph. Flow* 13, 23–31.
- Ooms, G., Segal, A., van der Wees, A.J., Meerhoff, R., Oliemans, R.V.A., 1983. A theoretical model for core-annular flow of a very viscous oil core and a water annulus through a horizontal pipe. *Int. J. Multiph. Flow* 10, 41–60.
- Pan, J., 2010. Gas Entrainment in Two-Phase Gas-Liquid Slug Flow (PhD Thesis). Imperial College London.
- Pearson, K.G., Jowitt, D., Cooper, C.A., 1984. The THETIS 80% blocked cluster experiment. Part 5. London, UK.
- Perez, V.H., 2007. Gas-liquid two phase flow in inclined pipes (PhD Thesis). University of Nottingham, United Kingdom.
- Richard, M., Emil, A., 2003. Heavy Oil and Natural Bitumen-Strategic Petroleum Resources [WWW Document]. U.S. Geol. Surv. Fact Sheet 70-03, East. Publ. Gr. URL <http://pubs.usgs.gov/fs/fs070-03/fs070-03.html> (accessed 6.27.13).
- Rodriguez, O.M.H., Baldani, L.S., 2012. Prediction of pressure gradient and holdup in wavy stratified liquid–liquid inclined pipe flow. *J. Pet. Sci. Eng.* 96-97, 140–151.
- Rodriguez, O.M.H., Oliemans, R.V.A., 2006. Experimental study on oil–water flow in horizontal and slightly inclined pipes. *Int. J. Multiph. Flow* 32, 323–343.
- Romero, C.H., Márquez, M.A., Vergara, S.D., Valecillos, M.T., 2012. Experimental Determination of Hydrodynamic Parameters of Air-Water Two-Phase Slug Flow in Horizontal Pipes. In: Proceedings of the ASME 2012 Fluids Engineering Summer Meeting. ASME, Rio Grande, Puerto Rico, USA,.
- Ros, N.C.J., 1961. Simultaneous Flow of Gas and Liquid As Encountered in Well

- Tubing. Soc. Pet. Eng. 13.
- Schulkes, R., 2011. Slug Frequencies Revisited. In: 15th International Conference on Multiphase Production Technology. BHR Group, Cannes, France.
- Scott, S.L., Shoham, O., Brill, J.P., 1989. Prediction of Slug Length in Horizontal, Large-Diameter Pipes. Soc. Pet. Eng. 4.
- Shah, A., Fishwick, R., Wood, J., Leeke, G., Rigby, S., Greaves, M., 2010. A review of novel techniques for heavy oil and bitumen extraction and upgrading. Energy Environ. Sci. 3, 700.
- Sonnenburg, H.G., 1989. Full-range drift-flux model base on the combination of drift-flux theory with envelope theory. Germany.
- Sugimoto, F.K., Mazza, R.A., 2015. Experimental Analysis of Pressure Gradients on a Liquid-Liquid Two Phase Flow. Journeys in MultiphaseFlows 10.
- Taitel, Y., Barnea, D., 1990. Two-Phase Slug Flow. In: Transfer, J.P.H. and T.F.I.B.T.-A. in H. (Ed.), ADVANCES IN HEAT TRANSFER. Elsevier, pp. 83–132.
- Taitel, Y., Barnea, D., Dukler, A.E., 1980. Modelling flow pattern transitions for steady upward gas-liquid flow in vertical tubes. AIChE J. 26, 345–354.
- Taitel, Y., Dukler, A.E., 1976. A model for predicting flow regime transitions in horizontal and near horizontal gas-liquid flow. AIChE J. 22, 47–55.
- Thome, J.R., 2004. Void Fractions in Two-Phase Flows. In: Engineering Data Book III. Wolverine Tube Inc., Switzerland, pp. 1–33.
- Trallero, J.L., 1995. Oil-water flows in horizontal pipes. University of Tulsa.
- Van Hout, R., Barnea, D., Shemer, L., 2001. Evolution of statistical parameters of gas-liquid slug flow along vertical pipes. Int. J. Multiph. Flow 27, 1579–1602.
- Vuong, D.H., Zhang, H., Sarica, C., Li, M., 2009. Experimental Study on High Viscosity Oil / Water Flow in Horizontal and Vertical Pipes. In: SPE Annual Technical Conference and Exhibition. Society of Petroleum Engineers, New Orleans, Louisiana, pp. 1–10.
- Wallis, G.B., 1969. One-dimensional two-phase flow, New York: McGraw-Hill Book

Comp. American Institute of Chemical Engineers, Newyork.

Wang, S., 2012. Experiments and Model Development For High-Viscosity Oil / Water / Gas Horizontal And Upward Vertical Pipe Flows. University of Tulsa.

Wang, W., Cheng, W., Kai Li, C. Lou, Jing Gong, 2013. Flow Patterns Transition Law of Oil-Water Two-Phase Flow under a Wide Range of Oil Phase Viscosity Condition. J. Appl. Math.

Weisman, J., Duncan, D., Gibson, J., Crawford, T., 1979. Effects of Fluid Properties and Pipe Diameter on Two-Phase Flow Patterns in Horizontal Line. Int. J. Multiph. Flow 5, 437–462.

Xiao, J.J., Shonham, O., Brill, J.P., 1990. A Comprehensive Mechanistic Model for Two-Phase Flow in Pipelines. In: SPE Annual Technical Conference and Exhibition. Society of Petroleum Engineers, New Orleans, Louisiana, USA.

Yusuf, N., Al-Wahaibi, Y., Al-Wahaibi, T., Al-Ajmi, A., Olawale, A.S., Mohammed, I.A., 2012. Effect of oil viscosity on the flow structure and pressure gradient in horizontal oil–water flow. Chem. Eng. Res. Des. 90, 1019–1030.

Zabaras, G.J., 1999. Prediction of Slug Frequency for Gas/Liquid Flows. In: SPE Annual Technical Conference and Exhibition,. Society of Petroleum Engineers, Houston, Texas, USA.

Zhang, H., Sarica, C., Pereyra, E., 2012. Review of High-Viscosity Oil Multiphase Pipe Flow. Energy & Fuels 26, 3979–3985.

Zhang, H.-Q., Wang, Q., Sarica, C., Brill, J.P., 2003a. Unified Model for Gas-Liquid Pipe Flow via Slug Dynamics—Part 1: Model Development. J. Energy Resour. Technol. 125, 266–273.

Zhang, H.-Q., Wang, Q., Sarica, C., Brill, J.P., 2003b. Unified Model for Gas-Liquid Pipe Flow via Slug Dynamics—Part 2: Model Validation. J. Energy Resour. Technol. 125, 274.

Zhang, H.-Q., Wang, Q., Sarica, C., Brill, J.P., 2003c. A unified mechanistic model for slug liquid holdup and transition between slug and dispersed bubble flows. Int. J. Multiph. Flow 29, 97–107.

- Zhang, L., Wang, H., 2010. Identification of oil–gas two-phase flow pattern based on SVM and electrical capacitance tomography technique. *Flow Meas. Instrum.* 21, 20–24.
- Zhao, Y., 2014. High Viscosity Liquid Two-phase Flow (PhD Thesis). Cranfield University, United Kingdom, United Kingdom.
- Zhao, Y., Lao, L., Yeung, H., 2015. Investigation and prediction of slug flow characteristics in highly viscous liquid and gas flows in horizontal pipes. *Chem. Eng. Res. Des.* 102, 124–137.
- Zhao, Y., Yeung, H., Lao, L., 2013. Slug frequency in high viscosity liquid and gas flow in horizontal pipes. In: 16th International Conference on Multiphase Production Technology. BHR Group, Cannes, France.
- Zhao, Y., Yeung, H., Zorgani, E.E., Archibong, A.E., 2013. High viscosity effect on characteristics of oil and gas two - phase flow in horizontal pipes. *Chem. Eng. Sci.* 38.
- Zuber, N., Findlay, J.A., 1965. Average Volumetric Concentration in Two-Phase Flow Systems. *J. Heat Transfer* 87, 453–468.

# APPENDICES

## A Estimating Uncertainties

Uncertainty is defined in the International Standard Organisation (ISO)'s "Guide to the Expression of Uncertainty in Measurement" (GUM) as a parameter (e.g. standard deviation), associated with the result of a measurement, that characterizes the dispersion of the values that could reasonably be attributed to the measurand. It is often expressed in a "range" and at a "level of confidence". Uncertainty can be estimated by using analytical or Monte Carlo methods, in this work, uncertainty is evaluated using the analytical approach.

The common method of repeating experimental measurement at the same condition to obtain the uncertainty interval is impractical and expensive especially due to the transient nature of multiphase flow. An example of this is in the estimation of the frictional pressure gradient were slight variations in ambient or system temperature can lead to a change in the viscosity of fluids and thus the measured frictional pressure gradient.

The analytical concepts become a viable solution in handling this type scenario. A detailed step-wise process given by Yan (2011) in estimating uncertainty is stated below:

1. If an experimentally measured output,  $y$  is a function of inputs  $x_1, x_2, x_3 \dots x_n$  then:

$$y = f(x_1, x_2, x_n \dots x_n) \quad (\text{A-1})$$

2. Estimate uncertainty of  $x_i$

$u(x_i)$  – uncertainty in absolute terms

$u(x_i)$  – uncertainty in fractional terms

3. Compute sensitivity of  $y$  to changes in  $x_i$ , i.e. partial differentiation for each input. The absolute and fractional inputs are given by:

$$c_i = \frac{\partial y}{\partial x_i} \quad (\text{A-2})$$

$$c_i^* = \frac{\partial y}{\partial x_i} \cdot \frac{x_i}{y} \quad (\text{A-3})$$

4. A combination of the uncertainties for a set of uncorrelated inputs is obtained by summation of uncertainties for each input. The absolute and fractional terms are expressed as:

$$u_c(y) = \sqrt{\sum_{i=1}^n (c_i \cdot u(x_i))^2} \quad (\text{A-4})$$

$$u_c^*(y) = \sqrt{\sum_{i=1}^n (c_i^* \cdot u^*(x_i))^2} \quad (\text{A-5})$$

Uncertainties in the superficial liquid and gas liquid velocities, liquid holdup, pressure gradient and liquid viscosity is described in the following sections together with sample calculation.

### A.1.1 Uncertainty in superficial liquid velocity

The liquid superficial velocity,  $V_{SL}$  is a function of the mass flow rate,  $\dot{M}_L$  liquid density,  $\rho_L$  and flow area,  $A$ . For the purpose of this evaluation, the pipe diameter and hence the flow area will be considered constant. The Coriolis mass flow meter is used to obtain the mass flow rate and liquid density, from the manufacturer's guide, the maximum error in measurement are  $\pm 0.5\%$  and  $\pm 0.5 \text{ kg/m}^3$  for mass flow rate and liquid density respectively. In evaluating the uncertainty, we follow the steps that were previously highlighted thus:

Determine standard uncertainty of each of the functions based on their respective measurement equipment and confidence level. Assuming a 95.4% confidence level;

$$V_{SL} = \frac{\dot{M}_L}{\rho_L A} = \frac{4\dot{M}_L}{\rho_L \pi D^2} \quad (\text{A-6})$$

Partial derivatives of the inputs,  $Q_L$  and  $\rho_L$  is given by:

$$\frac{\partial V_{SL}}{\partial \dot{M}_L} = \frac{4}{\rho_L \pi D^2} \quad (A-7)$$

$$\frac{\partial V_{SL}}{\partial \rho_L} = -\frac{4 \dot{M}_L}{\pi (\rho_L D)^2} \quad (A-8)$$

Combined uncertainty in measurement of the superficial liquid velocity is thus:

$$u_c(V_{SL}) = \sqrt{\sum_{i=1}^n (c_i^* \cdot u^*(V_{SL}))^2} = \sqrt{\left(u_c^*(\dot{M}_L) \cdot \frac{\partial V_{SL}}{\partial \dot{M}_L}\right)^2 + \left(u_c^*(\rho_L) \cdot \frac{-4 \dot{M}_L}{\pi (\rho_L D)^2}\right)^2} \quad (A-8)$$

### Case Study

In a test case for the 0.0254 m pipe ID test facility,  $V_{SL} = 0.10$  m/s,  $\dot{M}_L = 180.5$  kg/h,  $\rho_L = 905.8$  kg/m<sup>3</sup>. As earlier stated, pipe diameter is considered a constant while the uncertainty for  $\rho_L$  and  $\dot{M}_L$  are as given in the manufacturer's manual. As shown in the spreadsheet in Table B-1 below, the combined uncertainty at 95.4 % confidence level for this condition is  $\pm 0.55$  %.

Table B-1: Table showing sample uncertainty computations

Superficial Liquid Velocity	Mass Flow Rate	Liquid Density	Pipe Diameter	Standard uncert., u* Mass Flow	Standard uncert., u* Density	Sensitivity, ci*	Sensitivity, ci*	Combined Uncert., U* (95.4% Confidence)
m/s	kg/s	kg/m <sup>3</sup>	m			Mass Flow	Density	
0.1	0.0501	905.8	0.0254	0.0025	0.25	4.348832125	1.091561212	0.54621358

### A.1.2 Uncertainty in superficial gas velocity

The vortex flow meter is used in measuring the gas volumetric flow rate based on which the superficial gas velocity is obtained. The uncertainty in the flow meter is given in the manufacturer's guide as  $\pm 1\%$ . The gas superficial velocity is given as a function of the measured volumetric flow rate,  $Q_{FM}$ , pressure at the flow meter,  $P_{FM}$  and temperature at the flow meter,  $T_{FM}$ . It is also a function of the corresponding measurements of pressure,  $P_{GI}$  and temperature,  $T_{GI}$  at the gas injection point into the main test section. Mathematically, it is expressed as:

$$V_{SG} = \frac{Q_G}{A} = \frac{4P_{FM} Q_{FM} T_{GI}}{P_{GI} T_{FM} \pi D^2} \quad (\text{A-9})$$

Partial derivatives of the inputs are expressed as:

$$\frac{\partial V_{SG}}{\partial P_{FM}} = \frac{4 Q_{FM} T_{GI}}{P_{GI} T_{FM} \pi D^2} \quad (\text{A-10})$$

$$\frac{\partial V_{SG}}{\partial Q_{FM}} = \frac{4 P_{FM} T_{GI}}{P_{GI} T_{FM} \pi D^2} \quad (\text{A-11})$$

$$\frac{\partial V_{SG}}{\partial T_{GI}} = \frac{4 P_{FM} Q_{FM}}{P_{GI} T_{FM} \pi D^2} \quad (\text{A-12})$$

$$\frac{\partial V_{SG}}{\partial P_{GI}} = -\frac{4 P_{FM} Q_{FM} T_{GI}}{P_{GI}^2 T_{FM} \pi D^2} \quad (\text{0-23})$$

$$\frac{\partial V_{SG}}{\partial T_{FM}} = -\frac{4 P_{FM} Q_{FM} T_{GI}}{P_{GI} T_{FM}^2 \pi D^2} \quad (\text{A-14})$$

Combined uncertainty in measurement of the superficial gas velocity is thus:

$$u_c(V_{SG}) = \sqrt{\left( u_c^*(P_{GI}) \cdot \left( -\frac{4 P_{FM} Q_{FM} T_{GI}}{P_{GI}^2 T_{FM} \pi D^2} \right) \right)^2 + \left( u_c^*(T_{FM}) \cdot \left( -\frac{4 P_{FM} Q_{FM} T_{GI}}{P_{GI} T_{FM}^2 \pi D^2} \right) \right)^2 + \left( u_c^*(P_{FM}) \cdot \frac{4 Q_{FM} T_{GI}}{P_{GI} T_{FM} \pi D^2} \right)^2 + \left( u_c^*(Q_{FM}) \cdot \frac{4 P_{FM} T_{GI}}{P_{GI} T_{FM} \pi D^2} \right)^2 + \left( u_c^*(T_{GI}) \cdot \frac{4 P_{FM} Q_{FM}}{P_{GI} T_{FM} \pi D^2} \right)^2} \quad (\text{A-35})$$

### Case Study

In a test case for the 0.0254 m pipe ID test facility,  $V_{SG} = 0.36$  m/s,  $Q_{FM} = 180.5$  kg/h,  $\rho_L = 905.8$  kg/m<sup>3</sup>. As earlier stated, pipe diameter is considered a constant while the uncertainty for  $Q_{FM}$ ,  $P_{FM,GI}$  and  $T_{FM,GI}$  is  $\pm 0.1\%$  as given in the manufacturer's manual. As shown in the spreadsheet in Table B-1 below, the combined uncertainty at 95.4 % confidence level for this condition is  $\pm 7.73\%$ .



Table A-1: Table showing sample uncertainty computations

Superficial Gas Velocity	Volumetric Flow Rate	Pressure at FM	Pressure at GI	Temperature, T FM	Temperature, TGI	Standard uncert., u* Volumetric Flow Rate	Standard uncert., u* P FM	Standard uncert., u* P GI
m/s	m <sup>3</sup> /s	bara	bara	degC	degC			
0.36	0.011322222	4.9	2.4	6	11.5	0.0005	0.0005	0.0005

Standard uncert., u* T FM	Standard uncert., u* T GI	Sensitivity, ci*	Sensitivity, ci*	Sensitivity, ci*	Sensitivity, ci*	Sensitivity, ci*	Combined Uncert., U* (95.4% Confidence)
		Volumetric Flow	P FM	P GI	T FM	TGI	
0.0005	0.0005	14.91036366	7.96085E-05	7.9608E-05	1.44529E-05	0.009625222	7.72532525

## A.2 Uncertainty in pressure gradient

Pressure gradient in this work was obtained directly from measurements by the differential and point pressure transducers. Based upon this premise, the uncertainty in the measurements of pressure gradient is sourced directly from the stated uncertainties in the manufacturer's guide. For measurements using the single points and the differential pressure transducers, the uncertainties were given as  $\pm 2$  and  $\pm 0.04\%$  for the range of 0 – 6 barg and -200 to +200 mbar respectively.

## A.3 Uncertainty in liquid holdup

Uncertainty in measurement for the liquid holdup was obtained from the Gamma densitometer systems used in measurements of this parameter. They were sourced from static calibrations of the instruments as highlighted in Chapter 3. They are given as  $\pm 10\%$ .

## A.4 Uncertainty in liquid viscosity

The uncertainty in liquid viscosity measurement is obtained from the viscometer supplied by Brookfield. The accuracy of the viscometer is given as  $\pm 1\%$  of the full range with a repeatability of  $\pm 0.2\%$  of the full range.

## B Error Analysis

### B.1 Estimating Errors

When measurements are obtained from experiments, an assumption that some true or exact value exists based on certain definition of the quantity being measured is usually assumed. The deviation of the actual measured value from this exact value is termed the error in measurement. Possible sources of error in experiments include: Environment (temperature, pressure, vibration etc.), instrument performance (bias, drift, resolution, wear etc.) process stability (bends, pulsation, valve etc.) calibration uncertainty etc.

Six statistical parameters previously used by (Gokcal 2008 and Zhao 2014) have been utilized in this study to evaluate the performance of existing predictions models/ correlations against present data and developed correlations. There are calculated based on relative error and actual error. Equation (B-1 to B-8) gives the mathematical definition of this parameters

$$e_{ri} = \frac{(E_{i,Cal} - E_{i,Mea})}{E_{i,Mea}} \times 100 \quad (B-1)$$

$$e_i = E_{i,Cal} - E_{i,Mea} \quad (B-2)$$

Average percentage relative error is:

$$\varepsilon_1 = \frac{1}{N} \sum_1^N e_{ri} \quad (B-3)$$

Average absolute percentage relative error is:

$$\varepsilon_2 = \frac{1}{N} \sum_1^N |e_{ri}| \quad (B-4)$$

Standard deviation about average relative error is:

$$\varepsilon_3 = \sqrt{\frac{\sum_1^N (e_{ri} - \varepsilon_1)^2}{N-1}} \quad (B-5)$$

Average actual error is:

$$\varepsilon_4 = \frac{1}{N} \sum_1^N e_i \quad (\text{B-6})$$

Average absolute actual error is:

$$\varepsilon_5 = \frac{1}{N} \sum_1^N |e_i| \quad (\text{B-7})$$

Standard deviation about average actual error is:

$$\varepsilon_6 = \sqrt{\frac{\sum_1^N (e_i - \varepsilon_4)^2}{N-1}} \quad (\text{B-8})$$

## C List of Models/Correlations Used For Comparison

### C-1 Liquid Holdup

The general drift flux model for liquid holdup is given by

$$H_L = 1 - \frac{U_{SG}}{C_o U_M + V_D} \quad (\text{D-1})$$

Liquid holdup  $H_L$  can be estimated from equation D-1 above, if the distribution parameter  $C_o$  and drift velocity  $V_D$  are known.

Authors	$C_o$	$V_D$	Data Source
(Zuber and Findlay, 1965)	1.2	$1.53 \left[ \frac{g\sigma(\rho_L - \rho_G)}{\rho_L^2} \right]^{1/4}$	Air-Water Vertical systems
(Ishii, 1977)	$1.2 - 0.2 \sqrt{\frac{\rho_G}{\rho_L} (1 - \exp(18\alpha_G))}$	$(C_o - 1)V_M + \sqrt{2} \left[ \frac{g\sigma(\rho_L - \rho_G)}{\rho_L^2} \right]^{1/4}$	---
(Kataoka and Ishii, 1939)	$1.2 - 0.2 \sqrt{\frac{gd\Delta\rho}{\rho_g}}$	$0.92 \left( \frac{\rho_G}{\rho_L} \right)^{-0.157}$	---
(Pearson et al., 1984)	$1 + 0.796 * \exp(0.061 \sqrt{\frac{\rho_G}{\rho_L}})$	$0.034 \left( \sqrt{\frac{\rho_G}{\rho_L}} - 1 \right)$	---
(Sonnenburg, 1989)	$1 + (0.32 - 0.32 \sqrt{\frac{\rho_G}{\rho_L}})$	$\frac{C_o(1 - C_o\alpha_G)}{(C_o\alpha_G/\sqrt{gd\Delta\rho/\rho_G}) + C_o\alpha_G/\sqrt{g}}$	----
(Bestion, 1990)	1	$0.188 \sqrt{\frac{gd\Delta\rho}{\rho_g}}$	---
(Choi et al., 2012)	$\frac{2.27}{1 + (Re/1000)^2} + \frac{1.2 - 0.2 \sqrt{(\rho_G/\rho_L)(1 - \exp(18\alpha_G))}}{1 + (1000/Re)^2}$	$A \cos \theta + B \left[ \frac{g\sigma(\rho_L - \rho_G)}{\rho_L^2} \right]^{1/4} \sin \theta$	2 inch, oil-gas, 0.001 - 0.601 Pa.s
(Beggs and Brill, 1973)	$H_L = \frac{0.845\lambda_L}{Fr^{0.0346}}$ where $\lambda_L = \frac{V_{SL}}{V_{SG} + V_{SL}}$		1 and 1.5 inch ID, Air-water experiments

(Xiao et al., 1990)	$H_L = \frac{V_t E_s + V_b(1 - E_s) - V_{sg}}{V_t}$	----
---------------------	---	------

## C-2 Slug Frequency

Authors	Correlation/Models	Data Source
(Gregory and Scott, 1969)	$0.0226 \left(\frac{V_{SL}}{gD}\right)^{1.2} \cdot \left(\frac{19.75}{V_M} + V_M\right)^{1.2}$	0.019 m Pipe ID, CO <sub>2</sub> -Water, 0.0001 Pa.s
(Greskovich and Shrier, 1972)	$0.0226 \left(\frac{V_{SL}}{V_M}\right)^{1.2} \cdot \left(\frac{19.75}{D} + \frac{V_M^2}{gD}\right)^{1.2}$	Modified (Gregory and Scott, 1969)
(Heywood and Richardson, 1979)	$0.0434 \left[\left(\frac{V_{SL}}{gD}\right) \left(\frac{19.75}{V_M} + V_M\right)\right]^{1.2}$	Slight modification to (Gregory and Scott, 1969)
(Nydal, 1991)	$0.088 \frac{(V_{SL} + 1.5)^2}{gD}$	---
(Zabaras, 1999)	$0.0226 \left[\frac{V_{SL}}{gD} \left(\frac{19.75}{V_M} + V_M\right)\right]^{1.2} + 2.75 \sin \theta$	0.0254 – 0.2032 m pipe ID, air-water
(Bahadir Gokcal et al., 2009)	$2.63 \frac{1}{N_F^{0.612}} \frac{V_{SL}}{D}$	0.0508 m pipe ID, oil-gas, 0.183-0.580 Pa.s
(Al-Safran, 2009b)	$\ln F_s = 0.8 + 1.53 \ln(V_{sl}) + 0.27 \left(\frac{V_s}{V_m}\right) - 34.1 D_1$	0.0508 m pipe ID, oil-gas, 0.183-0.580 Pa.s
(Okezue, 2013)	$\left(\frac{3.6102}{V_M}\right) \left(\frac{V_{SL}^{1.299}}{V_M^{0.299}}\right) \left(\frac{Fr_m^{0.497}}{Re_M^{0.531}}\right)$	0.074 m ID Pipe, Oil-Gas, 1-4.0 Pa.s
(Y Zhao et al., 2013)	$\frac{F}{\Psi(\alpha)} = \begin{cases} 10.836 Re_{SL}^{-0.337} & Re_{SG} \leq 4000 \\ 6.40 Re_{SL}^{-0.141} & Re_{SG} > 4000 \end{cases} \text{ for } Re_{SL} < 4000$	0.074 m ID Pipe, Oil-Gas, 1.0-7.0 Pa.s

(Archibong, 2015)	$\ln F_s = \psi_1 \ln(Fr) - \psi_2 \ln(V_{sgd}) + \psi_3 \ln(\lambda) - \psi_4 \ln(M_R) \text{ where}$ $Fr = \frac{V_m}{\sqrt{gD}}; V_{sgd} = \frac{V_{sg} \left[ \sqrt{[(\rho_l - \rho_g)/\rho_g]} \right]}{\sqrt{gD}} ;$ $M_R = \frac{Re_{sl} V_{sl}^2}{Re_{sg} V_{sg}^2}; \lambda = \frac{V_{sl}}{V_M};$ <p>And <math>\psi_1, \psi_2, \psi_3</math> and <math>\psi_4</math> were obtained from his dataset as 0.138, 0.801, 1.661 and 0.277 respectively.</p>	0.0254 m ID Pipe, Oil-Gas, 1.0-7.0 Pa.s
-------------------	--	---

### C-3 Slug Liquid Holdup

Authors	Correlation/Models	Data Source
(Gregory et al., 1978)	$Hl_s = \frac{1}{1 + \left(\frac{V_M}{8.66}\right)^{1.39}}$	0.0258 and 0.0512 m ID pipe
(Malnes, 1983)	$Hl_s = 1 - \frac{V_M}{\left[ V_M + 83 \left( \frac{g\sigma_{GL}}{\rho_L} \right)^{1/4} \right]}$	Modified (Gregory et al., 1978)
(Gomez et al., 2000)	$Hl_s = e^{-(0.45\theta + C Re)} \quad 0 < \theta \leq 90^\circ$ $C = 2.48 \times 10^{-6}, Re = \frac{\rho_L V_M D}{\mu_L}$	0.051-0.203 m ID pipe, air-kerosene
(Abdul-Majeed, 2000)	$Hl_s = (1.009 - CV_M)A$ <p>Where <math>C = \left( 0.006 + 1.3377 \frac{\mu_G}{\mu_L} \right)</math></p>	0.025-0.203 m ID pipe, air-water, 0.001-0.007 Pa.s
(Felizola, 1992)	$Hl_s = A_1 + A_2 V_M + A_3 V_M^2 \text{ where } A_1=0.775, A_2 = 0.041, A_3=0.019$	0.051 m ID pipe, Kerosene-air,

(Kora et al., 2011)	$Hl_s = \begin{cases} 1.012 \exp(-0.085 Fr N_\mu^{0.2}) & 0.15 < Fr N_\mu^{0.2} < 1.5 \\ 0.9473 \exp(-0.041 Fr N_\mu^{0.2}) & Fr N_\mu^{0.2} \geq 1.5 \\ 1.0 & Fr N_\mu^{0.2} \leq 0.15 \end{cases}$	0.0508 m ID, oil-gas 0.257 and 0.181 Pa.s
(Al-Safran et al., 2013)	$Hl_s = 0.85 - 0.75\varphi + 0.057\sqrt{\varphi^2 + 2.27}; \quad \varphi = Fr N_\mu^{0.2} - 0.89$	0.0508 m ID, oil-gas, 0.180 – 0.587 Pa.s
(Archibong, 2015)	$Hl_s = 1 - 0.03336 N_{Fr} N_\mu^{0.11}$	0.026 m Pipe ID, oil-gas, 0.8-7.0 Pa.s

#### C-4 Slug Translational Velocity

Authors	Correlation/Models	Data Source
Nicklin et al. (1962)	$V_T = C_0 V_m + V_D$	----
(Hubbard, 1965)	$V_T = (1 + C_0) V_m + V_D$	----
(Kouba and Jepson, 1990)	$V_T = 1.21(0.1134 + 0.94V_{sl} + V_{sg})$	0.15 m ID pipe, air-water
(Benjamin, 1968)	$C_o=1.2; V_D = 0.542\sqrt{gD}$	---
(Choi et al., 2012)	$C_o = \frac{2.27}{1 + (Re/1000)^2} + \frac{1.2 - 0.2\sqrt{(\rho_G/\rho_L)}(1 - \exp(18\alpha_G))}{1 + (1000/Re)^2}$ $V_D = A \cos \theta + B \left[ \frac{g\sigma(\rho_L - \rho_G)}{\rho_L^2} \right]^{1/4} \sin \theta$	2 inch, oil-gas, 0.001 – 0.601 Pa.s

(Benin Chelinsky Jeyachandra et al., 2012)	$Co = \frac{2.27}{1 + (Re/1000)^2} + \frac{1.2 - 0.2\sqrt{(\rho_G/\rho_L)}(1 - \exp(18\alpha_G))}{1 + (1000/Re)^2}$ $V_D = Fr_\theta = Fr^h \cos \theta + Fr^v \sin \theta,$	0.0508, 0.0762 and 1.524 m Pipe ID, 0-90 degree, 0.001 to 0.7 Pa.s
--	--	--

### C-5 Slug Body Length

Authors	Correlation/Models	Data Source
(Brill et al., 1981)	$\ln(L_S) = -3.851 + 0.059 \ln\left(\frac{V_m}{0.3048}\right) + 5.445 \left[ \ln\left(\frac{D}{0.0254}\right) \right]^{0.5}$	Alaska Prudhoe Bay field data
(Norris, 1982)	$\ln\left(\frac{L_S}{0.3048}\right) = -2.099 + 4.859 \sqrt{\ln\frac{D}{0.0254}}$	Modified (Brill et al., 1981)
(Gordon and Fairhurst, 1987)	$\ln L_S = -3.287 + 4.859\sqrt{\ln D + 3.673} + 0.059 \ln(V_m)$	0.3048 m, 0.4064 m and 0.508 m internal diameter pipes:
(Gordon and Fairhurst, 1987)	$\ln L_S = -3.287 + 4.859\sqrt{\ln D + 3.673}$	0.588m ID pipe
(Scott et al., 1989)	$\ln L_S = -26.6 + 28.495 \left[ \ln\left(\frac{D}{0.0254}\right) \right]^{0.1}$	Alaska Prudhoe Bay field data
(Wang, 2012)	$L_S = \left\{ 10.1 + \frac{16.8}{1 + \text{Exp}[-3.57 * (\ln(N_f) - 5.4)]} \right\} \left[ \cos^2 \theta + \frac{\sin^2 \theta}{2} \right] D$	0.0525 m ID pipe, 0.15 to 0.57 Pa.s



(Al-Safran et al., 2013)	$\frac{L_S}{D} = 2.63 \frac{\left[ D^{2/3} \sqrt{\rho_L (\rho_L - \rho_G)} \right]^{0.321}}{\mu_L}$	0.0508 m ID pipe, 0.181 – 0.589 Pa.s
--------------------------	---	---